Life on N_2O

On the ecophysiology on nitrous oxide reduction & its potential as a greenhouse gas sink in wastewater treatment

Conthe Calvo, Monica

DOI
10.4233/uuid:6cdf5170-69f6-48c5-b953-a790bc611ac8

Publication date
2018

Document Version
Final published version

Citation (APA)
Conthe Calvo, M. (2018). *Life on N_2O: On the ecophysiology on nitrous oxide reduction & its potential as a greenhouse gas sink in wastewater treatment*. [Dissertation (TU Delft), Delft University of Technology]. https://doi.org/10.4233/uuid:6cdf5170-69f6-48c5-b953-a790bc611ac8

Life on N_2O

On the ecophysiology on nitrous oxide reduction
& its potential as a greenhouse gas sink in wastewater treatment

Dissertation

for the purpose of obtaining the degree of doctor
at Delft University of Technology
by the authority of the Rector Magnificus, prof.dr.ir. T.H.J.J. van der Hagen,
chair of the Board for Doctorates
to be defended publicly on
Tuesday 11th of December, 2018 at 10:00 o'clock

by

Mónica CONTHE CALVO
Master of Microbiology, Universidad Autónoma de Madrid, Spain
born in Madrid, Spain

This dissertation has been approved by the promotors.

Composition of the doctoral committee:

Rector Magnificus,	chairperson
Prof.dr.ir. M.C.M. van Loosdrecht	Delft University of Technology, promotor
Dr.ir. R. Kleerebezem	Delft University of Technology, copromotor

Independent members:

Prof.dr. Å. Frostegård	Norwegian University of Life Sciences, Norway
Prof.dr. H. Daims	University of Vienna, Austria
Prof.dr. J.T. Pronk	Delft University of Technology
Dr. C. Welte	Radboud University, The Netherlands
Prof.dr. P. Daran-Lapujade	Delft University of Technology, reserve member

Other members:

Prof.dr.ir. J G. Kuenen	Delft University of Technology

This research was funded by the European Commission through the Marie Skłodowska-Curie Actions

Printed by: Ridderprint BV | www.ridderprint.nl
ISBN: 978-94-6375-222-0

Table of contents

Summary

With its rapidly rising concentration in the atmosphere and its high global warming potential, N_2O is arguably *the* greenhouse gas of the 21st century. The research carried out within the Nitrous Oxide Research Alliance (NORA) – of which this thesis forms part of – focused on the microbial conversions of N_2O within the nitrogen cycle, the ultimate aim being to develop N_2O mitigation strategies for natural and managed ecosystems such as agricultural soils and wastewater treatment plants. A variety of pathways in the nitrogen cycle *produce* N_2O, but respiratory N_2O reduction to N_2 by microorganisms harboring an N_2O reductase enzyme (encoded by the gene *nosZ*), is the only known microbial conversion that consumes N_2O. N_2O-respiring microorganisms may thus be key in this endeavour.

Studies in literature reporting the cultivation of denitrifying bacteria with N_2O as a sole electron acceptor date back to the 1950s and in recent years, there have been important discoveries of novel groups of denitrifying and non-denitrifying N_2O reducing bacteria and archaea, and their importance for N_2O reduction in the environment. Nevertheless, essential aspects of N_2O reduction remain unclear and the aim of this thesis was to fill in some of the existing knowledge gaps regarding N_2O-reducer ecophysiology, using wastewater treatment as a frame of reference.

Our main approach was to study simplified, naturally selected, N_2O reducing bacterial communities in chemostat enrichment cultures fed with N_2O as the sole electron acceptor and acetate as electron donor. Continuous cultivation, which selects for a fairly simple community, is ideal for ecophysiology studies as it bridges the gap between ecosystem studies and pure culture work. Furthermore, it allows for cultivation under constant and limiting conditions.

With this approach:

- we studied the efficiency of N_2O respiration as reflected in the growth yields of the enrichment cultures during N_2O limiting as well as electron-donor limiting conditions (**Chapters 2**, **3**, and **4**)
- we were able to compare the thermodynamic efficiency of *nosZ* clade II versus clade I associated electron transport chains and to gain further insight into the role of the NosZ type in the microbial competition for N_2O (**Chapters 2** and **3**)

- we could assess the effect of O_2 availability on the N_2O sink capacity of a microbial community: i.e. (i) the extent to which simultaneous respiration of N_2O and O_2 can occur, (ii) the mechanism governing the competition for N_2O and O_2, and (iii) how the N_2O-reducing capacity of a community is affected by dynamic aerobic/anoxic shifts (**Chapter 5**)
- we could search for previously undescribed microbial metabolisms involving N_2O (**Chapter 6**)

We complemented the chemostat enrichment methodology with continuous cultivation of a pure culture (*Pseudomonas stutzeri*, **Chapter 2**) and with short-term batch tests with the enrichment cultures (**Chapters 2** and **4**). In **Chapter 6**, we addressed NO_x and N_2O kinetics with short-term batch tests *directly* on natural community from a full-scale Activated sludge system. In the final chapter of this thesis we present some insight into the modularity of denitrifying communities applying the chemostat enrichment approach to NO_3^- reducing communities.

We hope that the research presented in this thesis will be of help in the development of N_2O mitigation strategies – not only in wastewater treatment systems, but in managed ecosystems in general.

Samevatting

Met de snel toenemende concentratie van N_2O in de atmosfeer en diens hoge potentieel voor opwarming van de aarde, wordt N_2O gezien als *het* broeikasgas van de 21e eeuw. Het onderzoek dat is uitgevoerd binnen de 'Nitrous Oxide Research Alliance' (NORA) – van welke dit proefschrift onderdeel uitmaakt – was gericht op de microbiële conversies van N_2O binnen de stikstofkringloop, met het uiteindelijke doel om strategieën voor N_2O mitigatie te ontwikkelen voor natuurlijke en beheerde ecosystemen, zoals landbouwgrond en afvalwaterzuiveringen. Verscheidene omzettingen in de stikstofkringloop *produceren* N_2O, maar er is maar één microbiële omzetting bekend die N_2O consumeert: de respiratoire reductie van N_2O naar N_2. Dit proces kan worden uitgevoerd door micro-organismen die een N_2O reductase enzym bezitten, dat wordt gecodeerd door het *nosZ* gen. N_2O respirerende micro-organismen kunnen daarom de sleutel zijn tot N_2O mitigatie.

Studies in de wetenschappelijke literatuur die rapporteren over de cultivatie van denitrificerende bacteriën met N_2O als enige elektronacceptor gaan terug tot de jaren '50. Meer recent zijn er belangrijke ontdekkingen gedaan aangaande nieuwe groepen denitrificerende en niet-denitrificerende N_2O reducerende bacteriën en archaea, en hun belang in de reductie van N_2O in het milieu. Desondanks zijn essentiële aspecten van N_2O reductie nog onduidelijk. Het doel van dit proefschrift was om deze kennishiaten met betrekking tot de ecofysiologie van de N_2O-reduceerders in te vullen, waarbij afvalwaterzuivering als referentiekader wordt gebruikt.

Wij hebben dit voornamelijk bestudeerd in vereenvoudigde, natuurlijk geselecteerde, N_2O reducerende bacteriële populaties in chemostaat verrijkingsculturen gevoed met N_2O als enige elektronacceptor en azijnzuur als elektrondonor. Continue cultivatie, wat selecteert voor een vrij simpele populatie, is ideaal voor ecofysiologische studies, omdat het de kloof tussen ecosysteem studies en het werk met pure cultures overbrugt. Daarnaast kun je met een continu systeem cultiveren onder constante en limiterende condities.

Met deze aanpak:

- hebben we de efficiëntie van N_2O respiratie bestudeerd, welke is gereflecteerd in de groeiopbrengst van de verrijkingsculturen tijdens N_2O gelimiteerde en elektrondonor gelimiteerde condities (**Hoofdstuk 2**, **3** en **4**).

- waren we in staat om de thermodynamische efficiëntie van de elektronentransportketens van *nosZ* clade II en clade I te vergelijken, en om meer inzicht te krijgen in de rol van het NosZ type in de microbiële competitie voor N_2O (**Hoofdstuk 2** en **3**).
- waren we in staat om het effect van de beschikbaarheid van O_2 op de N_2O reducerende capaciteit van de populatie te evalueren: d.i. (i) in hoeverre gelijktijdige respiratie van N_2O en O_2 kan voorkomen, (ii) het mechanisme dat de competitie voor N_2O en O_2 stuurt, en (iii) hoe de N_2O reducerende capaciteit van een populatie wordt beïnvloed door dynamische omschakelingen tussen aerobe en anoxische condities (**Hoofstuk 5**).
- waren we in staat om naar nieuwe microbiële metabolismes met betrekking tot N_2O te zoeken (**Hoofdstuk 6**).

We hebben de chemostaat verrijking methodologie aangevuld met continue cultivatie van een pure cultuur (*Pseudomonas stutzeri*, **Hoofdstuk 2**) en met korte termijn batch testen met de verrijkingsculturen (**Hoofstuk 2** en **4**). In **Hoofdstuk 6** hebben we ons gericht op de kinetiek van NO_x en N_2O, met korte termijn batch testen, *direct* toegepast op een natuurlijke populatie uit actief slib van een waterzuivering. In het laatste hoofdstuk van dit proefschrift presenteren we inzichten in de modulariteit van denitrificerende populaties, door het toepassen van de chemostaat verrijking methodologie op NO_3^- reducerende populaties.

We hopen dat het onderzoek in dit proefschrift zal bijdragen aan het ontwikkelen van strategieën voor N_2O mitigatie – niet alleen in afvalwaterzuiveringen, maar in beheerde ecosystemen in het algemeen.


N_2O

1

Introduction

A. N_2O - a greenhouse gas in the nitrogen cycle

- *The Nitrogen cycle*

Nitrogen (N) is an essential element for life on Earth. All living beings contain a significant proportion of N in their cells in the form of nucleic acids and proteins (see for example, the general molecular formula for bacterial biomass: $CH_{1.8}O_{0.6}\mathbf{N_{0.2}}$; Roels, 1980). In general, N availability is one of the factors limiting biomass growth in ecosystems: even though N_2 is abundant in the atmosphere (making up 79% of the Earth's atmosphere), organisms can only assimilate *reactive forms* of N, i.e. NH_4^+, NO_3^-. Thus, before the invention of synthetic fertilizers, biomass growth in terrestrial and marine ecosystems was limited by the rate of *nitrogen fixation* by bacteria harboring a *nitrogenase* gene.

Because N can exist in 8 different redox states (ranging from **+V**, NO_3^-, to **–III**, NH_3), N compounds, apart from their assimilatory role, play an important role as an electron source or sink in the *dissimilatory* metabolism of different types of microorganisms –**Figure 1.1**. More oxidized states of N can serve as electron acceptors for microbial respiration (in a process generally termed *denitrification*) while more reduced forms can be used as electron donors when other sources are scarce (see *nitrification*). Via these redox reactions, microbes are the primary mediators of Earth's Nitrogen geochemical cycle.

- *N_2O is to fertilizer what CO_2 is to fossil fuel*

Nitrous oxide (N_2O; +I) is part of the N cycle, a product of NO reduction (or hydroxylamine oxidation) and a substrate for the nitrous oxide reductase enzyme (generally abbreviated NOS). The global N_2O *inventory* (2000 Tg according to estimations by Kuypers *et al.*, 2018) is relatively small compared to those of N_2, NO_3^-, and organic N (**Figure 1.1-A**). However, even in relatively small quantities, N_2O can have an important environmental impact being (i) a very potent greenhouse gas (GHG), with a *global warming potential* roughly 300 times greater than that of CO_2, and currently (ii) the major threat to ozone depletion in the atmosphere (Ravishankara *et al.*, 2009)

Historical records show that N_2O has been naturally present in the atmosphere in ppb concentrations for as far as we can measure (**Figure 1.2 - A)**. However, the dramatic increase in the past decades - corresponding to the intensive use of synthetic nitrogen-based fertilizers in agriculture - are a cause for alarm. The industrial-scale (and energy-intensive) conversion of inert N_2 gas into NH_3 (i.e the *Haber Bosch process*) has more than doubled the annual terrestrial input of

reactive nitrogen to the global nitrogen cycle (**Figure 1.1 – B**). As a result - apart from other serious ecological consequences like eutrophication and rain - the N_2O concentration in the atmosphere is increasing exponentially.

- *The Nitrous Oxide Research Alliance*

A "forgotten greenhouse gas" until recent years (Thomson *et al.*, 2012) due to its relatively low atmospheric concentration compared to CO_2 (ppb vs. ppm) – N_2O is now a recognized global concern. The Intergovernmental Panel on Climate Change (IPCC) reports that N_2O accounted for roughly 8% of global anthropogenic GHG emissions as of 2010, a number predicted to increase with the global population's exponential growth. The EU-funded Nitrous Oxide Research Alliance (NORA – nora.nmbu.no) was one of the arising initiatives to understand the complex and interrelated microbial processes involved in N_2O emissions on a biochemical, physiological and ecosystem level, the ultimate goal of which was to develop effective climate change mitigation options.

Within the NORA consortium TU Delft focused on N_2O conversions in wastewater treatment (WWT) processes in particular. Of overall anthropogenic N_2O emissions, those traceable to the global "water and wastewater" sector account for a relatively small fraction compared to the "agriculture" sector (roughly 3% vs 75 % respectively according to IPCC 2010, **Figure 1.2 – B**). Nevertheless, N_2O is a major concern in the development and sustainable implementation of new WWT technologies, e.g. Nereda® and Nitritation-Anammox processes and attention to N_2O in the more conventional full-scale nitrification-denitrification processes is an essential step towards achieving carbon neutral WWTP given that measures implemented to reduce CO_2 emissions, such as reducing aeration, can paradoxically result in a higher overall *carbon footprint* as a consequence of increased levels of N_2O (Kampschreur *et al.*, 2009).

We generally approached our research from the perspective of *conventional activated sludge-based WWT systems* given that is is, by far, the most widespread form of biological nitrogen removal to treat municipal wastewater: e.g. activated sludge was used (i) as the seed community for lab-scale chemostat enrichments (**Ch 2-5**), and (ii) for the study of maximum NO_x reduction rates in a full-scale system (**Ch 6**). Nevertheless, wastewater treatment is an engineered form of processes that occur in nature (albeit on a shorter time scale), and the research presented in this thesis addresses fundamental concepts applicable to N-cycling systems in general, including other WWT technologies as well as soils (see **BOX 1.1**).

BOX 1.1: N transformation processes in WWT *vs*. soils

Removal of nitrogen entering a WWTP - primarily in the form of NH_4^+- is generally achieved via a combination of *nitrification* (oxic) and *denitrification* (anoxic) by microorganisms growing in Activated Sludge flocs (see **Figure 1.3** for N removal variations/alternatives including *partial nitritation-anammox*).

While beneficial for WWT, *nitrification* and *denitrification* are detrimental processes in agriculture: *nitrification-denitrification* in soils results in nutrient loss from fields and eutrophication of aquatic ecosystems – in the form of leaching of NO_x.

The nitrification and denitrification processes are fundamentally the same in WWTP and soils, yet some general differences to be considered, regarding N_2O emissions, concern:

- The microbial communities:
  - Ammonia oxidizing archaea (AOA) are abundant in soils but rare in WWT (where ammonia oxidizing bacteria – AOB – predominate; Kampschreur *et al.*, 2009). This is potentially an important difference - as a recent study suggests that AOA have lower N_2O accumulation than AOB during ammonium oxidation (Hink *et al.*, 2016).
  - Soil is far more heterogeneous in conditions then a wastewater treatment plant giving space to a much more diverse community.

- Growth rates and limiting nutrients:
  - Soils are intrinsically oligotrophic systems, and WWTP eutrophic.
  - Growth rates in WWT are higher than in soils. Any given organism in a WWTP will likely undergo more rapid and frequent changes in its surrounding environment than organisms in soil.

Figure 1.1 - next page - (**A)** Global nitrogen inventory according to Kuypers *et al.* (2018). NH_3 is abundant in rocks and sediments, but only becomes available upon erosion and therefore its contribution to the N cycle is negligible in an anthropocentric time scale. (**B**) Microbial redox reactions mediating N cycling between inventories. Rather than forming one balanced N cycle, these processes have very different fluxes: those relevant to this thesis are shown in green – for terrestrial fluxes – and blue – for marine fluxes in Tg/year (again, based on Kuypers *et al.*, 2018). Industrial nitrogen fixation and its corresponding flux is shown in red and labeled HB for Haber-Bosch.

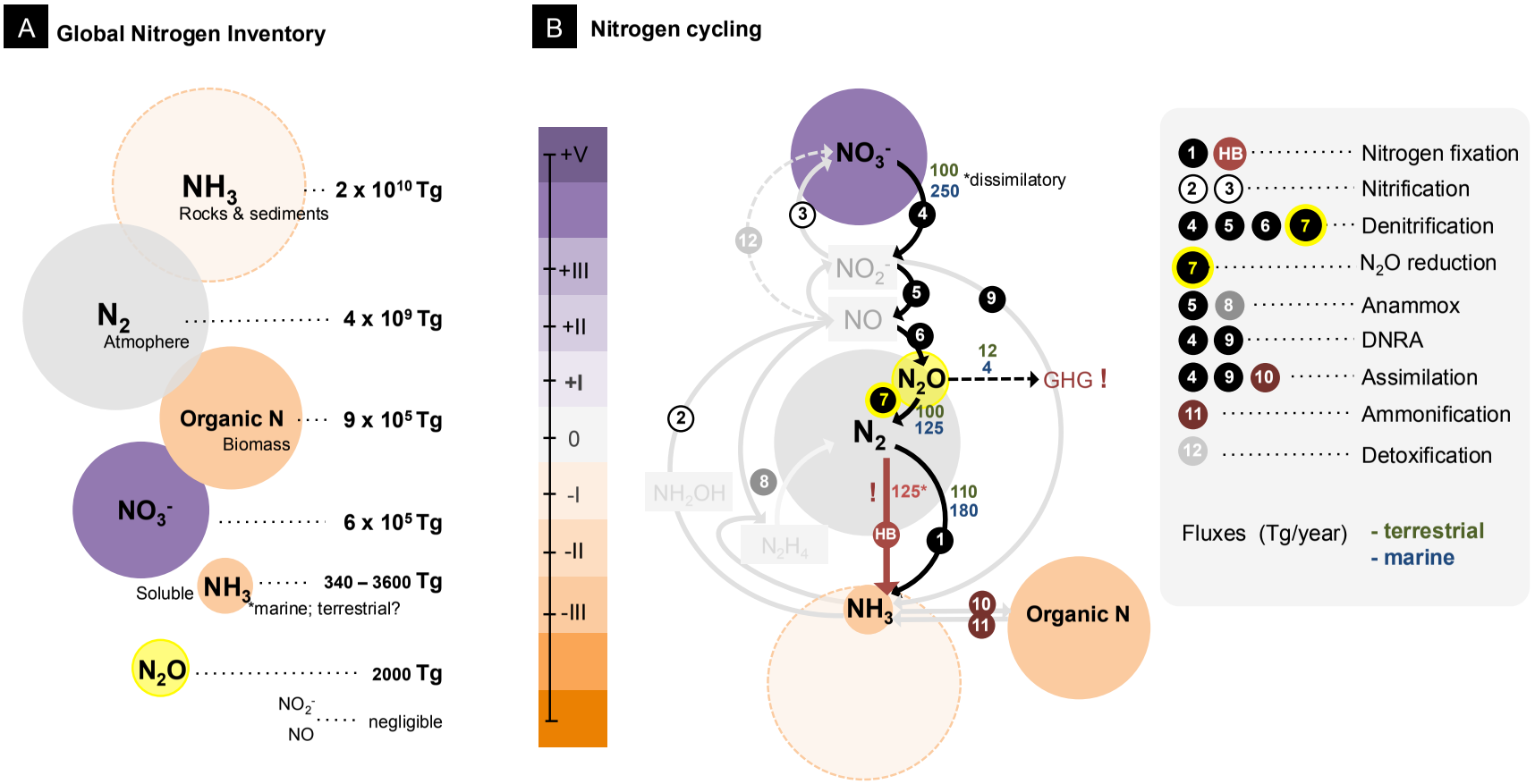
A
Global Nitrogen Inventory
NH3
Rocks & sediments
2 x 10^10 Tg
N2
Atmophere
4 x 10^9 Tg
Organic N
Biomass
9 x 10^5 Tg
NO3-
6 x 10^5 Tg
Soluble NH3
340 – 3600 Tg
*marine; terrestrial?
N2O
2000 Tg
NO2-
NO
negligible
B
Nitrogen cycling
+V
+III
+II
+I
0
-I
-II
-III
NO3-
100
250
*dissimilatory
NO2-
NO
N2O
GHG !
12
4
100
125
N2
NH2OH
N2H4
!
125*
110
180
HB
NH3
Organic N
1 HB Nitrogen fixation
2 3 Nitrification
4 5 6 7 Denitrification
7 N2O reduction
5 8 Anammox
4 9 DNRA
4 9 10 Assimilation
11 Ammonification
12 Detoxification
Fluxes (Tg/year)
- terrestrial
- marine

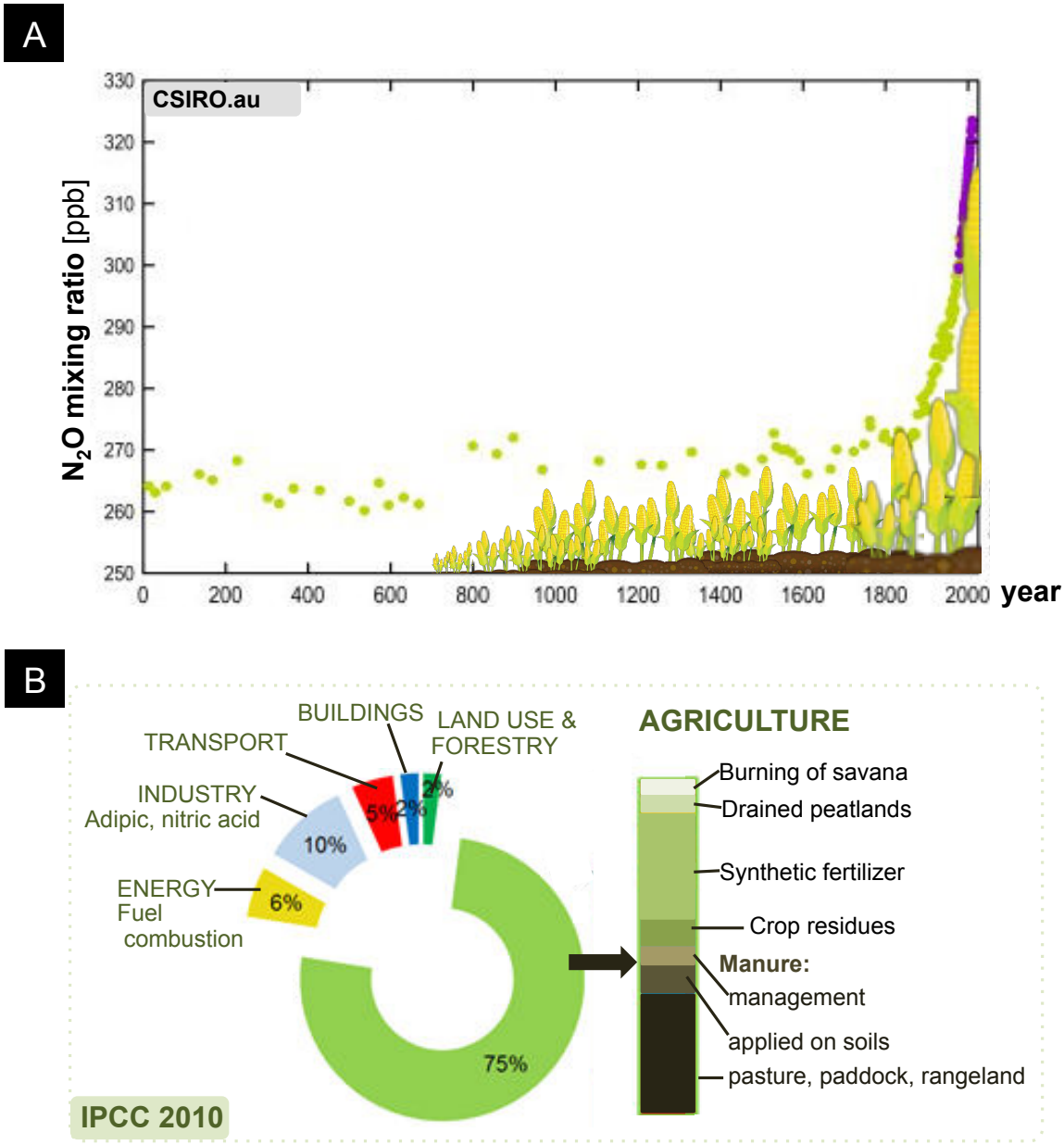

Figure 1.2 (**A**) Historical record of N_2O concentration in the atmosphere. **Source**: CSIRO Marine and Atmospheric Research; Australian Bureau of Meteorology (Cape Grim Baseline Air Pollution Station) – capegrim.csiro.au. The purple data points were obtained *in situ* at the Cape Grim Baseline Air Pollution Station (Tasmania, Australia). The green data points correspond to air samples collected in Antartic ice at Law dome. (**B**) Relative anthropogenic N_2O emissions traceable to different sectors. **Source**: From working group III contribution to the IPCC Fifth assessment report (2010).

B. N_2O emissions during wastewater treatment

- *Sources of N_2O during biological nitrogen removal*

N_2O can be a major contributor to the carbon footprint of a wastewater treatment plant, sometimes surpassing CO_2 and CH_4, as shown from full-scale GHG emission studies (Daelman *et al.*, 2013; Ahn *et al.*, 2010). In the process designed to remove NH_4^+ from wastewater, N_2O can accumulate as a byproduct of nitrification by ammonia oxidizing bacteria (AOBs) - via (1) hydroxylamine oxidation or (2) nitrifier denitrification - and/or as a result of (3) incomplete denitrification by - primarily heterotrophic - denitrifying bacteria (**Figure 1.3**; Schreiber *et al.*, 2012; Kampschreur *et al.*, 2009).

Resolving the relative contribution of nitrification and denitrification to the overall N_2O emissions of a WWTP is not a straightforward task. The fact that most of the emission occurs in aerated nitrification zones (Ahn *et al.*, 2010) could be taken to suggest that nitrification is the primary source of N_2O. But the N_2O stripped off by aeration could also originate from (i) non-aerated anoxic zones or (ii) denitrification in anoxic - and possibly anoxic - microsites within the aerated nitrification zones. Dissolved O_2 concentrations in the aerated *mixed liquor* of a WWTP are typically low and diffusion limitation may result in even lower local concentrations within the activated sludge flocs. In addition to the N_2O produced during nitrification and denitrification, N_2O can be a product of abiotic reactions between intermediates of these processes, e.g. between hydroxylamine and NO_2^- (Soler-Jofra *et al.*, 2016) or NO_2^- and reduced iron species (Kampschreur *et al.*, 2011). Unfortunately, natural isotope fractionation analyses (Wunderlin *et al.*, 2013) or correlating a wide range of process variables to emissions in a long term N_2O-monitoring campaign (Daelman *et al.*, 2015; Vasilaki *et al.*, 2018) have not been conclusive in correlating emissions to the specific culprit. Furthermore the data collected in the long term monitoring campaign of Daelman *et al.*, 2015 showed a surprisingly high daily and seasonal variability in overall N_2O emissions, which did not show the same patter the subsequent year (personal communication).

The uncertainty surrounding the sources of N_2O in WWT makes it difficult to develop effective GHG mitigation strategies: e.g. measures taken to reduce N_2O production due to nitrifier denitrification, like increasing aeration, could result in higher N_2O production as a result of hydroxylamine oxidation or inhibition of N_2O reduction in denitrifiers (see **Figure 1.3**).

- *Tapping into the N_2O sink capacity as a mitigation strategy*

The flip side of N_2O is that it is a very potent electron acceptor/oxidant (**Figure 1.4, Box 1.2**). Given the complexity of N_2O producing processes, favoring N_2O reduction to innocuous N_2 gas may be the most straightforward strategy to reduce emissions. For this reason, we focused primarily on the *consumption* of N_2O catalyzed by NOS (rather than on the *production* of N_2O, which is more often the focus, e.g. Perez-Garcia *et al.*, 2017; Lu and Chandran, 2010; Wunderlin *et al.*, 2012; Ribera-Guardia *et al.*, 2014). Because N_2O reduction is associated to denitrification – a process which is both a source a sink of N_2O -, we considered the denitrification pathway in more detail than the other N transformations.

BOX 1.2:

Seeing the glass half full: The CANDO process

The same oxidative power that makes N_2O a nuisance also makes it a valuable resource. With this frame of mind a new N removal process has been proposed: CANDO - Coupled Aerobic-anoxic Nitrous Decomposition Operation (Scherson *et al.*, 2013, 2014; Gao *et al.*, 2017). The CANDO process involves three steps: (i) partial nitrification of NH_4^+ to NO_2^-; (ii) partial anoxic reduction of NO_2^- to N_2O; and (3) N_2O conversion to N_2 with energy recovery by either catalytic decomposition to N_2 and O_2 or use of N_2O to oxidize biogas CH_4.

Figure 1.3 - next page - (**A**) Sources of N_2O emissions during N removal via nitrification-denitrification and factors associated to increased emissions based on Kampschreur *et al.*, (2009). (1) hydroxilamine oxidation, (2) “nitrifier denitrification”, (3) incomplete denitrification. Generally, most of the N_2O stripping occurs in the oxic (i.e. aerated) stage. (**B**) Most common reactor configurations for N removal. Biomass is most often in the form of Activated sludge flocs, but can also grow as a biofilm on carriers (e.g. ceramic particles – Biofor®) or even granules (Nereda®). (i) A+B stage (common COD sources added: glycerol, ethanol, acetate), (ii) MLE (modified Ludzack-Ettinger), (iii) oxidation ditch, and (iv) sequence batch reactor (SBR) with aerobic granules. (**C**) N removal via partial nitritation-anammox: N_2O can be produced during nitritation, but also if denitrification occurs in the anoxic space. Despite its advantages over nitrification-denitrification (e.g. less O_2 consumption & sludge production, no need for addition of COD), currently it has only been implemented in the full-scale for high strength wastewaters at relatively high temperatures.

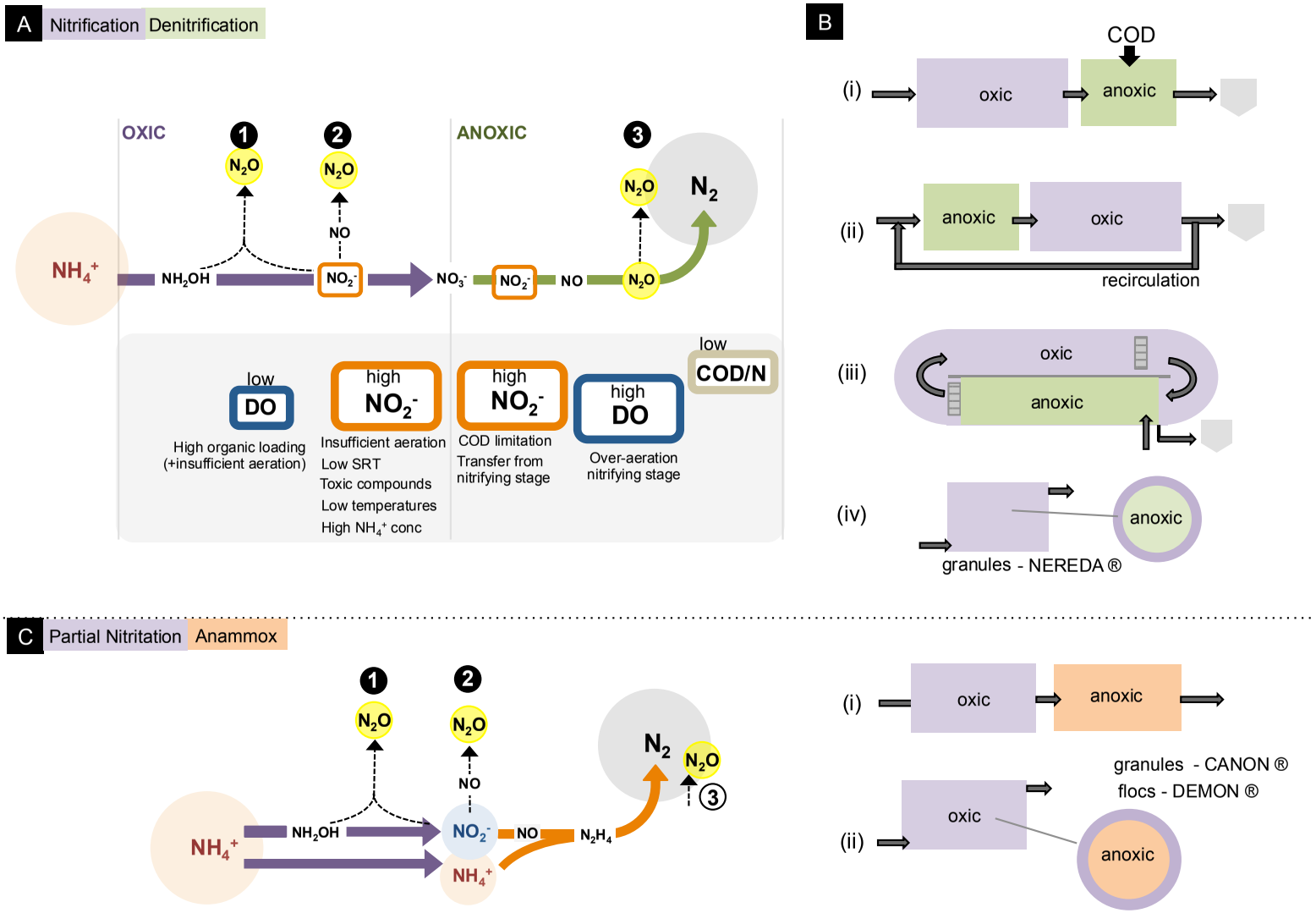
A Nitrification Denitrification
OXIC
ANOXIC
1
2
3
N_2O
NO
N_2
NH_4^+
NH_2OH
NO_2^-
NO_3^-
low
DO
high
NO_2^-
high
NO_2^-
high
DO
low
COD/N
High organic loading
(+insufficient aeration)
Insufficient aeration
Low SRT
Toxic compounds
Low temperatures
High NH_4^+ conc
COD limitation
Transfer from
nitrifying stage
Over-aeration
nitrifying stage
B
COD
(i)
oxic
anoxic
(ii)
anoxic
oxic
recirculation
(iii)
oxic
anoxic
(iv)
anoxic
granules - NEREDA ®
C Partial Nitritation Anammox
N_2H_4
(i)
oxic
anoxic
granules - CANON ®
flocs - DEMON ®
(ii)
oxic
anoxic

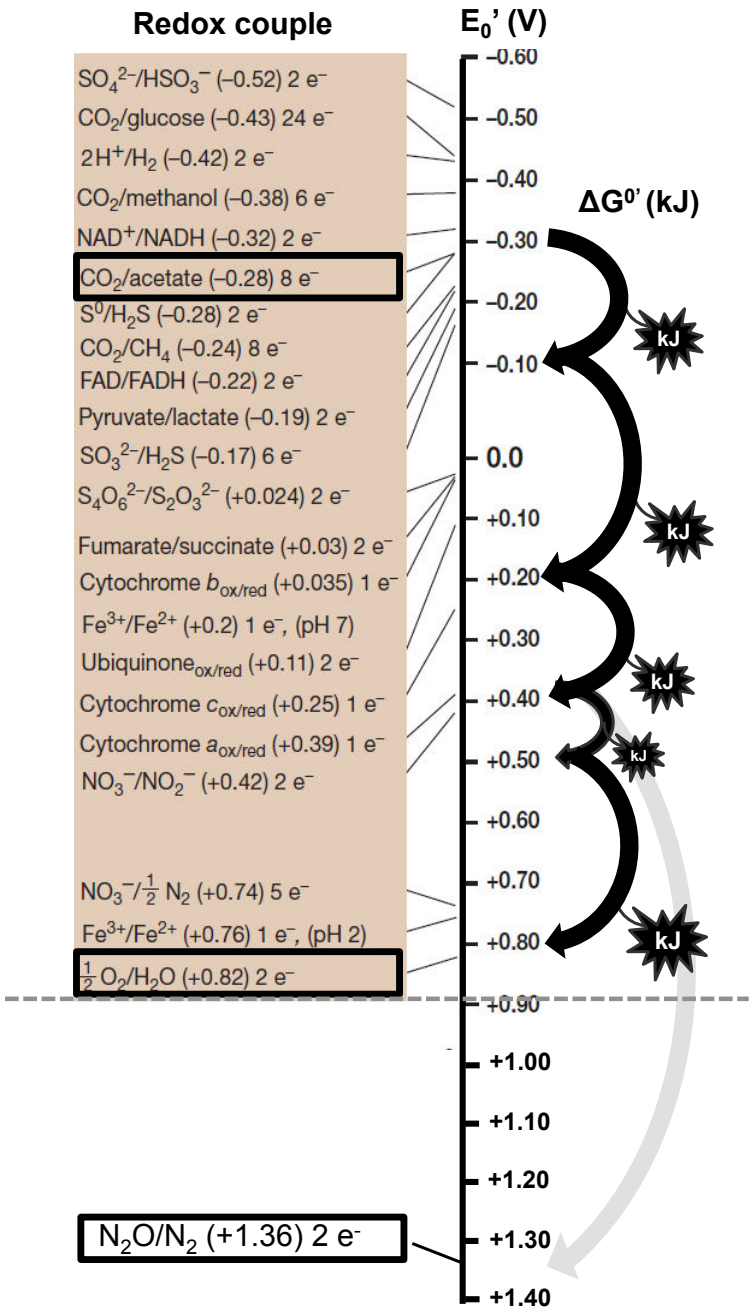

Figure 1.4 Redox tower as presented in textbooks (notably Brock's Biology of Microorganisms) – depicted with O_2/H_2O at the bottom – modified to include the N_2O/N_2 redox couple (+1.36 V). The free energy liberated in each redox step of the ETC with acetate and O_2 as electron donor and acceptor (respectively) is represented by the black arrows. In theory there is much more energy available using N_2O as an electron donor.

C. Denitrification as an N_2O sink & source

- *An inherently modular (and communal?) process*

The term “denitrification” was coined at the end of the 19th century to describe the - at the time - unexplained phenomenon by which soluble nitrogen species (i.e. NO_x) were seemingly lost in a “fermenting” microbial community. To this day, this has been the term kept to refer to the microbial process, on a cell or ecosystem level, in which NO_3^- is used as an electron acceptor for respiration, and is converted to inert N_2 gas via the intermediates NO_2^-, NO and N_2O (Zumft, 1997). Even though it is typically referred to as a whole and many organisms possess the whole pathway, denitrification is actually inherently modular, catalyzed by four independent and structurally distinct reductases, encoded by four separate gene operons which are subject to different (and often independent) regulatory mechanisms (**Figure 1.5; Table 1.1**).

Denitrification genes are organized in “superclusters” in some bacteria, e.g *Pseudomonas stutzeri* – historically one of the most studied denitrifiying microorganism together with *Paracoccus denitrificans* (Zumft, 1997). However, with increasing knowledge of microbial diversity it has become clear that it is common for microorganisms to have some, but not all, of the genes (or modules) encoding denitrifying reductases (i.e. any form of *nar/nap*, *nir*, *nor*, and *nos*; Graf *et al.*, 2014; Lycus *et al.*, 2017; Shapleigh, 2013; Roco *et al.*, 2016, **Figure 1.6**). There also appears to be no universal regulatory network for denitrification – rather it varies from one microorganism to another, yielding different “regulatory phenotypes” even in closely related species (Liu *et al.*, 2013). **Figure 1.5** shows the variety and complexity of positive and negative regulation mechanisms, in response to O_2 concentration, NO_3^-/NO_2^-, NO and redox conditions, as presented in Torres *et al.*, 2016.

In the context of N-cycling ecosystems, this modularity implies that denitrification can be a result of (i) microbial species performing full denitrification or (ii) different microbial species specializing in specific steps (i.e. NO_3^- reduction to NO_2^-, NO_2^- to NO, NO to N_2O, and N_2O to N_2) and working in a sort of “denitrifying tandem/communal symbiosis”, the product of one being the substrate of another. Denitrifying “tandems” could be composed of *truncated denitrifiers* but also, in theory, of cells with the genetic potential to perform full denitrification, which would gain a competitive advantage in specialization: e.g. Lilja and Johnson (2016) suggest that a segregation of the denitrification steps in different microbial cells (even within one same species)

could be advantageous to reduce the accumulation of the potentially toxic intermediates NO and NO_2^- (see also Cooper and West, 2018).

- *N_2O accumulation due to pathway imbalances: on cell or community level?*

As mentioned above, it is not uncommon for microorganisms to harbor in their genome some, but not all, of the genes encoding the reductases that catalyze the four steps in the denitrification pathway (or for that matter to harbor reductases with a seemingly redundant function - e.g. *nirS* and *nirK*; **Figure 1.6**). Most interesting, from the N_2O emission point of view, are denitrifiers lacking the *nosZ* gene encoding NOS (e.g. most/all Actinobacteria and the fungal phylum Ascomycota), and organisms *solely* equipped with *nosZ,* coined non-denitrifying N_2O reducers (Sanford *et al.*, 2012; Hallin *et al.*, 2018). As a result of this genotypic diversity, microbial community composition can be an important factor determining whether an ecosystem is more likely to act as a sink or a source of N_2O (the opposite sides of the spectrum being (1) a community composed solely of truncated denitrifiers lacking NOS, inevitably an N_2O source, versus (2) a strong N_2O sink community abundant in non-denitrifying N_2O reducers.

Nevertheless, N_2O accumulation can occur, even in *nosZ*-rich communities, if NOS *activity* is low compared to other denitrifying reductases. N_2O accumulation in complex communities, but also fully denitrifying pure cultures, has been associated to e.g. the presence of O_2, the accumulation of NO_2^-, dynamic environmental conditions, and storage polymer metabolism (Law *et al.*, 2012; Wunderlin *et al.*, 2012; Foley *et al.*, 2010; Kampschreur *et al.*, 2008 - see **Figure 1.3 - B** -; Lu and Chandran, 2010; Otte *et al.*, 1996). Transcriptional and post transcriptional regulation dependent on environmental conditions (Liu *et al.*, 2013; Lycus *et al.*, 2017) as well as kinetic phenomena (Betlach and Tiedje, 1981) likely play a role in N_2O accumulation in cells equipped with NOS. There is abundant literature addressing “regulatory phenotypes” and the kinetics of denitrification (e.g. Bergaust *et al.*, 2011; Roco *et al.*, 2016), but, as mentioned before, there is no universal model, and it is still very difficult to predict when a denitrifying community or cell will accumulate N_2O.

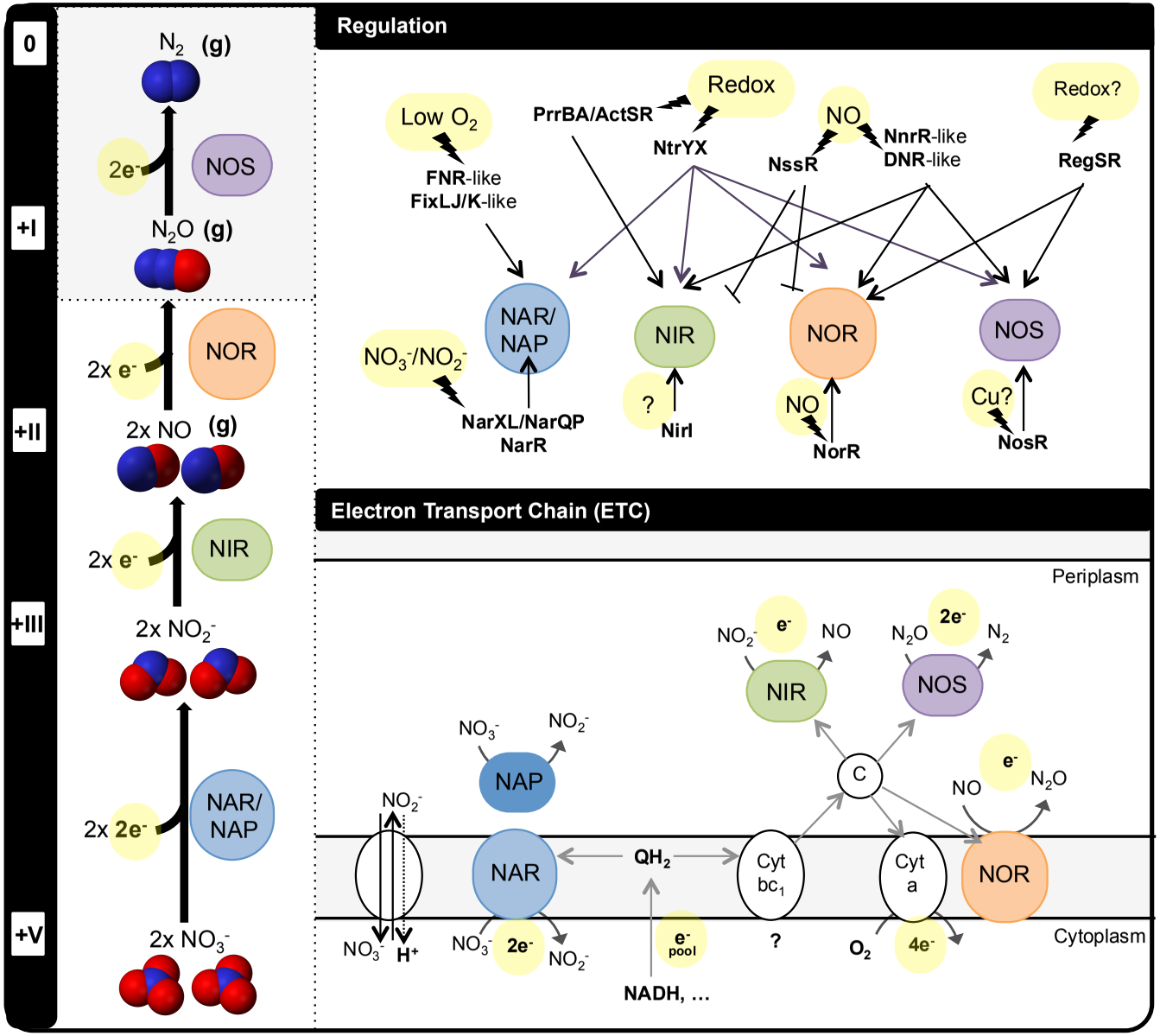
0
+I
+II
+III
+V
N2 (g)
2e-
NOS
N2O (g)
2x e-
NOR
2x NO (g)
2x e-
NIR
2x NO2-
2x 2e-
NAR/ NAP
2x NO3-
Regulation
Low O2
FNR-like
FixLJ/K-like
PrrBA/ActSR
Redox
NtrYX
NO
NssR
NnrR-like
DNR-like
Redox?
RegSR
NO3-/NO2-
NarXL/NarQP
NarR
NAR/ NAP
?
NirI
NIR
NO
NorR
NOR
Cu?
NosR
NOS
Electron Transport Chain (ETC)
Periplasm
Cytoplasm
NO2-
e-
NO
N2O
2e-
N2
NIR
NOS
NO3-
NO2-
NAP
C
NO2-
NO3-
H+
NAR
QH2
Cyt bc1
Cyt a
NOR
e-
NO
N2O
NO3-
2e-
NO2-
e- pool
?
O2
4e-
NADH, …

Figure 1.5 - previous page - The denitrification pathway: regulatory mechanisms adapted from (Torres *et al.*, 2016) and topography of the electron transport chain based on our knowledge of biochemistry in *Paracoccus denitrificans* (see van Spanning and Richardson, 2007). Note that in the nosZII-harboring non-denitrying *Wollinella succinogenes*, there are differences in regulation and possibly electron donor protein to NOS (Kern and Simon, 2016; Simon and Klotz, 2013). This is described further in section 4.

Table 1.1. Characteristics of reductases involved in denitrification.

Enzyme	Structural gene	Location	Characteristics
NAR/NAP NO_3^- reductase	*narG*	Cytoplasmic membrane	**Low affinity, high activity** Active site in cytoplasm → NO_3^- transport required H^+ pumping
	napA	Periplasm*	**High affinity, low activity** Expressed in presence of O_2
NIR NO_2^- reductase	*nirS*	Periplasm*	**Fe**- dependent Complex enzyme (many genes involved)
	nirK	Periplasm*	**Cu**-dependent One gene; one enzyme
NOR NO reductase	*qnorB* *cnorB*	Cytoplasmic membrane	Different types Also involved in NO detox (?)
NOS N_2O reductase	*nosZI* *nosZII*	Periplasm*	**Cu**-dependent Differences in **affinity/activity** not known

In *Bacillus azotoformans* periplasmic proteins are membrane-bound (Suharti and de Vries, 2005), and this may be the general case for G(+) microorganisms in general (since they lack a periplasmic membrane).

.

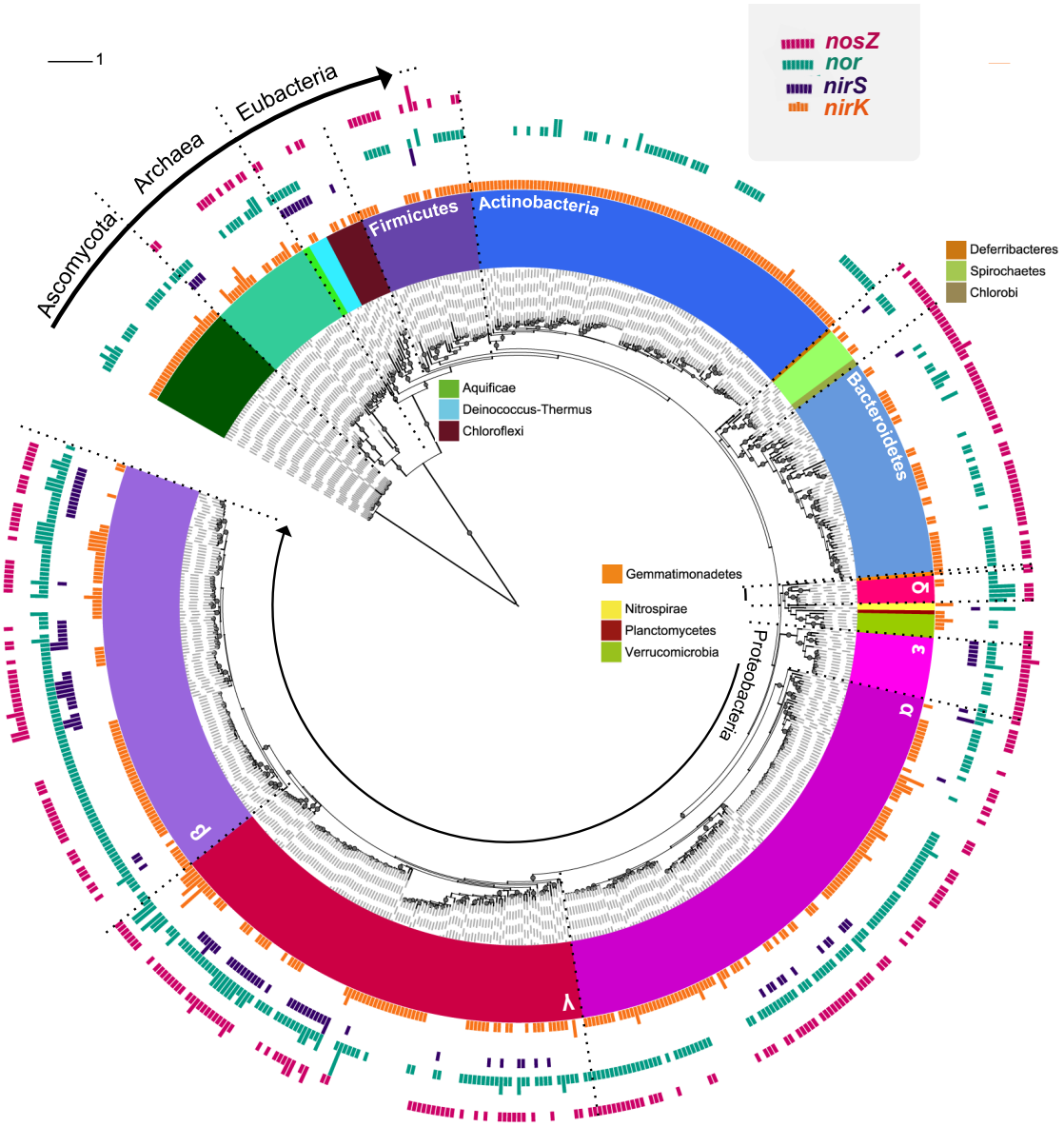

Figure 1.6 Phylogenetic tree of the 16S/18S rRNA gene in sequenced genomes harboring the genes associated to denitrification *nirK*, *nirS*, *nor* and *nosZ,* indicating which of these genes are present in each genome (and their copy number). Adapted from (Graf *et al.*, 2014)

D. A spotlight on N_2O reducing organisms

Due to the fact that N_2O reduction by microbial NOS is the only reaction known to transform N_2O under physiological conditions, bacteria and archaea harboring the nosZ-type genes - in particular those classified as non-denitrifiers - are receiving increasing attention in the search to combat N_2O emissions (Hallin et al., 2018).

- *N_2OR: phylogeny & function*

Like other denitrifying reductase genes, *nosZ* genes are widespread in terms of phylogeny and habitats: present in all subclasses of proteobacteria as well as several halophilic and thermophilic archaea (yet, interestingly, missing in the fungal Ascomycota phylum; **Figure 1.6; 1.7 – A**; Jones *et al.*, 2014; Zumft and Kroneck, 2006).

nosZ encodes a soluble periplasmic *metalloenzyme* made up of 2 subunits, each equipped with 2 multinuclear Cu centers which are active sites for electron transport. The assembly and maturation of NosZ is a complex process and requires accessory genes: including genes for Cu insertion and export to the periplasm. These genes (*nosF*, *nosL*, *nosY, …*) as well as genes involved in regulation (possibly *nosR*) and/or electron donation (possibly *nosR*, or *nosB*) compose the Nos *operon* (**Figure 1.7 – B)**.

As far as we know, the primary function of microbial NOS is the conservation of energy for growth: N_2O respiration generates a proton motive force (pmf) across the bacterial ETC and can fully sustain the energetic needs of a cell (see **Figure 1.5** – note that NOS cannot contribute directly to protons translocation/charge separation, as it is not a transmembrane protein). The respiratory role of NOS is evident from pure culture studies using N_2O as the sole electron acceptor (see **Figure 1.8**) and the basis for the enrichments presented in **Ch 2 - 5**.

It has also been proposed that NOS may serve as an electron sink/spill – not contributing to energy conservation but to redox homeostasis - e.g. in the ubiquitous soil bacteria of the phylum Gemmatimonadetes (Zumft, 1997; Park *et al.*, 2017) - or as a detoxification mechanism – presuming N_2O has a toxic effect on bacteria with Vit B12 dependent pathways (of relevance **Ch 2 and 5;** Sullivan *et al.*, 2013)**.**

- *Two types of N_2OR: nosZI and nosZII*

The *nosZ* gene can be divided into two major phylogenetic clades denominated clade I and II (*nosZ*I and *nosZ*II in short; **Figure 1.7 – A**; Sanford *et al.*, 2012;

Jones *et al.*, 2014) which, as far as we known, are mutually exclusive (i.e. no sequenced genome harbors both clades). Differences between clade I and clade II apparent on the genome level include (1) the presence of a cytochrome domain fused to the C-terminal of clade II-type NOS, potentially involved in electron transport to the active site, and (2) *sec* vs*. tat protein export* sequence for the translocation of NOS to the periplasm. In addition to this, some accessory genes forming part of the *nos* operon are exclusively associated to *nosZ*II and others to *nosZ*I (see **Figure 1.7-B**, Sanford *et al.*, 2012; Hallin *et al.*, 2018). Furthermore, *nosZ*I and II differ in the co-occurrence with other denitrification genes: *nosZ* clade II is more often associated to non-denitrifiers while *nosZ* clade I is more often associated to *nir* genes (and *nirS* in particular, Graf *et al.*, 2014).

Whether the differences on the genome level translate into differences in the *ecophysiology* of N_2O reducers harboring clade I or clade II is not yet fully understood. A differentiation in putative electron transport accessory proteins (e.g. NosR and NosB) could be indicative of differences in the electron transport chain that could result in (1) additional proton extrusion to the periplasm per electron accepted, and thus a greater energy conservation, as proposed by Simon *et al.* (2004), or (2) a lower affinity constant (K_S) of NOS for N_2O. Niche differentiation of clade I and II has been reported in natural ecosystems, like the rhizosphere, soils, and sediments (Graf *et al.*, 2016; Wittorf *et al.*, 2016; Juhanson *et al.*, 2017; Domeignoz-Horta *et al.*, 2017). Of particular interest from the N_2O mitigation point of view is the fact that a high abundance and diversity of *nosZ* clade II, in particular, is linked to an increased N_2O reduction sink capacity in soils, as well as lower *in situ* N_2O emissions (Jones *et al.*, 2014; Domeignoz-Horta *et al.*, 2017). To date our knowledge of clade II-type-N_2O reducer biochemistry is limited almost exclusively to the fermentative host-associated epsilon-proteobacteria *Wollinella succinogenes* (see Kern and Simon, 2016; Simon *et al.*, 2004) and a mechanistic explanation backing up these observations is lacking.

Recently, a study comparing the growth kinetics and yields of N_2O reducing bacterial species with *nosZ*I (of the genus *Pseudomonas* and *Shewanella*) and *nosZ*II (*Dechloromonas* and *Anaeromyxobacter*), reported the latter to have: (1) a generally lower affinity constant (K_s) for N_2O, which in theory would confer *nosZ* clade II N_2O reducers a selective advantage during competition for limiting amounts of N_2O and (2) up to 1.5 times higher biomass yields per mole of N_2O, implying a greater efficiency of energy conservation in the *nosZ* clade II-associated ETC. Such differences in affinity and yields could explain niche

partitioning of both clades and the lower *in situ* N_2O emissions in clade II-enriched soils. However, conclusive statements appearing in literature based on these results are yet to be avoided given the limited number of microorganisms in the study (versus the broad taxonomic diversity of N_2O reducers detected in the environment e.g. Jones *et al.*, 2014; Wittorf *et al.*, 2016), the apparent continuum (more than a dichotomy) of K_s values obtained in the study, and, lastly, the limitations of batch experiments for such physiological studies (Kuenen 2015). We explored this further in **Ch 2 and 3**.

Figure 1.7 - next page - (**A**) *nosZ* gene phylogeny adapted from *J*ones *et al.* (2013) and (**B**) accessory genes in the *nos* operon common to one or both clades based on Hallin *et al.*, (2018).

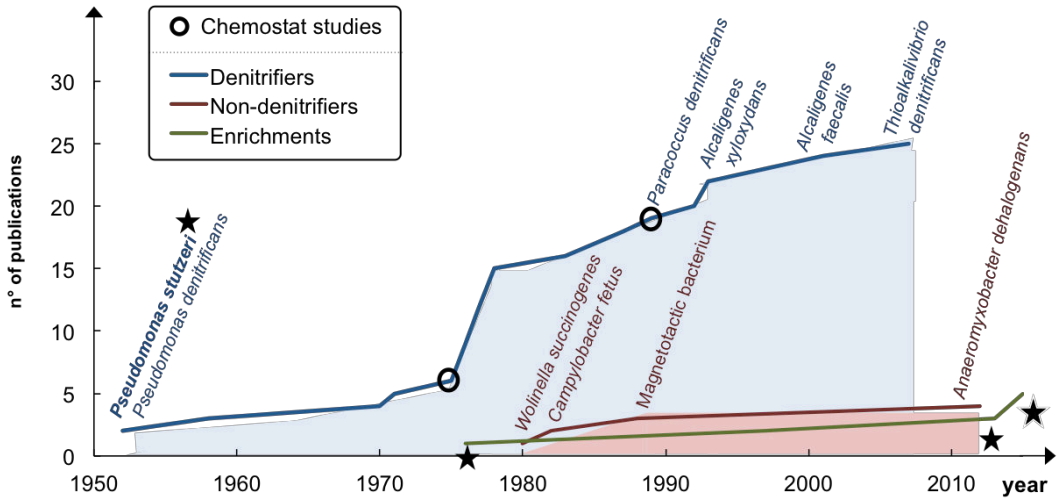

Figure 1.8: Cumulative number of scientific publications found using N_2O as sole electron acceptor for microbial growth in the lab.

A **Phylogenetic tree of *nosZ* sequences found in complete genomes** - from Jones *et al*. 2013

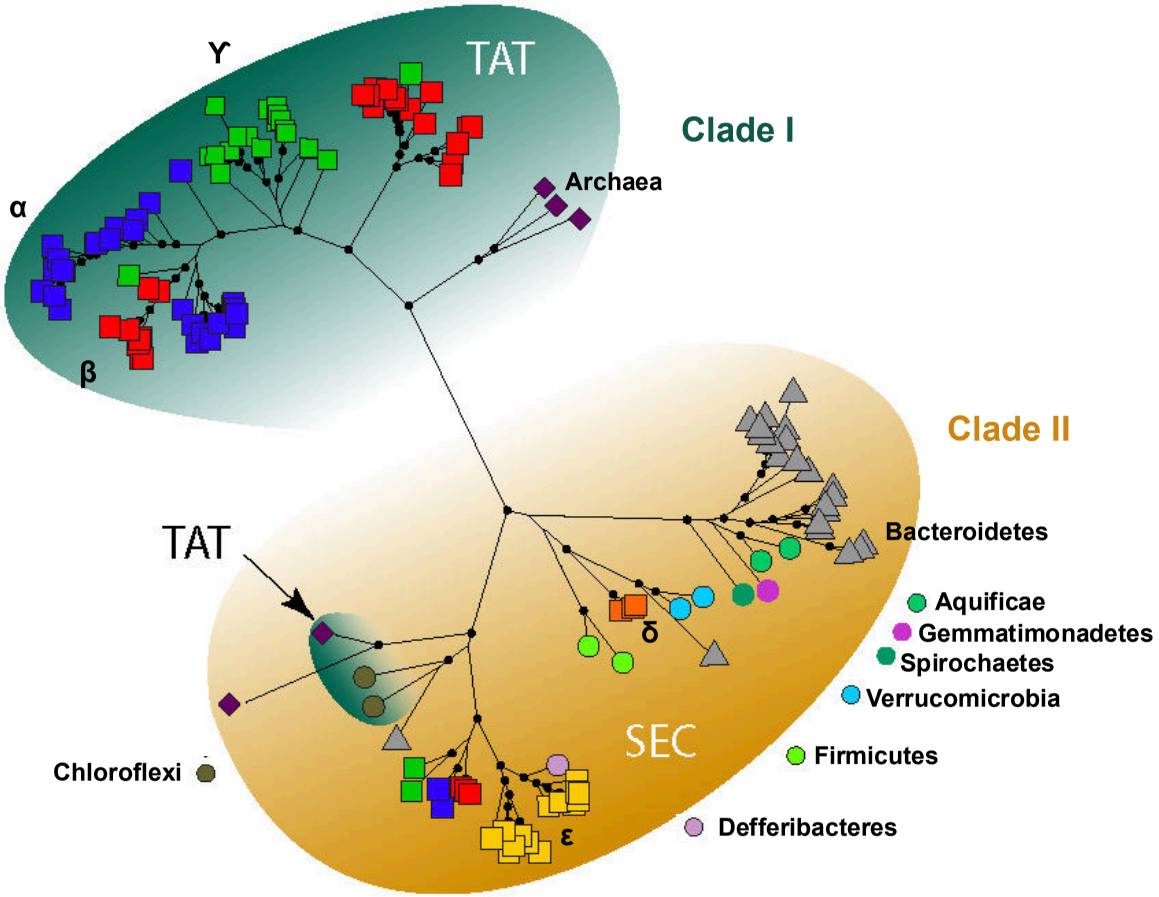

B **Accessory genes in nos operon**

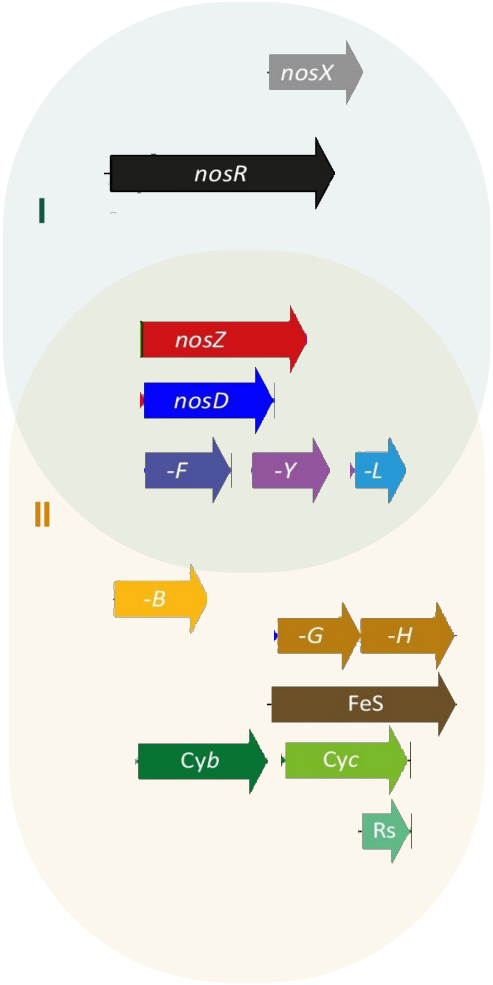

E. To breathe or not to breathe N_2O

- *Branched – not linear - Electron Transport Chains: electron acceptor mixotrophies*

Denitrification is usually presented as a sequential process, the product of one reductase being the substrate of the next (NO_3^-→NO_2^-→NO→N_2O→N_2). Nevertheless, all four denitrifying reductases constitute independent modules which accept electrons - in parallel - not sequentially – from a common electron pool, provided the presence of the corresponding electron acceptor (NO_3^-, NO_2^-, NO, N_2O; as shown in **Figure 1.5,** Chen and Strous, 2013). From this point of view, the denitrification pathway allows cells to simultaneously use the intermediates and hence permits true *mixotrophy* of electron acceptors. Accumulation of NO_2^-, NO, and, most importantly from a greenhouse gas mitigation point of view, N_2O, can occur if, for whatever reason, there is a preferential flow of electrons to one type of reductase over another. In **Ch 6,** we compared electron flow rates to N_2O vs. NO_3^- in activated sludge samples from a full-scale WWTP.

Electron acceptor mixotrophy of O_2 and N_2O is also relevant from a greenhouse gas mitigation perspective, and we address this topic in **Ch 4** with an enrichment culture grown on N_2O. To our knowledge, all denitrifiers - and presumably non-denitrifying N_2O-reducers - are primarily aerobes and in model organisms, like *Paracoccus denitrificans,* denitrifying reductases and reductases involved in aerobic respiration share the core of the ETC and thus a common electron pool (Chen and Strous, 2013). It is often stated in literature that, when both O_2 and other NO_x are available, denitrifiers will respire O_2 preferentially over other NO_x (including N_2O) likely based on (i) the *diauxic* growth curves of pure culture model denitrifiers like *Paracoccus denitrificans* growing on NO_3^- and O_2 in batch mode (e.g Bergaust *et al.*, 2010), and (ii), particulary in the case of N_2O, the fact that the purified NOS enzyme is inhibited by O_2 *in vitro* (Zumft and Kroneck, 2006). However, there are numerous studies pointing towards the occurrence of *aerobic denitrification* (the simultaneous consumption of NO_x and O_2; see Chen and Strous, 2013 and references therein) in both lab cultures and ecosystems and recent studies suggest that the NOS reductase can maintain its activity in in the presence of O_2 *in vivo* (Qu *et al.*, 2015).

What we know about transcriptional regulation in model dentirifiers could partly explain why N_2O reduction may not occur in the presence of O_2, since

transcription of nosZ is induced by a low redox potential (see **Figure 1.5**, and possibly also by low O_2 concentrations via an FNR-like regulator, Bergaust *et al.*, 2012). However in a system like a WWTP where microorganisms are subjected to relatively rapid and dynamic changes of O_2 and NO_x concentrations multiple times per generation, a *short-term* and *rapidly reversible* regulation mechanism – e.g. allosteric inhibition of NOS by O_2 or simply electron flow via the path of less resistance, would probably be more important than transcriptional regulation. A clear mechanistic explanation explaining a preferential flow of electrons entering the ETC to O_2 over N_2O – if this is indeed the case - is lacking.

- *Biochemical vs. thermodynamic boundaries in the efficiency of N_2O respiration*

In lack of a better explanation, thermodynamics is often used to explain why cells prioritize aerobic respiration over denitrification, the O_2/H_2O redox couple being lower in the "redox tower" than NO_3^-/N_2 (van Spanning *et al.*, 2007). However, N_2O/N_2 is a stronger redox couple than O_2/H_2O for any given electron donor (**Figure 1.4**) and cells could, in theory, obtain higher growth yields by using N_2O rather than O_2 (or O_2 and N_2O simultaneously) as an electron acceptor. Still, there *is* evidence that cells obtain less energy for growth during respiration of N_2O compared to aerobic respiration - as reflected in biomass yields per electron-equivalents consumed. The biomass yields obtained with different NOx in the studies by Beun *et al.*, 2000; Koike and Hattori, 1975; Murnleitner *et al.*, 1997 fit well with what is known of ETC biochemistry in model denitrifying organisms (**Figure 1.5** and **Table 1.1**), suggesting that in certain cases biochemistry – and not thermodynamics – is what drives metabolic fluxes in nature. Nevertheless, the Anammox pathway, was predicted based on thermodynamic considerations before it was discovered (Broda, 1977) and in **Ch 5** we speculate about the existence of a more energy efficient N_2O reduction process (via e.g. nosZ of clade II or an unknown enzyme) than the one studied so far.

F. Experimental approach and structure of this thesis

- *Continuous enrichment cultures as a bridge between pure culture and ecosystem studies*

The *chemostat* was the main experimental tool of choice in this thesis. Chemostat cultivation ensures controlled and prolonged steady state conditions at a fixed (non-maximal) growth rate limited by the supply of (generally) one nutrient (=limiting nutrient). When working with enrichments/mixed microbial communities, chemostat cultures allow for competition experiments based on affinity for a limiting substrate– likely a selective pressure more significant in natural environments than the maximum growth rate (the selective advantage in a batch culture). We could also study the difference between having the electron donor (in this case, acetate) or the electron acceptor (N_2O, or NO_3^-) as the limiting growth factor.

Working with open mixed cultures has the added advantage of allowing the potential formation of denitrifying "tandems" – when using NO_x as an electron acceptor - as well as other potentially important microbial interactions (e.g. cross-feeding, inhibition, etc.) that may be relevant to conditions in natural ecosystems. Furthermore, it allows physiology studies of microorganisms, which may otherwise never be isolated in a pure culture.

We used continuous enrichment cultures for the study of:

- ⇨ N_2O reducing communities growing on N_2O as the sole electron acceptor for a large number of generations: the effect of N_2O versus acetate limitation; and the potential dichotomy in N_2O reducer ecophysiology in terms of competition for N_2O (affinity) and thermodynamic efficiency (**Ch 2 and 3**)
- ⇨ the possibility of N_2O and O_2 mixotrophy (**Ch 4**)
- ⇨ the existence of unknown N_2O–reducing metabolisms: selecting an enrichment based on its ability to grow under severe limitation of reactive nitrogen species (**Ch 5**)
- ⇨ the modularity of denitrifying communities in relation to N_2O emissions: effect of electron donor vs. electron acceptor limitation, induction, etc. (preliminary results presented in **Ch 7**)

In **Ch 2** we complemented the enrichment work with data obtained from a pure culture of *Pseudomonas stutzeri*. Finally, in **Ch 6** we addressed NO_x and N_2O kinetics with short-term batch tests, directly on natural community from a full-scale Activated sludge system.

- *Outline of the Chapters and corresponding publications*

1 Introduction

2 Life on N_2O: deciphering the ecophysiology of N_2O respiring bacterial communities in a continuous culture

- Published as: Conthe M, Wittorf L, Kuenen JG, Kleerebezem R, van Loosdrecht MCM, Hallin S. (2018). *ISMEJ*

3 Growth yield and selection of *nosZ* clade II-types in a continuous enrichment culture of N_2O respiring bacteria

- Published as: Conthe M, Wittorf L, Kuenen JG, Kleerebezem R, Hallin S, van Loosdrecht MCM. (2018). *Environ Microbiol Rep*.

4 O_2 *versus* N_2O respiration in a continuous microbial enrichment

- Published as: Conthe M, Parchen C, Stouten G, Kleerebezem R, MCM van Loosdrecht MCM. (2018). *App Microbiol & Biotech*.

5 Exploring microbial N_2O reduction: a continuous enrichment in nitrogen free medium supplied with N_2O

- Published as: Conthe M, Kuenen JG, Kleerebezem R, van Loosdrecht MCM. (2018). *Environ Microbiol Rep*.

6 Denitrification as an N_2O sink

- Under revision in *Water Research* as: Conthe M, Lycus P, Arntzen MØ, Ramos Da Silva A, Frostergård Å, Bakken LR, Kleerebezem R, van Loosdrecht MCM.

7 Outlook – including preliminary data from denitrifying chemostats

G. References

Ahn JH, Kim S, Park H, Rahm B, Pagilla K, Chandran K. (2010). N_2O emissions from activated sludge processes, 2008-2009: Results of a national monitoring survey in the united states. *Environ Sci Technol* **44**: 4505–4511.

Bergaust L, Bakken LR, Frostegård A. (2011). Denitrification regulatory phenotype, a new term for the characterization of denitrifying bacteria. *Biochem Soc Trans* **39**: 207–12.

Bergaust L, Mao Y, Bakken LR, Frostegård A. (2010). Denitrification response patterns during the transition to anoxic respiration and posttranscriptional effects of suboptimal pH on nitrous oxide reductase in *Paracoccus denitrificans*. *Appl Environ Microbiol* **76**: 6387–96.

Bergaust L, van Spanning RJM, Frostegård A, Bakken LR. (2012). Expression of nitrous oxide reductase in *Paracoccus denitrificans* is regulated by oxygen and nitric oxide through FnrP and NNR. *Microbiology* **158**: 826–34.

Betlach MR, Tiedje JM. (1981). Kinetic explanation for accumulation of nitrite, nitric oxide, and nitrous oxide during bacterial denitrification. *Appl Environ Microbiol* **42**: 1074–84.

Beun JJ, Verhoef EV., Van Loosdrecht MCM, Heijnen JJ. (2000). Stoichiometry and kinetics of poly-β-hydroxybutyrate metabolism under denitrifying conditions in activated sludge cultures. *Biotechnol Bioeng* **68**: 496–507.

Broda E. (1977). Two kinds of lithotrophs missing in nature. *Zeitschrift für Allg Microbiol* **17**: 491–493.

Chen J, Strous M. (2013). Denitrification and aerobic respiration, hybrid electron transport chains and co-evolution. *Biochim Biophys Acta - Bioenerg* **1827**: 136–144.

Cooper GA, West SA. (2018). Division of labour and the evolution of extreme specialization. *Nat Ecol Evol* **2**: 1161–1167.

Daelman MRJ, De Baets B, van Loosdrecht MCM, Volcke EIP. (2013). Influence of sampling strategies on the estimated nitrous oxide emission from wastewater treatment plants. *Water Res* **47**: 3120–30.

Daelman MRJ, van Voorthuizen EM, van Dongen UGJM, Volcke EIP, van Loosdrecht MCM. (2015). Seasonal and diurnal variability of N_2O emissions from a full-scale municipal wastewater treatment plant. *Sci Total Environ* **536**: 1–11.

Domeignoz-Horta LA, Philippot L, Peyrard C, Bru D, Breuil M-C, Bizouard F, *et al.* (2017). Peaks of in situ N_2O emissions are influenced by N_2O-producing and reducing microbial communities across arable soils. *Glob Chang Biol* **24**: 360–370.

Foley J, de Haas D, Yuan Z, Lant P. (2010). Nitrous oxide generation in full-scale biological nutrient removal wastewater treatment plants. *Water Res* **44**: 831–44.

Gao H, Liu M, Griffin JS, Xu L, Xiang D, Scherson YD, *et al.* (2017). Complete Nutrient Removal Coupled to Nitrous Oxide Production as a Bioenergy Source by Denitrifying Polyphosphate-Accumulating Organisms. *Environ Sci Technol* **51**: 4531–4540.

Graf DRH, Jones CM, Hallin S. (2014). Intergenomic comparisons highlight modularity of the denitrification pathway and underpin the importance of community structure for N_2O emissions. *PLoS One* **9**: e114118.

Graf DRH, Zhao M, Jones CM, Hallin S. (2016). Soil type overrides plant effect on genetic and enzymatic N_2O production potential in arable soils. *Soil Biol Biochem* **100**: 125–128.

Hallin S, Philippot L, Löffler FE, Sanford RA, Jones CM. (2018). Genomics and ecology of novel N_2O-reducing microorganisms. *Trends Microbiol*. **26**:43-55.

Hink L, Nicol GW, Prosser JI. (2016). Archaea produce lower yields of N_2O than bacteria during aerobic ammonia oxidation in soil. *Environ Microbiol*. **19**: 4829–4837.

Jones CM, Graf DR, Bru D, Philippot L, Hallin S. (2013). The unaccounted yet abundant nitrous oxide-reducing microbial community: a potential nitrous oxide sink. *ISME J* **7**: 417–426.

Jones CM, Spor A, Brennan FP, Breuil M-C, Bru D, Lemanceau P, *et al.* (2014). Recently identified microbial guild mediates soil N_2O sink capacity. *Nat Clim Chang* **4**: 801–805.

Juhanson J, Hallin S, Söderström M, Stenberg M, Jones CM. (2017). Spatial and phyloecological analyses of *nosZ* genes underscore niche differentiation amongst terrestrial N_2O reducing communities. *Soil Biol Biochem* **115**: 82–91.

Kampschreur MJ, Kleerebezem R, de Vet WWJM, van Loosdrecht MCM. (2011). Reduced iron induced nitric oxide and nitrous oxide emission. *Water Res* **45**: 5945–52.

Kampschreur MJ, van der Star WRL, Wielders H a, Mulder JW, Jetten MSM, van Loosdrecht MCM. (2008). Dynamics of nitric oxide and nitrous oxide emission during full-scale reject water treatment. *Water Res* **42**: 812–26.

Kampschreur MJ, Temmink H, Kleerebezem R, Jetten MSM, van Loosdrecht MCM. (2009). Nitrous oxide emission during wastewater treatment. *Water Res* **43**: 4093–103.

Kern M, Simon J. (2016). Three transcription regulators of the Nss family mediate the adaptive response induced by nitrate, nitric oxide or nitrous oxide in *Wolinella succinogenes*. *Environ Microbiol* **18**: 2899–2912.

Koike I, Hattori A. (1975). Energy yield of denitrification: an estimate from growth yield in continuous cultures of *Pseudomonas denitrificans* under nitrate-, nitrite- and oxide-limited conditions. *J Gen Microbiol* **88**: 11–9.

Kuenen JG (2015). Continuous Cultures (Chemostats). In: Reference Module in Biomedical Sciences. Elsevier, Philadelphia, 2015.

Kuypers MM, Marchant HK, Kartal B. (2018). The microbial nitrogen-cycling network. *Nat Rev Microbiol* **16**: 263–276.

Law Y, Ye L, Pan Y, Yuan Z. (2012). Nitrous oxide emissions from wastewater treatment processes. *Philos Trans R Soc Lond B Biol Sci* **367**: 1265–77.

Lilja EE, Johnson DR. (2016). Segregating metabolic processes into different microbial cells accelerates the consumption of inhibitory substrates. *ISME J* **10**: 1568–78.

Liu B, Mao Y, Bergaust L, Bakken LR, Frostegård Å. (2013). Strains in the genus *Thauera* exhibit remarkably different denitrification regulatory phenotypes. *Environ Microbiol* **15**: 2816–2828.

Lu H, Chandran K. (2010). Factors promoting emissions of nitrous oxide and nitric oxide from denitrifying sequencing batch reactors operated with methanol and ethanol as electron donors. *Biotechnol Bioeng* **106**: 390–398.

Lycus P, Lovise Bøthun K, Bergaust L, Shapleigh JP, Bakken LR, Frostegård Å. (2017). Phenotypic and genotypic richness of denitrifiers revealed by a novel isolation strategy. *ISME J* **10**: 2219-2232.

Murnleitner E, Kuba T, van Loosdrecht MCM, Heijnen JJ. (1997). An integrated metabolic model for the aerobic and denitrifying biological phosphorus removal. *Biotechnol Bioeng* **54**: 434–450.

Otte S, Grobben NG, Robertson LA, Jetten MS, Kuenen JG. (1996). Nitrous oxide production by *Alcaligenes faecalis* under transient and dynamic aerobic and anaerobic conditions. *Appl Environ Microbiol* **62**: 2421–2426.

Park D, Kim H, Yoon S. (2017). Nitrous oxide reduction by an obligate aerobic bacterium, *Gemmatimonas aurantiaca* strain T-27. *Appl Environ Microbiol* **83**: e00502-17.

Perez-Garcia O, Mankelow C, Chandran K, Villas-Boas SG, Singhal N. (2017). Modulation of Nitrous Oxide (N_2O) Accumulation by Primary Metabolites in Denitrifying Cultures Adapting to Changes in Environmental C and N. *Environ Sci Technol* **51**: 13678-13688.

Qu Z, Bakken LR, Molstad L, Frostegård Å, Bergaust L. (2015). Transcriptional and metabolic regulation of denitrification in *Paracoccus denitrificans* allows low but significant activity of nitrous oxide reductase under oxic conditions. *Environ Microbiol*. **18**: 2951–2963.

Ravishankara AR, Daniel JS, Portmann RW. (2009). Nitrous Oxide (N_2O): The Dominant Ozone-Depleting Substance Emitted in the 21st Century. *Science* **326**: 123–125.

Ribera-Guardia A, Kassotaki E, Gutierrez O, Pijuan M. (2014). Effect of carbon source and competition for electrons on nitrous oxide reduction in a mixed denitrifying microbial community. *Process Biochem* **49**: 2228–2234.

Roco CA, Bergaust LL, Bakken LR, Yavitt JB, Shapleigh JP. (2016). Modularity of nitrogen-oxide reducing soil bacteria: Linking phenotype to genotype. *Environ Microbiol* **19**: 2507–2519.

Roels JA. (1980). Simple model for the energetics of growth on substrates with different degrees of reduction. *Biotechnol Bioeng* **22**: 33–53.

Sanford RA, Wagner DD, Wu Q, Chee-Sanford JC, Thomas SH, Cruz-García C, *et al.* (2012). Unexpected nondenitrifier nitrous oxide reductase gene diversity and abundance in soils. *Proc Natl Acad Sci U S A* **109**: 19709–14.

Scherson YD, Wells GF, Woo S-G, Lee J, Park J, Cantwell BJ, *et al.* (2013). Nitrogen removal with energy recovery through N_2O decomposition. *Energy Environ Sci* **6**: 241–248.

Scherson YD, Woo S-G, Criddle CS. (2014). Production of nitrous oxide from anaerobic digester centrate and its use as a co-oxidant of biogas to enhance energy recovery. *Environ Sci Technol* **48**: 5612–5619.

Schreiber F, Wunderlin P, Udert KM, Wells GF. (2012). Nitric oxide and nitrous oxide turnover in natural and engineered microbial communities: biological pathways, chemical reactions, and novel technologies. *Front Microbiol* **3**: 372.

Shapleigh JP. (2013). Denitrifying Prokaryotes. In: Rosenberg E, DeLong EF, Lory S, Stackebrandt E, Thompson F (eds). *The Prokaryotes: Prokaryotic Physiology and Biochemistry*. Springer Berlin Heidelberg: Berlin, Heidelberg, pp 405–425.

Simon J, Einsle O, Kroneck PM., Zumft WG. (2004). The unprecedented *nos* gene cluster of *Wolinella succinogenes* encodes a novel respiratory electron transfer pathway to cytochrome *c* nitrous oxide reductase. *FEBS Lett* **569**: 7–12.

Simon J, Klotz MG. (2013). Diversity and evolution of bioenergetic systems involved in microbial nitrogen compound transformations. *Biochim Biophys Acta* **1827**: 114–35.

Soler-Jofra A, Stevens B, Hoekstra M, Picioreanu C, Sorokin D, van Loosdrecht MCM, *et al.* (2016). Importance of abiotic hydroxylamine conversion on nitrous oxide emissions during nitritation of reject water. *Chem Eng J* **287**: 720–726.

van Spanning RJM, Richardson DJ, Ferguson SJ. (2007). Introduction to the Biochemistry and Molecular Biology of Denitrification. Biology of the Nitrogen Cycle.

Suharti, de Vries S. (2005). Membrane-bound denitrification in the Gram-positive bacterium Bacillus azotoformans. *Biochem Soc Trans* **33**: 130–3.

Thomson AJ, Giannopoulos G, Pretty J, Baggs EM, Richardson DJ. (2012). Biological sources and sinks of nitrous oxide and strategies to mitigate emissions. *Philos Trans R Soc Lond B Biol Sci* **367**: 1157–68.

Torres MJ, Simon J, Rowley G, Bedmar EJ, Richardson DJ, Gates AJ, *et al.* (2016). Nitrous Oxide Metabolism in Nitrate-Reducing Bacteria: Physiology and Regulatory Mechanisms. In: Vol. 68. *Advances in Microbial Physiology*. Academic Press, pp 61–79.

Vasilaki V, Volcke EIP, Nandi AK, van Loosdrecht MCM, Katsou E. (2018). Relating N_2O emissions during biological nitrogen removal with operating conditions using multivariate statistical techniques. *Water Res* **140**: 387–402.

Wittorf L, Bonilla-Rosso G, Jones CM, Bäckman O, Hulth S, Hallin S. (2016). Habitat partitioning of marine benthic denitrifier communities in response to oxygen availability. *Environ Microbiol Rep* **8**: 486–492.

Wunderlin P, Lehmann MF, Siegrist H, Tuzson B, Joss A, Emmenegger L, *et al.* (2013). Isotope signatures of N_2O in a mixed microbial population system: Constraints on N_2O producing pathways in wastewater treatment. *Environ Sci Technol* **47**: 1339–1348.

Wunderlin P, Mohn J, Joss A, Emmenegger L, Siegrist H. (2012). Mechanisms of N_2O production in biological wastewater treatment under nitrifying and denitrifying conditions. *Water Res* **46**: 1027–37.

Yoon S, Nissen S, Park D, Sanford RA, Löffler FE. (2016). Nitrous Oxide Reduction Kinetics Distinguish Bacteria Harboring Clade I NosZ from Those Harboring Clade II NosZ. *Appl Environ Microbiol* **82**: 3793–800.

Zumft WG. (1997). Cell biology and molecular basis of Cell Biology and Molecular Basis of Denitrification. *Microbiology* **61**.

Zumft WG, Kroneck PMH. (2006). Respiratory Transformation of Nitrous Oxide (N_2O) to Dinitrogen by Bacteria and Archaea. *Adv Microb Physiol* **52**: 107–227.

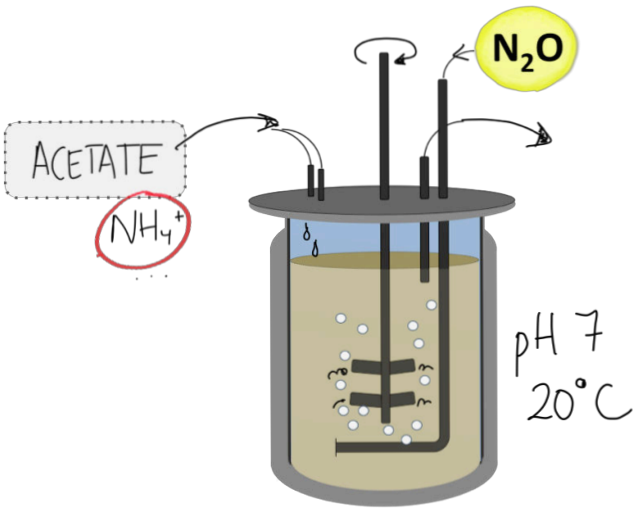
N_2O
ACETATE
NH_4^+
pH 7
20°C

2

Life on N_2O: deciphering the ecophysiology of N_2O respiring bacterial communities in a continuous culture

Conthe M, Wittorf L, Kuenen JG, Kleerebezem R, Van Loosdrecht MCM, Hallin S.

ISME J (2018) **12**: 1142–1153

+ SUPPLEMENTARY INFORMATION

The ISME Journal (2018) 12:1142–1153
https://doi.org/10.1038/s41396-018-0063-7

ARTICLE

Life on N_2O: deciphering the ecophysiology of N_2O respiring bacterial communities in a continuous culture

Monica Conthe[1] · Lea Wittorf[2] · J. Gijs Kuenen[1] · Robbert Kleerebezem[1] · Mark C. M. van Loosdrecht[1] · Sara Hallin[2]

Received: 21 September 2017 / Revised: 19 December 2017 / Accepted: 29 December 2017 / Published online: 7 February 2018

Abstract

Reduction of the greenhouse gas N_2O to N_2 is a trait among denitrifying and non-denitrifying microorganisms having an N_2O reductase, encoded by *nosZ*. The *nosZ* phylogeny has two major clades, I and II, and physiological differences among organisms within the clades may affect N_2O emissions from ecosystems. To increase our understanding of the ecophysiology of N_2O reducers, we determined the thermodynamic growth efficiency of N_2O reduction and the selection of N_2O reducers under N_2O- or acetate-limiting conditions in a continuous culture enriched from a natural community with N_2O as electron acceptor and acetate as electron donor. The biomass yields were higher during N_2O limitation, irrespective of dilution rate and community composition. The former was corroborated in a continuous culture of *Pseudomonas stutzeri* and was potentially due to cytotoxic effects of surplus N_2O. Denitrifiers were favored over non-denitrifying N_2O reducers under all conditions and Proteobacteria harboring clade I *nosZ* dominated. The abundance of *nosZ* clade II increased when allowing for lower growth rates, but bacteria with *nosZ* clade I had a higher affinity for N_2O, as defined by μ_{max}/K_s. Thus, the specific growth rate is likely a key factor determining the composition of communities living on N_2O respiration under growth-limited conditions.

Introduction

Nitrous oxide (N_2O) is a potent greenhouse gas and the major ozone-depleting substance in the atmosphere [1]. In the era of global warming, it is imperative to find strategies to mitigate N_2O emissions, especially from managed ecosystems with high nitrogen loadings like agricultural soils and wastewater treatment plants. For this reason, there is an increasing interest to understand the ecophysiology of N_2O-reducing microorganisms [2], which have received much less attention than microbial and chemical processes that can lead to the formation of N_2O [3].

The N_2O reductase (NosZ), encoded by the gene *nosZ*, is the only known enzyme converting N_2O, by reducing it to N_2. There are two major clades in the *nosZ* phylogeny—clade I and the recently described clade II [4, 5]—and genome comparisons as well as studies focusing on the ecology and physiology of N_2O reducers have suggested differences, for example regarding niches and composition of the electron transport chain, between organisms harboring the two clades [2]. Nitrous oxide reduction as part of the denitrification pathway has been extensively studied in model organisms (e.g., *Paracoccus denitrificans* and *Pseudomonas stutzeri*) but N_2O reduction is not a metabolic feature restricted to denitrifiers. Many non-denitrifying N_2O-reducing organisms possess N_2O reductases, but lack all or some of the other reductases in the denitrification pathway [6]. Hence, there is an emerging body of literature focusing on non-denitrifying N_2O-reducing organisms (which often possess clade II type *nosZ*; [2] and references therein), since they have the potential to increase the N_2O sink capacity of soils and other environments [7, 8].

Nitrous oxide reduction conserves energy and can fully sustain the energetic needs of a cell, as organisms

✉ Sara Hallin
Sara.Hallin@slu.se

[1] Department of Biotechnology, Delft University of Technology, Delft, The Netherlands

[2] Department of Forest Mycology and Plant Pathology, Swedish University of Agricultural Sciences, Uppsala, Sweden

Table 1 Chemostat operational conditions

Period	N_2O/Acetate provided (mol/mol)	Limiting nutrient	(No. of days)	D (h^{-1})	Concentration in the chemostat		
					CH_3COO^- (mM)	N_2O^a (mM)	Biomass (g VSS l^{-1})
I	2.7	N_2O	56	0.086 ± 0.003	4.2 ± 0.3	n.d.	0.67 ± 0.01
II	26.1	Acetate	29	0.089 ± 0.003	n.d.	5.5 ± 0.6	0.60 ± 0.01
III	15.9/7.6	Acetate	61	0.028 ± 0.001	n.d.	1.2 ± 0.1	0.59 ± 0.02
IV	2.3	N_2O	43	0.027 ± 0.001	16.5 ± 1.8	n.d.	0.54 ± 0.03

n.d. (not detected), below detection limit

[a]N_2O concentration in the liquid was calculated from the N_2O concentration in the off-gas using mass transfer laws

possessing either *nosZ* clade I or clade II have been successfully grown using N_2O as a sole electron acceptor [9–11]. Recent work based on a small selection of pure cultures report a lower whole-cell half-saturation constant (K_s) for N_2O and up to 1.5 times higher biomass yields among organisms with *nosZ* clade II compared to those with clade I [5, 12, 13]. A higher energy conservation per electron accepted could potentially be due to differences between the two clades regarding the *nos* gene cluster, which encodes proteins involved in the electron transport to NosZ [5, 14]. However, the physiological and bioenergetic implications of possessing *nosZ* clade I or clade II are largely unknown considering the broad taxonomic diversity of N_2O reducers detected in the environment (e.g., refs. [7, 15]). To date, there are no reports on long-term growth of bacteria based on their N_2O-reducing capacity and the selective effect of N_2O as sole electron acceptor in natural communities.

Our aim was to increase the understanding of the ecophysiology of N_2O-reducing microorganisms, and more specifically determine (i) the selection of bacteria, and associated *nosZ* genes, in an environmental community specializing in N_2O reduction under N_2O-limiting as well as acetate-limiting conditions, and (ii) the thermodynamic growth efficiency of N_2O reduction and the efficiency of N_2O respiration as reflected in the growth yields of the enrichment cultures under said conditions. We hypothesized that organisms harboring *nosZ* clade II genes would dominate the enrichment culture during N_2O-limiting conditions since these organisms have been suggested to have a lower K_s [13] and thus, likely have a higher overall affinity for N_2O (as defined by the ratio of μ_{max} over K_s). For our purpose, we employed chemostat enrichment cultures using activated sludge from a wastewater treatment plant as our seed community and fed with N_2O as the sole electron acceptor and acetate as the only energy and carbon source. We worked at two different dilution rates and with either the electron acceptor (N_2O-limiting condition) or the donor as a limiting factor (acetate-limiting condition). With the enrichment approach, we could monitor the abundance, diversity, and bioenergetics of naturally occurring N_2O reducers potentially relevant in wastewater treatment or other environments instead of narrowing our view to a few model organisms. In contrast to batch cultures, the chemostat set-up also allowed us to effectively address the effects of limiting conditions. We chose acetate as a carbon and energy source mainly to avoid enrichment of non-N_2O-reducing microorganisms, as acetate cannot be readily converted in the absence of an external electron acceptor. It also allowed us to compare our results to other studies reporting differences in physiology among *nosZ* clade I and II organisms grown on acetate [5, 13]. As a control, a pure culture of *Pseudomonas stutzeri*, closely related to the dominant population in the enrichment culture during high dilution rates, was grown under similar conditions.

Materials and methods

Chemostat operation for enrichment of N_2O reducers

An acetate-consuming N_2O-reducing culture was enriched from activated sludge and cultivated in a double-jacket glass bioreactor with a working volume of 2 l (Applikon, Delft, the Netherlands) operated as a continuous stirred tank reactor (i.e., a flow-controlled chemostat) during 195 days. Mixing was achieved with a stirrer having two standard geometry six-blade turbines turning at 750 rpm. The dilution rate was controlled by two peristaltic pumps feeding-concentrated medium and water to the system and an effluent pump controlled by a level sensor. The reactor temperature was maintained at 20 ± 1 °C using a cryostat bath (Lauda, Lauda-Königshofen, Germany). The pH was monitored with a pH electrode (Mettler Toledo) and maintained at 7.0 ± 0.05 by titration of 1 M HCl controlled by an ADI 1030 biocontroller (Applikon).

During the experiment, the chemostat system was operated under four different operational conditions, referred to as periods I–IV (Table 1 and Figure S1), with a minimum of 30 volume changes each. The shifts between N_2O and acetate limitation were achieved by changing the N_2O supply rate (Fig. S1). A variable flow of N_2 and N_2O (summing up to a total of 100–800 ml min^{-1}) was sparged into the reactor, controlled by two separate mass flow controllers (Brooks Instruments, Ede, the Netherlands). While N_2O served as the electron acceptor, N_2 gas was used as a dilution gas to increase mixing and enhance gas–liquid mass transfer for both N_2O and CO_2. The N_2O concentration was not directly measured in the liquid, but calculations based on the N_2O concentration in the off-gas using mass transfer laws show that N_2O was growth limiting when acetate was present in excess (Table 1). The medium was supplied in two separate flows of concentrated acetate and mineral medium, respectively. A second peristaltic pump supplied tap water to the system to dilute the medium. The final influent contained 45.3 mmol acetate ($NaCH_3COO{\cdot}3H_2O$), 13.3 mmol NH_4Cl, 7.4 mmol KH_2PO_4, 2.1 mmol $MgSO_4{\cdot}7H_2O$, 0.5 mmol NaOH, 2 mg yeast extract and 2.5 ml trace element solution [16] per liter.

Prior to the experimental periods I–IV, the reactor was inoculated with activated sludge from the wastewater treatment plant of Harnaschpolder, the Netherlands, and run for a period of 118 days with similar conditions as in the experimental periods I and II (Table S1). When changing dilution rate, and one additional time shortly after changing to periods III and IV, the reactor was re-inoculated with 20–100 ml sludge from Dokhaven wastewater treatment plant to minimize legacy effects of the previous periods for selection of bacteria under the actual conditions in each period. The operation of the Harnaschpolder and Dokhaven plants is described in Gonzalez-Martinez et al. [17]. The chemostat was operated under non-sterile conditions and cleaned approximately every 3 weeks to remove any biofilm present. The contribution of biofilm growth to the amount of biomass inside the reactor was negligible.

Before terminating the chemostat experiment, a batch experiment was performed on day 192 to compare the maximum acetate conversion rate of the enrichment with either N_2O or NO_3^- as an electron acceptor. During these tests, the influent and effluent pumps of the chemostat were stopped, but flushing with N_2 gas was kept constant (at 800 ml min^{-1}). The sparging with N_2O was initially increased to obtain maximum conversion rates on N_2O and then stopped before adding 1 mM NO_3^- and monitoring its reduction.

Growth of *P. stutzeri* JM300 under N_2O and acetate-limiting conditions

A pure culture of *P. stutzeri* JM300, a strain closely related to the dominant population in the enrichment culture during periods I and II, was grown under alternating N_2O and acetate-limiting conditions. The chemostat reactor set-up was similar to the one described above, except for operating at 30 ± 1 °C, under sterile conditions, and using 1 M H_2SO_4 for pH control. The substrate and mineral medium were fed simultaneously, but final concentrations in the influent were the same as in the enrichment culture. The mineral medium was adjusted to a defined medium by removing the yeast extract. The chemostat was inoculated with a pre-culture of *P. stutzeri* JM300 grown aerobically in a shake flask and harvested at exponential phase. Start-up of the reactor was initially in batch mode with the defined mineral medium supplemented with 30 mM NO_3^- to induce denitrification. Once the NO_3^- was depleted, N_2O sparging was initiated, and medium was added at a dilution rate of 0.044 h^{-1}. Like in the enrichment, the N_2O supply rate varied to achieve N_2O-limiting vs. acetate-limiting conditions. The concentration of N_2O, diluted in N_2 supplied at a rate of 600 ml min^{-1}, was 0.62–0.93%.

Analytical procedures

Samples from the reactor for analysis of acetate and NH_4^+ were immediately filtered after sampling (0.45-µm pore size poly-vinylidene difluoride membrane, Merck Millipore, Carrigtohill, Ireland). Acetate was measured with a Chrompack CP 9001 gas chromatograph (Chrompack, Middelburg, the Netherlands) equipped with an HP Innowax column (Algilent Technologies, Santa Clara, CA,

USA) and a flame ionization detector. Ammonium, as well as NO_3^- and NO_2^-, was determined spectrophotometrically using cuvette test kits (Hach Lange, Düsseldorf, Germany). For the estimation of biomass concentration, the volatile suspended solids (VSS) concentration was determined by centrifuging 0.2 l of the enrichment, drying the pellet overnight at 105 °C, and then burning the pellet at 550 °C for 2 h to determine the ash content. Concentrations of N_2O, N_2, and CO_2 in the headspace of the reactor were monitored in dried gas, either by using an infrared gas analyzer (NGA 2000, Rosemount, Chanhassen, MN, USA) or through mass spectrometry (Prima BT, Thermo Scientific).

Elemental and electron balances were set up to determine the conversions taking place within the chemostat. To convert VSS to biomass, a biomass composition of $CH_{1.8}O_{0.5}N_{0.2}$ was assumed [18]. The N_2O consumption and N_2 and CO_2 production rates were computed from the off-gas partial pressure and the gas supply rate. Dissolved N_2O as well as dissolved CO_2 and ionized species were included in the mass balances. For the electron balance, an average of the N_2O consumption and the N_2 production was used to estimate the moles of electrons accepted.

To monitor the microbial community structure of the enrichment, the reactor was sampled regularly for microscopy, FISH (fluorescent in situ hybridization), and DNA extraction for quantitative PCR and sequencing as described below.

DNA extraction and quantitative PCR of nirK, nirS, nosZ, and 16S rRNA genes

DNA was extracted from a pellet retrieved from 2 ml of the enrichment culture at each sampling occasion, and from the activated sludge samples used as inoculum using the PowerLyzer PowerSoil DNA Isolation Kit (MoBio Laboratories). DNA was quantified using the Qubit Fluorometer (Life Technologies Corporation).

To determine the abundance of the denitrifier, nitrous oxide reducing, and total bacterial communities in the enrichment, the genes *nirS* and *nirK*, *nosZ* clade I and II, and the 16S rRNA gene were quantified using quantitative real-time PCR (qPCR). Each independent duplicate reaction contained 5 ng template DNA, iQ SYBR Green Supermix (BioRad), 0.1% BSA, and primer concentrations of 0.25 µM for *nirK*, 0.5 µM for the 16S rRNA gene and *nirS*, and 0.8 µM for both *nosZ* clades. Primer sequences and thermal cycling conditions are available in Table S2. Standard curves were obtained using serial dilutions of linearized plasmids containing fragments of the respective genes. We tested for PCR inhibitors in all DNA extracts with a plasmid-specific qPCR assay (pGEM-T; Promega) and no inhibition was detected when comparing to controls with only the plasmid added.

Amplicon sequencing of 16S rRNA genes and nosZ clade I and II

The composition of the bacterial and N_2O-reducing communities were determined by amplicon sequencing of 16S rRNA genes and the *nosZ* genes of both clades. A two-step PCR protocol was used [19]. The 16S rRNA genes were amplified in duplicate using $25 + 8$ cycles and the primers pro341F and pro805R [20]. Amplicons were pooled and purified with the AMPure Beads Purification kit (Agilent Technologies) in between and after the final amplification step. The PCR contained 10 ng template DNA, Phusion High-Fidelity PCR Master Mix (Thermo Scientific), 0.75 µg µL^{-1} BSA and 0.25 µM of each primer, equipped with Nextera adapter sequences in the second PCR. The amplification of *nosZ* clade I and II were done in duplicate with $20 + 12$ cycles for *nosZ*I and $25 + 15$ cycles for *nosZ*II as described in Jones et al. [7]. The AMPure Beads Purification kit was used for purification of the final PCR. The reactions contained 20 ng template DNA, DreamTaq Green PCR Master Mix (Fermentas), 0.1% BSA, 1 mM $MgCl_2$, and 0.8 µM of either *nosZ* clade I or II specific primers. Primer sequences and cycling conditions are listed in Table S2. Sequencing was performed by Microsynth (Microsynth AG) on the MiSeq platform (Illumina) using 2×300 bp paired-end chemistry for 16S rRNA genes and on a 454 FLX Genome Sequencer (Roche) using Titanium FLX + chemistry for the *nosZ* genes. The sequences obtained in this study are available at The Sequence Read Archive under the accession number PRJNA398140.

Bioinformatic analysis

The 16S rRNA gene sequences were trimmed with the FASTX-Toolkit (http://hannonlab.cshl.edu/fastx_toolkit) and paired-end reads were merged with PEAR [21] using a minimum overlap of 30 bp. Further quality filtering was done using VSEARCH [22]. The sequences were clustered at 97% nucleotide similarity into operational taxonomic units (OTU), followed by de novo and reference-based chimera checking (Gold database retrieved from UCHIME; [23]). All OTUs that comprised less than 1% of all sequences within each sample were removed from the data set. This resulted in a total of 2,210,612 sequences clustering into 82 OTUs. Taxonomy assignment was done with the SINA aligner using the SILVA taxonomy [24].

The *nosZ* sequence data were screened and demultiplexed using QIIME [25]. Frameshift correction and removal of contaminating sequences was performed using HMMFRAME [26], with HMM profiles based on separate reference alignments of full-length *nosZ* amino acid

Table 2 Average conversion rates in the chemostat (negative numbers = consumption, positive numbers = production) and carbon (C) and electron (e^-) balances indicating recovery

Period	Limiting nutrient	D (h^{-1})	Compound conversion rates (mmol h^{-1})					C-bal (%)	e^- bal (%)
			CH_3COO^-	N_2O	N_2	NH_4^+	$CH_{1.8}O_{0.5}N_{0.2}$[a]	CO_2	
I	N_2O	0.086 ± 0.003	−6.90 ± 0.56	−17.21 ± 1.43	16.72 ± 0.72	−1.24 ± 0.06	4.49 ± 0.15	7.57 ± 0.33	91	95
II	Acetate	0.089 ± 0.003	−7.74 ± 0.24	−23.97 ± 1.05	24.38 ± 1.07	−1.15 ± 0.07	4.11 ± 0.15	9.94 ± 0.45	94	106
III	Acetate	0.028 ± 0.001	−2.54 ± 0.10	−7.78 ± 0.42	7.49 ± 0.38	−0.32 ± 0.03	1.26 ± 0.07	3.35 ± 0.19	92	101
IV	N_2O	0.027 ± 0.001	−1.78 ± 0.20	−5.09 ± 0.90	3.88 ± 0.21	−0.30 ± 0.01	1.14 ± 0.08	2.15 ± 0.13	93	97

[a]Calculated from volatile suspended solids (VSS) using theoretical chemical composition of biomass [18]

sequences obtained from genomes for each clade [27]. Chimera checking (de novo and reference-based using the *nosZ* database retrieved from FunGene; [28]) and OTU clustering at 97% nucleotide similarity were performed using USEARCH in QIIME. The full set of OTUs was reduced in the same way as for the 16S rRNA gene data set, which resulted in 300,554 sequences for clade I and 143,185 for clade II corresponding to 79 and 102 OTUs, respectively. The representative sequences of all 181 OTUs were aligned to the reference alignment containing 624 full-length *nosZ* amino acid sequences using HMMER [29] and the alignment was edited manually using ARB [30]. The final *nosZ* phylogeny was generated from the amino acid alignment with FastTree 2 [31] using the WAG + CAT substitution model [32].

FISH and microscopic analysis of the culture

FISH was performed using the probes listed in Table S3 as described by Johnson et al., [33], using a hybridization buffer containing 35% (v/v) formamide. Slides were observed with an epifluorescence microscope (Axioplan 2, Zeiss, Sliedrecht, the Netherlands) and images were acquired with a Zeiss MRM camera, compiled with the Zeiss microscopy image acquisition software (AxioVision version 4.7, Zeiss)

Results

Conversion rates and biomass yields of the enrichment culture and *P. stutzeri* JM300

An enrichment culture using acetate as a carbon source and exogenous N_2O as the sole electron acceptor was successfully maintained during a period of 195 days under two different dilution rate regimes and subjected to either electron donor (acetate) or electron acceptor (N_2O)-limiting conditions (Table 1). The limiting substrates could not be detected in the chemostat, which supports that we had obtained limiting conditions (Table 1). That N_2O was growth limiting when acetate was present in excess was further verified by shortly increasing the N_2O supply rate and observing an increase in biomass-specific N_2O conversion rates during an N_2O-limiting period (data not shown). The conversion rates were averaged for each of the four conditions, and checked for consistency by evaluating the carbon and electron balances (>90% of C and electrons recovered; Table 2). The stoichiometry deduced from the conversion rates (Table 2) and the biomass yields (Table 3) shows that the N_2O:acetate ratio used by the culture was 2.5–3.1 mol/mol depending on the limitation regime.

Table 3 Biomass yields and NH_4^+ consumption of the enrichment culture and the *Pseudomonas stutzeri* JM300 culture

Period	Limiting nutrient	D (h^{-1})	Y_{XAc} (CmolX/CmolS)	Y_{XN2O} (CmolX/molN_2O)	NH_4^+ consumption (molN/CmolX)
I	N_2O	0.086 ± 0.003	0.33 ± 0.03	0.26 ± 0.02	0.25 ± 0.02
II	Acetate	0.089 ± 0.003	0.27 ± 0.01	0.17 ± 0.01	0.28 ± 0.01
III	Acetate	0.028 ± 0.001	0.25 ± 0.02	0.16 ± 0.01	0.28 ± 0.02
IV	N_2O	0.027 ± 0.001	0.32 ± 0.04	0.22 ± 0.04	0.26 ± 0.01
P. stutzeri JM300	Acetate	0.044 ± 0.002	0.18 ± 0.01	–	0.38 ± 0.02
P. stutzeri JM300	N_2O	0.044 ± 0.002	0.26 ± 0.01	–	0.33 ± 0.01

X = biomass, *YXAc* = biomass yield on acetate in carbon mole biomass produced (CmolX) per carbon mole of substrate consumed (CmolS), YXN_2O = biomass yield per mole of N_2O consumed

When deriving the biomass yield of the culture from the conversion rates (Table 2), we found higher values during the N_2O-limited conditions (periods I and IV) compared to the acetate-limited conditions (periods II and III; Table 3). To validate these results, we determined the biomass growth yields during N_2O versus acetate-limiting conditions in a pure culture of *Pseudomonas stutzeri* JM300, a strain closely related to the dominant OTU in the enrichment culture when the dilution rate was high (periods I and II; see below). Although biomass yields overall were lower for *P. stutzeri* JM300 compared to the enrichment, the pattern with lower growth per mole of substrate (almost 30% lower) during acetate-limited growth compared to N_2O-limited growth was similar (Table 3). Moreover, the NH_4^+ consumption was higher than expected (Table 3) and this was also the case in the enrichment when considering the measured nitrogen content in the biomass (0.21–0.23 mole N/C-mole biomass; data not shown). At the end of the experiment, on day 192, the enrichment culture was able to reduce NO_3^- with transient accumulation of NO_2^- and NO, but no detectable N_2O. The maximum acetate oxidation rate during NO_3^- reduction was roughly 60% of that during N_2O reduction (1.05 vs. 1.65 mM h^{-1} acetate, respectively; Figure S4).

Abundance of bacterial community and functional genes during chemostat operation

Organisms harboring *nosZ* clade I dominated the system over those with *nosZ* clade II throughout operation of the chemostat (Fig. 1). At the higher dilution rate (periods I and II), *nosZ* clade I gene abundance was in the same order of magnitude as that of the 16S rRNA genes and was unaffected by the limitation regime. After the shift to a lower dilution rate (periods III and IV), *nosZ* clade I remained the dominant clade, although the average gene copy number decreased by one order of magnitude. This co-occurred with an increase by one to two orders of magnitude of the *nosZ* clade II abundance.

The *nirS* and *nirK* genes were abundant in the enrichment culture throughout the entire time of operation (Fig. 1). Overall, *nirS* dominated over *nirK*, except for a short period in which both genes were equally abundant (period II). The abundance of *nirS* was strongly affected by the shift from nitrous oxide to acetate limitation during the low dilution rate, whereas *nirK* and *nosZ* genes were mainly affected by the change in dilution rate.

Composition of the enriched N_2O-reducing community

A relatively simple community was selected in the N_2O-reducing enrichment culture with four to five *nosZ* OTUs representing the majority of the sequences at any given time period (Fig. 2). At the higher dilution rate, both the *nosZ* clade I and clade II community structure remained similar regardless of whether the electron acceptor (N_2O) or donor (acetate) was the growth-limiting substrate. After decreasing the dilution rate, the community composition changed and then changed again when switching from acetate limitation to N_2O limitation. The *nosZ* clade I OTUs included sequences clustering closely with *nosZ* from the families *Pseudomonadaceae*, *Rhodocyclaceae*, *Rhodobacteraceae*, and *Comamonadaceae*, the latter including the genus *Acidovorax* (Fig. 2 and S2). The *nosZ*II-harboring community was more diverse and most dominant OTUs clustered with *Rhodocyclaceae* (including the genera *Azonexus* and *Dechloromonas*) and *Flavobacteriaceae* (including *Chryseobacterium* and *Riemerella*).

Composition of the overall, taxa-based bacterial community

In line with the results for the *nosZ* communities, the analysis of the 16S rRNA gene reads revealed that a relatively simple community was enriched, dominated by a few OTUs, and the changes in patterns over time were similar to those observed for the *nosZ* communities (Fig. 3). The main

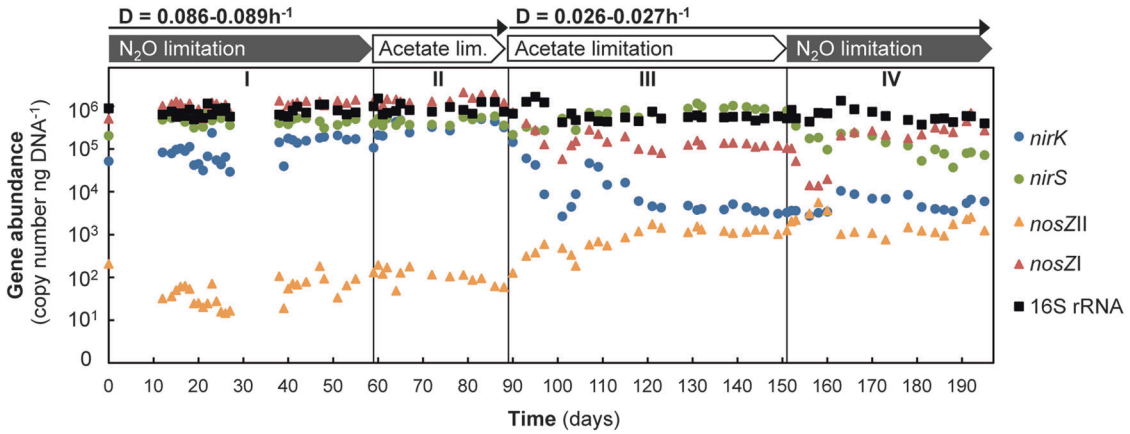

Fig. 1 Abundances of 16S rRNA, *nosZ*I, *nosZ*II, *nirS*, and *nirK* genes during operation of the N_2O-reducing chemostat under four conditions (I–IV) with either acetate or N_2O as growth-limiting factor, under two different dilution rates (D)

OTU at the high dilution rate belonged to the genus *Pseudomonas*, and coexisted with OTUs related to *Comamonadaceae*, *Rhizobium*, *Flavobacteriaceae*, and the phylum Gracilibacteria (Fig. 3a and Table S4). With a lower dilution rate and acetate limitation, the enrichment became dominated by Betaproteobacteria sequences, notably *Azoarcus*-like, but also transiently by sequences affiliated with *Rhodocyclaceae*. From the relative abundance patterns of 16S rRNA and *nosZ* gene sequences we could, with some caution, assign some of the main 16S rRNA OTUs to the *nosZ* OTUs (Fig. 3b). The *Pseudomonas* sp. (16S rRNA OTU 1), which dominated the community during periods I and II, might have been poorly resolved as two divergent copies of *nosZ*I (*nosZ*I OTUs 0 and 1) co-occurred with this taxon. Alternatively, it possessed two different copies of the gene. It is likely closely related to *Pseudomonas stutzeri* TS44 (which possesses two closely related copies of *nosZ*I). OTU 2 in the *nosZ*I community, assigned as *Rhodocyclaceae*, could not be assigned at the genus level, but likely corresponds to the same organism as OTU 3 of the 16S rRNA gene survey, as shown in Fig. 3b. No *nosZ* OTU matched the relative abundance pattern of the 16S rRNA OTU 2 belonging to the Gracilibacteria phylum.

When the relative abundances of the main groups present in the enrichment were independently validated using FISH, the results roughly corroborated those obtained by 16S rRNA sequencing (Figure S4). For example, Gammaproteobacteria dominated the enrichment during periods I and II, and were later washed out and replaced by Betaproteobacteria. Microscopy did not reveal the presence of other cells than prokaryotes.

Discussion

An enrichment culture growing by N_2O reduction to N_2 at the expense of acetate oxidation was maintained for an extended number of generations. The availability of N_2O was not a selective driver for non-denitrifying N_2O reducers, as mainly bacteria with a denitrification pathway were selected in the enrichment, irrespective of N_2O-limiting or acetate-limiting conditions. This was inferred from the abundances of *nir* and *nosZ* genes, phylogenetic placement of *nosZ* genes, classification of 16S rRNA gene sequences and what is known about these organisms. Both the *nosZ* clade I and II communities were dominated by Proteobacteria and all major OTUs from the 16S rRNA gene survey were affiliated with this phylum. The dominant 16S rRNA gene-based OTUs were closely related to *Pseudomonas stuzeri* (periods I and II) and *Azoarcus* (period III). These taxa are well-known denitrifiers that possess both *nir* and *nosZ* clade I genes [6]. The most abundant *nosZ* clade II OTU selected in the enrichment was closely related to *nosZ* in *Dechloromonas*—a Betaproteobacteria known to perform full denitrification—even though, in general, *nosZ* clade II represents a taxonomically highly diverse clade dominated by non-denitrifying N_2O reducers [2]. The ratio of *nir* to *nosZ* gene abundances based on qPCR also indicates selection for complete denitrifying bacteria. This is further supported by the batch test performed on day 192 to compare the maximum conversion rates of the enrichment with either N_2O or NO_3^- as an electron acceptor. The NO_3^--reducing capacity of the culture was in the same order of magnitude as the N_2O-reducing capacity. Moreover, these tests showed that the full denitrification pathway was constitutively or rapidly induced even after growth with N_2O as a sole electron acceptor for a long period. Apart from the expected N_2O reducers, the presence of a relatively abundant OTU closely related to Gracilibacteria is intriguing, since organisms belonging to this phylum are most probably fermentative organisms lacking any type of electron transport chain [34]. However, this phylum is understudied and might include members with other metabolic features than what is currently described. Their presence could also

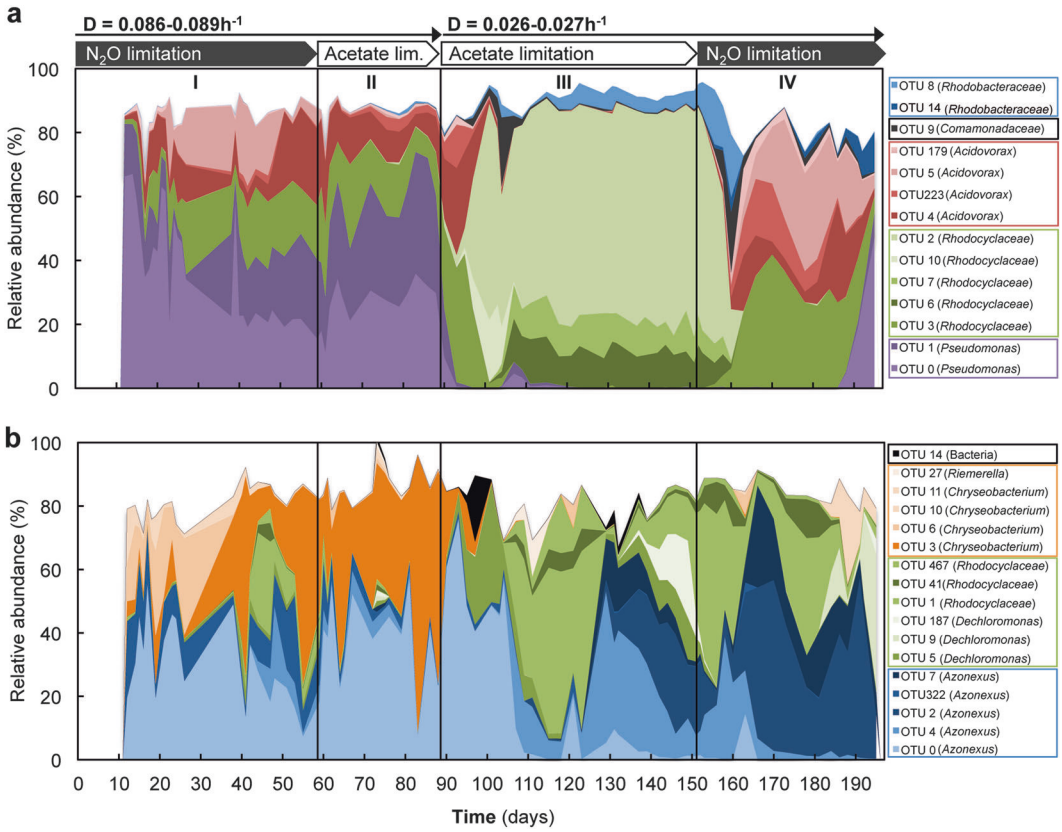

Fig. 2 Relative abundance of *nosZ*I (**a**) and *nosZ*II (**b**) OTUs with >10% of the sequences at any given date during operation of the N_2O-reducing chemostat under four conditions (I–IV). The OTUs are listed on the right-hand side with genus/family indicated in parenthesis (see Figure S2). Closely related OTUs are shown in shades of the same color

indicate important microbial interactions that we cannot account for (e.g., cross-feeding, secretion of inhibiting substances, etc.) resulting in the co-existence of N_2O-reducing denitrifiers and other organisms . We can only speculate about the Gracilibacteria living off the fermentation of byproducts excreted by denitrifiers or products of cell lysis.

In contrast to what was suggested by Yoon et al. [13], our results indicate that organisms with *nosZ* clade I display a higher overall affinity for N_2O under the conditions studied, since organisms harboring *nosZ* clade I genes dominated the enrichment even when N_2O was limiting. This does not necessarily imply that organisms with *nosZ* clade I have a lower affinity constant (K_S) for N_2O, as the overall affinity for a substrate in a continuous culture is determined not only by the K_s, but by the ratio of μ_{max} to K_S [35]. During the periods with a high dilution rate, an OTU closely related to *P. stutzeri*, known to be a fast grower with a high maximum growth rate on a variety of substrates [36, 37], dominated the enrichment. Enrichments with N_2O as electron acceptor in batch cultures, where maximum growth rate is the selective factor, often select for this species [38, 39]. Although the apparent K_s for N_2O is claimed to be relatively high in certain *P. stutzeri* strains [13], its high maximum specific growth rate may have very well compensated for it when competing for N_2O uptake during N_2O-limiting conditions in our reactor. The OTU related to *P. stutzeri* that dominated under both N_2O and acetate-limiting conditions is likely two closely related strains harboring two divergent gene copies of *nosZ* (clade I) according to the *nosZ* phylogeny. One could speculate that these divergent copies offer different advantages if they are expressed and translated into functional proteins under different conditions. Within a single isolate of a *Bacillus* sp. having two phylogenetically divergent *nosZ* clade II genes, N_2O reduction could be maintained at different pH values when compared to closely related strains with only one *nosZ* copy [40].

After the switch to a lower dilution rate, the *P. stutzeri*-dominated community was washed out and replaced by a more diverse community, but still dominated by *nosZ* clade I bacteria. The dilution rate imposed in this study was low enough to be able to sustain growth of the *nosZ* clade II bacterium *Dechloromonas aromatica*, but too high for the three other *nosZ* clade II species for which μ_{max} has been determined [13]. The evidence for a lower μ_{max} among organisms with clade II than organisms with *nosZ* type I is limited, but if this would be the case, *nosZ* clade II could potentially increase when decreasing the dilution rate even

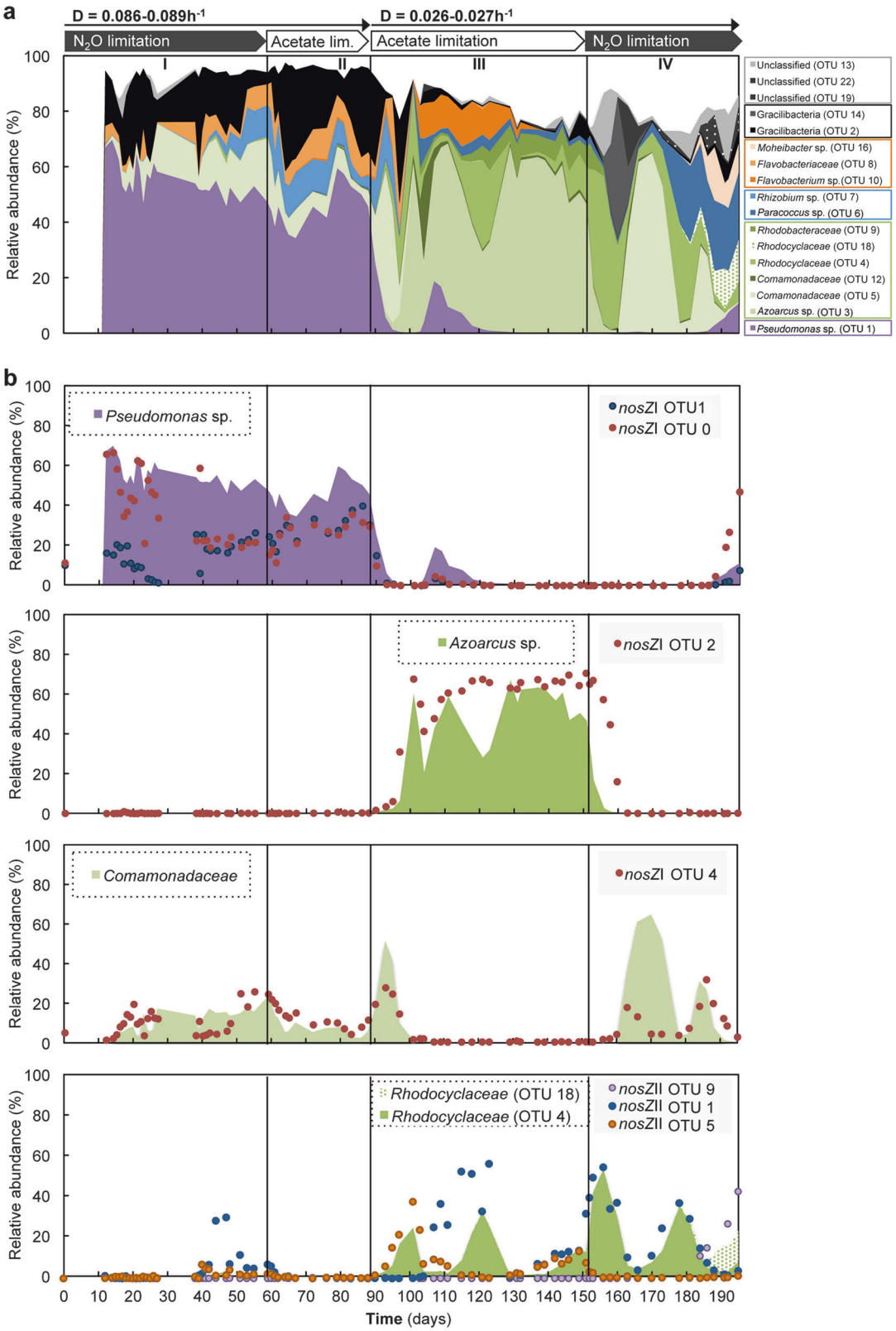

Fig. 3 Changes in the relative abundance of the main 16S rRNA gene OTUs and the related *nosZ* OTUs during operation of the N_2O-reducing chemostat under four conditions (I–IV). **a** Contribution of the main 16S rRNA gene OTUs with >10% of the sequences at any given date. **b** Comparison between the major 16S rRNA gene OTUs and the *nosZ* OTUs with corresponding relative abundance patterns. For taxonomy assignment of the 16S rRNA gene OTUs, see Table S4

further. In agreement, the qPCR results indicate a significant increase in the abundance of *nosZ* clade II when the dilution rate was lowered, irrespective of the limiting substrate. In natural and engineered systems, microorganisms typically grow at rates lower than those used in our experiment (e.g., in the order of 0.2–0.05 d^{-1} in activated sludge WWTP). This could explain why *nosZ* clade II genes are often detected in equal or higher abundance compared to *nosZ* clade I in many environments [4]. In contrast, the ratios between *nosZ* clade I and II observed in root-associated communities are higher compared to those in bulk soil [41, 42]. The rhizosphere is an example of an environment where carbon supply is high, and high growth rate or overall affinity would be a competitive advantage. It would be interesting to address the competition of *nosZ* clade I vs. clade II under N_2O limitation under a larger range of growth rates, especially lower than those used here.

The growth yield per electron accepted of the enrichment was in the same range (or lower) as the reported yields of denitrifying pure cultures using acetate as a carbon source (refs. [5, 13, 43]; Table S6). However, growth yields were significantly different depending on whether acetate or N_2O was the limiting substrate, independent of the dilution rate. The biomass yield per electron accepted identified during the N_2O-limiting periods was comparable to two denitrifying enrichments grown under either acetate or NO_3^- limitation with comparable conditions regarding pH, temperature, inoculum, etc. (0.38 ± 0.04 and 0.34 ± 0.05 CmolX/CmolS, respectively; data not shown). This suggests that the yield during acetate limitation was unexpectedly low. The difference in yield cannot be related to the selection of different communities with different electron transport pathways for N_2O respiration, since it was observed not only between periods I and II, which had a similar community structure, but also in the pure culture of *P. stutzeri* JM300. We therefore hypothesize that the stunted growth during acetate limitation was caused by cytotoxic effects of excess N_2O. Cytotoxicity of N_2O with concentrations as low as 0.1 µM, which is far below the concentration in our system during acetate limitation, has been reported for *Paracoccus denitrificans* [44]. This effect was attributed to the destruction of vitamin B12, which is necessary for methionine and DNA synthesis. In *P. denitrificans*, high levels of N_2O presumably lead to a switch to vitamin B12-independent pathways, which are energetically costly. An increased energy expense in the presence of excess N_2O could explain why we found lower growth yields in the enrichment during the acetate-limited periods. In broader perspective, cytotoxic effects of N_2O on certain organisms would be another mechanism of selection effects of N_2O in a community, in addition to the organisms' μ_{max} and K_S for N_2O. Metatranscriptomics when N_2O is present in excess may provide more supporting evidence for this hypothesis. In the environment, N_2O reduction could be a detoxification mechanism without being linked to energy conservation. The relative importance of detoxification and anaerobic respiration for N_2O reduction in the environment is not known [2], but in our chemostat, N_2O reducers would necessarily have to harvest energy during N_2O reduction, as it was the sole electron acceptor provided.

Overall, denitrifying bacteria were favored over non-denitrifying N_2O reducers when N_2O was the sole electron acceptor, even under N_2O-limiting conditions. A high affinity for N_2O may be advantageous for complete denitrifiers to avoid scavenging, by other microorganisms, of the N_2O produced in the first steps of denitrification. This strategy would allow them to harvest the energy available in N_2O reduction to N_2 in addition to the rest of the denitrification steps, which may be particularly advantageous when there is limited access to electron acceptors in the environment. Denitrifiers with *nosZ* clade I were favored over microorganisms with *nosZ* clade II under all conditions and our results suggest that the μ_{max} was important in the selection of different N_2O-reducing communities. The conditions are not typical for specific ecosystems, but rather reflect growth-limited conditions determined by substrate supply rates. We cannot exclude that the choice of acetate as an electron donor and carbon source, or the absence of O_2 and N oxides other than N_2O, which are known to be involved in the regulation of *nosZ* expression in model denitrifiers (e.g., *Paracoccus denitrificans* [45, 46]) and in *Gemmatimonas aurantiaca* (*nosZ* clade II [47]), influenced the clade I vs. clade II competition, and further studies are required to look into this. Thus, other conditions than evaluated in the present study could be needed to enrich and study the elusive non-denitrifying N_2O reducers with clade II *nosZ*. Recent work suggests that these organisms form biotic interactions with truncated denitrifiers in soils and sediments [27, 48] and further work should address if these interactions could be exploited in engineered and managed systems to mitigate N_2O emissions.

Acknowledgements This work was funded by the European Commission (Marie Curie ITN NORA, FP7-316472) and the Swedish Research Council (VR grant 2016-03551 to SH). We like to warmly thank Koen Verhagen for carrying out preliminary work with the N_2O chemostat and Gerben Stouten for his help with the off-gas measurements.

Funding The European Commission (Marie Sklodpowska-Curie ITN NORA, FP7-316472) and the Swedish Research Council (grant 2016-03551)

Compliance with ethical standards

Conflict of interest The authors declare that they have no conflict of interest.

References

1. Ravishankara AR, Daniel JS, Portmann RW. Nitrous oxide (N_2O): the dominant ozone-depleting substance emitted in the 21st century. Science. 2009;326:123–5.
2. Hallin S, Philippot L, Löffler FE, Sanford RA, Jones CM. Genomics and ecology of novel N_2O-reducing microorganisms. Trends Microbiol. 2018;26:43–55.
3. Schreiber F, Wunderlin P, Udert KM, Wells GF. Nitric oxide and nitrous oxide turnover in natural and engineered microbial communities: biological pathways, chemical reactions, and novel technologies. Front Microbiol. 2012;3:372.
4. Jones CM, Graf DRH, Bru D, Philippot L, Hallin S. The unaccounted yet abundant nitrous oxide¯reducing microbial community: a potential nitrous oxide sink. ISME J. 2013;7:417–26.
5. Sanford RA, Wagner DD, Wu Q, Chee-Sanford JC, Thomas SH, Cruz-García C, et al. Unexpected nondenitrifier nitrous oxide reductase gene diversity and abundance in soils. Proc Natl Acad Sci USA. 2012;109:19709–14.
6. Graf DRH, Jones CM, Hallin S. Intergenomic comparisons highlight modularity of the denitrification pathway and underpin the importance of community structure for N_2O emissions. PLoS ONE. 2014;9:e114118.
7. Jones CM, Spor A, Brennan FP, Breuil M-C, Bru D, Lemanceau P, et al. Recently identified microbial guild mediates soil N_2O sink capacity. Nat Clim Chang. 2014;4:801–5.
8. Domeignoz-Horta LA, Putz M, Spor A, Bru D, Breuil MC, Hallin S, et al. Non-denitrifying nitrous oxide-reducing bacteria - an effective N_2O sink in soil. Soil Biol Biochem. 2016;103:376–9.
9. Allen MB, Van Niel CB. Experiments on bacterial denitrification. J Bacteriol. 1952;64:397–412.
10. Sacks LE, Barker HA. Substrate oxidation and nitrous oxide utilization in denitrification. J Bacteriol. 1952;64:247–52.
11. Yoshinari T. N_2O reduction by *Vibrio succinogenes*. Appl Environ Microbiol. 1980;39:81–84.
12. Kern M, Simon J. Three transcription regulators of the Nss family mediate the adaptive response induced by nitrate, nitric oxide or nitrous oxide in *Wolinella succinogenes*. Environ Microbiol. 2016;18:2899–912.
13. Yoon S, Nissen S, Park D, Sanford RA, Löffler FE. Nitrous oxide reduction kinetics distinguish bacteria harboring clade I NosZ from those harboring clade II NosZ. Appl Environ Microbiol. 2016;82:3793–800.
14. Simon J, Klotz MG. Diversity and evolution of bioenergetic systems involved in microbial nitrogen compound transformations. Biochim Biophys Acta. 2013;1827:114–35.
15. Wittorf L, Bonilla-Rosso G, Jones CM, Bäckman O, Hulth S, Hallin S. Habitat partitioning of marine benthic denitrifier communities in response to oxygen availability. Environ Microbiol Rep. 2016;8:486–92.
16. Vishniac W, Santer M. The Thiobacilli. Microbiol Mol Biol Rev. 1957;21:195–213.
17. Gonzalez-Martinez A, Rodriguez-Sanchez A, Lotti T, Garcia-Ruiz MJ, Osorio F, Gonzalez-Lopez J, et al. Comparison of bacterial communities of conventional and A-stage activated sludge systems. Sci Rep. 2016;6:18786.
18. Roels JA. Simple model for the energetics of growth on substrates with different degrees of reduction. Biotechnol Bioeng. 1980;22:33–53.
19. Berry D, Ben Mahfoudh K, Wagner M, Loy A. Barcoded primers used in multiplex amplicon pyrosequencing bias amplification. Appl Environ Microbiol. 2011;77:7846–9.
20. Takahashi S, Tomita J, Nishioka K, Hisada T, Nishijima M. Development of a prokaryotic universal primer for simultaneous analysis of Bacteria and Archaea using next-generation sequencing Bourtzis K (ed). PLoS ONE. 2014;9:e105592.
21. Zhang J, Kobert K, Flouri T, Stamatakis A. PEAR: a fast and accurate Illumina paired-end reAd mergeR. Bioinformatics. 2014;30:614–20.
22. Rognes T, Flouri T, Nichols B, Quince C, Mahé F. VSEARCH: a versatile open source tool for metagenomics. PeerJ. 2016;4:e2584.
23. Edgar RC, Haas BJ, Clemente JC, Quince C, Knight R. UCHIME improves sensitivity and speed of chimera detection. Bioinformatics. 2011;27:2194–2200.
24. Pruesse E, Peplies J, Glöckner FO. SINA: accurate high-throughput multiple sequence alignment of ribosomal RNA genes. Bioinformatics. 2012;28:1823–9.
25. Caporaso J, Kuczynski J, Stombaugh J, Bittinger K, Bushman FD. QIIME allows analysis of high-throughput community sequencing data. Nat Methods. 2010;7:335–6.
26. Zhang Y, Sun Y. HMM-FRAME: accurate protein domain classification for metagenomic sequences containing frameshift errors. BMC Bioinforma. 2011;12:198.
27. Juhanson J, Hallin S, Söderström M, Stenberg M, Jones CM. Spatial and phyloecological analyses of *nosZ* genes underscore niche differentiation amongst terrestrial N_2O reducing communities. Soil Biol Biochem. 2017;115:82–91.
28. Fish J, Chai B, Wang Q, Sun Y, Brown CT. FunGene: the functional gene pipeline and repository. Front Microbiol. 2013;4:291.
29. Eddy SR. Profile hidden Markov models. Bioinformatics. 1998;14:755–63.
30. Ludwig W, Strunk O, Westram R, Richter L, Meier H, Yadhukumar A, et al. ARB: a software environment for sequence data. Nucleic Acids Res. 2004;32:1363–71.
31. Price MN, Dehal PS, Arkin AP. FastTree 2 - approximately maximum-likelihood trees for large alignments Poon AFY (ed). PLoS ONE. 2010;5:e9490.
32. Whelan S, Goldman N. A general empirical model of protein evolution derived from multiple protein families using a maximum-likelihood approach. Mol Biol Evol. 2001;18:691–9.
33. Johnson K, Jiang Y, Kleerebezem R, Muyzer G, Van Loosdrecht MCM. Enrichment of a mixed bacterial culture with a high polyhydroxyalkanoate storage capacity. Biomacromolecules. 2009;10:670–6. American Chemical Society
34. Rinke C, Schwientek P, Sczyrba A, Ivanova NN, Anderson IJ, Cheng J-F, et al. Insights into the phylogeny and coding potential of microbial dark matter. Nature. 2013;499:431–7.
35. Kuenen JG. Continuous cultures (Chemostats). Reference Module in Biomedical Sciences. Philadelphia: Elsevier; 2015. 2015
36. Lalucat J, Bennasar A, Bosch R, García-Valdés E, Palleroni NJ. Biology of *Pseudomonas stutzeri*. Microbiol Mol Biol Rev. 2006;70:510–47.
37. Sorokin DY, Teske A, Robertson LA, Kuenen JG. Anaerobic oxidation of thiosulfate to tetrathionate by obligately heterotrophic

bacteria, belonging to the *Pseudomonas stutzeri* group. FEMS Microbiol Ecol. 1999;30:113–23.
38. Pichinoty F, Mandel M, Greenway B, Garcia J-L. Isolation and properties of a denitrifying bacterium related to *Pseudomonas lemoignei*. Int J Syst Bacteriol. 1977;27:346–8.
39. Desloover J, Roobroeck D, Heylen K, Puig S, Boeckx P, Verstraete W, et al. Pathway of nitrous oxide consumption in isolated *Pseudomonas stutzeri* strains under anoxic and oxic conditions. Environ Microbiol. 2014;16:3143–52.
40. Jones CM, Welsh A, Throbäck IN, Dörsch P, Bakken LR, Hallin S. Phenotypic and genotypic heterogeneity among closely related soil-borne N_2- and N_2O-producing *Bacillus* isolates harboring the *nosZ* gene. FEMS Microbiol Ecol. 2011;76:541–52.
41. Graf DRH, Zhao M, Jones CM, Hallin S. Soil type overrides plant effect on genetic and enzymatic N_2O production potential in arable soils. Soil Biol Biochem. 2016;100:125–8.
42. Zhao M, Jones CM, Meijer J, Lundquist PO, Fransson P, Carlsson G, et al. Intercropping affects genetic potential for inorganic nitrogen cycling by root-associated microorganisms in *Medicago sativa* and *Dactylis glomerata*. Appl Soil Ecol. 2017;119:260–6.
43. Strohm TO, Griffin B, Zumft WG, Schink B. Growth yields in bacterial denitrification and nitrate ammonification. Appl Environ Microbiol. 2007;73:1420–4.
44. Sullivan MJ, Gates AJ, Appia-Ayme C, Rowley G, Richardson DJ. Copper control of bacterial nitrous oxide emission and its impact on vitamin B12-dependent metabolism. Proc Natl Acad Sci USA. 2013;110:19926–31.
45. Bergaust L, van Spanning RJM, Frostegård A, Bakken LR. Expression of nitrous oxide reductase in *Paracoccus denitrificans* is regulated by oxygen and nitric oxide through FnrP and NNR. Microbiology. 2012;158:826–34.
46. Qu Z, Bakken LR, Molstad L, Frostegård Å, Bergaust L. Transcriptional and metabolic regulation of denitrification in *Paracoccus denitrificans* allows low but significant activity of nitrous oxide reductase under oxic conditions. Environ Microbiol. 2015;18:2951–63. https://doi.org/10.1111/1462-2920.13128.
47. Park D, Kim H, Yoon S. Nitrous oxide reduction by an obligate aerobic bacterium, *Gemmatimonas aurantiaca* strain T-27. Appl Environ Microbiol. 2017;83:e00502–17.
48. Baker BJ, Lazar CS, Teske AP, Dick GJ. Genomic resolution of linkages in carbon, nitrogen, and sulfur cycling among widespread estuary sediment bacteria. Microbiome. 2015;3:14.

Table S1 Chemostat operational conditions prior to the experimental period presented in the main text. pH 7, 20°C. D= dilution rate

Day	Mode	D (h^{-1})	Limiting nutrient
0-5	Start up- Batch operation	---	---
5-18	Step-wise increase of D	0.028; 0.042	Acetate
18-90	Continuous	0.083	Acetate
90-118	Continuous	0.083	N_2O

Table S2 Primers and thermal cycling conditions for quantification and sequencing of 16S rRNA, *nosZ*I and *nosZ*II genes. Eff = efficiency qPCR reaction

Genes Primer names	**Sequences** (5'-3')	**References**	**Thermal cycling**	**Eff**
16S rRNA			(95°C, 7 min) x 1	
341F	CCT ACG GGA GGC AGC AG	López-Gutiérrez *et al.*, 2004	(95°C, 15 s; 60°C, 30 s; 72°C, 30 s; 80°C, 30 s) x 35	93%
534R	ATT ACC GCG GCT GCT GGC A		(95°C, 15 s;(60 to 95° C, 10 s, increment 0.5°)), x 1	
nirK			(95°C, 7 min) x 1	
876F	ATYGGCGGVCAYGGCGA	Henry *et al.*, 2004	(95°C, 15s;(63°C – 58°C, -1°/cycle), 30s; 72°C, 30s) x6	85%
R3Cu	GCCTCGATCAGRTTGTGGTT	Hallin and Lindgren, 1999	(95°C, 15 s; 58°C, 30 s; 72°C, 30 s; 80°C, 30 s) x 35	
			(95°C, 15 s;(60 to 95° C, 10 s, increment 0.5°)), x 1	
nirS			(95°C, 7 min) x 1	
cd3aFm	AACGYSAAGGARACSGG	Throbäck *et al.*, 2004	(95°C, 15s;(65°C – 60°C, -1°/cycle), 30s; 72°C, 30s) x6	65%
R3cdm	GASTTCGGRTGSGTCTTSAYGAA		(95°C, 15 s; 60°C, 30 s; 72°C, 30 s; 80°C, 30 s) x 35	
			(95°C, 15 s;(60 to 95° C, 10 s, increment 0.5°)), x 1	
nosZI			(95°C, 7 min) x 1	
1840F	CGC RAC GGC AAS AAG GTS MSS GT	Henry *et al.*, 2004	(95°C, 15s;(65°C – 60°C, -1°/cycle), 30s; 72°C, 30s) x6	78%
2090R	CAK RTG CAK SGC RTG GCA GAA		(95°C, 15 s; 60°C, 30 s; 72°C, 30 s; 80°C, 30 s) x 35	
			(95°C, 15 s;(60 to 95° C, 10 s, increment 0.5°)), x 1	
nosZII			(95°C, 7 min) x 1	
nosZII-F	CTI GGI CCI YTK CAY AC	Jones *et al.*, 2013	(95°C, 15 s; 54°C, 30 s; 72°C, 30 s; 80°C, 30 s) x 40	70%
nosZII-R	GCI GAR CAR AAI TCB GTR C		(95°C, 15 s;(60 to 95° C, 10 s, increment 0.5°)), x 1	
16S rRNA (sequencing)			(98°C, 3 min) x 1	
Pro341F	CCTACGGGNBGCASCAG	Takahashi *et al.*, 2014	(98°C, 30 s; 55°C, 30 s; 72°C, 30 s) x 25+8	
Pro805R	GACTACNVGGGTATCTAATCC		(72°C , 10 min) x 1	
nosZI (sequencing)			(95°C, 7 min) x 1	
nosZF1mod2	CGC TST TYM TIG AYA GYC AG	Philippot *et al.*, 2013 (mod.)	(95°C, 45 s; 54°C, 60 s; 72°C, 60 s) x 20+20	
nosZ2Rmod	CAK RTG CAI SGC RTG GCA GAA		(72°C , 10 min) x 1	
nosZII (sequencing)			(95°C, 7 min) x 1	
nosZII-F	CTI GGI CCI YTK CAY AC	Jones *et al.*, 2013	(95°C, 45 s; 54°C, 60 s; 72°C, 60 s) x 20+15	
nosZII-R	GCI GAR CAR AAI TCB GTR C		(72°C , 10 min) x 1	

Table S3 Probes used in FISH analysis of the culture

Probe	Sequence (5'→ 3')	Dye	Specificity	Ref
Eub338mix	gc**w**gcc**w**cccgtagg**w**gt	Cy5	Most bacteria	Amann *et al.* (1990); Daims *et al.* (1999)
Gam42a	gccttcccacatcgttt	Fluos/Cy3	Gammaproteobacteria	Manz *et al.* (1992)
Bet42a	gccttcccacttcgttt	Cy3/Fluos	Betaproteobacteria	Manz *et al.* (1992)

Table S4 Assigned taxonomy for the main 16S rRNA-based OTUs using the Silva database. The main OTUs were considered to be those with >10% sequences on any given sampling date, also see figure 2

OTU	Kingdom	Phylum	Class	Order	Family	Genus	Identity (%)
1	Bacteria	Proteobacteria	Gammaproteobacteria	Pseudomonales	*Pseudomonadaceae*	*Pseudomonas*	98.9
2	Bacteria	Gracilibacteria					94.8
3	Bacteria	Proteobacteria	Betaproteobacteria	Rhodocyclales	*Rhodocyclaceae*	*Azoarcus*	98.5
4	Bacteria	Proteobacteria	Betaproteobacteria	Rhodocyclales	*Rhodocyclaceae*		99.4
5	Bacteria	Proteobacteria	Betaproteobacteria	Burkholderiales	*Comamonadaceae*		98.1
6	Bacteria	Proteobacteria	Alphaproteobacteria	Rhodobacterales	*Rhodobacteraceae*	*Paracoccus*	98.2
7	Bacteria	Proteobacteria	Alphaproteobacteria	Rhizobiales	*Rhizobiaceae*	*Rhizobium*	98.2
8	Bacteria	Proteobacteria	Flavobacteria	Flavobacteriales	*Flavobacteriaceae*		95.7
9	Bacteria	Proteobacteria	Alphaproteobacteria	Rhodobacterales	*Rhodobacteraceae*		95.9
10	Bacteria	Proteobacteria	Flavobacteria	Flavobacteriales	*Flavobacteriaceae*	*Flavobacterium*	98.7
12	Bacteria	Proteobacteria	Betaproteobacteria	Burkholderiales	*Comamonadaceae*		99.4
13	Unclassified						83.0
14	Bacteria	Gracilibacteria					82.8
16	Bacteria	Proteobacteria	Flavobacteria	Flavobacteriales	*Flavobacteriaceae*	*Moheibacter*	93.9
18	Bacteria	Proteobacteria	Betaproteobacteria	Rhodocyclales	*Rhodocyclaceae*		97.0
19	Unclassified						85.2
22	Unclassified						93.2

Table S5 Assigned taxonomy for the main 16S rRNA-based OTUs (those with >10% sequences) of the activated sludge inocula using the Silva database

OTU	Kingdom	Phylum	Class	Order	Family	Genus	Identity (%)
4	Bacteria	Proteobacteria	Betaproteobacteria	Rhodocyclales	*Rhodocyclaceae*		99.4
12	Bacteria	Proteobacteria	Betaproteobacteria	Burkholderiales	*Comamonadaceae*		99.4
20	Bacteria	Proteobacteria	Flavobacteriia	Flavobacteriales	*Flavobacteriaceae*	*Cloacibacterium*	99.3
42	Bacteria	Bacteroidetes	Bacteroidia	Bacteroidales	*Porphyromonadaceae*	*Macellibacteroides*	98.7
62	Bacteria	Proteobacteria	Flavobacteriia	Flavobacteriales	*Flavobacteriaceae*	*Flavobacterium*	98.3
71	Bacteria						98.6
92	Bacteria	Proteobacteria	Betaproteobacteria	Burkholderiales	*Comamonadaceae*		99.1
98	Bacteria	Firmicutes	Bacilli	Lactobacillales	*Carnobacteriaceae*	*Trichococcus*	99.4
102	Bacteria	Proteobacteria	Flavobacteriia	Flavobacteriales	*Flavobacteriaceae*	*Flavobacterium*	98.9
107	Bacteria	Proteobacteria	Gammaproteobacteria	Pseudomonales	*Moraxellaceae*	*Acinetobacter*	99.1
122	Bacteria	Proteobacteria	Betaproteobacteria	Burkholderiales	*Comamonadaceae*	*Aquabacterium*	99.6
140	Bacteria	Chloroflexi					96.8
142	Bacteria	Nitrospirae	Nitrospira	Nitrospirales	*Nitrospiraceae*	*Nitrospira*	99.6
143	Bacteria	Proteobacteria	Betaproteobacteria	Burkholderiales	*Comamonadaceae*	*Acidovorax*	99.6
164	Bacteria	Proteobacteria	Betaproteobacteria	Rhodocyclales	*Rhodocyclaceae*	*Zooglea*	97.4
207	Bacteria	Proteobacteria	Betaproteobacteria	Burkholderiales	*Comamonadaceae*		98.7
312	Bacteria	Bacteroidetes	Shingobacteriia	Sphingobacteriales	*Saprospiraceae*		99.3
314	Bacteria	Actinobacteria	Acidimicrobiia	Acidomicrobiales			95.3
316	Bacteria	Actinobacteria	Actinobacteria	Micrococcales	*Instrasporangiaceae*		98.7
323	Bacteria	Bacteroidetes	Shingobacteriia	Sphingobacteriales	*Saprospiraceae*		89.4
328	Bacteria	Proteobacteria	Betaproteobacteria				98.7
832	Bacteria	Proteobacteria	Betaproteobacteria	Rhodocyclales	*Rhodocyclaceae*	*Zooglea*	98.5
15503	Bacteria	Proteobacteria	Flavobacteriia	Flavobacteriales	*Flavobacteriaceae*	*Flavobacterium*	97.2
15554	Bacteria	Proteobacteria	Flavobacteriia	Flavobacteriales	*Flavobacteriaceae*	*Flavobacterium*	98.0

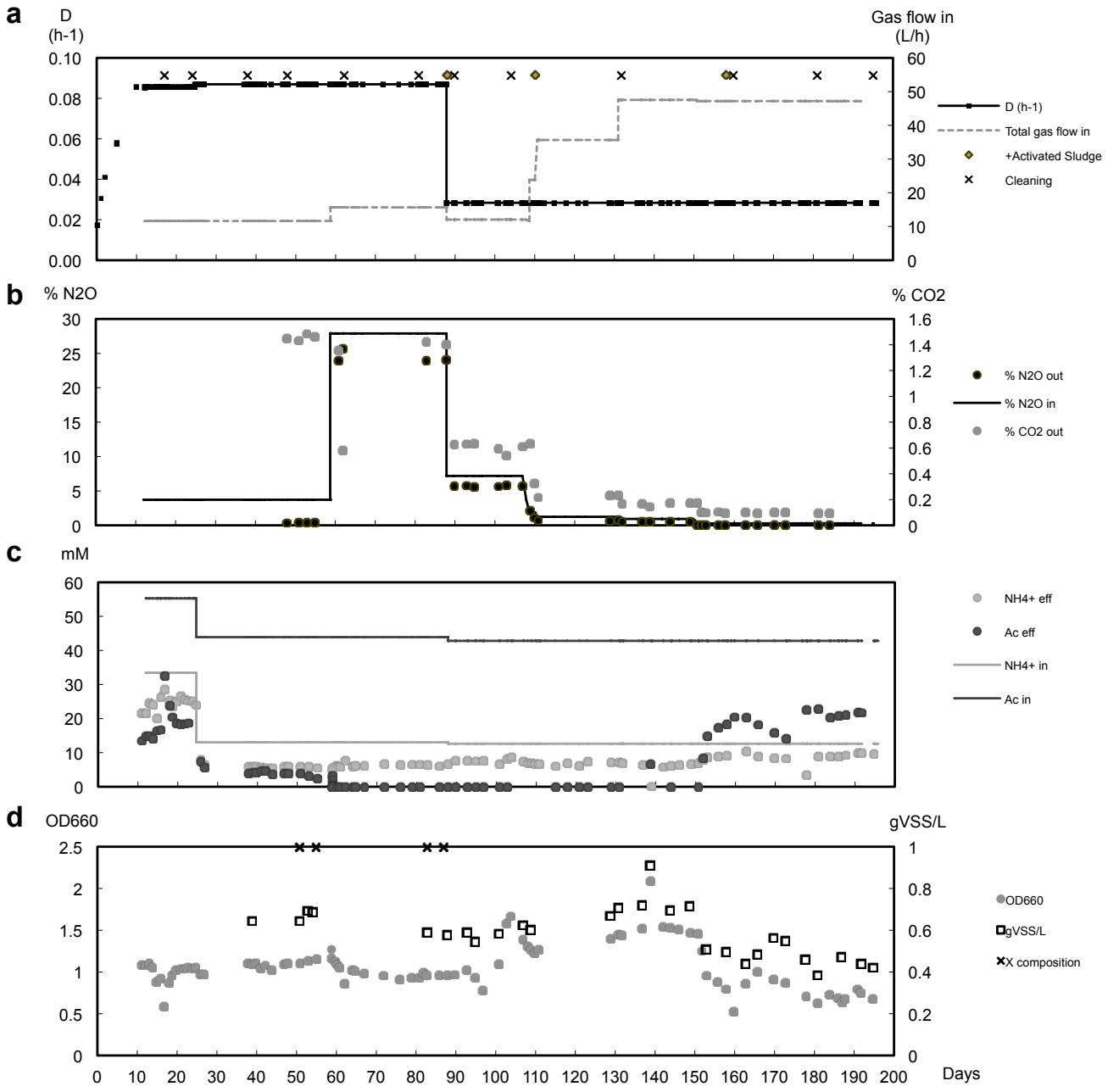

Figure S1 Chemostat operation over 195 days showing (**a**) dilution rate (D), total gas flow, (**b**) N_2O concentration in the in-gas, N_2O and CO_2 concentrations in the off-gas, (**c**) incoming and outgoing acetate and NH_4^+ concentrations, and (**d**) biomass concentration and optical density of the culture. The time points at which the reactor was cleaned or re-inoculated with activated sludge are indicated, as well as the points in which biomass samples were collected to determine the nitrogen content of the culture.

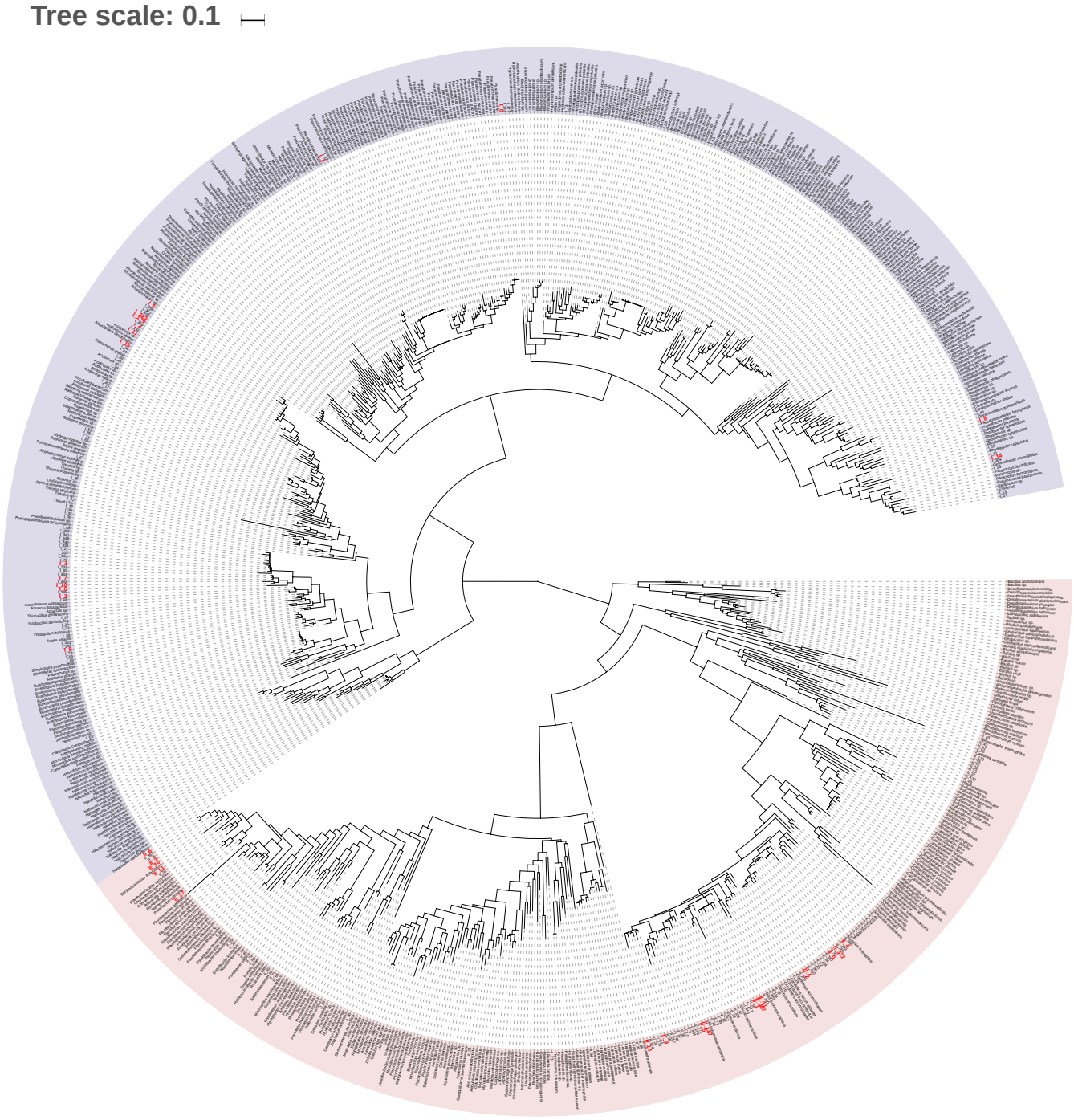

Figure S2. Phylogenetic tree of genomic *nosZ* reference sequences and representative sequences of the OTUs. The two clades are indicated in blue (clade I) and pink (clade II). The major OTUs found in the enrichment are highlighted in red.

Table S6 Reported biomass yields of pure cultures during N_2O respiration in batch experiments with acetate as carbon and energy source. To obtain the yield in C mole biomass per mole N_2O, a molecular weight of 24.63 mg per C-mmol of biomass was assumed according to the biomass composition formula in Roels 1980.

Reference	Strain	Y_{XN2O}	
		mg biomass/mmol N_2O	CmolX/molN_2O
Yoon *et al.* 2016	*Pseudomonas stutzeri* DCP-Ps1	7,24	0,29
	Shewanella loihica	6,31	0,26
	Dechloromonas aromatica	10,2	0,41
	Anaeromyxobacter dehalogenans 2CP-C	11,2	0,45
Sanford *et al.* 2012	*Anaeromyxobacter dehalogenans* 2CP-C	6,4	0,26
	Pseudomonas stutzeri DCP-Ps1	4,3	0,17
Strohm *et al*. 2007	*Pseudomonas stutzeri*	5,5	0,22
	Paracoccus denitrificans	3,15	0,13

Characterization of the activated sludge samples used for inoculation

The two activated sludge samples used as inocula were different in terms of overall bacterial abundance and community composition (**Figures S2** and **S3**). The two clades of *nosZ* genes were equally abundant in the activated sludge sample from Harnashpolder, while in the Dokhaven sample *nosZ* clade I had approximately one order of magnitude higher gene copy number than clade II (**Figure S3**). In both samples, *nirS* was roughly two orders of magnitude more abundant than *nirK*. As expected, both the *nosZ* clade I and II and the 16S rRNA-based community composition was more complex in the activated sludge samples as compared to the enrichment. The community of Dokhaven was dominated by 16S rRNA OTUs related to Betaproteobacteria and Bacteroidetes, whereas the main OTU in the activated sludge of Harnashpolder was closely related to uncultured Bacteria and the remaining sequences clustered in a diverse range of OTUs related to Actinobacteria, Nitrospirae, Firmicutes, Chloroflexi, Bacteroidetes and Betaproteobacteria. The majority of *nosZ* clade I OTUs were similar to *nosZ* in Betaproteobacteria of the Comamonadaceae and Rhodocyclaceae families in both samples, but they differed regarding the composition of the *nosZ* clade II communities. In Dokhaven, the main OTUs were placed among *Rhodocyclaceae* sequences, while the OTUs of the Harnaschpolder AS were much more diverse, with significant amounts of *nosZ* related to *nosZ* in *Caldilineaceae* (Chloroflexi) and Gemmatimonadaceae.

Figure S3 (next page) Characterization of the activated sludge inocula from the wastewater treatment plants of Harnaschpolder and Dokhaven used for inoculation. (**a**) Abundances of *nosZI*, *nosZII*, *nirS*, *nirK* and 16S rRNA genes, (**b**) relative abundances of the 16S rRNA OTUs, (**c**) *nosZ* clade I OTUs and (**d**) *nosZ* clade II OTUs. Sequences labeled OTHER correspond to OTUs making up less than 10% of the sequences. The activated sludge from Harnaschpolder was sampled in February 2015 and that from Dokhaven in June 2015 from the B-stage.

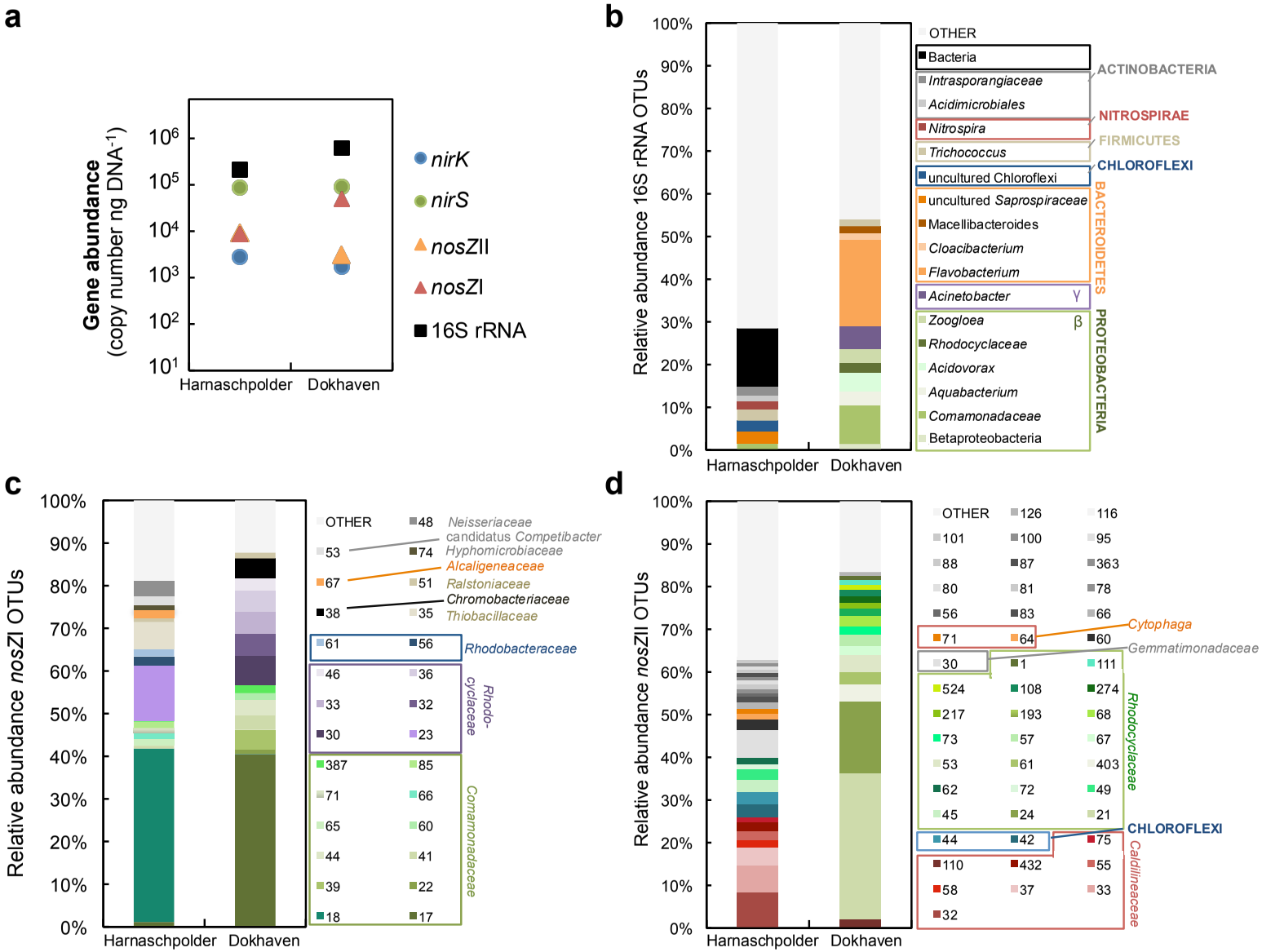
a
Gene abundance
(copy number ng DNA-1)
10^6
10^5
10^4
10^3
10^2
10^1
Harnaschpolder
Dokhaven
nirK
nirS
nosZII
nosZI
16S rRNA
b
Relative abundance 16S rRNA OTUs
100%
90%
80%
70%
60%
50%
40%
30%
20%
10%
0%
Harnaschpolder
Dokhaven
OTHER
Bacteria
Intrasporangiaceae
Acidimicrobiales
Nitrospira
Trichococcus
uncultured Chloroflexi
uncultured Saprospiraceae
Macellibacteroides
Cloacibacterium
Flavobacterium
Acinetobacter
Zoogloea
Rhodocyclaceae
Acidovorax
Aquabacterium
Comamonadaceae
Betaproteobacteria
ACTINOBACTERIA
NITROSPIRAE
FIRMICUTES
CHLOROFLEXI
BACTEROIDETES
γ
β
PROTEOBACTERIA
c
Relative abundance nosZI OTUs
100%
90%
80%
70%
60%
50%
40%
30%
20%
10%
0%
Harnaschpolder
Dokhaven
OTHER
48
53
74
67
51
38
35
61
56
46
36
33
32
30
23
387
85
71
66
65
60
44
41
39
22
18
17
Neisseriaceae
candidatus Competibacter
Hyphomicrobiaceae
Alcaligeneaceae
Ralstoniaceae
Chromobacteriaceae
Thiobacillaceae
Rhodobacteraceae
Rhodo-cyclaceae
Comamonadaceae
d
Relative abundance nosZII OTUs
100%
90%
80%
70%
60%
50%
40%
30%
20%
10%
0%
Harnaschpolder
Dokhaven
OTHER
126
116
101
100
95
88
87
363
80
81
78
56
83
66
71
64
60
30
1
111
524
108
274
217
193
68
73
57
67
53
61
403
62
72
49
45
24
21
44
42
75
110
432
55
58
37
33
32
Cytophaga
Gemmatimonadaceae
Rhodocyclaceae
CHLOROFLEXI
Caldilineaceae

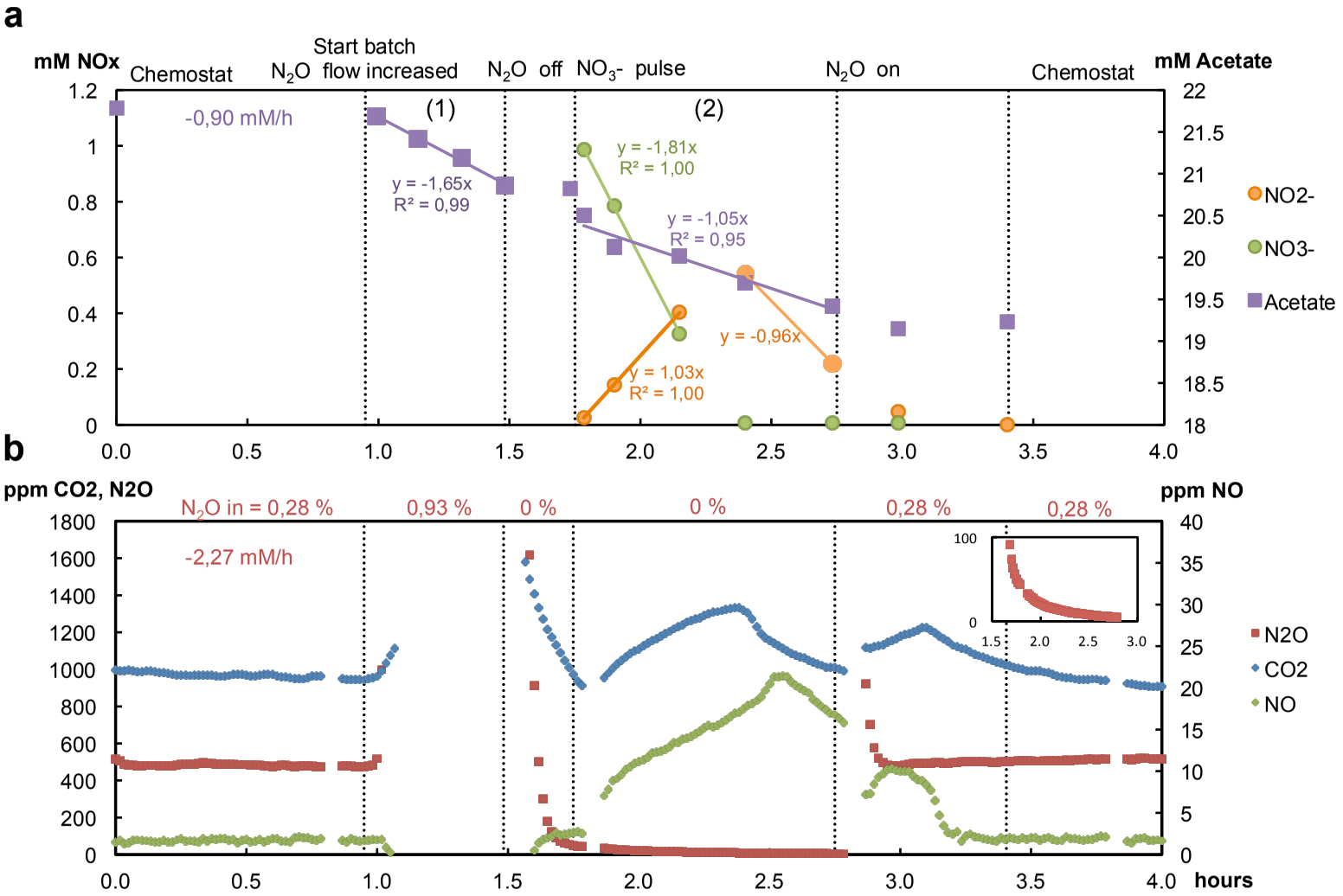

Figure S4 Semi-batch experiments on day 192 of the chemostat enrichment operation. The influent and effluent pumps of the chemostat were stopped during the batch tests, but flushing with N_2 gas was kept constant (at 800ml/min). N_2O sparging in the reactor was initially increased to obtain maximum conversion rates on N2O (1), then completely stopped for a NO_3^- consumption experiment (2), and re-started after NO_3^- was depleted. (**a**) Acetate, nitrate (NO_3^-) and nitrite (NO_2^-) concentrations in the reactor during batch tests. The rates of acetate and nitrate consumption, and nitrite production and consumption are indicated in the graph (in mM/h). (**b**) N_2O, CO_2 and NO concentration in the offgas. Concentrations of N_2O, NO and CO_2 in the headspace of the reactor were monitored with an infrared gas analyzer.

Eub338mix – Cy5 (→blue) Beta42a – Cy3 (→green) Gamma42a – FLUOS (→pink)	Eub338mix – Cy5 (→blue) Beta42a - FLUOS (→pink) Gamma42a – Cy3 (→green)
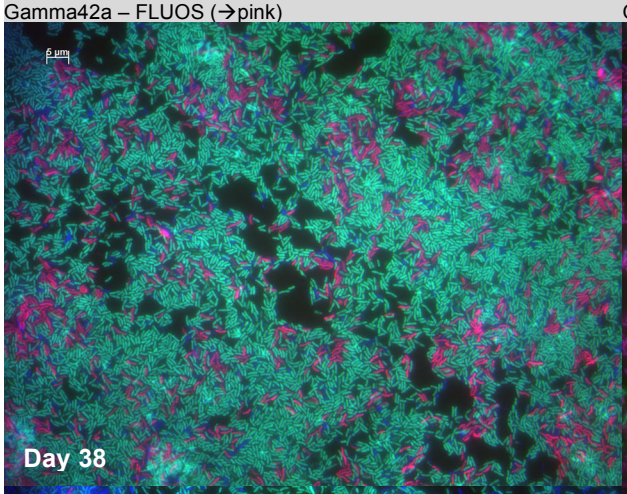	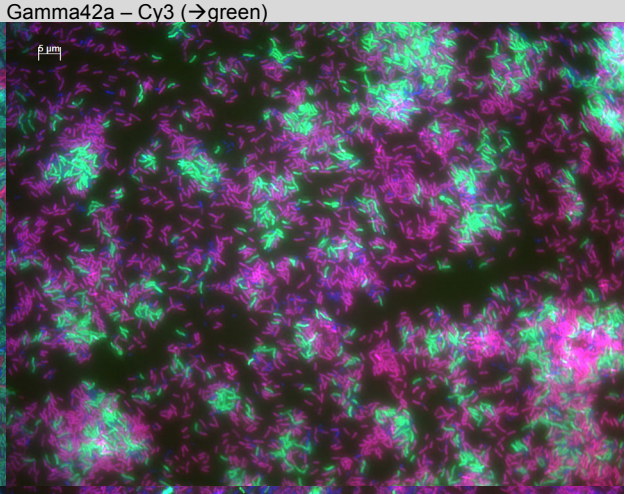
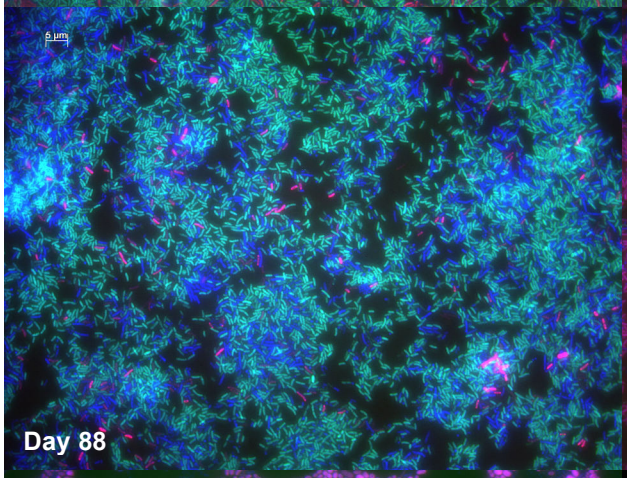	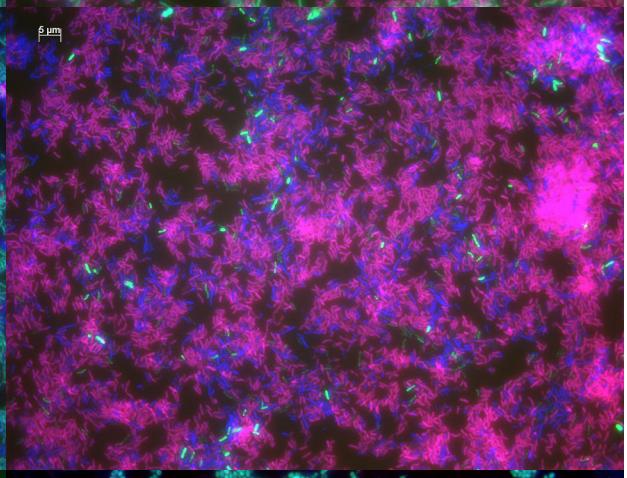
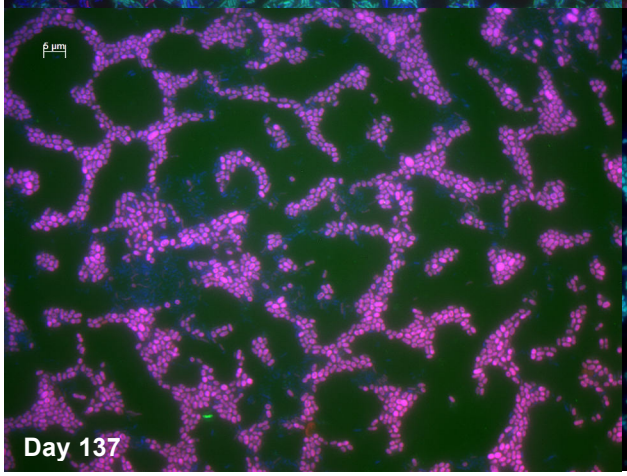	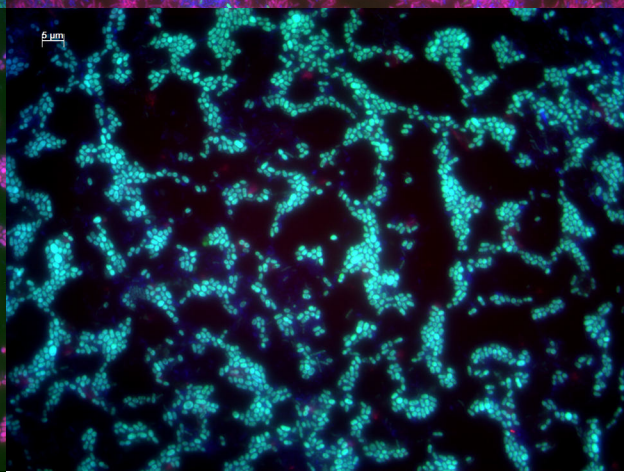

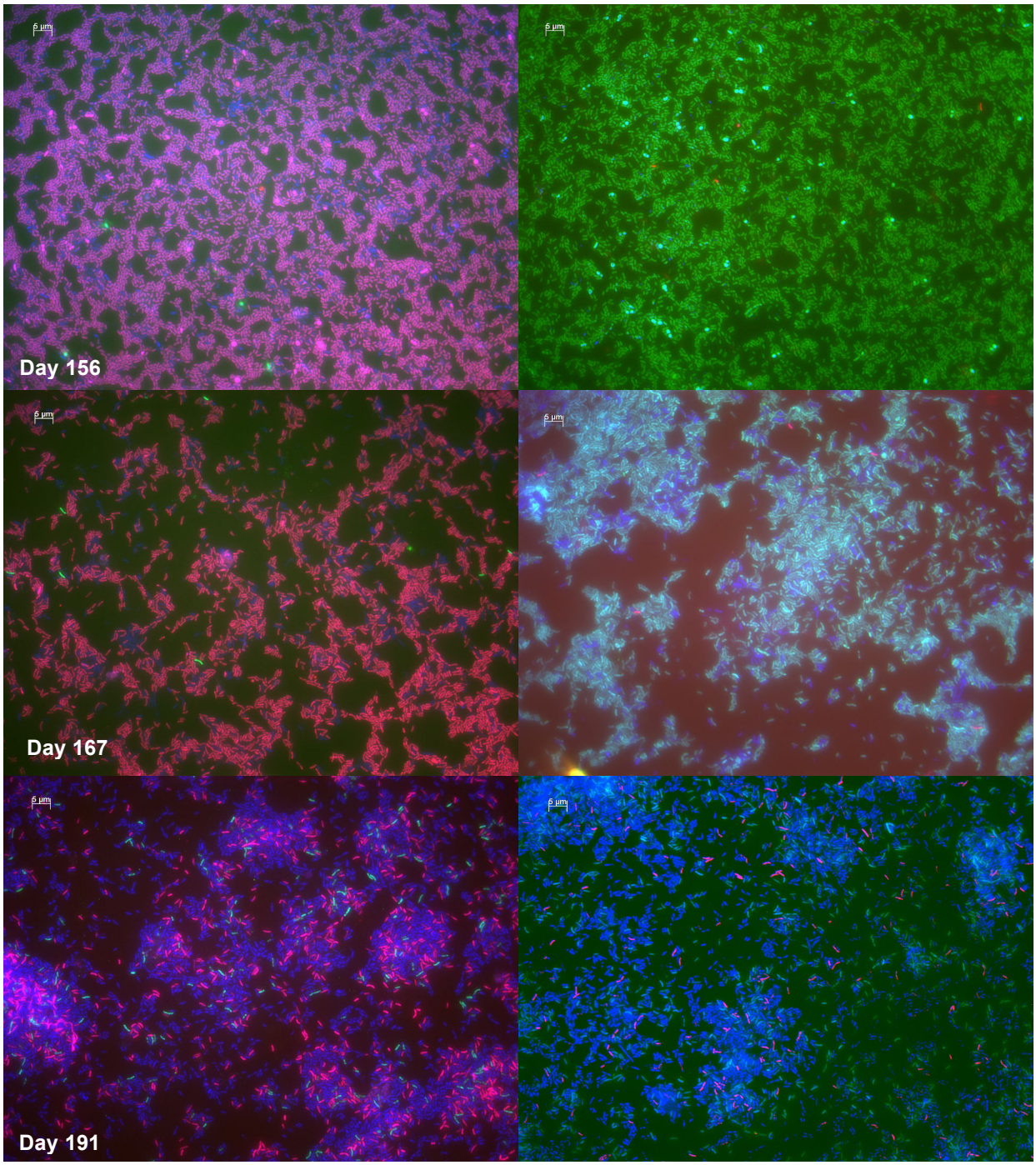

Figure S5 FISH images of the culture on days 38, 88, 137, 156, 167 and 191 of operation stained with Cy5-labeled probe for bacteria (EUB338 mix, blue), fluorescein-labeled probe for most gammaproteobacteria (Gamma42a, red) and Cy3-labeled probe for most betaproteobacteria (Beta42a, green) on the left column, and fluorescein-labeled probe Beta42a and Cy3-labeled Gamma42a, on the right column. Blue color indicates only EUB338mix hybridized. The pink color indicates both EUB338mix and Gamma42a/Beta42a hybridized.

References

Amann, R.I., Binder, B.J., Olson, R.J., Chisholm, S.W., Devereux, R., and Stahl, D.A. (1990) Combination of 16S rRNA-targeted oligonucleotide probes with flow cytometry for analyzing mixed microbial populations. *Appl. Environ. Microbiol*. **56**: 1919–25.

Hallin, S. and Lindgren, P.-E. (1999) PCR Detection of Genes Encoding Nitrite Reductase in Denitrifying Bacteria. *Appl. Envir. Microbiol.* **65**: 1652–1657.

Henry, S., Baudoin, E., López-Gutiérrez, J.C., Martin-Laurent, F., Brauman, A., and Philippot, L. (2004) Quantification of denitrifying bacteria in soils by *nirK* gene targeted real-time PCR. *J. Microbiol. Methods* **59**: 327–35.

Jones, C.M., Graf, D.R.H., Bru, D., Philippot, L., and Hallin, S. (2013) The unaccounted yet abundant nitrous oxide-reducing microbial community: a potential nitrous oxide sink.*ISME J.* **7**: 417–26.

López-Gutiérrez, J.C., Henry, S., Hallet, S., Martin-Laurent, F., Catroux, G., and Philippot, L. (2004) Quantification of a novel group of nitrate-reducing bacteria in the environment by real-time PCR. *J. Microbiol. Methods* **57**: 399–407.

Manz, W., Amann, R., Ludwig, W., Wagner, M., and Schleifer, K.-H. (1992) Phylogenetic Oligodeoxynucleotide Probes for the Major Subclasses of Proteobacteria: Problems and Solutions. *Syst. Appl. Microbiol*. **15**: 593–600.

Philippot, L., Spor, A., Hénault, C., Bru, D., Bizouard, F., Jones, C.M., et al. (2013) Loss in microbial diversity affects nitrogen cycling in soil. *ISME J.* **7**: 1609–19.

Roels JA. (1980). Simple model for the energetics of growth on substrates with different degrees of reduction. *Biotechnol Bioeng* **22**: 33–53.

Sanford, R.A., Wagner, D.D., Wu, Q., Chee-Sanford, J.C., Thomas, S.H., Cruz-García, C., et al. (2012) Unexpected nondenitrifier nitrous oxide reductase gene diversity and abundance in soils. *Proc. Natl. Acad. Sci. U. S. A*. **109**: 19709–14.

Strohm, T.O., Griffin, B., Zumft, W.G., and Schink, B. (2007) Growth yields in bacterial denitrification and nitrate ammonification. *Appl. Environ. Microbiol*. **73**: 1420–4.

Takahashi, S., Tomita, J., Nishioka, K., Hisada, T., and Nishijima, M. (2014) Development of a Prokaryotic Universal Primer for Simultaneous Analysis of Bacteria and Archaea Using Next Generation Sequencing. *PLoS One*. **9**: e105592.

Throbäck, I.N., Enwall, K., Jarvis, A., and Hallin, S. (2004) Reassessing PCR primers targeting *nirS*, *nirK* and *nosZ* genes for community surveys of denitrifying bacteria with DGGE. *FEMS Microbiol. Ecol.* **49**: 401–17.

Yoon, S., Nissen, S., Park, D., Sanford, R.A., and Löffler, F.E. (2016) Nitrous Oxide Reduction Kinetics Distinguish Bacteria Harboring Clade I NosZ from Those Harboring Clade II NosZ. *Appl. Environ. Microbiol*. **82**: 3793–800.

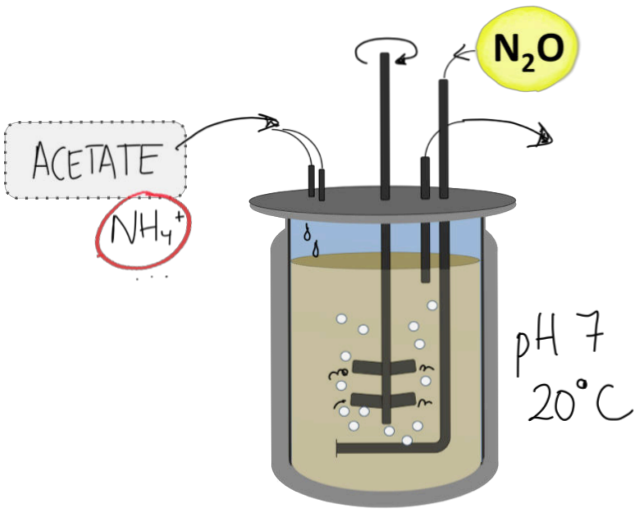
N_2O
ACETATE
NH_4^+
pH 7
20°C

3

Growth yield and selection of *nosZ* clade II-types in a continuous enrichment culture of N_2O respiring bacteria

Conthe M, Wittorf L, Kuenen JG, Kleerebezem R, Hallin S, van Loosdrecht MCM.

Environ Microbiol Rep (2018) **10**: 239–244.

+ SUPPLEMENTARY INFORMATION

Environmental Microbiology Reports (2018) **10**(3), 239–244 doi:10.1111/1758-2229.12630

Growth yield and selection of *nosZ* clade II types in a continuous enrichment culture of N_2O respiring bacteria

Monica Conthe,[1]* Lea Wittorf,[2] J. Gijs Kuenen,[1] Robbert Kleerebezem,[1] Sara Hallin[2] and Mark C.M. van Loosdrecht[1]

[1]*Department of Biotechnology, Delft University of Technology, Delft, The Netherlands.*

[2]*Department of Forest Mycology and Plant Pathology, Swedish University of Agricultural Sciences, Uppsala, Sweden.*

Summary

Nitrous oxide (N_2O) reducing microorganisms may be key in the mitigation of N_2O emissions from managed ecosystems. However, there is still no clear understanding of the physiological and bioenergetic implications of microorganisms possessing either of the two N_2O reductase genes (*nosZ*), clade I and the more recently described clade II type *nosZ*. It has been suggested that organisms with *nosZ* clade II have higher growth yields and a lower affinity constant (K_s) for N_2O. We compared N_2O reducing communities with different *nosZ*I/*nosZ*II ratios selected in chemostat enrichment cultures, inoculated with activated sludge, fed with N_2O as a sole electron acceptor and growth limiting factor and acetate as electron donor. From the sequencing of the 16S rRNA gene, FISH and quantitative PCR of *nosZ* and *nir* genes, we concluded that betaproteobacterial denitrifying organisms dominated the enrichments with members within the family *Rhodocyclaceae* being highly abundant. When comparing cultures with different *nosZ*I/*nosZ*II ratios, we did not find support for (i) a more energy conserving N_2O respiration pathway in *nosZ* clade II systems, as reflected in the growth yield per mole of substrate, or (ii) a higher affinity for N_2O, defined by μ_{max}/K_s, in organisms with *nosZ* clade II.

Introduction

Nitrous oxide (N_2O) reducing microorganisms, both denitrifying and non-denitrifying, can contribute to the N_2O sink capacity of ecosystems and may be key in reducing emissions of this potent greenhouse gas (Hallin *et al.*, 2018). The phylogeny of the nitrous oxide reductase (NosZ), encoded by the *nosZ* gene, has two major clades, clade I and II (Jones *et al.*, 2013). A high abundance and diversity of N_2O reducing bacteria harboring *nosZ* clade II, in particular, has been linked to an increased N_2O reduction potential in soils as well as lower *in situ* N_2O emissions (Jones *et al.*, 2014; Domeignoz-Horta *et al.*, 2017), but a mechanistic explanation for this is lacking. *nosZ* clade I and clade II differ in (i) the co-occurrence with other denitrification genes, with *nosZ* clade II being more often associated to non-denitrifiers (Graf *et al.*, 2014) and (ii) the accessory proteins associated to the *nos* operon. For example, *nosR* and *nosB* genes encode proteins likely to be involved in electron transport to the NosZ of clade I and clade II respectively (Sanford *et al.*, 2012). It is not understood if these differences between the two types of NosZ, apparent on the genome level, result in a differentiation in the ecophysiology of N_2O reducers harboring either *nosZ* clade.

Physiological studies with clade II-type N_2O reducers are scarce, but Yoon and colleagues (2016) recently compared five N_2O reducing bacterial species and reported lower whole-cell half-saturation constants (K_s) for N_2O and up to 1.5 times higher biomass yields per mole of N_2O for the *nosZ* clade II N_2O reducers compared to those harboring *nosZ* clade I. A lower K_s would confer *nosZ* clade II N_2O reducers a selective advantage during competition for limiting amounts of N_2O, whereas a higher biomass yield implies a greater efficiency of energy conservation in the *nosZ* clade II-associated electron transport chain (ETC). Extra charge separations during N_2O reduction could hypothetically be mediated by the predicted transmembrane protein encoded by *nosB* present in *nosZ* clade II organisms. It is an attractive hypothesis that *nosZ*II-associated ETCs generate a greater proton motive force per electron accepted than the *nosZ*I equivalent, which would explain niche

Table 1. Conversion rates in the chemostats (negative numbers = consumption, positive = production) under N_2O limitation and carbon (C) and electron (e^-) balances over the conversions (mean ± SD, n = 5).

		Compound conversion rates (mmol h^{-1})							
	Dilution rate (h^{-1})	CH_3COO^-	N_2O	N_2	NH_4^+	$CH_{1.8}O_{0.5}N_{0.2}$	CO_2	C-bal (%)	e^--bal (%)
Conthe and colleagues (2018)[a]	0.027 ± 0.001	−1.78 ± 0.20	−5.09 ± 0.90	3.88 ± 0.81	−0.30 ± 0.01	1.14 ± 0.08	2.25 ± 0.13	93	97
This study	0.026 ± 0.001	−1.94 ± 0.10	−4.40 ± 0.09	4.34 ± 0.05	−0.39 ± 0.04	1.39 ± 0.15	2.27 ± 0.07	106 ± 12	104 ± 12

a. During period IV of operation.
b. After day 21.

differentiation between the two clades. To test the competition between *nosZ* clade I and clade II N_2O reducers, we recently analyzed the performance of an enrichment culture growing for a large number of generations with N_2O as the sole electron acceptor under different dilution rates and with either the electron donor (acetate) or N_2O as the limiting factor (Conthe *et al.*, 2018). Continuous systems with enrichment cultures are optimal to study the potential dichotomy in N_2O reducer ecophysiology, as it allows competition experiments based on the affinity for a limiting substrate within a fairly complex community and provides prolonged steady state conditions to obtain reliable biomass yields. Nevertheless, irrespective of whether N_2O or acetate was the growth limiting substrate in the culture, *nosZ* clade I N_2O reducers dominated the enrichment. This led us to reject the hypothesis that *nosZ* clade II-harboring organisms have a higher overall affinity for N_2O than organisms with *nosZ* clade I, with affinity being determined by the ratio of μ_{max} over K_s. Since we did not enrich for a significant community of *nosZ* clade II N_2O reducers under the different operational conditions, we were unable to compare growth yields amongst N_2O reducers of both clades (Conthe *et al.*, 2018). However, we did observe an increase in *nosZ* clade II when the dilution rate switched from high to low, which suggest that the μ_{max} was important in the selection of N_2O reducers.

The aim of the present study was to compare the results from the period with low dilution rate and N_2O limitation from our previous experiment with an independently enriched N_2O-fed chemostat culture subject to the same conditions. Even though a functional steady state had been achieved in the previous study, a steady state in terms of microbial community composition and *nosZ*II/*nosZ*I ratio had not. Additionally, the history of reactor operation likely affects the selection of community members, and in the present study, we directly started off with continuous operation under conditions of N_2O limitation and low dilution rate without a preceding period of higher dilution rate or acetate limiting conditions. With the new enrichment approach, the abundance of *nosZ* clade II bacteria was significantly increased, which allowed us to compare the thermodynamic efficiency of *nosZ* clade II- versus clade I-associated ETCs and to gain further insight into the role of the NosZ type in the microbial competition for N_2O. The abundance of N_2O reducers was determined using quantitative real-time PCR (qPCR) of *nosZ*I and *nosZ*II along with the nitrite reductase genes *nirS* and *nirK* characteristic of denitrifying organisms. Additionally, the 16S rRNA genes were sequenced to obtain the composition of the enriched community, and fluorescent *in situ* hybridization (FISH) with probes targeting Bacteria and

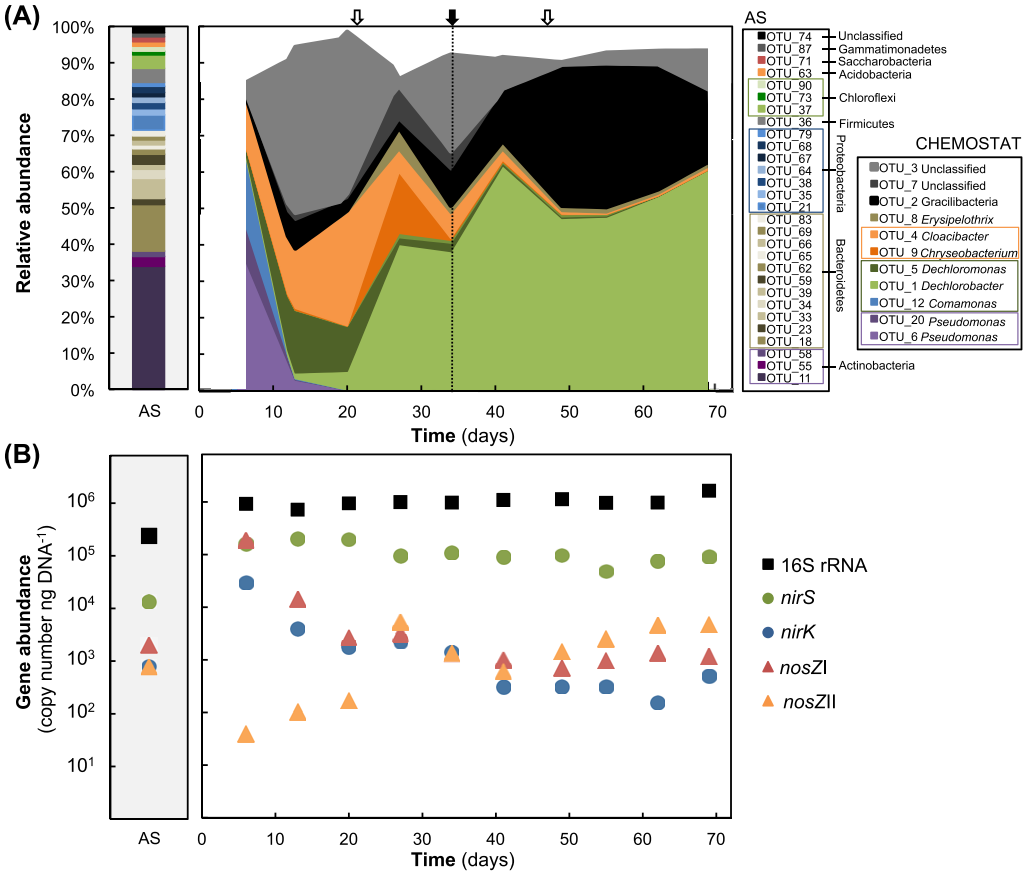

Fig. 1. Relative abundances of the 16S rRNA gene OTUs with > 5% of the sequences (A) and abundances of 16S rRNA and denitrification genes (B) in the activated sludge sample used as inoculum (AS) and in the enrichment culture throughout the operation of the chemostat. The white arrow on day 21 indicates when the influent pump tubing was changed, leading to a decrease in the dilution rate from 0.028 ± 0.001 to 0.026 ± 0.001, while the white arrow on day 47 indicates the switch from N_2 to Argon and recirculation of gas (200 ml min^{-1} of in-gas composed of Argon and N_2O with 700 ml min^{-1} of recycling, keeping the flow of N_2O constant). The black arrow indicates the time point corresponding to the FISH image (Fig. 2). Sequences are available at NCBI under BioProject accession number PRJNA430066. The procedures for DNA extraction, Illumina sequencing and bioinformatic analyses of 16S rRNA gene sequences as well as the qPCR of *nosZ* and *nir* genes can be found in Conthe and colleagues (2018). qPCR efficiencies were 97% for 16S rRNA, 80% for *nosZ*I, 87% for *nosZ*II, 93% for *nirK* and 75% for *nirS*.

Beta- and Gammaproteobacteria was performed to independently quantify the relative abundance of these taxa.

Results and discussion

Prolonged heterotrophic growth sustained by N_2O respiration

Activated sludge from the wastewater treatment plant of Harnaschpolder (the Netherlands) was used as the inoculum to enrich a microbial community growing with N_2O as the sole electron acceptor and using acetate as an electron donor at pH 7 and 20°C. After an initial batch start-up phase of 48 h, the culture was operated in continuous mode under N_2O limiting conditions during 72 days at a dilution rate of 0.027 h^{-1} (specifically at 0.028 ± 0.001 h^{-1} days 0–20 and 0.026 ± 0.001 h^{-1} days 21–72; Supporting Information Fig. S1). Nitrous oxide was supplied to the reactor at a constant rate (Supporting Information Fig. S1) and the reactor set-up, medium composition, operation and sampling are described in detail in Conthe and colleagues (2018). The microbial community was growing by N_2O reduction to N_2 at the expense of acetate oxidation, as confirmed by the elemental and electron balances (Table 1), with acetate present in excess throughout the operation (Supporting Information Fig. S1). The compound conversion rates were comparable to those obtained in our previous experiment, showing that the community functioning was similar in the two, independent enrichments (Table 1). To confirm that N_2O was growth limiting in the system, the N_2O sparging rate was increased, which resulted in an immediate increase in the biomass specific N_2O conversion rates (data not shown).

The N_2O reducing community was dominated by betaproteobacterial denitrifiers

The composition of the enrichment culture, sampled on 10 different days during chemostat operation, and of the activated sludge used as inoculum was determined by Illumina sequencing of the 16S rRNA gene (Fig. 1A and Supporting Information Tables S1 and S2). Bacteria belonging to the family *Rhodocyclaceae*, despite representing only a small percentage of sequences in the activated sludge inoculum, made up a significant part of the enrichment with a single OTU (1) covering 40 to 60% of the reads after day 30. However, FISH performed on day 34 suggests that the relative abundance of the dominant OTU, as reflected in the abundance of bacteria hybridizing with the betaproteobacterial probe, was even much higher than estimated by sequencing (70–90% of the biovolume *vs*. 40% of sequences; Fig. 2). As far as we could see, the cells stained with the betaproteobacterial probe had the same morphology. The initial decrease of *Pseudomonas* sp. and *Comamonas* sp. that dominated at the startup of the reactor operation was followed by an increase in *Cloacibacterium* sp., *Chryseobacterium* sp. and *Dechloromonas* sp. This shift in community composition coincided with a decrease in *nosZ* clade I abundance and an increase in *nosZ* clade II (Fig. 1B). In agreement, sequenced genomes of the genera *Pseudomonas* and *Comamonas* harbor clade I *nosZ*, whereas *Dechloromonas* sp. and N_2O reducers within *Flavobacteriaceae* harbor *nosZ* clade II. After day 20, *Rhodocyclaceae* (*Dechlorobacter* sp.) dominated the enrichment. Different species within the *Rhodocyclaceae* have been shown to harbor either *nosZ* clade I or II (Jones *et al*., 2014). The only sequenced genome of *Dechlorobacter* so far has a *nosZ* sequence similar to the *nosZ* clade I from *Rhodoferax ferrireducens* and *Ralstonia pickettii* (Conthe *et al*., 2018). However, while OTU 1 was assigned to *Dechlorobacter* when using the Silva taxonomy, it was assigned to the genus *Azonexus* when using the rdp classifier, and sequenced genomes of *Azonexus* harbor *nosZ* clade II rather than clade I. This makes it difficult to speculate about the type of *nosZ* associated to this OTU. Instead, the similar abundance of both *nosZ* types suggests that OTU 1 could be a mix of closely related species within the *Rhodocyclaceae* family. Interestingly, reads related to *nosZ* clade II from *Azonexus* dominated the *nosZ* clade II community in the previous experiment under the same conditions used in the present study, although the corresponding 16S rRNA gene sequences could only be assigned at the family level (Conthe *et al*., 2018). Bacteria of the genus *Pseudomonas*, *Comamonas* and *Dechloromonas*, as well as many *Rhodocyclaceae* also possess genetic potential for denitrification

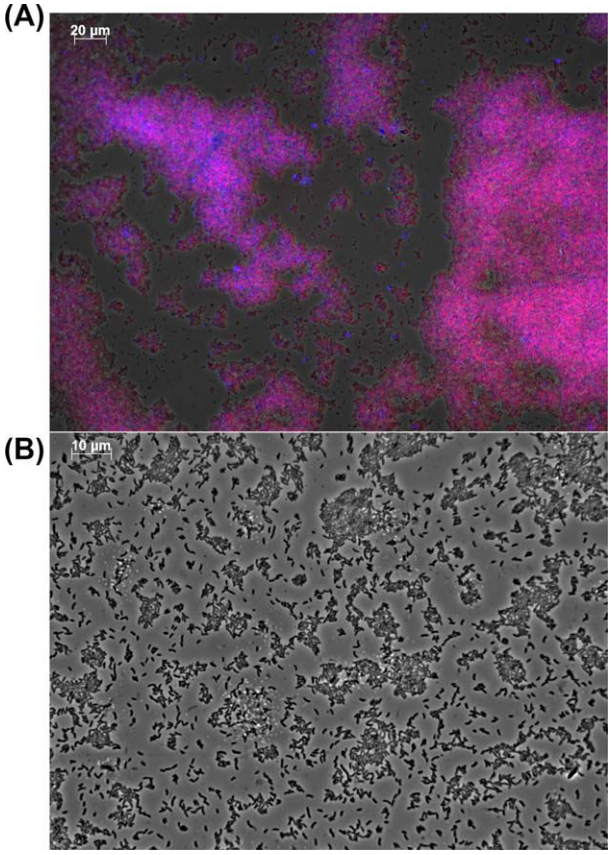

Fig. 2. FISH microscopic photographs of the enrichment.
A. FISH image (40×) of the culture on day 34 stained with a Cy5-labelled probe targeting Bacteria (EUB338, blue), a Cy3-labelled probe targeting Betaproteobacteria (Beta42a, red) and a FLUOS-labelled probe for Gammaproteobacteria (Gamma42a, green). Cells in blue only hybridized with EUB332, while cells in pink hybridized with both EUB338 and Beta42a. Gammaproteobacteria were absent from the culture. Details about the probes and protocol used for FISH can be found in Conthe and colleagues (2018).
B. 100× microscopic image of the cells.

(Graf *et al*., 2014), but for the *Cloacibacterium* sp. and *Chryseobacterium* sp. knowledge is limited. The *nir* genes, characteristic of denitrifying organisms, were highly abundant in the culture (Fig. 1B), indicating that the N_2O reducers dominating the enrichment were likely denitrifiers rather than non-denitrifying N_2O reducers. This shows that the availability of N_2O, even under N_2O limiting conditions, is not a selective driver for non-denitrifying N_2O reducers and highlights the strong competitive advantage of proteobacterial *nirS*-type denitrifiers under these conditions.

The vast majority of the community members were presumed to harbor the *nosZ* gene required for sustained growth on N_2O respiration, translated in similar abundances of *nosZ* and 16S rRNA genes. However, the total *nosZ* gene copy numbers were two to three orders of magnitude lower than that of the 16S rRNA genes and two orders lower than the abundance of *nir*

Table 2. Biomass yields and gene copy number ratios of the enrichment cultures.

			Gene copy number ratios[a]		
	Dilution rate (h^{-1})	Y_{XAc} CmolX/CmolAc	*nosZ*II/*nosZ*I	*nosZ*/*nir*[a]	*nosZ*/16S rRNA[b]
Conthe and colleagues (2018)[c]	0.027 ± 0.001	0.32 ± 0.04	0.005 ± 0.002	3.253 ± 2.220	0.542 ± 0.272
This study	0.026 ± 0.001	0.36 ± 0.04	3.025 ± 0.896	0.060 ± 0.026	0.004 ± 0.002

X = biomass; Y_{XAc} = biomass yield on acetate in carbon mole biomass produced (CmolX) per carbon mole of substrate consumed (CmolS).

a. From qPCR values averaged over relevant periods (days 49–69 in this study *vs.* days 163–195 in Conthe and colleagues 2018).

b. *nosZ* includes the sum of *nosZ*I and *nosZ*II gene copy number. *nir* includes the sum on *nirS* and *nirK* gene copy number.

c. During period IV of operation.

genes after the community shift on day 21 (Fig. 1B and Table 2). This is potentially due to an underestimation of *nosZ* genes or the presence of a population incapable of N_2O reduction that was not captured when sequencing the 16S rRNA gene. We also detected a relatively high abundance of the phylum Gracilibacteria and unclassified bacteria (Fig. 1A). The only genomes of Gracilibacteria available so far were obtained from single-cell sequencing of cells from the vicinity of hydrothermal vents of the East Pacific rise. Both of the two retrieved genomes are closely related, have low G + C content and are characterized as fermentative bacteria (Rinke *et al.*, 2013). They do not have any *nos* genes that would indicate capacity for N_2O reduction, although they have a nitric oxide reductase. They may have co-existed in the chemostat by living off products of cell lysis or cross-feeding with N_2O reducers. The Gracilibacteria were also present in the enrichment in Conthe and colleagues (2018).

nosZ *clade type is not a selective driver in the competition for* N_2O

The *nosZ*II/*nosZ*I abundance ratio in the present enrichment culture was higher compared to that reported by Conthe *et al.* despite similar operating conditions (Table 2). Differences in the bacterial community composition of the inoculum or in reactor operation history, as well as a certain degree of stochasticity to be expected during colonization of any ecosystem (Roeselers *et al.*, 2006), could explain the difference in community composition between the two enrichment cultures. However, the small difference in dilution rate between the studies (0.026 ± 0.001 in this study *vs.* 0.027 ± 0.001 in Conthe *et al.*, 2018) could be an explanation considering that the minor change in dilution rate on day 21 coincided with a dramatic shift in the composition of the bacterial community (Fig. 1). Changes in community composition, either due to minor operational differences or due to potential interactions among community members, suggest that the competitive differences between *nosZ* clade I and II are small during N_2O limiting conditions.

The fact that the relative abundance of the two clades differed substantially between the two independent enrichment cultures, while conversion rates and biomass yields were very similar (Tables 1 and 2), suggests that competition among community members was not driven by the type of NosZ and that the overall energy conservation was similar in *nosZ* clade I- and *nosZ* clade II-associated ETCs present in our system. Our finding that N_2O reduction kinetics and stoichiometric yields do not distinguish bacteria harboring NosZ clade I from those with NosZ clade II contradicts the study reporting lower whole-cell K_s values and 50–80% higher growth yields in *nosZ* clade II N_2O reducers compared to organisms with *nosZ* clade I during growth on N_2O as the sole electron acceptor (Yoon *et al.*, 2016). The species that were studied might not be representative for the extant diversity known for the two clades of NosZ and furthermore, the difference in apparent K_s among the clade II species was as large as the differences among the clade I species, suggesting that differences in affinity might be taxa dependent rather than between *nosZ* clade I and II organisms. We conclude that there is no simple answer explaining the divergence and ecological differences of the two clades of NosZ observed in several studies of soils, sediments and rhizosphere (e.g., Tsiknia *et al.*, 2015; Wittorf *et al.*, 2016; Graf *et al.*, 2016; Dini-Andreote *et al.*, 2016; Juhanson *et al.*, 2017).

Acknowledgements

This work was funded by the European Union (Marie Curie ITN NORA, FP7–316472) and the Swedish Research Council (VR grant 2016–03551 to SH). The authors would like to thank Camiel Parchen and Gerben Stouten for their help with the lab work.

References

Conthe, M., Wittorf, L., Kuenen, J.G., Kleerebezem, R., van Loosdrecht, M.C.M., and Hallin, S. (2018) Life on N_2O:

deciphering the ecophysiology of N_2O respiring bacterial communities in a continuous culture. *ISME J* 1.
Dini-Andreote, F., Brossi, MJ. D L., van Elsas, J.D., and Salles, J.F. (2016) Reconstructing the genetic potential of the microbially-mediated nitrogen cycle in a salt marsh ecosystem. *Front Microbiol* **7**: 9023389–9023902.
Domeignoz-Horta, L.A., Philippot, L., Peyrard, C., Bru, D., Breuil, M.-C., Bizouard, F., *et al.* (2017) Peaks of in situ N_2O emissions are influenced by N_2O-producing and reducing microbial communities across arable soils. *Glob Chang Biol* **24**: 360–370.
Graf, D.R.H., Jones, C.M., and Hallin, S. (2014) Intergenomic comparisons highlight modularity of the denitrification pathway and underpin the importance of community structure for N_2O emissions. *PLoS One* **9**: e114118.
Graf, D.R.H., Zhao, M., Jones, C.M., and Hallin, S. (2016) Soil type overrides plant effect on genetic and enzymatic N_2O production potential in arable soils. *Soil Biol Biochem* **100**: 125–128.
Hallin, S., Philippot, L., Löffler, F.E., Sanford, R.A., and Jones, C.M. (2018) Genomics and ecology of novel N_2O-reducing microorganisms. *Trends Microbiol* **26**: 43–55.
Jones, C.M., Graf, D.R.H., Bru, D., Philippot, L., and Hallin, S. (2013) The unaccounted yet abundant nitrous oxide-reducing microbial community: a potential nitrous oxide sink. *ISME J* **7**: 417–426.
Jones, C.M., Spor, A., Brennan, F.P., Breuil, M.-C., Bru, D., Lemanceau, P., *et al.* (2014) Recently identified microbial guild mediates soil N_2O sink capacity. *Nat Clim Chang* **4**: 801–805.
Juhanson, J., Hallin, S., Söderström, M., Stenberg, M., and Jones, C.M. (2017) Spatial and phyloecological analyses of nosZ genes underscore niche differentiation amongst terrestrial N_2O reducing communities. *Soil Biol Biochem* **115**: 82–91.
Rinke, C., Schwientek, P., Sczyrba, A., Ivanova, N.N., Anderson, I.J., Cheng, J.-F., *et al.* (2013) Insights into the phylogeny and coding potential of microbial dark matter. *Nature* **499**: 431–437.
Roeselers, G., Zippel, B., Staal, M., Van Loosdrecht, M., and Muyzer, G. (2006) On the reproducibility of microcosm experiments – different community composition in parallel phototrophic biofilm microcosms. *FEMS Microbiol Ecol* **58**: 169–178.
Sanford, R.A., Wagner, D.D., Wu, Q., Chee-Sanford, J.C., Thomas, S.H., Cruz-García, C., *et al.* (2012) Unexpected nondenitrifier nitrous oxide reductase gene diversity and abundance in soils. *Proc Natl Acad Sci USA* **109**: 19709–19714.
Tsiknia, M., Paranychianakis, N.V., Varouchakis, E.A., and Nikolaidis, N.P. (2015) Environmental drivers of the distribution of nitrogen functional genes at a watershed scale. *FEMS Microbiol Ecol* **91**. doi:10.1093/femsec/fiv052.
Vishniac, W., and Santer, M. (1957) The Thiobacilli. *Microbiol Mol Biol Rev* **21**: 195–213.
Wittorf, L., Bonilla-Rosso, G., Jones, C.M., Bäckman, O., Hulth, S., and Hallin, S. (2016) Habitat partitioning of marine benthic denitrifier communities in response to oxygen availability. *Environ Microbiol Rep* **8**: 486–492.
Yoon, S., Nissen, S., Park, D., Sanford, R.A., and Löffler, F.E. (2016) Nitrous oxide reduction kinetics distinguish bacteria harboring clade I NosZ from those harboring clade II NosZ. *Appl Environ Microbiol* **82**: 3793–3800.

Supporting Information

Additional Supporting Information may be found in the online version of this article at the publisher's web-site:

Fig. S1. Chemostat operation over 72 days showing (a) the liquid medium and gas flow rates (the total gas flow consisting of pure N_2O diluted in N_2 or Argon) going into the reactor, (b) the incoming and outgoing acetate and NH_4^+ concentrations in the medium and effluent and (c) the biomass concentration and optical density of the culture. Day 0 corresponds to the start of continuous operation. Medium A contained 90.6 mmol acetate ($NaCH_3COO{\cdot}3H_2O$) per liter, and medium B contained 26.6 mmol NH_4Cl, 14.8 mmol KH_2PO_4, 4.2 mmol $MgSO_4{\cdot}7H_2O$, 1 mmol NaOH, 4 mg yeast extract and 5 ml trace element solution (Vishniac and Santer, 1957) per liter. Both media were fed to the chemostat by means of one peristaltic pump with two pump heads. Even though the biomass concentration increased after day 21, growth yields remained the same. This is because the HRT decreased after replacing the influent pump tubing feeding mediums A and B to the reactor while the growth limiting substrate – N_2O – was supplied to the reactor at a constant gas flow rate. Recirculation was implemented on day 47 with the intention of reducing the amount of Argon gas used and to increase the mass transfer of gaseous N_2O to the liquid phase. However, the resulting increase in N_2O availability in the liquid was too small to be detected in the biomass yield of the culture.
Table S1. Assigned taxonomy for the main 16S rRNA-based OTUs (those with $>$ 10% sequences) of the activated sludge inoculum using the Silva database.
Table S2. Assigned taxonomy for the main 16S rRNA-based OTUs in the enrichment using the Silva database. The main OTUs were considered to be those with $>$ 5% sequences on any given sampling date, also see Fig. 1.

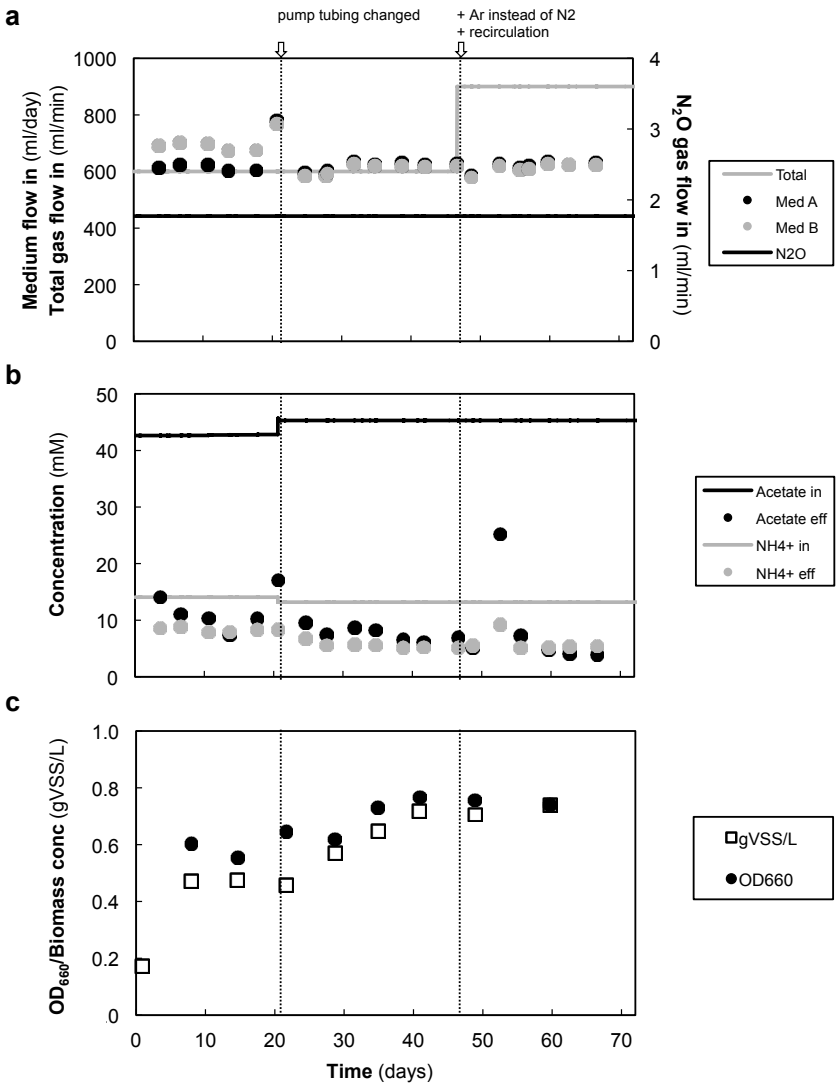

Fig. S1. Chemostat operation over 72 days showing (a) the liquid medium and gas flow rates (the total gas flow consisting of pure N_2O diluted in N_2 or Argon) going into the reactor, (b) the incoming and outgoing acetate and NH_4^+ concentrations in the medium and effluent, and (c) the biomass concentration and optical density of the culture. Day 0 corresponds to the start of continuous operation. Medium A contained 90.6 mmol acetate ($NaCH_3COO.3H_2O$) per liter, and Medium B 26.6 mmol NH_4Cl, 14.8 mmol KH_2PO_4, 4.2 mmol $MgSO_4.7H_2O$, 1 mmol NaOH, 4 mg yeast extract and 5 ml trace element solution (Vishniac and Santer, 1957) per liter. Both media were fed to the chemostat by means of one peristaltic pump with two pump heads. Even though the biomass concentration increased after day 21, growth yields remained the same. This is because the HRT decreased after replacing the influent pump tubing feeding mediums A and B to the reactor while the growth limiting substrate - N_2O - was supplied to the reactor at a constant gas flow rate. Recirculation was implemented on day 47 with the intention of reducing the amount of Argon gas used and to increase mass transfer of gaseous N_2O to the liquid phase. However, the resulting increase in N_2O availability in the liquid was too small to be detected in the biomass yield of the culture

Table S1. Assigned taxonomy for the main 16S rRNA-based OTUs (those with >10% sequences) of the Activated sludge inoculum using the Silva database

OTU	Kingdom	Phylum	Class	Order	Family	Genus	Identity (%)
11	Bacteria	Actinobacteria	Acidimicrobiia	Acidomicrobiales	*Microthrixaceae*	Candidatus *Microthrix*	98.8
18	Bacteria	Bacteroidetes	Shingobacteriia	Sphingobacteriales	*Saprospiraceae*	---	97.9
21	Bacteria	Proteobacteria	Betaproteobacteria	Burkholderiales	*Comamonadaceae*	---	98.8
23	Bacteria	Firmicutes	Bacilli	Lactobacillales	*Carnobacteriaceae*	---	99.1
33	Bacteria	Bacteroidetes	Shingobacteriia	Sphingobacteriales	*Saprospiraceae*	---	96.6
34	Bacteria	Bacteroidetes	Shingobacteriia	Sphingobacteriales	*Saprospiraceae*	---	97.0
35	Bacteria	Proteobacteria	Epsilonproteobacteria	Campylobacterales	*Campylobacteraceae*	*Arcobacter*	99.0
36	Bacteria	Firmicutes	Bacilli	Lactobacillales	*Carnobacteriaceae*	---	99.0
37	Bacteria	Chloroflexi	---	---	---	---	98.4
38	Bacteria	Proteobacteria	Betaproteobacteria	Burkholderiales	*Comamonadaceae*	---	99.3
39	Bacteria	---	---	---	---	---	95.0
55	Bacteria	Actinobacteria	Actinobacteria	Micrococcales	*Instrasporangiaceae*	---	98.7
58	Bacteria	Actinobacteria	Acidimicrobiia	Acidomicrobiales	*Acidimicrobiaceae*	---	98.5
62	Bacteria	Bacteroidetes	Shingobacteriia	Sphingobacteriales	*Saprospiraceae*	---	95.6
63	Bacteria	Acidobacteria	Blastocatellia	Blastocatellales	*Blastocatellaceae*	---	98.8
64	Bacteria	Proteobacteria	Betaproteobacteria	Burkholderiales	*Comamonadaceae*	---	98.8
65	Bacteria	Bacteroidetes	Shingobacteriia	Sphingobacteriales	*Saprospiraceae*	---	95.8
66	Bacteria	Bacteroidetes	Shingobacteriia	Sphingobacteriales	*Saprospiraceae*	---	98.7
67	Bacteria	Proteobacteria	Gammaproteobacteria	---	---	---	97.0
68	Bacteria	Proteobacteria	Alphaproteobacteria	Rhodospirillales	*Acetobacteraceae*	*Stella*	96.0
69	Bacteria	Bacteroidetes	Shingobacteriia	Sphingobacteriales	*Saprospiraceae*	---	99.0
71	Bacteria	Bacteroidetes	---	---	---	---	95.1
73	Bacteria	Chloroflexi	Anaerolineae	Anaerolineales	*Anaerolineaceae*	---	96.5
74	Unclassified	---	---	---	---	---	97.5
79	Bacteria	Proteobacteria	Gammaproteobacteria	Xanthomonadales	*Competibacteraceae*	Candidatus *Competibacter*	99.0
83	Bacteria	Bacteroidetes	Shingobacteriia	Sphingobacteriales	*Chitinophagaceae*	*Terrimonas*	98.1
87	Bacteria	Gemmatimonadetes	Gemmatimonadetes	Gemmatimonadales	*Gemmatimonadaceae*	---	98.0
90	Bacteria	Chloroflexi	---	---	---	---	97.2

Table S2. Assigned taxonomy for the main 16S rRNA-based OTUs in the enrichment using the Silva database. The main OTUs were considered to be those with >5% sequences on any given sampling date, also see figure 1

OTU	Kingdom	Phylum	Class	Order	Family	Genus	Identity (%)
1	Bacteria	Proteobacteria	Betaproteobacteria	Rhodocyclales	*Rhodocyclaceae*	*Dechlorobacter*	96.3
2	Bacteria	Gracilibacteria	---	---	---	---	94.8
3	Unclassified	---	---	---	---	---	83.2
4	Bacteria	Bacteroidetes	Flavobacteria	Flavobacteriales	*Flavobacteriaceae*	*Cloacibacterium*	98.5
5	Bacteria	Proteobacteria	Betaproteobacteria	Rhodocyclales	*Rhodocyclaceae*	*Dechloromonas*	99.4
6	Bacteria	Proteobacteria	Gammaproteobacteria	Pseudomonales	*Pseudomonadaceae*	*Pseudomonas*	98.9
7	Unclassified	---	---	---	---	---	85.0
8	Bacteria	Firmicutes	Erysipelotrichi	Erysipelotrichales	*Erysipelotrichaceae*	*Erysipelothrix*	93.1
9	Bacteria	Bacteroidetes	Flavobacteria	Flavobacteriales	*Flavobacteriaceae*	*Chryseobacterium*	95.0
10	Bacteria	Proteobacteria	Betaproteobacteria	Rhodocyclales	*Rhodocyclaceae*	*Azonexus*	97.6
12	Bacteria	Proteobacteria	Betaproteobacteria	Burkholderiales	*Comamonadaceae*	*Comamonas*	99.4
20	Bacteria	Proteobacteria	Gammaproteobacteria	Pseudomonales	*Pseudomonadaceae*	*Pseudomonas*	97.8

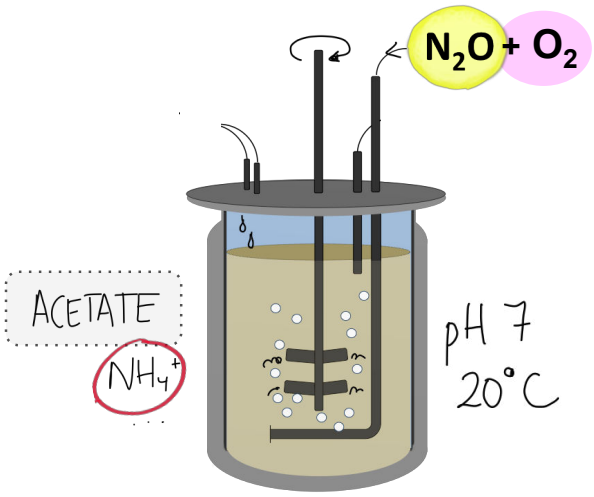
$N_2O + O_2$
ACETATE
NH_4^+
pH 7
20°C

4

O_2 versus N_2O respiration in a continuous microbial enrichment

Conthe M, Parchen C, Stouten G, Kleerebezem R, van Loosdrecht MCM

Appl Microbiol Biotechnol (2018) **102** (20) 8943-8950

+ SUPPLEMENTARY INFORMATION

Applied Microbiology and Biotechnology
https://doi.org/10.1007/s00253-018-9247-3

ENVIRONMENTAL BIOTECHNOLOGY

O_2 versus N_2O respiration in a continuous microbial enrichment

Monica Conthe[1] · Camiel Parchen[1] · Gerben Stouten[1] · Robbert Kleerebezem[1] · Mark C. M. van Loosdrecht[1]

Received: 14 April 2018 / Revised: 13 July 2018 / Accepted: 15 July 2018

Abstract
Despite its ecological importance, essential aspects of microbial N_2O reduction—such as the effect of O_2 availability on the N_2O sink capacity of a community—remain unclear. We studied N_2O vs. aerobic respiration in a chemostat culture to explore (i) the extent to which simultaneous respiration of N_2O and O_2 can occur, (ii) the mechanism governing the competition for N_2O and O_2, and (iii) how the N_2O-reducing capacity of a community is affected by dynamic oxic/anoxic shifts such as those that may occur during nitrogen removal in wastewater treatment systems. Despite its prolonged growth and enrichment with N_2O as the sole electron acceptor, the culture readily switched to aerobic respiration upon exposure to O_2. When supplied simultaneously, N_2O reduction to N_2 was only detected when the O_2 concentration was limiting the respiration rate. The biomass yields per electron accepted during growth on N_2O are in agreement with our current knowledge of electron transport chain biochemistry in model denitrifiers like *Paracoccus denitrificans*. The culture's affinity constant (K_S) for O_2 was found to be two orders of magnitude lower than the value for N_2O, explaining the preferential use of O_2 over N_2O under most environmentally relevant conditions.

Keywords Nitrous oxide · Mixotrophy · Enrichment · Chemostat

Introduction

Coping with rising levels of the potent greenhouse gas nitrous oxide (N_2O) in the atmosphere calls for the development of mitigation strategies to reduce N_2O accumulation and emission in soil management and wastewater treatment (WWT). The presence and activity of N_2O-reducing organisms in fertilized soils and WWT plants, such as bacteria and archaea harboring *nosZ*-type genes, may be key in such mitigating strategies (Thomson et al. 2012). Nitrous oxide reductase (N_2OR), the enzyme encoded by the *nosZ* gene, is a terminal reductase present in some microbial respiratory electron transport chains (ETC) that catalyzes the only microbial reaction known to consume N_2O, converting it to innocuous N_2 (which constitutes 79% of the Earth's atmosphere). Although N_2O reduction is generally associated to denitrifying organisms, many N_2O reducers lack reductases other than N_2OR (i.e., nitrate-, nitrite-, or nitric oxide-reductase; Hallin et al. 2018). However, most, if not all, denitrifiers—and presumably N_2O reducers—are facultative aerobes, having the terminal oxidases necessary for O_2 respiration (van Spanning and Richardson 2007).

Based on what is known on the biochemistry of model organisms like *Paracoccus denitrificans*, N_2O and O_2 respiration presumably share the core of the ETC (Chen and Strous 2013), with electrons branching out to O_2 (via cytochrome oxidases), N_2O (via N_2OR), or other NO_x (in denitrifying N_2O reducers) depending on electron acceptor availability. It is a common notion that, when both N_2O and O_2 are available, N_2O reducers will consume O_2 preferentially over N_2O (and other N oxides; Shapleigh 2013). Even though N_2O is a stronger electron acceptor than O_2 in terms of thermodynamics, a number of authors have shown that N_2O respiration is energetically less efficient than aerobic respiration, resulting in lower biomass growth yields per substrate (Koike and Hattori 1975; Stouthamer et al. 1982; Beun et al. 2000). We cannot rule out the existence of a more energy-efficient N_2O reduction process (Conthe et al. 2018a), considering the broad phylogenetic diversity of N_2O reducers and our limited knowledge regarding non-denitrifying N_2O reducers in particular. However, given the growth yields reported in literature, it

✉ Monica Conthe
M.conthecalvo-24@tudelft.nl

[1] Department of Biotechnology, Delft University of Technology, Van der Maasweg 9, 2629 HZ Delft, The Netherlands

would make evolutionary sense for microorganisms to favor aerobic respiration over the respiration of N compounds to optimize energy conservation in the cell. Intriguingly, the physical mechanism directing electrons to O_2 preferentially over other N compounds, when both electron acceptors are available, remains unclear.

Regulatory systems on a transcriptional or post-transcriptional level have been shown to shut down denitrification in the presence of oxygen in a variety of organisms (Zumft 1997). For instance, the NosZ protein of *Paracoccus denitrificans* and *Pseudomonas stutzeri* is inhibited by O_2 in vitro (Coyle et al. 1985; Alefounder and Ferguson 1982), which could be a form of allosteric regulation in vivo. It has also been proposed that N_2OR is—for reasons unknown—less competent than the cytochrome oxidases involved in respiration of O_2 in the "competition" for electrons in the ETC (Qu et al. 2015). Nevertheless, diverse studies have reported the occurrence of denitrification in the presence of O_2 (termed aerobic denitrification; Chen and Strous 2013 and references therein). Regarding N_2O reduction more specifically, a significant degree of N_2OR transcription and activity has been found under aerated conditions (Körner and Zumft 1989; Qu et al. 2015).

From a greenhouse gas mitigation point of view, it is interesting to study O_2 and N_2O mixotrophy—or the capability of microorganisms to simultaneously respire O_2 and N_2O—in order to understand how frequent oxic-anoxic shifts during nitrogen removal from wastewater, in space or time, may affect the N_2O-reducing capacity of activated sludge. WWTP design and operation vary greatly, but universal questions to address are, e.g., (a) if N_2OR activity can persist in aerated zones consuming nitrification-derived N_2O potentially minimizing greenhouse gas emissions or (b) if, on the contrary, N_2OR is relatively less active than the other NO_x reductases in the presence of O_2, leading to N_2O accumulation in the aerobic-anoxic transition zones.

We explored O_2 versus N_2O respiration in a continuous enrichment culture selected and grown with N_2O as the sole electron acceptor and fully characterized—in terms of stoichiometry and community composition—in a previous study (Conthe et al. 2018b). The culture had been found to be composed of a relatively simple microbial community dominated by *Dechlorobacter*-like *Betaproteobacteria*. In this study, operation of the chemostat was continued and the N_2O-limited steady-state conditions were intermittently interrupted to perform short-term batch experiments in situ, with varying concentrations of N_2O, O_2, or both N_2O and O_2 simultaneously, to determine (i) whether O_2 is, in fact, preferentially consumed over N_2O when both electron acceptors are available, (ii) under which O_2 concentrations (if any) N_2O consumption can take place, and (iii) to begin to unravel the mechanism governing the electron flow in the ETC to O_2 or N_2O.

Materials and methods

Chemostat operation

Following the work presented in Conthe et al. (2018b), a microbial enrichment using acetate as a carbon and energy source and exogenous N_2O as the sole electron acceptor was maintained under N_2O-limiting conditions in a continuous culture at 20 °C, pH 7, and a dilution rate of 0.026 ± 0.001 h^{-1}. The reactor set-up, operation, sampling, and medium composition are described in detail in Conthe et al. (2018b, c). One hundred percent pure N_2O gas diluted in Argon gas was fed to the chemostat at a total flow rate of 200 ml/min and the offgas from the reactor was recirculated at a rate of 700 ml/min, resulting in an incoming N_2O concentration of roughly 0.30%. The stability of the culture in terms of conversion rates and microbial community composition was monitored by regular sampling of the broth and biomass and via online monitoring of the acid (1 M HCl) dosing (a proxy for acetate consumption in the system) and offgas composition.

Batch experiments

The steady-state conditions of the culture were briefly interrupted on different operation days in order to perform batch experiments in situ and determine the maximum conversion rates of the enrichment under non-limiting conditions (Figure S1). The medium and effluent pumps were switched off and the gas supply rates of O_2 (from a bottle of pure O_2) and/or N_2O were modified to achieve different electron acceptor concentrations within the system in random steps. Two main types of batches were performed: (1) supplying a single electron acceptor—either N_2O or O_2—at different concentrations or (2) supplying N_2O and O_2 simultaneously, keeping the N_2O gas supply rate constant and varying that of O_2. Additionally, we performed a batch test in which a constant O_2 gas supply rate was maintained while varying that of N_2O as well as short batch tests with either NO_3^- or NO_2^- to assess the denitrifying capacity of the culture. Note that gas recirculation was maintained during the experiments, causing an apparent delay between the conversions in the chemostat and the offgas concentration values measured. To avoid acetate depletion, a concentrated solution of sodium acetate was added to the broth at the start of the experiments and the 1 M HCl solution used for pH control during continuous operation was replaced by 1 M acetic acid for the duration of the experiment. For the batch tests with NO_3^- and NO_2^-, these compounds were supplied as 1 M KNO_3 or 1 M KNO_2.

Analytical procedures

Samples from the reactor for analysis of acetate and NH_4^+ were immediately filtered after sampling (0.45-μm pore size

poly-vinylidene difluoride membrane, Merck Millipore, Carrigtohill, Ireland). Acetate was measured with a Chrompack CP 9001 gas chromatograph (Chrompack, Middelburg, The Netherlands) equipped with an HP Innowax column (Agilent Technologies, Santa Clara, CA, USA) and a flame ionization detector. Ammonium, NO_3^-, and NO_2^- concentrations were determined spectrophotometrically using cuvette test kits (Hach Lange, Düsseldorf, Germany). For the estimation of biomass concentration, the volatile suspended solids (VSS) concentration was determined by centrifuging 0.2 L of the enrichment, drying the pellet overnight at 105 °C, and then burning the pellet at 550 °C for 2 h to determine the ash content. Additionally, the optical density of the culture (at a wavelength of 660; OD_{660}) was monitored. Concentrations of N_2O, N_2 and CO_2, Argon, and O_2 in the headspace of the reactor were measured online via mass spectrometry (Prima BT, Thermo Scientific). The dissolved O_2 concentration in the broth during the batch tests with O_2 was measured with two types of oxygen sensors: a Clark electrode calibrated in the range of 0–20.8% and an optical oxygen probe calibrated in range 0–2% (Presens, Regensburg, Germany).

Calculations

Elemental and electron balances during steady state were set up as described in Conthe et al. (2018a, b, c). During the batch tests, the conversion rates (r, in mol h^{-1}) for O_2 and N_2O were calculated from the measured ingoing and outgoing gas composition and the argon supply rate (see Figures S2–S6 and Tables S2–S6 for details). The average biomass concentration value for each experimental step was derived from the ammonium uptake rates (see for example Figure S4b) and used to calculate the corresponding biomass specific rates (q, in mol $CmolX^{-1}$ h^{-1}). A standard and constant biomass composition of $CH_{1.8}O_{0.5}N_{0.2}$ (Roels 1980). The qO_2 and qN_2O obtained for each step were plotted against the corresponding concentration of dissolved O_2 or N_2O in the broth in order to determine the q_{max} and K_s of the enrichment for O_2 and N_2O. The concentration of dissolved O_2 was obtained experimentally with the DO probes while the concentration of dissolved N_2O was estimated given a k_La_{N2O} of 180 h^{-1}—obtained by scaling the experimentally derived k_La_{O2} (Janssen and Warmoeskerken 1987) and deriving the corresponding K_La_{broth} and $K_La_{headspace}$ assuming a t_{broth} of 6 s (1800 and 50 h^{-1}, respectively). A Monod model fitting the results was obtained by minimizing the sum of squared errors using the Microsoft Excel software.

The thermodynamic efficiency of metabolic growth using acetate as an electron donor and O_2, N_2O, or NO_3^- as an electron acceptor can be interpreted by the Gibbs free energy ($\Delta G01$) dissipated per C mole of biomass growth or per electron-equivalent used for respiration. These values were calculated based on Kleerebezem and van Loosdrecht (2010) and using the thermodynamic values found in Thauer et al. (1977)—please refer to Table S7 for more details.

DNA extraction and 454 amplicon sequencing of 16S rRNA gene

The taxa-based community composition of the enriched culture during the period of operation presented in this study was determined by 454 amplicon sequencing of the 16S rRNA gene following the procedure described in Conthe et al. (2018a, b, c) and the sequences are available at NCBI under BioProject accession number PRJNA413885.

Results

Continuous operation and microbial community composition of the N_2O-reducing enrichment

A culture enriched from activated sludge using acetate as a carbon source and electron donor and exogenous N_2O as the sole electron acceptor was studied for a total period of 155 days (> 100 volume changes) in a chemostat under electron acceptor (N_2O) limiting conditions (Figure S1). The start-

Table 1 Average biomass-specific conversion rates during steady state and the batch experiments

	Compound biomass specific conversion rates (mmol/$mmol_X$ h^{-1})			
	$q_{N2O\text{-}N}$	$q_{NO3\text{-}N}$ or $q_{NO2\text{-}N}$	$q_{N2\text{-}N}$	$q_{Acetate\text{-}C}$
Steady state	-0.033 ± 0.001^b		0.034 ± 0.001^b	-0.017 ± 0.001^b
N_2O batch	-0.131 ± 0.004^b		0.126 ± 0.008^b	-0.067 ± 0.009^c
NO_3^- batch		-0.007 ± 0.000^c	0.004 ± 0.000^c	-0.003 ± 0.000^c
$N_2O + NO_2^-$ batch[a]	-0.033 ± 0.000^c		0.042 ± 0.000^c	

[a] N_2O gas supply was kept on during addition of 1 mM KNO_2^-

[b] Standard deviation calculated from at least three independent measurements

[c] Standard deviation calculated by LINEST least squares method

Table 2 Experimentally determined biomass yields per mole of electron donor or per mole of electron equivalents respired during growth with N_2O, NO_3^-, and O_2 as an electron acceptor and corresponding Gibbs free energy dissipation values based on these yields

	Parameter	Units	Growth on electron acceptor		
			N_2O[a]	NO_3^-[b]	O_2[c]
Y_{XS}	Biomass yield on acetate	$Cmol_X/Cmol_{Ac^-}$	0.36 ± 0.03	0.38	0.45
Y_{Xe}	Biomass yield on e^- transported in catabolic process	$Cmol_X/mol_{e^-}$	0.16 ± 0.01	0.15	0.19
ΔG^{01}_{MET}	Metabolic energy change per mole donor[d]	$kJ/Cmol_X$	− 1078	− 620	− 479
$\Delta G^{01}_{e\ CAT}$	Metabolic energy change per electron transferred in catabolism	kJ/mol_{e^-}	− 159	− 96	− 101

[a] Steady state data, this study

[b] Steady state data—no siginificant accumulation of intermediates (Conthe et al.; data unpublished)

[c] Batch experiment data in N_2O reducing enrichment, this study

up and characterization of the enrichment during the first 70 days of operation, in terms of conversion rates, stoichiometry, and microbial community composition, are described in Conthe et al. (2018b). During the subsequent period reported here, the conversion rates and corresponding biomass yields remained consistent with the previous period, characterized by steady-state growth on acetate oxidation coupled to N_2O reduction to N_2 (Tables 1 and 2). Furthermore, 454 amplicon sequencing of the 16S rRNA gene of the microbial community confirmed the continued prevalence of a *Dechlorobacter*-like OTU (Figure S1), transiently co-occurring (around day 100) with two other closely related OTUs classified as *Azonexus* and uncultured *Rhodocyclaceae*.

O_2 vs. N_2O batch tests: affinity and yields

Batch experiments with varying supply rates of either N_2O or O_2 were performed on days 106 and 132, respectively (Fig. 1). The maximum biomass specific conversion rates of N_2O (q^{max}_{N2O}) and acetate were identified by increasing the N_2O supply rate to non-limiting conditions. The q^{max}_{N2O} values

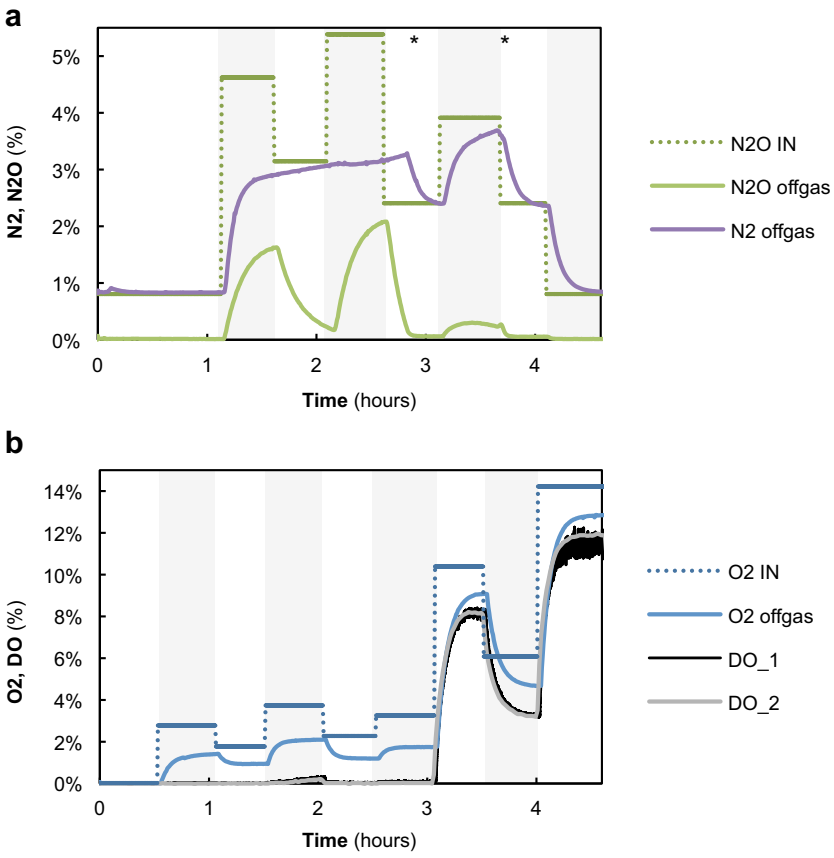

Fig. 1 Offgas data from the batch experiments with varying concentrations of **a** N_2O; day 106, **b** and O_2; day 132. For the experiment with O_2, the dissolved oxygen concentration (DO) was measured both with a Clark electrode (DO_1) and an optical sensor (DO_2). The affinity of the culture for N_2O and O_2 was determined from these experiments (see Fig. 5). The asterisk mark time points at which acetate had been depleted and was added to the culture

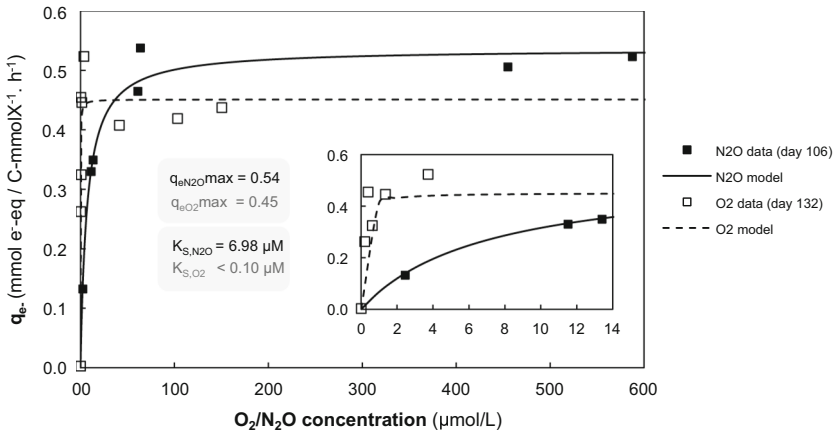

Fig. 2 Biomass specific transfer rates of electron equivalents (q_{e^-}) as a function of the electron acceptor concentration (either N_2O, in black, or O_2, in gray), along with the fitting Monod model (with the corresponding $q_{e^-}^{max}$ and K_s parameters). The inset is an enlargement of the graph at low O_2/N_2O concentrations. The rates presented were obtained from the experiments shown in Fig. 2

identified were roughly fourfold higher than the actual biomass specific conversion rates during steady state (Table 1). When exposed to varying concentrations of O_2, the culture was able to switch to aerobic respiration in the order of seconds. The maximum O_2 reducing capacity (q_{O2}^{max}) was comparable to N_2O respiration when expressed per mole electron accepted. NO_3^- and NO_2^- reducing capacities were much lower compared to N_2O or O_2 (< 15% of the maximum N_2O or O_2 reduction rate; Table 1).

Plotting the biomass-specific electron transfer rate (qe^-) at different dissolved O_2 (DO) or N_2O concentrations, we could determine the apparent K_s for O_2 or N_2O by fitting a Monod model to the data (Fig. 2). Given the confidence intervals, the absolute value for this parameter could not be identified accurately, but the results demonstrate clearly that the K_s value for O_2 is 1 or 2 orders of magnitude smaller compared to K_s-N_2O. The maximum biomass-specific conversion rate of O_2 (q_{O2}^{max}) was roughly two times lower than that of N_2O (q_{N2O}^{max}) per mole of electron acceptor but the conversion rates expressed as electron equivalents (q_e^{max}) were comparable for both processes, since double the electrons are taken up during the reduction of O_2 to H_2O compared to N_2O to N_2.

The biomass yields per mole of electron donor (determined from the steady-state growth on N_2O in the chemostat, and from the batch experiments with O_2 as the sole electron acceptor) are presented in Table 2.

Simultaneous O_2 and N_2O batch tests

Batch experiments with excess N_2O and varying concentrations of O_2, supplied simultaneously, were performed on days 110 and 155 (Figs. 3 and 4). The maximum electron transfer rate (q_e^{max})—combining the electron transfer capacities of N_2O and O_2—summed up to a value comparable with the

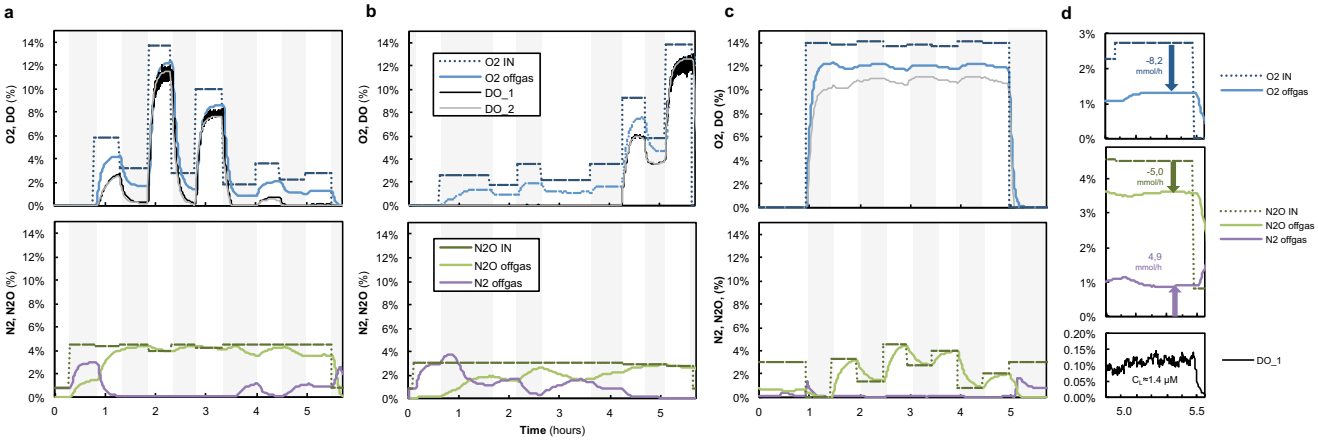

Fig. 3 Offgas data from the batch experiments with excess N_2O and varying concentrations of O_2 on **a** day 125 and **b** day 155. The dissolved oxygen concentration (DO) was measured both with a Clark electrode (DO_1) and an optical sensor (DO_2). The biomass specific electron transfer rates to either N_2O or O_2 during these experiments are shown in Fig. 4. The asterisk marking the last two steps of the batch experiment on day 155 indicates the culture ran out of NH_4^+ for growth, and thus the rates during these steps was not considered. **c** Offgas data of batch experiment with excess O_2 and varying concentrations of N_2O on day 113. Detailed data from these experiments can be found in the Supplementary Materiasl—Tables xxx–xxx and Figures xxx to xxx. **d** Detailed view of one of the steps from the batch experiment depicted in (**a**) showing the simultaneous consumption of O_2 and N_2O, and subsequent production of N_2

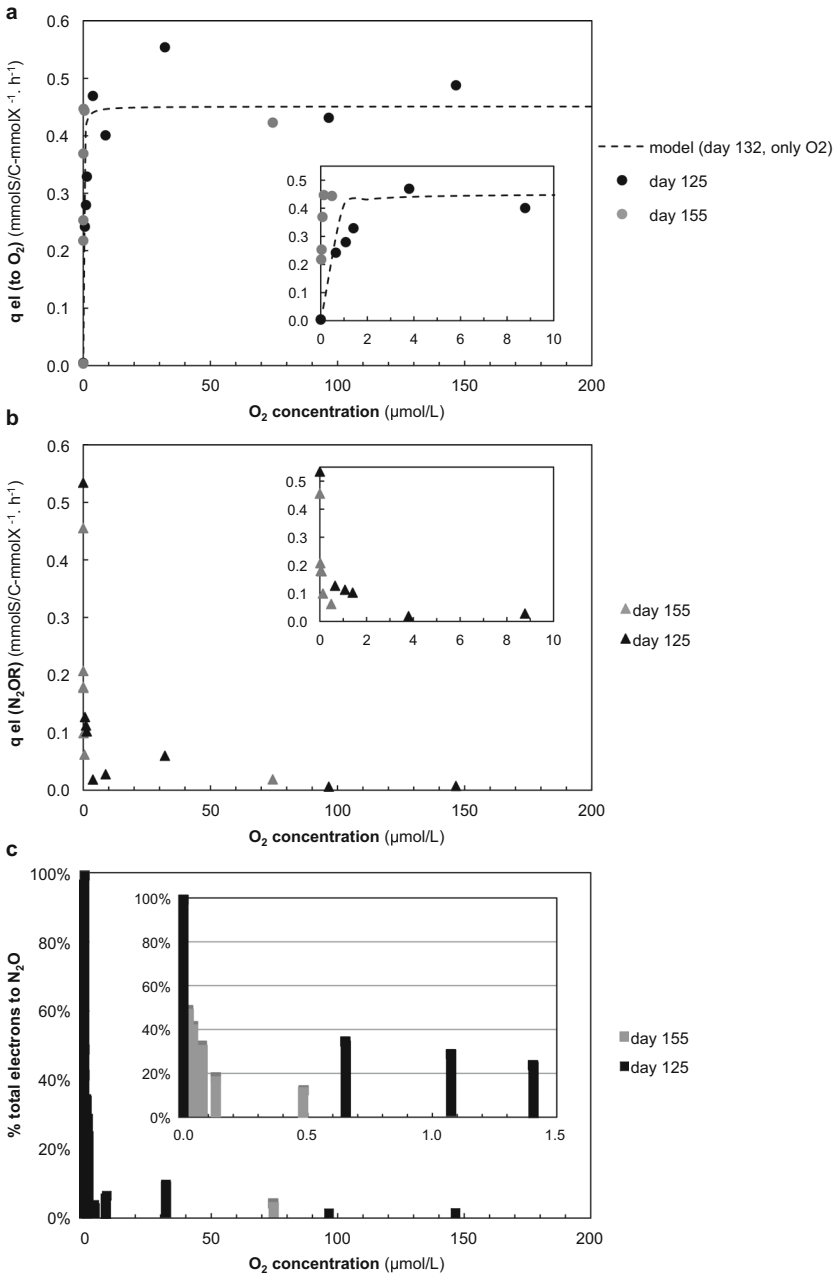

Fig. 4 Biomass specific transfers rate of electron equivalents (q_{e^-}) (**a**) to O_2 and **b** N_2O and **c** percentage of total electrons being shuttled to N_2O vs. O_2 at varying O_2 concentrations during the batch tests on day 125 (in black) and day 155 (in gray). The Monod model of O_2 consumption in the absence of N_2O (shown in Fig. 3) is included in (**a**) for comparison. The inset in (**c**) is an enlargement of the graph at low O_2 concentrations

q_e^{max} found during the N_2O- or O_2-only experiments. N_2O reduction to N_2 co-occurred with aerobic respiration only at relatively low concentrations of O_2 (Fig. 3d). The experiments performed on days 110 and 155 differed regarding the O_2 concentration range at which N_2O reduction could co-occur (roughly < 4 and < 1.5 μM O_2 on days 110 and 155, respectively) but, nevertheless, N_2O reduction in the presence of O_2 contributed to no more than a small fraction of the total electron acceptor capacity (generally < 20% of qe¯tot; Fig. 4). An additional batch experiment on day 113, with a constant supply of O_2 and a varying supply of N_2O, also showed that N_2O reduction was undetectable in the presence of relatively high concentrations of O_2 (≈5 μM; Fig. 3c).

Discussion

Aerobic respiration was distinctly favored over N_2O respiration in the enrichment despite the fact that the culture had been operated for an extensive number of generations with N_2O as only electron acceptor. Upon a sudden change in supply from N_2O to O_2, the culture readily switched to O_2 respiration and, when both electron acceptors were available, N_2O reduction was only observed at relatively low concentrations of O_2 (< 4 μM = 0.13 mg O_2/L). Under conditions of electron acceptor excess (N_2O and/or O_2), growth in the system was likely limited by the electron supply rate to the electron transport chain (see Fig. 5) and not by the capacity of N_2OR or O_2 reductases.

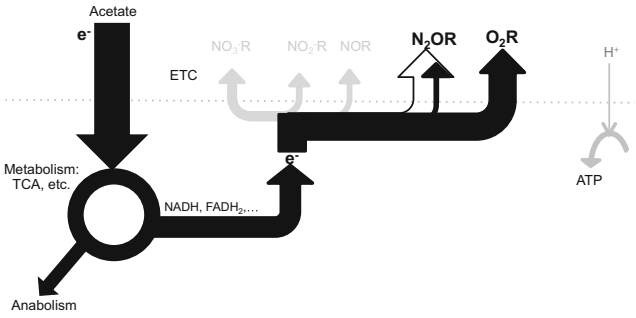

Fig. 5 Simplified representation of the proportional distribution of electrons (e^-) in the electron transport chain (ETC) during batch tests with only N_2O (open arrow) versus batch tests with the simultaneous addition of O_2 and N_2O (black arrows) showing that there is a preferential shuttling of electrons to O_2R than to N_2OR. This simplified schematic is based on the assumptions that (i) both enzymes share a common electron pool (/quinone pool) and (ii) that all cells have a similar electron distribution among terminal reductases (whereas it would be possible for the majority of cells to switch fully to aerobic respiration, and a small fraction to continue respiring N_2O)

This was inferred from the fact that the maximum electron acceptor capacity of the culture was comparable for N_2O and O_2 respiration (i.e., $q^{max}_{e^-N2O} \approx q^{max}_{e^-O2}$), and could be due to kinetic limitations in acetate uptake, acetate oxidation in the citric acid cycle, or in some shared component of the ETC itself.

The overall electron transfer capacity during the simultaneous respiration of N_2O and O_2 (i.e., $q^{max}_{e^-TOT}$) was comparable to $q^{max}_{e^-N2O}$ or $q^{max}_{e^-O22}$. This suggests that "aerobic N_2O respiration" (by analogy to aerobic denitrification) generally occurs if the electron supply rate to the ETC exceeds the electron accepting capacity of the O_2 reductases. In other words, N_2O respiration complements aerobic respiration primarily when O_2 is limiting. Nonetheless, our results indicate that, under O_2-limiting conditions, N_2O reducers can use O_2 and N_2O mixotrophically as proposed by Chen and Strous 2013 (Fig. 5). We cannot exclude heterogeneity in electron acceptor use within the population in our bioreactor leading for example to most of the culture respiring O_2 and a side population reducing N_2O. Under the microscope, we did not observe formation of aggregates or biofilms which could create anoxic niches in spite of the O_2 supply (data not shown), yet oxygen gradients and anoxic microzones could still form around suspended cells if O_2 diffusion rate is slower than the respiration rate. Nevertheless, with the strong sparging and mixing conditions imposed on the culture, we would expect that most cells would be exposed to comparable environmental conditions.

The K_s values of the enrichment culture were in the same range as the K_m values reported for purified N_2OR and different O_2 reductases in literature, i.e., in the μM range for N_2O and nM range for O_2 (Pouvreau et al. 2008 and references therein, Yoon et al. 2016). The relatively high $K_{S,N2O}$ (two orders of magnitude higher than for O_2) is noteworthy in a culture presumably well-adapted to N_2O-limiting conditions. Also the observation that, even after a prolonged absence of O_2 in the environment, the cellular machinery specific for aerobic respiration (i.e., cytochrome oxidases) was constitutively present (in contrast to NO_3^- and NO_2^- reductases). According to these results, the preferential use of O_2 over N_2O in natural systems could be attributed to a difference in affinity ($\mu max/K_s$) for O_2 and N_2O.

With regard to efficiency of N_2O respiration versus O_2 respiration, our chemostat enrichment cultures corroborate studies in literature (Koike and Hattori 1975; Stouthamer et al. 1982; Beun et al. 2000) and predictions based on our knowledge of the ETC in model denitrifiers (Chen and Strous 2013): with biomass yields per mole of acetate during growth with N_2O (or NO_3) roughly 1/3 lower than yields during O_2 respiration (Table 2). The relatively low growth yields on N_2O imply that N_2O reduction to N_2 is, thermodynamically, a very inefficient process with high energy dissipation. Thus, ensuring the maximization of energy conservation during microbial growth may be the evolutionary driver behind the preferential flow of electrons to O_2 over N_2O.

We cannot provide a conclusive answer regarding which cellular mechanism governs the preferential use of O_2 in the presence of excess N_2O observed. However, the instantaneous switch from N_2O to O_2 respiration suggests that the preference for O_2 over N_2O is regulated at the metabolome level and is independent from transcriptional regulation, e.g., by control of enzyme activity, like allosteric inhibition of N_2OR, or simply a higher affinity of O_2 reductases for the electrons coming from a common quinone pool.

Translated to the environmental conditions in a WWT plant, the results from this study suggest that oxic-anoxic transitions are unlikely to result in N_2O emissions associated to denitrification as a result of N_2OR inhibition by O_2 since the enrichment culture readily switched back and forth between O_2 and N_2O respiration. This implies that (a) either N_2OR is not directly inhibited by O_2 in vivo or (b) inhibition is readily reversible once O_2 is depleted.

On the other hand, the fact that aerobic respiration is so strongly favored over N_2O respiration would make it a challenge to exploit the N_2O sink capacity of activated sludge in the aerated/nitrification zones of WWT plants. The range in which significant N_2O consumption co-occurred with O_2 consumption in our experiments was narrow: roughly up to 1.5–4 μM O_2, i.e., 0.05–0.13 mg O_2/L, presumably below common DO values in the aerated tanks of WWTP (Tchobanoglous and Burton 2002). The very high affinity for oxygen minimizes the range of dissolved oxygen concentrations in which O_2 and N_2O respiration could occur in parallel. However, a beneficial difference in full-scale systems compared to our enrichment, in terms of avoiding N_2O accumulation, may be that mass transfer limitation induced oxygen limitation within the activated sludge flocs provide anoxic zones, prone to N_2O reduction, even when O_2 is present in the bulk liquid (Picioreanu et al. 2016). This, together with the fact that N_2O is much more soluble than O_2, could perhaps be exploited to enhance the N_2O sink capacity of activated sludge.

Acknowledgements The authors would like to thank Gijs Kuenen for his comments on the manuscript and Mitchell Geleijnse and Ben Abbas for their great help with the molecular analysis of microbial community composition.

Funding This work was funded by the European Commission (Marie Curie ITN NORA, FP7-316472).

Compliance with ethical standards

Conflict of interest The authors declare that they have no conflict of interest.

Ethical approval This article does not contain any studies with human participants or animals performed by any of the authors.

References

Alefounder PR, Ferguson SJ (1982) Electron transport-linked nitrous oxide synthesis and reduction by Paracoccusdenitrificans monitored with an electrode. Biochem Biophys Res Commun 104 (3):1149–1155

Beun JJ, Verhoef EV, Van Loosdrecht MCM, Heijnen JJ (2000) Stoichiometry and kinetics of poly-β-hydroxybutyrate metabolism under denitrifying conditions in activated sludge cultures. Biotechnol Bioeng 68:496–507

Chen J, Strous M (2013) Denitrification and aerobic respiration, hybrid electron transport chains and co-evolution. Biochim Biophys Acta Bioenerg 1827:136–144

Conthe M, Kuenen JG, Kleerebezem R, van Loosdrecht MCM (2018a) Exploring microbial N_2O reduction: a continuous enrichment in nitrogen free medium. Environ Microbiol Rep 10:102–107. https://doi.org/10.1111/1758-2229.12615

Conthe M, Wittorf L, Kuenen JG, Kleerebezem R, Hallin S, van Loosdrecht MCM (2018b) Growth yield and selection of nosZ clade II-types in a continuous enrichment culture of N_2O respiring bacteria. Environ Microbiol Rep 10:239–244. https://doi.org/10.1111/1758-2229.12630

Conthe M, Wittorf L, Kuenen JG, Kleerebezem R, van Loosdrecht MCM, Hallin S (2018c) Life on N_2O: deciphering the ecophysiology of N_2O respiring bacterial communities in a continuous culture. ISME J. https://doi.org/10.1038/s41396-018-0063-7

Coyle CL, Zumft WG, Kroneck PMH, Körner H, Jakob W (1985) Nitrous oxide reductase from denitrifying: *Pseudomonas perfectomarina* purification and properties of a novel multicopper enzyme. Eur J Biochem 153:459–467

Hallin S, Philippot L, Löffler FE, Sanford RA, Jones CM (2018) Genomics and ecology of novel N_2O-reducing microorganisms. Trends Microbiol 26:43–55

Janssen LPBM, Warmoeskerken MMCG (2006) Transport phenomena data companion, Third edit edn. VSSD, Delft

Kleerebezem R, van Loosdrecht MCM (2010) A generalized method for thermodynamic state analysis of environmental systems. Crit Rev Env Sci Technol 40(1):1–54

Koike I, Hattori A (1975) Energy yield of denitrification: an estimate from growth yield in continuous cultures of *Pseudomonas denitrificans* under nitrate-, nitrite- and oxide-limited conditions. J Gen Microbiol 88:11–19

Körner H, Zumft WG (1989) Expression of denitrification enzymes in response to the dissolved oxygen level and respiratory substrate in continuous culture of *Pseudomonas stutzeri*. Appl Environ Microbiol 55:1670–1676

Picioreanu C, Perez JP, Van Loosdrecht MCM (2016) Impact of cell cluster size on apparent half-saturation coefficients for oxygen in nitrifying sludge and biofilms. https://doi.org/10.1016/j.watres.2016.10.017

Pouvreau LAM, Strampraad MJF, Van Berloo S, Kattenberg JH, de Vries S (2008) NO, N_2O, and O_2 reaction kinetics: scope and limitations of the Clark electrode. Methods Enzymol 436:97–112

Qu Z, Bakken LR, Molstad L, Frostegård Å, Bergaust L (2015) Transcriptional and metabolic regulation of denitrification in *Paracoccus denitrificans* allows low but significant activity of nitrous oxide reductase under oxic conditions. Environ Microbiol 18:2951–2963. https://doi.org/10.1111/1462-2920.13128

Roels JA (1980) Simple model for the energetics of growth on substrates with different degrees of reduction. Biotechnol Bioeng 22:33–53

Shapleigh JP (2013) Denitrifying Prokaryotes. In: Rosenberg E, DeLong EF, Lory S, Stackebrandt E, Thompson F (eds) The prokaryotes: prokaryotic physiology and biochemistry. Springer Berlin Heidelberg, Berlin, pp 405–425

Stouthamer AH, Boogerd FC, van Verseveld HW (1982) The bioenergetics of denitrification. Antonie Van Leeuwenhoek 48:545–553

Thauer RK, Jungermann K, Decker K (1977) Energy conservation in chemotrophic anaerobic bacteria. Bacteriol Rev 41:100–180

Tchobanoglous G, Burton F, Stensel HD (2006) Wastewater engineering—treatment and reuse. McGraw-Hill, New York

Thomson AJ, Giannopoulos G, Pretty J, Baggs EM, Richardson DJ (2012) Biological sources and sinks of nitrous oxide and strategies to mitigate emissions. Philos Trans R Soc Lond Ser B Biol Sci 367:1157–1168

van Spanning RJM, Richardson DJ, Ferguson SJ (2007) Introduction to the biochemistry and molecular biology of Denitrification. Biology of the Nitrogen Cycle 3–20. https://doi.org/10.1016/B978-044452857-5.50002-3

Yoon S, Nissen S, Park D, Sanford RA, Löffler FE (2016) Nitrous oxide reduction kinetics distinguish bacteria harboring clade I NosZ from those harboring clade II NosZ. Appl Environ Microbiol 82:3793–3800

Zumft WG (1997) Cell biology and molecular basis of cell biology and molecular basis of Denitrification. Microbiology 61(4):533

Table S1 Assigned taxonomy for the main 16S rRNA sequences (i.e. those with > 5 % of total sequences in any given sample) using the Silva database

OTU	Kingdom	Phylum	Class	Order	Family	Genus	Identity (%) avg ± stdev
1	*Bacteria*	*Proteobacteria*	*Betaproteobacteria*	*Rhodocyclales*	*Rhodocyclaceae*	*Quatrionicoccus*	97.1 ± 0.6
2	*Bacteria*	*Proteobacteria*	*Betaproteobacteria*	*Rhodocyclales*	*Rhodocyclaceae*	uncultured	96.8 ± 0.9
3	*Bacteria*	*Proteobacteria*	*Betaproteobacteria*	*Rhodocyclales*	*Rhodocyclaceae*	*Azonexus*	97.6 ± 1.0
4	*Bacteria*	*Bacteroidetes*	*Flavobacteria*	*Flavobacteriales*	*Flavobacteriaceae*	*Cloacibacterium*	98.7 ± 0.8
5	*Bacteria*	*Bacteroidetes*	*Flavobacteria*	*Flavobacteriales*	Flavobacteriaceae	Chryseobacterium	97.9 ± 1.7
6	*Bacteria*	*Gracilibacteria*	---	---	---	---	84.8 ± 2.0

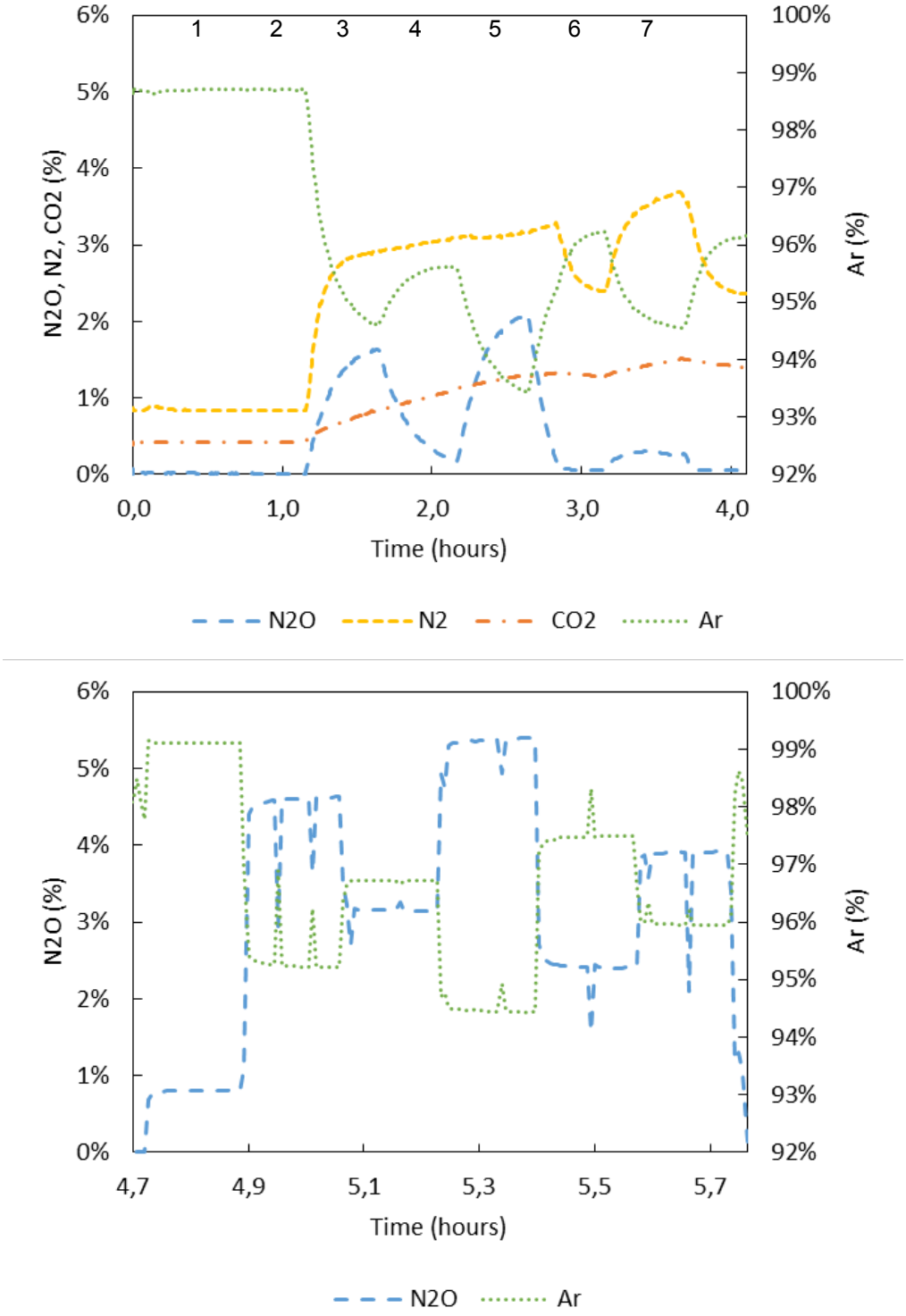

Figure S2 Concentration of N_2O, N_2, CO_2 and Argon in the offgas (above) and incoming gas (below) of the experiment on day 106 - N_2O only, presented in the main text as **Figure 1a**. The averaged data for each step – numbered in the graph - is presented in **Table S2**. Acetate was added manually to the culture during steps 5 and 7 to ensure that it was present in excess. NH_4^+ was also in excess throughout the experiment. pH was kept constant at 7.0 ± 0.1

Table S2 Average concentration and rates of N_2O, N_2, CO_2, O_2 and Argon supplied and produced during each of the steps (numbered 1 through 7) in the experiment with only N_2O on day 106 – presented in **Figure 1a** and **Figure S2.** Step 1 corresponds to steady state operation.

		IN-GAS			***OFF-gas***			***R***	***q_s***	***C_L***
			ml/min	*mmol/ h*		*ml/min*	*mmol/h*	*mmol/h*	*mol/ (mol h)*	*µM*
	N_2	0,04%	0,07	0,20	0,83%	1,67	4,48	4,28	0,067	
	CO_2	0,03%	0,05	0,14	0,43%	0,86	2,29	2,15	0,034	
1	N_2O	0,81%	1,61	4,31	0,01%	0,03	0,07	-4,24	**-0,066**	**0,1**
	Ar	99,11%	197,97	530,27	98,70%	197,97	530,27	0	0,000	
	O_2	0,02%	0,05	0,13	0,02%	0,05	0,13	0	0,000	
	N_2	0,06%	0,13	0,35	2,89%	6,05	16,20	15,85	0,239	
	CO_2	0,07%	0,14	0,38	0,81%	1,69	4,53	4,16	0,063	
2	N_2O	4,62%	9,61	25,75	1,60%	3,34	8,96	-16,79	**-0,253**	**443,7**
	Ar	95,21%	197,97	530,27	94,67%	197,97	530,27	0	0,000	
	O_2	0,03%	0,07	0,18	0,03%	0,06	0,17	-0,01	0,000	
	N_2	0,05%	0,11	0,28	3,06%	6,35	17,00	16,71	0,243	
	CO_2	0,05%	0,10	0,26	1,07%	2,22	5,94	5,67	0,083	
3	N_2O	3,15%	6,44	17,25	0,23%	0,48	1,27	-15,98	**-0,232**	**50,2**
	Ar	96,72%	197,97	530,27	95,61%	197,97	530,27	0	0,000	
	O_2	0,03%	0,06	0,16	0,03%	0,05	0,14	-0,02	0,000	
	N_2	0,07%	0,14	0,37	3,15%	6,68	17,89	17,52	0,247	
	CO_2	0,07%	0,15	0,41	1,28%	2,72	7,29	6,88	0,097	
4	N_2O	5,38%	11,29	30,23	2,06%	4,37	11,70	-18,54	**-0,261**	**574,1**
	Ar	94,44%	197,97	530,27	93,47%	197,97	530,27	0	0,000	
	O_2	0,03%	0,07	0,19	0,03%	0,06	0,15	-0,04	-0,001	
	N_2	0,05%	0,09	0,25	2,41%	4,96	13,30	13,05	0,179	
	CO_2	0,03%	0,07	0,18	1,29%	2,65	7,10	6,91	0,095	
5	N_2O	2,41%	4,89	13,09	0,06%	0,13	0,33	-12,76	**-0,175**	**4,3**
	Ar	97,49%	197,97	530,27	96,21%	197,97	530,27	0	0,000	
	O_2	0,03%	0,06	0,15	0,03%	0,06	0,15	0,00	0,000	
	N_2	0,05%	0,11	0,30	3,67%	7,69	20,59	20,30	0,269	
	CO_2	0,05%	0,11	0,30	1,49%	3,13	8,38	8,08	0,107	
6	N_2O	3,91%	8,07	21,62	0,24%	0,51	1,37	-20,25	**-0,269**	**48,1**
	Ar	95,95%	197,97	530,27	94,56%	197,97	530,27	0	0,000	
	O_2	0,03%	0,06	0,16	0,03%	0,06	0,15	-0,01	0,000	
	N_2	0,05%	0,09	0,25	2,37%	4,89	13,09	12,84	0,166	
	CO_2	0,03%	0,07	0,18	1,41%	2,90	7,76	7,58	0,098	
7	N_2O	2,41%	4,89	13,09	0,05%	0,11	0,30	-12,80	**-0,165**	**2,1**
	Ar	97,49%	197,97	530,27	96,14%	197,97	530,27	0	0,000	
	O_2	0,03%	0,06	0,15	0,03%	0,05	0,14	-0,01	0,000	

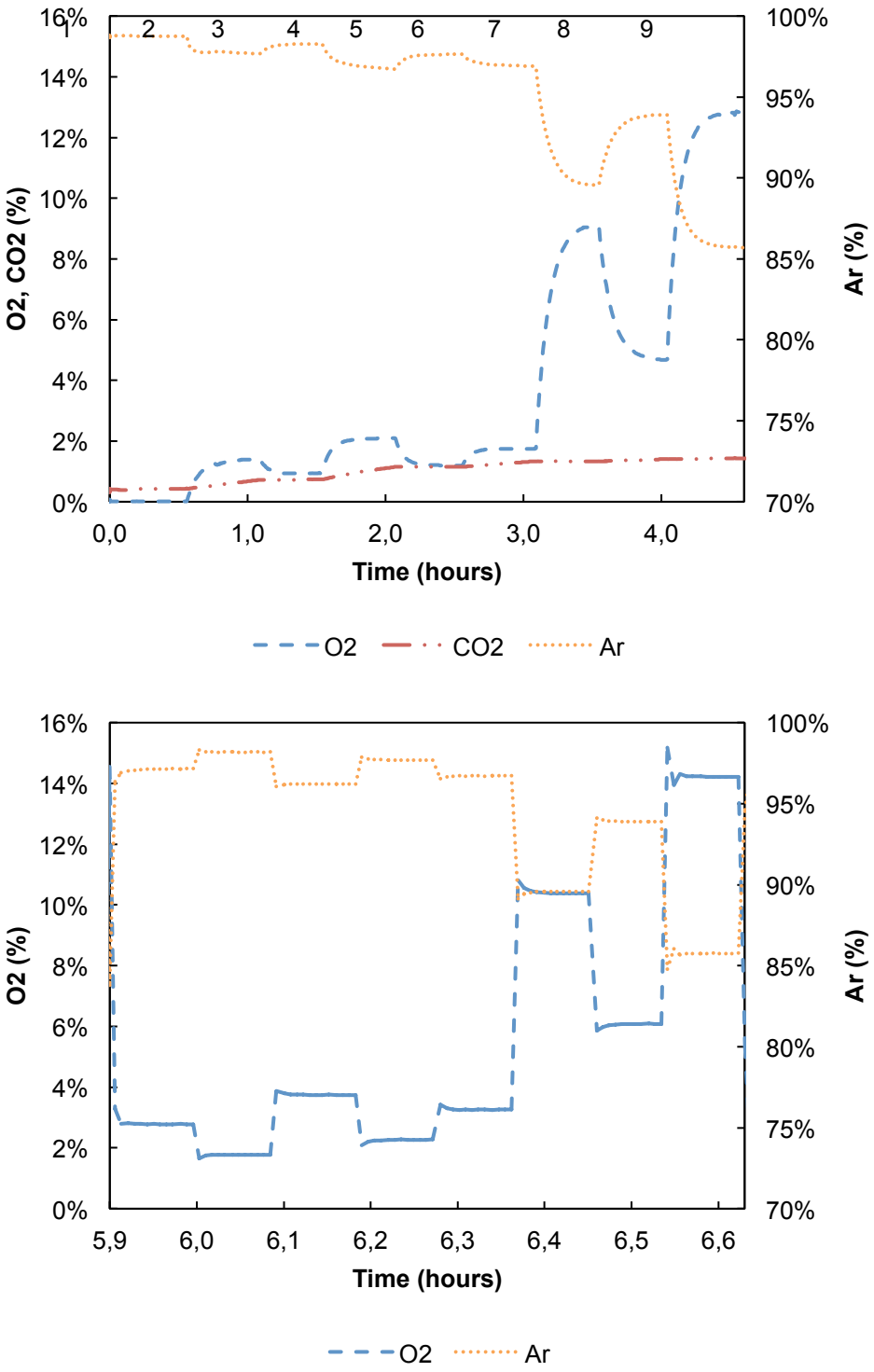

Figure S3 Concentration of N_2O, N_2, CO_2 and Argon in the offgas (above) as well as the incoming gas (below) of the experiment on day 132 (O_2 only) – presented in the main text as **Figure 1b**. The averaged data for each step – numbered in the graph - is presented in **Table S3**. Acetate and NH_4^+ were present in excess throughout the experiment. pH was kept constant at 7.0 ± 0.1

Table S3 Average concentration and rates of N_2O, N_2, CO_2, O_2 and Argon supplied and produced during each of the steps (1 through 9) in the experiment with only O_2 on day 132 – **Figure 1b** in the main text and **Figure S3**. Step 1 corresponds to steady state operation.

		IN-GAS			***OFF-gas***			***R***	***q_s***	***C_L***
			ml/min	*mmol/h*		*ml/min*	*mmol/h*	*mmol/h*	*mol/ (mol h)*	*µM*
	N_2	0,03%	0,06	0,17	0,80%	1,60	4,28	4,11	0,064	
	CO_2	0,02%	0,05	0,13	0,43%	0,85	2,29	2,15	0,034	
1	N_2O	0,77%	1,54	4,13	0,01%	0,02	0,04	-4,08	-0,064	
	Ar	99,15%	197,97	530,27	98,75%	197,97	530,27	0,00	0,000	
	O_2	0,02%	0,05	0,12	0,01%	0,03	0,08	-0,05	**-0,001**	**0,00**
	N_2	0,02%	0,04	0,10	0,21%	0,42	1,13	1,03	0,016	
	CO_2	0,01%	0,02	0,06	0,69%	1,40	3,75	3,69	0,056	
2	N_2O	0,03%	0,06	0,17	0,00%	0,00	0,00	-0,17	-0,003	
	Ar	97,16%	197,97	530,27	97,70%	197,97	530,27	0	0,000	
	O_2	2,78%	5,66	15,15	1,40%	2,84	7,60	-7,55	**-0,114**	**0,39**
	N_2	0,02%	0,04	0,10	0,06%	0,11	0,30	0,21	0,003	
	CO_2	0,01%	0,02	0,05	0,74%	1,48	3,97	3,92	0,057	
3	N_2O	0,01%	0,03	0,08	0,00%	0,00	0,00	-0,08	-0,001	
	Ar	98,18%	197,97	530,27	98,27%	197,97	530,27	0	0,000	
	O_2	1,77%	3,58	9,59	0,94%	1,89	5,07	-4,52	**-0,066**	**0,20**
	N_2	0,02%	0,04	0,10	0,04%	0,07	0,20	0,10	0,001	
	CO_2	0,01%	0,02	0,04	1,11%	2,28	6,10	6,06	0,087	
4	N_2O	0,01%	0,02	0,05	0,00%	0,00	0,00	-0,05	-0,001	
	Ar	96,22%	197,97	530,27	96,75%	197,97	530,27	0	0,000	
	O_2	3,74%	7,70	20,61	2,10%	4,29	11,50	-9,12	**-0,131**	**3,72**
	N_2	0,02%	0,04	0,10	0,03%	0,06	0,15	0,05	0,001	
	CO_2	0,01%	0,02	0,04	1,15%	2,33	6,23	6,19	0,086	
5	N_2O	0,00%	0,01	0,02	0,00%	0,00	0,00	-0,02	0,000	
	Ar	97,70%	197,97	530,27	97,63%	197,97	530,27	0	0,000	
	O_2	2,27%	4,60	12,33	1,19%	2,42	6,48	-5,85	**-0,081**	**0,62**
	N_2	0,02%	0,04	0,10	0,03%	0,06	0,16	0,06	0,001	
	CO_2	0,01%	0,01	0,04	1,31%	2,68	7,18	7,14	0,096	
6	N_2O	0,00%	0,00	0,01	0,00%	0,00	0,00	-0,01	0,000	
	Ar	96,71%	197,97	530,27	96,91%	197,97	530,27	0	0,000	
	O_2	3,26%	6,67	17,87	1,75%	3,57	9,56	-8,31	**-0,112**	**1,35**
	N_2	0,02%	0,04	0,11	0,02%	0,05	0,14	0,02	0,000	
	CO_2	0,01%	0,02	0,04	1,33%	2,93	7,84	7,80	0,104	
7	N_2O	0,00%	0,00	0,00	0,00%	0,00	0,00	0,00	0,000	
	Ar	89,58%	197,97	530,27	89,59%	197,97	530,27	0	0,000	
	O_2	10,39%	22,96	61,49	9,06%	20,02	53,64	-7,86	**-0,105**	**103,4**
	N_2	0,02%	0,04	0,10	0,02%	0,05	0,14	0,04	0,001	
	CO_2	0,01%	0,01	0,04	1,40%	2,94	7,89	7,85	0,101	
8	N_2O	0,00%	0,00	0,00	0,00%	0,00	0,00	0,00	0,000	
	Ar	93,89%	197,97	530,27	93,90%	197,97	530,27	0	0,000	
	O_2	6,08%	12,82	34,35	4,68%	9,87	26,45	-7,90	**-0,102**	**41,4**
	N_2	0,02%	0,04	0,10	0,02%	0,05	0,14	0,04	0,000	
	CO_2	0,01%	0,01	0,04	1,43%	3,30	8,83	8,79	0,110	
9	N_2O	0,00%	0,00	0,01	0,00%	0,00	0,00	-0,01	0,000	
	Ar	85,76%	197,97	530,27	85,74%	197,97	530,27	0	0,000	
	O_2	14,22%	32,82	87,91	12,80%	29,56	79,19	-8,72	**-0,109**	**150,5**

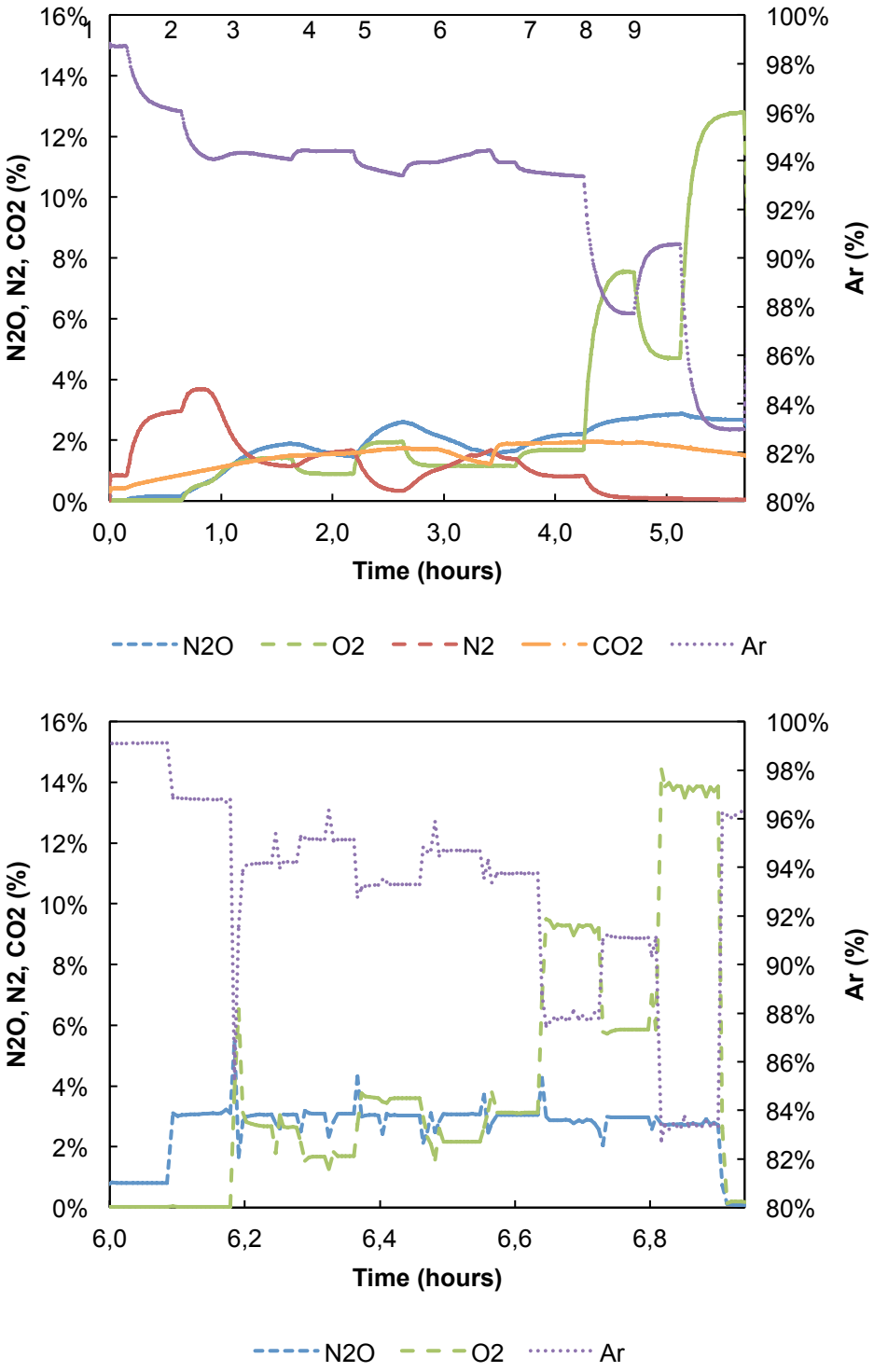

Figure S4 Concentration N_2O, N_2, CO_2, O_2 and Argon in the offgas (above) and incoming gas (below) of the experiment on day 110 (N_2O + O_2) – **Figure 3a** in the main text. The averaged data for each step – numbered in the graph - is presented in **Table S4**. Acetate and NH_4^+ were present in excess throughout the experiment. pH was kept constant at 7.0 ± 0.1

Table S4 Average concentration and rates of N_2O, N_2, CO_2, O_2 and Argon supplied and produced during each of the steps (numbered 1 through 9) in the experiment with simultaneous presence of O_2 and N_2O on day 110 – **Fig 3a** in the main text and **Fig S4**.

		IN-GAS			***OFF-gas***			***R***	***q_s***	***C_L***
			ml/min	*mmol/h*		*ml/min*	*mmol/h*	*mmol/h*	*mol/(mol h)*	*µM*
	N2	0,04%	0,08	0,21	2,94%	6,06	16,23	16,02	0,226	
	CO2	0,04%	0,08	0,22	0,82%	1,68	4,51	4,29	0,061	
1	N2O	3,09%	6,33	16,95	0,15%	0,30	0,82	-16,13	-0,228	
	Ar	96,80%	197,97	530,27	96,08%	197,97	530,27	0,00	0,000	
	O2	0,03%	0,06	0,16	0,02%	0,03	0,09	-0,06	-0,001	**0,00**
	N2	0,04%	0,08	0,22	1,15%	2,43	6,50	6,27	0,084	
	CO2	0,04%	0,08	0,20	1,48%	3,11	8,33	8,12	0,108	
2	N2O	3,06%	6,43	17,23	1,87%	3,94	10,55	-6,68	-0,089	
	Ar	94,22%	197,97	530,27	94,08%	197,97	530,27	0	0,000	
	O2	2,65%	5,56	14,89	1,41%	2,98	7,97	-6,92	-0,092	**0,07**
	N2	0,04%	0,08	0,21	1,65%	3,47	9,28	9,08	0,109	
	CO2	0,07%	0,14	0,38	1,57%	3,29	8,81	8,43	0,101	
3	N2O	3,04%	6,33	16,97	1,49%	3,12	8,35	-8,62	**-0,104**	
	Ar	95,14%	197,97	530,27	94,40%	197,97	530,27	0	0,000	
	O2	1,71%	3,57	9,55	0,90%	1,88	5,03	-4,52	**-0,054**	**0,02**
	N2	0,04%	0,08	0,23	0,34%	0,71	1,91	1,69	0,020	
	CO2	0,04%	0,08	0,20	1,74%	3,68	9,86	9,66	0,114	
4	N2O	3,04%	6,44	17,26	2,58%	5,46	14,62	-2,64	**-0,031**	
	Ar	93,29%	197,97	530,27	93,41%	197,97	530,27	0	0,000	
	O2	3,60%	7,63	20,44	1,94%	4,11	11,00	-9,44	**-0,111**	**0,48**
	N2	0,04%	0,08	0,22	1,39%	2,93	7,86	7,63	0,086	
	CO2	0,04%	0,07	0,20	1,88%	3,96	10,62	10,42	0,117	
5	N2O	3,08%	6,43	17,23	1,64%	3,45	9,24	-7,99	**-0,090**	
	Ar	94,68%	197,97	530,27	93,94%	197,97	530,27	0	0,000	
	O2	2,17%	4,53	12,14	1,15%	2,43	6,51	-5,63	**-0,063**	**0,04**
	N2	0,04%	0,08	0,23	0,82%	1,74	4,67	4,45	0,046	
	CO2	0,04%	0,08	0,21	1,94%	4,10	10,99	10,78	0,110	
6	N2O	3,05%	6,47	17,32	2,20%	4,66	12,48	-4,85	**-0,050**	
	Ar	93,29%	197,97	530,27	93,37%	197,97	530,27	0	0,000	
	O2	3,60%	7,63	20,44	1,68%	3,55	9,52	-10,92	**-0,112**	**0,13**
	N2	0,04%	0,09	0,25	0,11%	0,25	0,66	0,41	0,004	
	CO2	0,02%	0,05	0,13	1,91%	4,32	11,57	11,44	0,115	
7	N2O	2,87%	6,47	17,33	2,71%	6,12	16,40	-0,93	**-0,009**	
	Ar	87,78%	197,97	530,27	87,72%	197,97	530,27	0	0,000	
	O2	9,28%	20,94	56,08	7,54%	17,02	45,58	-10,50	**-0,106**	**74,5**
	N2	0,04%	0,09	0,23	0,08%	0,17	0,46	0,23	0,002	
	CO2	0,03%	0,07	0,19	1,80%	3,93	10,53	10,34	0,103	
8	N2O	2,97%	6,45	17,28	2,86%	6,25	16,73	-0,55	**-0,005**	
	Ar	91,10%	197,97	530,27	90,57%	197,97	530,27	0	0,000	
	O2	5,86%	12,74	34,11	4,70%	10,27	27,50	-6,61	**-0,066**	**46,6**
	N2	0,04%	0,09	0,24	0,05%	0,12	0,33	0,09	0,001	
	CO2	0,02%	0,04	0,12	1,56%	3,72	9,95	9,84	0,098	
9	N2O	2,75%	6,52	17,48	2,68%	6,39	17,13	-0,35	**-0,003**	
	Ar	83,39%	197,97	530,27	82,95%	197,97	530,27	0	0,000	
	O2	13,81%	32,79	87,82	12,76%	30,45	81,57	-6,25	**-0,062**	**160,0**

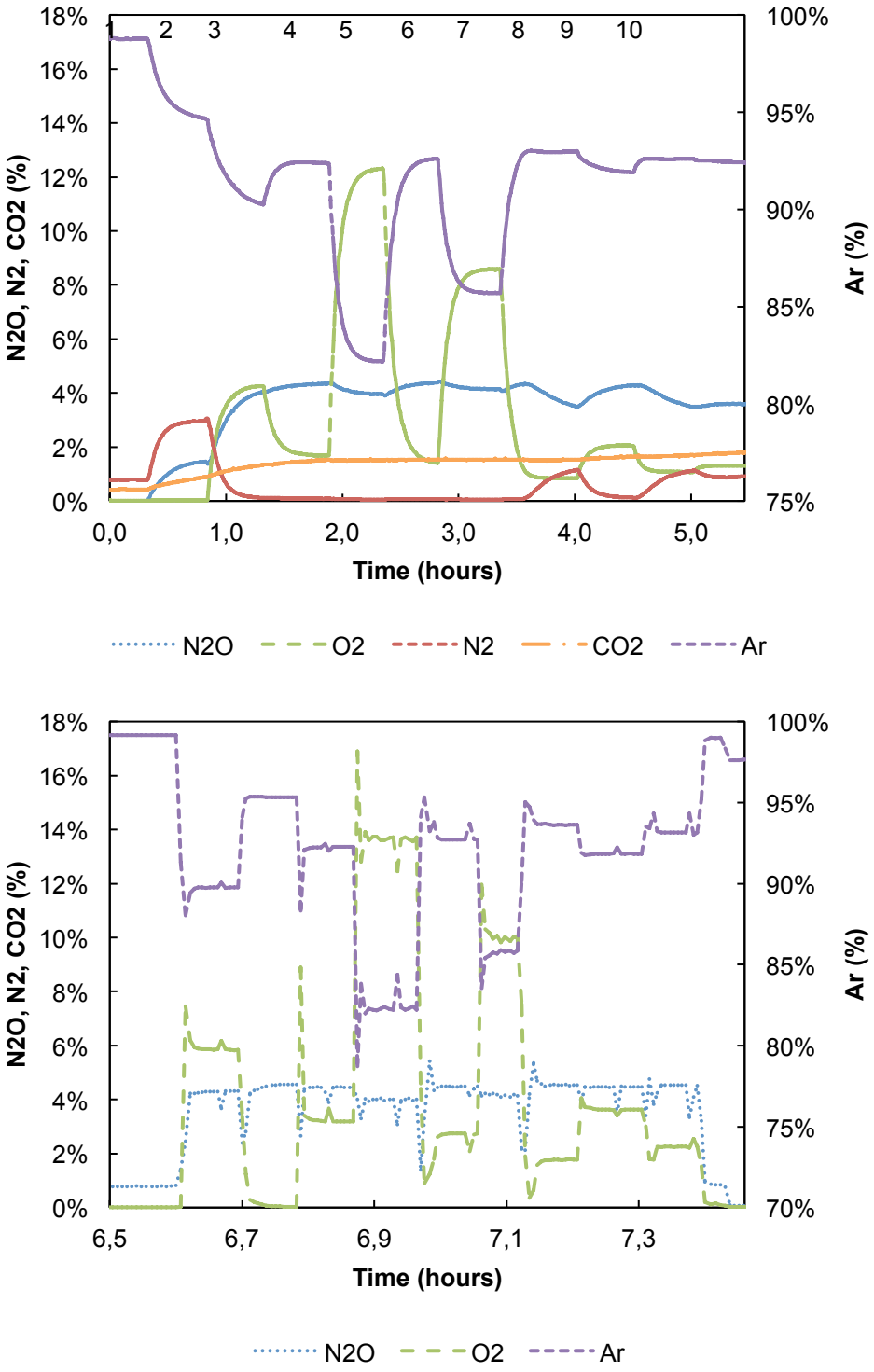

Figure S5 Concentration of N_2O, N_2, CO_2, O_2 and Argon in the offgas (above) and incoming gas (below) of the experiment on day 155 (N_2O + O_2) – **Figure 3b** in the main text. The averaged data for each step is presented in **Table S5**. Acetate and NH_4^+ were present in excess throughout the experiment. pH was kept constant at 7.0 ± 0.1

Table S5 Average concentration and rates of N_2O, N_2, CO_2, O_2 and Argon supplied and produced during each of the steps (numbered 1 through 10) in the experiment with simultaneous presence of O_2 and N_2O on day 155- **Fig 3b** in the main text and **Fig S5**.

		IN-GAS			***OFF-gas***			***R***	***q_s***	***C_L***
			ml/min	*mmol/h*		*ml/min*	*mmol/h*	*mmol/h*	*mol/ (mol h)*	*µM*
	N2	0,05%	0,10	0,26	2,96%	6,18	16,55	16,29	0,251	
	CO2	0,04%	0,08	0,23	0,84%	1,75	4,70	4,47	0,069	
1	N2O	4,56%	9,46	25,34	1,43%	2,98	7,98	-17,36	**-0,267**	
	Ar	95,33%	197,97	530,27	94,76%	197,97	530,27	0,00	0,000	
	O2	0,03%	0,06	0,17	0,02%	0,03	0,09	-0,08	**-0,001**	**0,00**
	N2	0,05%	0,11	0,29	0,13%	0,28	0,75	0,45	0,007	
	CO2	0,04%	0,09	0,23	1,31%	2,86	7,67	7,45	0,108	
2	N2O	4,31%	9,51	25,47	3,99%	8,73	23,40	-2,07	**-0,030**	
	Ar	89,76%	197,97	530,27	90,33%	197,97	530,27	0	0,000	
	O2	5,84%	12,89	34,52	4,25%	9,31	24,93	-9,59	**-0,139**	**32,1**
	N2	0,05%	0,10	0,27	0,08%	0,18	0,47	0,20	0,003	
	CO2	0,04%	0,08	0,22	1,51%	3,24	8,69	8,47	0,115	
3	N2O	4,46%	9,56	25,61	4,34%	9,31	24,93	-0,68	**-0,009**	
	Ar	92,27%	197,97	530,27	92,38%	197,97	530,27	0	0,000	
	O2	3,18%	6,83	18,28	1,68%	3,61	9,66	-8,63	**-0,117**	**3,79**
	N2	0,05%	0,11	0,30	0,06%	0,13	0,36	0,06	0,001	
	CO2	0,04%	0,09	0,24	1,51%	3,63	9,71	9,47	0,125	
4	N2O	4,01%	9,65	25,84	3,96%	9,54	25,56	-0,28	**-0,004**	
	Ar	82,19%	197,97	530,27	82,19%	197,97	530,27	0	0,000	
	O2	13,72%	33,04	88,49	12,28%	29,58	79,24	-9,25	**-0,122**	**146,6**
	N2	0,05%	0,10	0,27	0,06%	0,14	0,37	0,10	0,001	
	CO2	0,03%	0,06	0,16	1,53%	3,28	8,78	8,62	0,108	
5	N2O	4,49%	9,58	25,66	4,37%	9,35	25,04	-0,62	**-0,008**	
	Ar	92,70%	197,97	530,27	92,58%	197,97	530,27	0	0,000	
	O2	2,74%	5,85	15,66	1,45%	3,09	8,29	-7,37	**-0,092**	**2,55**
	N2	0,04%	0,10	0,27	0,05%	0,12	0,33	0,06	0,001	
	CO2	0,02%	0,05	0,14	1,53%	3,52	9,44	9,30	0,111	
6	N2O	4,18%	9,66	25,88	4,14%	9,57	25,63	-0,25	**-0,003**	
	Ar	85,71%	197,97	530,27	85,70%	197,97	530,27	0	0,000	
	O2	10,04%	23,19	62,11	8,57%	19,81	53,05	-9,05	**-0,108**	**96,6**
	N2	0,05%	0,10	0,26	1,11%	2,37	6,35	6,10	0,070	
	CO2	0,02%	0,05	0,14	1,53%	3,25	8,71	8,57	0,099	
7	N2O	4,54%	9,59	25,70	3,54%	7,54	20,20	-5,50	**-0,064**	
	Ar	93,62%	197,97	530,27	92,98%	197,97	530,27	0	0,000	
	O2	1,77%	3,74	10,03	0,84%	1,79	4,80	-5,23	**-0,060**	**0,65**
	N2	0,04%	0,09	0,25	0,14%	0,30	0,80	0,55	0,006	
	CO2	0,02%	0,05	0,14	1,63%	3,50	9,38	9,24	0,101	
8	N2O	4,47%	9,63	25,79	4,25%	9,16	24,52	-1,26	**-0,014**	
	Ar	91,84%	197,97	530,27	91,93%	197,97	530,27	0	0,000	
	O2	3,63%	7,83	20,97	2,05%	4,42	11,83	-9,14	**-0,100**	**8,78**
	N2	0,04%	0,09	0,25	1,06%	2,27	6,09	5,84	0,061	
	CO2	0,02%	0,05	0,13	1,69%	3,60	9,65	9,52	0,100	
9	N2O	4,53%	9,63	25,80	3,57%	7,63	20,43	-5,37	**-0,056**	
	Ar	93,15%	197,97	530,27	92,61%	197,97	530,27	0	0,000	
	O2	2,25%	4,79	12,83	1,08%	2,30	6,16	-6,66	**-0,070**	**1,07**

	N2	0,05%	0,10	0,27	0,90%	1,94	5,19	4,92	0,050	
	CO2	0,03%	0,06	0,16	1,79%	3,83	10,27	10,11	0,102	
10	N2O	4,49%	9,58	25,66	3,59%	7,69	20,59	-5,07	**-0,051**	
	Ar	92,70%	197,97	530,27	92,41%	197,97	530,27	0	0,000	
	O2	2,74%	5,85	15,66	1,31%	2,80	7,49	-8,17	**-0,082**	**1,40**

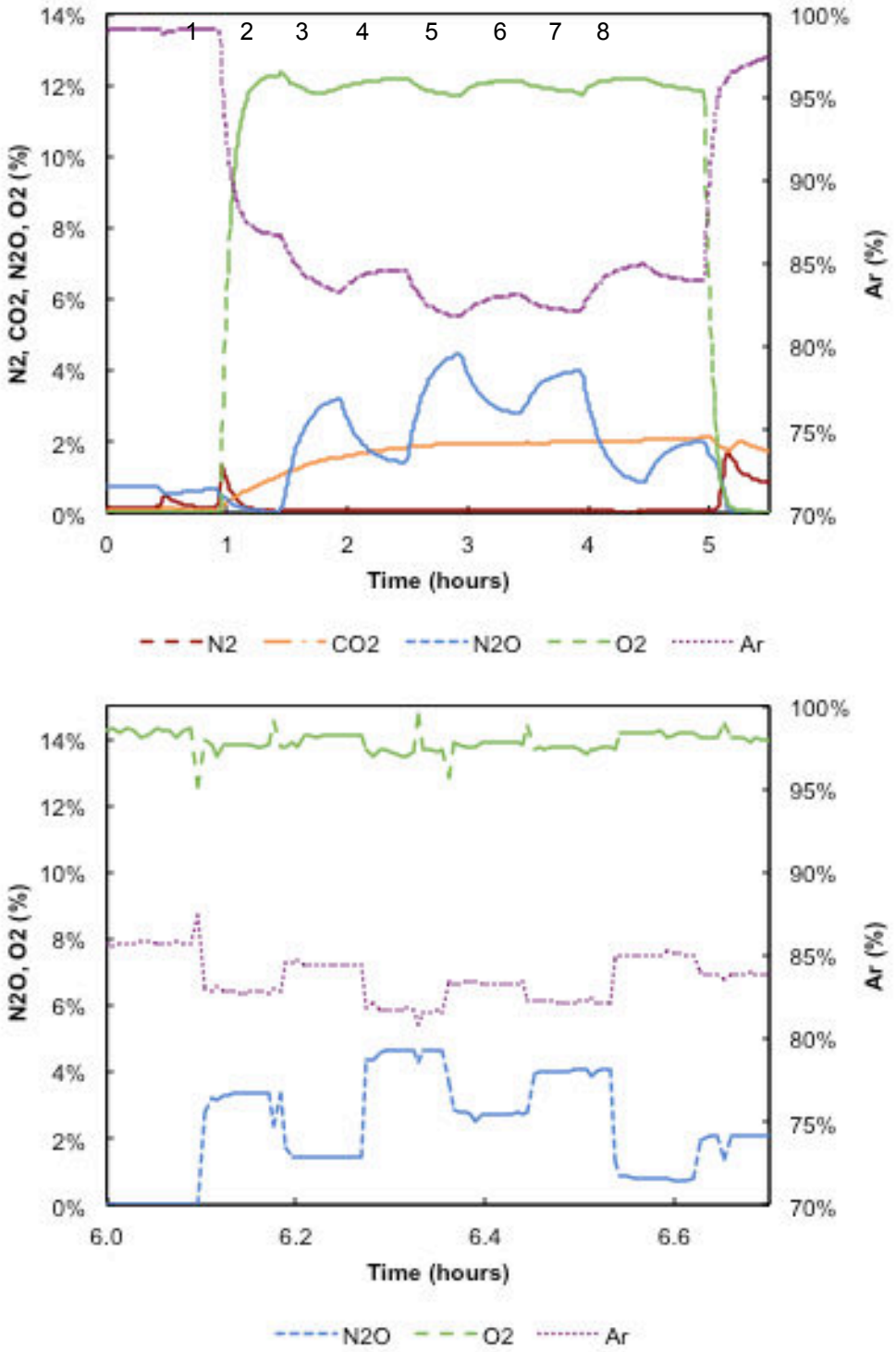

Figure S6 Concentration of N_2O, N_2, CO_2, O_2 and Argon in the offgas (above) and incoming gas (below) of the experiment on day 113 (O_2 + N_2O) – **Figure 3c** in the main text. The averaged data for each step is presented in **Table S5**. pH was kept constant at 7.0 ± 0.1

Table S6 Average concentration and rates of N_2O, N_2, CO_2, O_2 and Argon supplied and produced during each of the steps (numbered 1 through 8) in the experiment with simultaneous presence of O_2 and N_2O on day 113 – **Fig 3c** in the main text and **Figure S6**.

		IN-GAS			***OFF-gas***		***R***	***C_L***
			ml/min	*mmol/h*	*ml/min*	*mmol/h*	*mmol/h*	*µM*
	N2	0,02%	0,05	0,13	0,04%	0,09	0,25	0,1	
	CO2	0,01%	0,02	0,06	0,97%	2,21	5,91	5,8	
1	N2O	0,02%	0,05	0,12	0,03%	0,06	0,17	0,0	
	Ar	85,93%	197,97	530,27	86,73%	197,97	530,27	0,0	
	O2	14,02%	32,30	86,53	12,24%	27,93	74,82	-11,7	**5,1**
	N2	0,05%	0,11	0,30	0,08%	0,18	0,48	0,2	
	CO2	0,01%	0,03	0,09	1,54%	3,65	9,78	9,7	
2	N2O	3,32%	7,94	21,26	3,15%	7,47	20,00	-1,3	
	Ar	82,83%	197,97	530,27	83,38%	197,97	530,27	0	
	O2	13,79%	32,95	88,26	11,86%	28,15	75,40	-12,9	**4,9**
	N2	0,03%	0,07	0,20	0,05%	0,11	0,29	0,1	
	CO2	0,00%	0,00	0,00	1,81%	4,25	11,37	11,4	
3	N2O	1,41%	3,31	8,87	1,44%	3,37	9,03	0,2	
	Ar	84,45%	197,97	530,27	84,54%	197,97	530,27	0	
	O2	14,11%	33,07	88,59	12,16%	28,47	76,25	-12,3	**5,1**
	N2	0,06%	0,15	0,40	0,06%	0,19	0,50	0,1	
	CO2	0,01%	0,01	0,04	1,95%	4,72	12,63	12,6	
4	N2O	4,61%	11,18	29,95	4,43%	10,71	28,69	-1,3	
	Ar	81,60%	197,97	530,27	81,83%	197,97	530,27	0	
	O2	13,72%	33,29	89,17	89,17%	28,34	75,92	-13,2	**4,9**
	N2	0,04%	0,09	0,25	0,06%	0,14	0,39	0,1	
	CO2	0,04%	0,09	0,24	1,95%	4,65	12,45	12,2	
5	N2O	2,72%	6,46	17,29	2,80%	6,67	17,88	0,6	
	Ar	83,33%	197,97	530,27	83,10%	197,97	530,27	0	
	O2	13,88%	32,97	88,31	12,08%	28,78	77,09	-11,2	**5,0**
	N2	0,06%	0,13	0,36	0,07%	0,16	0,43	0,1	
	CO2	0,00%	0,01	0,02	1,99%	4,79	12,82	12,8	
6	N2O	4,02%	9,68	25,92	3,97%	9,56	25,60	-0,3	
	Ar	82,21%	197,97	530,27	82,17%	197,97	530,27	0	
	O2	13,71%	33,02	88,45	11,81%	28,45	76,20	-12,3	**4,9**
	N2	0,03%	0,06	0,16	0,04%	0,10	0,27	0,1	
	CO2	0,00%	0,00	0,01	2,03%	4,73	12,66	12,7	
7	N2O	0,77%	1,80	4,82	0,89%	2,07	5,54	0,7	
	Ar	85,02%	197,97	530,27	84,87%	197,97	530,27	0	
	O2	14,18%	33,02	88,44	12,17%	28,39	76,03	-12,4	**5,1**
	N2	0,03%	0,08	0,22	0,06%	0,15	0,39	0,2	
	CO2	0,07%	0,16	0,43	2,10%	4,95	13,27	12,8	
8	N2O	2,00%	4,71	12,62	2,00%	4,70	12,60	0,0	
	Ar	83,89%	197,97	530,27	83,99%	197,97	530,27	0	
	O2	14,02%	33,08	88,60	11,86%	27,95	74,85	-13,7	**4,9**

Table S7 Parameters and stoichiometry used to calculate the Gibbs free energy dissipation values during microbial growth following the methodology of Kleerebezem and Van Loosdrecht (2010). To obtain the overall stoichiometry of microbial metabolism (MET): first, the stoichiometry of the redox reactions describing the catabolism (**CAT**) and anabolism (**AN**) need to be established from the balanced redox half reactions (**D** for donor half reaction; **A** for acceptor half reaction and **An*** for the anabolic half reaction based on the C and N source – in this case acetate and ammonium). In a subsequent step, the stoichiometric coefficent – here λ_{cat}, derived from the experimentally determined biomass yields on substrate ($Y_{x/Acetate}$) - is used to couple the CAT and AN equations into the overall metabolic growth equation. The Gibbs free energy dissipation during the growth reaction is calculated by multiplying the stoichiometric coefficients obtained with the Gibbs free energy of formation of these compounds (G_f^0) corrected for non-ideality considering T = 20 °C and pH 7.

		G_f^0	D	A			An*	CAT			AN	MET		
		kJ mol^{-1}		N_2O	NO_3^-	O_2		N_2O	NO_3^-	O_2		N_2O	NO_3^-	O_2
$Y_{x/Acetate}$												-0,72	-0,75	-0,89
λ_{cat}												0,87	0,81	0,59
Ammonium	NH_4^+	-79,4					-0,2				-0,2	-0,2	-0,20	-0,20
Dinitrogen	N_2	0		1	1			4	0,8			3,49	0,65	
Nitrate	NO_3^-	-111,3			-2				-1,6				-1,29	
Nitrous oxide	N_2O	104,2		-1				-4				-3,49		
Carbon dioxide	CO_2	-394,4	2					2	2	2	0,05	1,79	1,67	1,24
Acetate	$C_2H_3O_2^-$	-369,4	-1				-0,5	-1	-1	-1	-0,525	-1,40	-1,33	-1,12
Biomass	$CH_{1.8}O_{0.5}N_{0.2}$	-67,0					1				1	1	1	1
Water	H_2O	-237,2	-2	1	6	2	0,5	2	2,8	2	0,45	2,19	2,71	1,64
Proton (HCl)	H^{+1}	0	7	-2	-12	-4	-0,5	-1	-2,6	-1	-0,325	-1,20	-2,43	-0,92
Oxygen	O_2	0				-1				-2				-1,19
Electron	e^{-1}	0	8	-2	-10	-4	-0,2							
ΔG^{01}	kJ $CmolX^{-1}$											-1078	-620	-479
ΔG^{01}	kJ mol N_2O or NO_3^- or O_2											-309	-479	-403
ΔG^{01}	kJ e^-mol through ETC											-155	-96	-101

References

Conthe M, Wittorf L, Kuenen JG, Kleerebezem R, Hallin S, van Loosdrecht MCM (2018b) Growth yield and selection of nosZ clade II-types in a continuous enrichment culture of N_2O respiring bacteria. Environ Microbiol Rep. doi: 10.1111/1758-2229.126307

Kleerebezem R, Van Loosdrecht MCM (2010) A generalized method for thermodynamic state analysis of environmental systems. Crit. Rev. Environ. Sci. Technol. 40:1–54

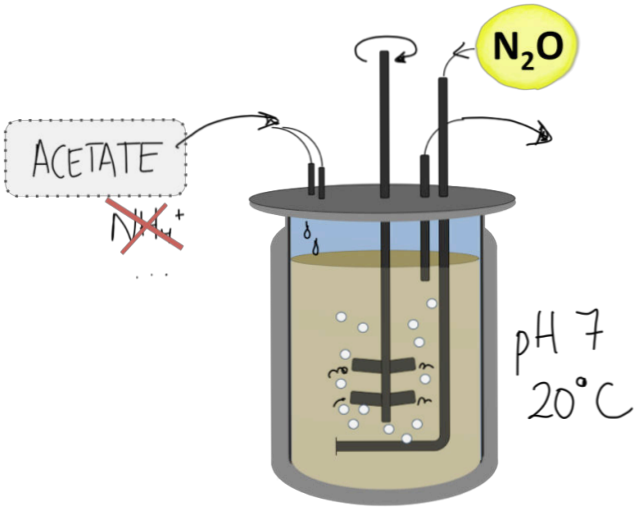
N_2O
ACETATE
NH_4^+
pH 7
20°C

5

Exploring microbial N_2O reduction: a continuous enrichment in nitrogen free medium supplied with N_2O

Conthe M, Kuenen JG, Kleerebezem R, van Loosdrecht MCM.

Environ Microbiol Rep (2018) **10**: 102–107.

Environmental Microbiology Reports (2018) **10**(1), 102–107 doi:10.1111/1758-2229.12615

Exploring microbial N_2O reduction: a continuous enrichment in nitrogen free medium

Monica Conthe,* J. Gijs Kuenen, Robbert Kleerebezem and Mark C. M. van Loosdrecht
Department of Biotechnology, Delft University of Technology, Delft, The Netherlands.

Summary

N_2O is a potent greenhouse gas, but also a potent electron acceptor. In search of thermodynamically favourable – yet undescribed – metabolic pathways involving N_2O reduction, we set up a continuous microbial enrichment, inoculated with activated sludge, fed with N_2O as the sole electron acceptor and acetate as an electron donor. A nitrogen-free mineral medium was used with the intention of creating a selective pressure towards organisms that would use N_2O directly as source of nitrogen for cell synthesis. Instead, we obtained a culture dominated by microorganisms of the *Rhodocyclaceae* family growing by N_2O reduction to N_2 coupled to N_2 fixation. Biomass yields of this culture were 40% lower than those of a previously reported culture grown under comparable conditions but with an NH_4^+-amended medium, as expected from the extra energy expense of N_2 fixation. Interestingly, we found no significant difference in yields whether N_2O or acetate was the growth-limiting substrate in the chemostat in contrast to the study with NH_4^+-amended medium, in which biomass yields were roughly 30% lower during acetate limiting conditions.

Introduction

N_2O, a potent greenhouse gas and the major ozone depleting substance of the 21st century (Ravishankara *et al*., 2009), is primarily transformed through reduction–oxidation reactions mediated by microbial communities in the biogeochemical nitrogen cycle. To deepen our understanding of these microbial conversions, resulting in the production and consumption of N_2O, will be essential in the development of mitigation strategies to reduce greenhouse gas emissions in agricultural production and wastewater treatment facilities.

While a variety of pathways lead to N_2O production, N_2O reduction to N_2 by the nitrous oxide reductase enzyme – encoded by the gene *nosZ* – is, to date, the only known pathway consuming N_2O. This metabolic step is present in denitrifying organisms as part of the denitrification pathway, but also as an independent step in non-denitrifying organisms (Hallin *et al*., 2018). Microorganisms reduce N_2O for energy conservation in the absence of O_2, but also as an electron sink in the presence of oxygen (Park *et al*., 2017), and possibly for detoxification purposes, as there is accumulating evidence that increased concentrations of N_2O may be cytotoxic to cells (Sullivan *et al*., 2013; Conthe *et al*., 2018) even though the mechanism behind this remains unclear.

New pathways in the nitrogen cycle are continuously being discovered: for example, anaerobic ammonium oxidation (Anammox; Strous *et al*., 1999), nitrite driven anaerobic methane oxidation (N-AMO; Raghoebarsing *et al*., 2006), complete ammonium oxidation (Comammox; Daims *et al*., 2015; Van Kessel *et al*., 2015). Prior to the enrichment of microorganisms capable of these conversions, the existence of the Anammox and N-AMO metabolisms had been proposed based on the thermodynamics of the electron acceptor and electron donor reactions (Broda, 1977; Raghoebarsing *et al*., 2006). As a strong electron acceptor, even stronger than O_2, N_2O opens up a realm of possibilities in the postulation of hypothetical metabolic pathways based on thermodynamic considerations (Strous *et al*., 2002; Heijnen and Kleerebezem, 2010; Table 1). Such pathways would be of interest, not only to deepen our understanding of the nitrogen cycle and N_2O turnover in natural ecosystems, but also as N_2O consuming pathways exploitable for the mitigation of N_2O emission.

We chose to work with a continuous microbial enrichment as a tool to search for such unknown N_2O-reducing metabolisms. Previously, we investigated microbial growth with N_2O as the sole electron acceptor and acetate as a carbon source and electron donor in chemostats inoculated with activated sludge (Conthe *et al*., 2018; Conthe *et al*., unpublished). However, whereas in previous studies we amended the mineral medium with NH_4^+ as a nitrogen source for biomass growth, here, the medium fed to the reactor was strongly limited in readily available

Table 1. Theoretical energy yields in the redox reactions of (1) aerobic respiration, (2) N_2O reduction to N_2, (3) N_2O reduction to NH_4^+ (hypothetical) and (4) nitrogen fixation with acetate as the electron donor and carbon source, as well as of (5) nitrification, (7) anammox and two other hypothetical pathways (6 and 8), calculated using the standard Gibbs free-energy values defined by Thauer *et al*., 1977.

	Pathway	Biochemistry	Reaction	ΔG^{01}_{CAT} (kJ/mole Ac^- or NH_4^+)	ΔG^{01}_e (kJ/e^-mol)
(1)	Aerobic respiration	Terminal reductases	$C_2H_3O_2^- + 2O_2 + H^+ \rightarrow 2CO_2 + 2H_2O$	−855	−107
(2)	N_2O reduction to N_2	N_2O reductase (*nosZ*)	$C_2H_3O_2^- + 4N_2O + H^+ \rightarrow 2CO_2 + 4N_2 + 2H_2O$	−1271	−159
(3)	N_2O reduction to NH_4^+	Hypothetical	$C_2H_3O_2^- + N_2O + 3H^+ + H_2O \rightarrow 2CO_2 + 2NH_4^+$	−327	−41
(4)	N_2 reduction to NH_4^+	Nitrogenase (*nif*)	$C_2H_3O_2^- + 1.3N_2 + 3.7H^+ + 2H_2O \rightarrow 2CO_2 + 2.7NH_4^+$	−13	−2
(5)	Nitrification	(*amo; hao*)	$NH_4^+ + 1.5O_2 \rightarrow NO_2^- + H_2O + 2H^+$	−269	−45
(6)	N_2O driven nitrification	Hypothetical	$NH_4^+ + 3N_2O \rightarrow NO_2^- + H_2O + 2H^+$	−581	−97
(7)	Anammox	(*nirS*; *hzs*; *hdh*)	$NH_4^+ + NO_2^- \rightarrow N_2 + 2H_2O$	−363	−61
(8)	N_2O driven anammox	Hypothetical	$NH_4^+ + 1.5N_2O \rightarrow 2N_2 + 1.5H_2O + H^+$	−472	−79

The hypothetical N_2O driven nitrification and Anammox pathways (6 and 8) are autotrophic, and their selection would not be expected in our acetate-fed system.

nitrogen sources like NH_4^+, NO_x compounds or organic nitrogen. The intention of this approach was to create a selective pressure towards organisms that would use N_2O directly as source of nitrogen for cellular growth.

The culture was enriched from a fresh activated sludge inoculum initially in batch mode and subsequently in continuous mode, under comparable conditions to the previous studies – that is, a dilution rate of 0.027 h^{-1}, pH 7, 20°C. During different phases of operation, the culture was subjected to varying ratios of electron acceptor (N_2O) to electron donor (acetate), as it was shown in Conthe *et al*. (2018) that whether N_2O is growth limiting or in excess can have an important effect on the N_2O reducing culture in terms of growth yields and microbial community composition. We monitored the conversions taking place in the enrichment, calculated the growth yields of the culture and monitored the enriched microbial community by 454 pyrosequencing of the 16S rRNA genes throughout the different operation periods.

Results and discussion

Conversions in the chemostat and microbial community selected

A microbial enrichment, inoculated with activated sludge, using acetate as a carbon and energy source and exogenous N_2O as the sole electron acceptor was successfully maintained using a nitrogen free medium during a period of approximately 74 days at a dilution rate of 0.027 h^{-1} at different N_2O/acetate ratios (Table 2, Fig. 1). This was achieved by increasing or decreasing the N_2O supply sparged into the reactor (diluted in N_2 gas to increase mass transfer and to facilitate the online measurement of the off-gas), while keeping the acetate concentration in the influent constant (operation phases a–e). The chemostat set-up, medium composition, sampling and analytical procedures are described in detail in Conthe *et al*. (2018) with the difference that NH_4Cl was not included in the medium. The trace amounts of yeast extract in the medium were maintained but provided $< 0.1\%$ of the nitrogen required for biomass growth at any given phase of operation. In the final stage of operation (phase f), NH_4^+ was supplied to the culture in the form of NH_4Cl during roughly five generations.

The batch start-up phase (i.e., the time necessary for the culture to fully consume the initial dose of acetate) was longer in the NH_4^+-free medium compared with the NH_4^+-amended culture in Conthe *et al*. (2018; 14 vs. 2 days, respectively – data not shown). The carbon and electron balances set up indicate that the culture was growing by N_2O reduction to N_2 at the expense of

Table 2. Average conversion rates in the chemostat during operation phases a–f

Phases	Limiting compound	Compound conversion rates (mmol h^{-1})					% recovery	
		Ac−	N_2O	$CH_{1.8}O_{0.5}N_{0.2}$*	CO_2	NH_4^+	C− bal	e− bal**
a	Acetate	−2.67 ± 0.09	−8.84 ± 0.91	1.19 ± 0.11	4.27 ± 0.42	—	102	110
b	N_2O	−1.37 ± 0.20	−4.97 ± 0.50	0.60 ± 0.04	1.80 ± 0.18	—	88	117
c	N_2O	−2.24 ± 0.13	−6.57 ± 0.66	0.98 ± 0.02	2.69 ± 0.26	—	82	100
d	N_2O	−2.55 ± 0.15	−8.09 ± 0.81	1.13 ± 0.04	3.53 ± 0.35	—	91	106
e	Acetate	−2.69 ± 0.16	−9.73 ± 0.98	1.04 ± 0.03	3.97 ± 0.39	—	93	113
f	Acetate (NH_4^+)	−2.70 ± 0.09	−9.92 ± 1.01	1.28 ± 0.01	4.02 ± 0.39	−0.28 ± 0.01	98	120

*Calculated from the measured volatile suspended solids, assuming theoretical biomass composition (Roels, 1980).
**Assuming degree of reduction of biomass to be 4.8 and considering only N_2O consumption and not N_2 production.

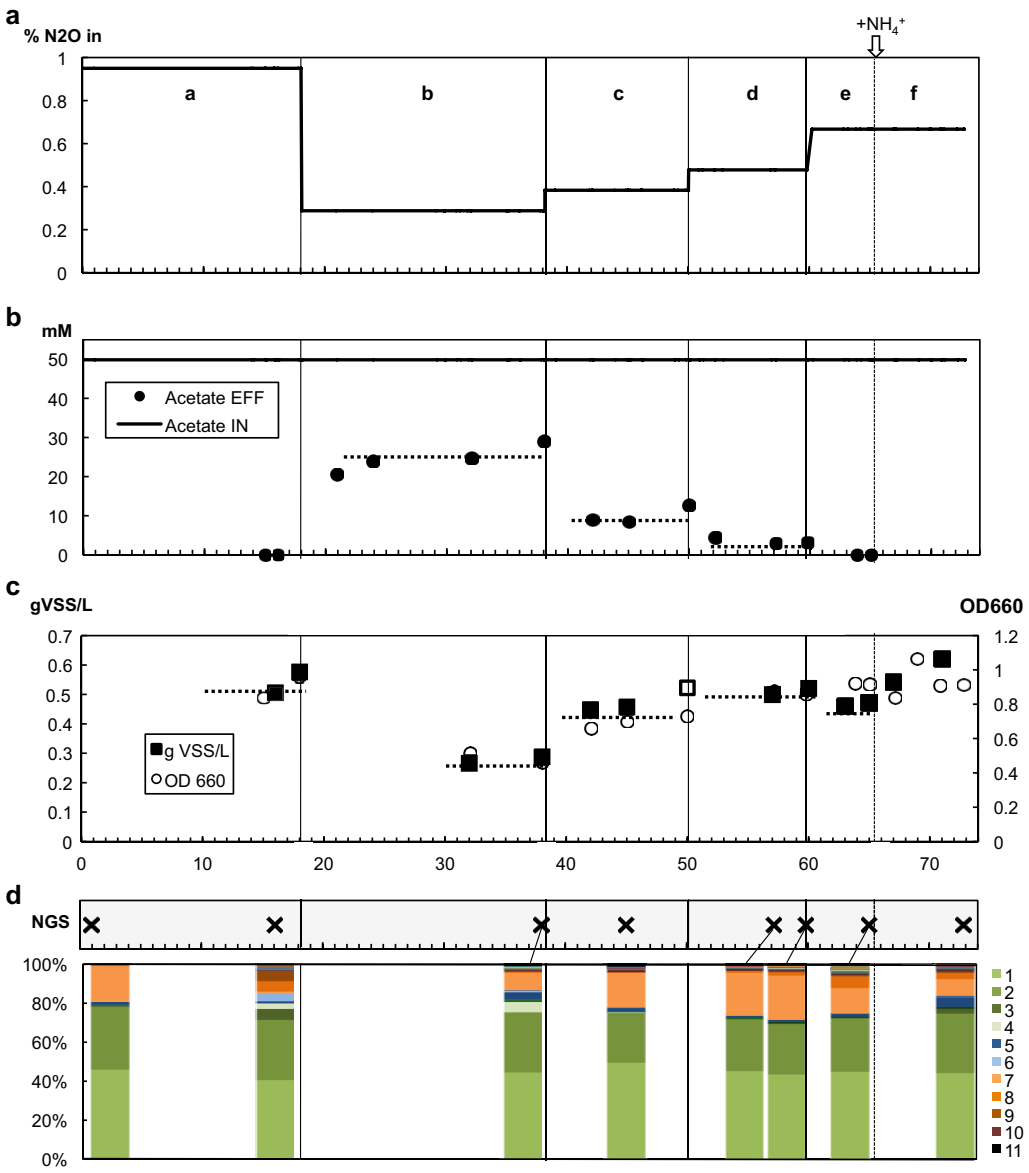

Fig. 1. Chemostat operation over 72 days showing (a) N_2O concentration in the gas supplied to the reactor, (b) incoming and outgoing acetate concentrations and (c) biomass concentration (in gVSS/L) and optical density of the culture. The relative abundance (in %) of the main 16S rRNA OTUs on different operation days determined by next generation sequencing (NGS) is presented in (d) where OTUs belonging to the Rhodocyclaceae family are shown in shades of green. The sequences are available at NCBI under BioProject accession number PRJNA413885 and the assigned taxonomy of the main OTUs is presented in Table 3. OTUs 1 and 2 have consensus sequences with 99% similarity. Day 0 marks the start of continuous operation. Previous to this, the enrichment was maintained in batch mode for approximately 14 days, until acetate was depleted. The different phases of operation regarding the N_2O to Acetate ratio supplied to the chemostat are labelled a through f. The point at which NH_4Cl was added to the medium (at a final concentration of 1.7 g/L) is indicated by a white arrow. Concentration of NH_4^+ in the effluent during phase f was below the detection limit, indicating that it was all consumed for biomass growth.

acetate oxidation (Table 2). Qualitative acetylene tests on days 60 and 63 showed that the culture had nitrogenase activity (Hardy *et al.*, 1968), evidence that growth in the nitrogen-free medium was dependent on cellular nitrogen fixation. The acetylene tests were performed by incubating 10 mL of freshly sampled culture with 1mM acetate in 20 mL sealed serum flasks with 1% O_2 and 7.5% acetylene in an Argon flushed headspace. After 24 h, gas chromatography of the headspace revealed an adjacent peak to the acetylene peak at a retention time coinciding with the retention time of an ethylene standard.

The microbial community was monitored by sequencing the 16S rRNA genes on different sampling dates throughout operation of the enrichment (Fig. 1d, Table 3). Starting from the complex activated sludge inoculum, a

Table 3. Assigned taxonomy for the main 16S rRNA gene sequences using the Silva database.

OTU	Phylum	Class	Family	Genus	Identity (%) avg ± stdev
1	Proteobacteria	Betaproteobacteria	*Rhodocyclaceae*	*Quatrionicoccus*	97.1 ± 0.6
2	Proteobacteria	Betaproteobacteria	*Rhodocyclaceae*	Uncultured	96.8 ± 0.9
3	Proteobacteria	Betaproteobacteria	*Rhodocyclaceae*	*Azonexus*	97.6 ± 1.0
4	Proteobacteria	Betaproteobacteria	*Rhodocyclaceae*	*Azoarcus*	97.6 ± 0.8
5	Proteobacteria	Alphaproteobacteria	*Rhodobacteraceae*	uncultured	97.0 ± 1.0
6	Proteobacteria	Alphaproteobacteria	*Rhizobiaceae*	*Rhizobium*	98.9 ± 0.9
7	Bacteroidetes	Flavobacteria	*Flavobacteriaceae*	*Moheibacter*	97.1 ± 0.6
8	Bacteroidetes	Flavobacteria	*Flavobacteriaceae*	*Flavobacterium*	98.2 ± 1.1
9	Bacteroidetes	Flavobacteria	*Flavobacteriaceae*	*Cloacibacterium*	98.7 ± 0.8
10	Bacteroidetes	Sphingobacteria	*Chitinophagaceae*	Uncultured	97.9 ± 1.7
11	Gracilibacteria	–	–	–	84.8 ± 2.0

Genomic DNA from 2 mL or reactor broth was extracted with the Ultraclean Microbial DNA extraction kit supplied by MOBIO laboratories Inc. (California), and used for a two-step PCR reaction targeting the 16S rRNA gene of most Bacteria and Archaea with the primers used by Wang *et al*. (2009). 2× iQ™ SYBR® Green Supermix (Bio-rad, CA), 500 nM primers and 1–50 ng genomic DNA, added to a final volume of 20 μL per well, was used for the first amplification with a protocol of: 5min denaturation at 95°C, 20 cycles of (i) 30 s at 95°C, (ii) 40 s at 50°C, (iii) 40 s at 72°C and a final extension of 7 min at 72°C. In the second amplification, 454-adapters (Roche) and MID tags were added to the products of step one at the U515F primer with a similar protocol but using Taq PCR Master Mix (Qiagen Inc, CA), 15 cycles, and a 10× diluted template from step one. Twelve PCR products were pooled and purified over an agarose gel using a GeneJET Gel Extraction Kit (Thermo Fisher Scientific, The Netherlands) and the resulting library was sent for 454 sequencing and run in 1/8 lane with titanium chemistry by Macrogen Inc. (Seoul, Korea). For the phylogenetic analysis, the reads were imported into CLC genomics workbench v7.5.1 (CLC Bio, Aarhus, DK; quality, limit = 0.05), trimmed to a minimum of 250 bp, and then de-multiplexed. A built-in SILVA 123.1 SSURef Nr99 taxonomic database was used for BLASTn analysis of the reads under default conditions and the top result was imported into an Excel spreadsheet and used to determine taxonomic affiliation and species abundance.

relatively simple community was enriched in the chemostat with two closely related 16S rRNA-based OTUs making up more than 70% of the sequences. Both of these OTUs (labelled 1 and 2) were Proteobacteria of the *Rhodocyclaceae* family. The fact that this family was also found in previous enrichments with NH_4^+-amended medium (Conthe *et al*., 2018; Conthe *et al*., unpublished) highlights the versatility and competitive advantage of these microorganisms in this type of system. Like in these previous studies, there was a background of microorganisms belonging to the *Flavobacteriaceae* family (OTUs 7, 8, 9) in the community throughout operation. Interestingly, the microbial community selected was resilient, unaffected by shifts in the N_2O/Acetate ratio or by the addition of NH_4^+ to the medium on day 65.

Growth by N_2O reduction to N_2 coupled to N_2 fixation

The biomass yield of the culture reported in this study (in C-moles of biomass per C mole of acetate) was roughly 40% lower than that of an NH_4^+-amended culture under comparable conditions (Table 4; N_2O limiting conditions). Assuming that 8 moles of ATP are required per mole of N fixed (Burgess and Lowe, 1996) and that microbial cells are composed of 0.2 moles of N per C-mole (Roels, 1980), 1.6 moles of ATP are needed for nitrogen fixation during the synthesis of 1 C-mole of biomass. Assuming also that, in the presence of NH_4^+ and with acetate as a C source, 2.45 moles of ATP are required for the synthesis of 1 C-mole of biomass (as determined by Stouthamer, 1973), roughly 40% more ATP is theoretically required for cell synthesis during nitrogen fixation via nitrogenase (2.45 + 1.6 = 4.05 moles ATP/C-mol biomass) than when a more readily available source of nitrogen is available. A pure continuous culture of *Azospirillum brasilense* Sp7 growing on N_2O, but with malate as a carbon and energy source, indeed yielded 50% lower biomass yields during growth on N_2 fixation than during growth in the presence of NH_4^+ as a nitrogen source (Danneberg *et al*., 1989). Our experimental observations on growth yields are in line with the theoretical impact of nitrogen fixation on growth yields.

Hence, taken together, our results indicate that the culture enriched in this study was growing by N_2O reduction to N_2 to fulfil the bioenergetic needs of the cells coupled to N_2 fixation as a source of nitrogen for cell synthesis. Different authors have speculated on the existence of a metabolic pathway in which N_2O is directly reduced to NH_4^+ – or assimilatory N_2O consumption – via the nitrogenase enzyme (Yamazaki *et al*., 1897; Jensen and Burris, 1986). However, like in this study, a batch enrichment study to search for this metabolic pathway led to the isolation of *Pseudomonas stutzeri* strains performing classic respiratory N_2O reduction coupled to N_2 fixation (as shown by following the fate of isotope labelled N_2O; Desloover *et al*., 2014).

The *Rhodocyclaceae* family includes nitrogen-fixing genera like *Azonexus*, *Azospira* and *Azovibrio* (Rosenberg,

Table 4. Biomass yields of the enrichment in this study compared to the yields of enrichments reported in previous studies under comparable conditions (acetate as carbon and energy source, D = dilution rate, substrate limitation, pH, temperature), but supplemented with NH_4^+ as a nitrogen source for growth.

Study	D (h^{-1})	Limiting compound	+ NH_4^+	Y_{XAc}	NH_4^+ consumption
				CmolX/CmolAc	molN/CmolX
Conthe *et al*. unpublished	0.027	N_2O	+	0.36 ± 0.04	0.27 ± 0.01
Conthe *et al*. in press	0.027	N_2O	+	0.32 ± 0.04	0.26 ± 0.01
Conthe *et al*. in press	0.027	Acetate	+	0.25 ± 0.02	0.28 ± 0.02
This study[a]	0.027	Acetate	+	0.24 ± 0.02	0.22 ± 0.02
This study[b]	0.027	Acetate	−	0.21 ± 0.02	–
This study[c]	0.027	N_2O	−	0.22 ± 0.02	–

[a]Yield calculated from conversion rates during phase f.
[b]Yield calculated from average conversion rates during phases a and e.
[c]Yield calculated from average conversion rates during phases b–d.

2013) and presumably the two OTUs dominating the enrichment also have the capability to fix nitrogen. The genetic potential for nitrogen fixation is ubiquitous in activated sludge (Yu and Zhang, 2012) and a number of organisms harbour genes for both nitrous oxide reduction (*nos*) and the nitrogen fixation (*nif*; Torres *et al*., 2016).

Excess N_2O may interfere with cellular assimilation of nitrogen

Unexpectedly, we found no significant difference in biomass yields, per mole of acetate, depending on whether N_2O or acetate was the growth-limiting substrate in the culture (operation phases a and e vs. b, c and d; Table 4). This is in stark contrast to an enrichment culture and a *Pseudomonas stutzeri* JM300 culture reported in Conthe *et al*. (2018), both of which presented substantially lower biomass yields during acetate limiting conditions when compared with the N_2O limiting conditions. Furthermore, the biomass yield obtained under acetate limiting conditions after NH_4Cl was supplied to the medium (operation phase f; Table 4) was similar to the yield during acetate limitation in Conthe *et al*. (2018). We can merely speculate about the reasons behind the different effect of acetate limitation on a NH_4^+-amended versus nitrogen-free culture, but it may suggest that a surplus N_2O concentration potentially interferes in specific steps of the NH_4^+ assimilation process (e.g., by inhibiting NH_4^+ transporters, favouring the energetically costly GDH NH_4^+ assimilation system over the GS/GOGAT or up/down regulation of genes), resulting in lower biomass yields. This would be an interesting hypothesis to address in future studies.

Outlook

We did not find the postulated metabolic pathway of N_2O reduction to NH_4^+ presented in Table 1, despite the fact that it is a thermodynamically favourable reaction that would save cells energy invested in the energetically costly process of N_2 fixation (Eq. 3 vs. 4). This illustrates how thermodynamics alone may not be enough to predict the existence of a metabolic pathway: the adequate biochemistry may not exist due to physical constraints or due to lack of evolutionary drive to select for it. Nonetheless, we believe it is of interest to continue the search for these undiscovered, yet thermodynamically favourable, pathways. Future studies should consider lower dilution rates than the ones used here (rare metabolisms typically require low growth rates), growth in biofilms and a variety of carbon sources. Autotrophic enrichments would be necessary in the search for N_2O driven nitrification or N_2O driven Anammox (Table 1, Eqs. 6 and 8, respectively). A thorough understanding of all pathways involving the oxidation or reduction of N_2O is not only interesting from an academic point of view, but may also be important in the development of mitigation strategies to control emissions of this potent greenhouse gas.

Conflict of Interest

The authors declare no conflict of interest.

Acknowledgements

This work was funded by the European Commission (Marie Curie ITN NORA, FP7–316472). The authors would like to thank Mitchell Geleijnse and Ben Abbas for their great help with the molecular analysis of microbial community composition.

References

Broda, E. (1977) Two kinds of lithotrophs missing in nature. *Zeitschrift Für Allg Microbiol* **17**: 491–493.

Burgess, B.K., and Lowe, D.J. (1996) Mechanism of molybdenum nitrogenase. *Chem Rev* **96**: 2983–3012.

Conthe, M., Wittorf, L., Kuenen, J.G., Kleerebezem, R., van Loosdrecht, M.C.M., and Hallin, S. (2018) Life on N_2O:

deciphering the ecophysiology of N_2O respiring bacterial communities in a continuous culture. *Isme J* (In press).

Daims, H., Lebedeva, E.V., Pjevac, P., Han, P., Herbold, C., Albertsen, M., *et al*. (2015) Complete nitrification by Nitrospira bacteria. *Nature* **528**: 504.

Danneberg, G., Zimmer, W., and Bothe, H. (1989) Energy transduction efficiencies in nitrogenous oxide respirations of Azospirillum brasilense Sp7. *Arch Microbiol* **151**: 445–453.

Desloover, J., Roobroeck, D., Heylen, K., Puig, S., Boeckx, P., Verstraete, W., *et al*. (2014) Pathway of nitrous oxide consumption in isolated Pseudomonas stutzeri strains under anoxic and oxic conditions. *Environ Microbiol* **16**: 3143–3152.

Hallin, S., Philippot, L., Löffler, F.E., Sanford, R.A., and Jones, C.M. (2018) Genomics and ecology of novel N2O-reducing microorganisms. *Trends Microbiol* **26**: 43–55.

Hardy, R.W.F., Holsten, R.D., Jackson, E.K., and Burns, R.C. (1968) The acetylene-ethylene assay for n2 fixation: laboratory and field evaluation. *Plant Physiol* **43**: 1185–1207.

Heijnen, J.J., and Kleerebezem, R. (2010) Bioenergetics of microbial growth. In *Encyclopedia of Bioprocess Technology*. Flickinger, M.C., and Drew, S.W. (eds). Hoboken, NJ: John Wiley & Sons, Inc.

Jensen, B.B., and Burris, R.H. (1986) N2O as a substrate and as a competitive inhibitor of nitrogenasase. *Biochemistry* **25**: 1083–1088.

Park, D., Kim, H., Yoon, S., and Kivisaar, M. (2017) Nitrous oxide reduction by an obligate aerobic bacterium, Gemmatimonas aurantiaca strain T-27. *Appl Environ Microbiol* **83**: e00502-e00517.

Raghoebarsing, A.A., Pol, A., van de Pas-Schoonen, K.T., Smolders, A.J.P., Ettwig, K.F., Rijpstra, W.I.C., *et al*. (2006) A microbial consortium couples anaerobic methane oxidation to denitrification. *Nature* **440**: 918–921.

Ravishankara, A.R., Daniel, J.S., and Portmann, R.W. (2009) Nitrous oxide (N2O): the dominant ozone-depleting substance emitted in the 21st century. *Science (80)* **326**: 123–125.

Roels, J.A. (1980) Simple model for the energetics of growth on substrates with different degrees of reduction. *Biotechnol Bioeng* **22**: 33–53.

Rosenberg, E. (2013) The family rhodocyclaceae. In *The Prokaryotes: Alphaproteobacteria and Betaproteobacteria*. DeLong, E.F., Lory, S., Stackebrandt, E., and Thompson, F.L. (eds). Berlin, Heidelberg: Springer, pp. 1–1012.

Stouthamer, A.H. (1973) A theoretical study on the amount of ATP required for synthesis of microbial cell material. *Antonie Van Leeuwenhoek* **39**: 545–565.

Strous, M., Fuerst, J.A., Kramer, E.H., Logemann, S., Muyzer, G., van de Pas-Schoonen, K.T., *et al*. (1999) Missing lithotroph identified as new planctomycete. *Nature* **400**: 446–449.

Strous, M., Kuenen, J.G., Fuerst, J.A., Wagner, M., and Jetten, M.S.M. (2002) The anammox case - A new experimental manifesto for microbiological eco-physiology. *Antonie van Leeuwenhoek Int J Gen Mol Microbiol* **81**: 693–702.

Sullivan, M.J., Gates, A.J., Appia-Ayme, C., Rowley, G., and Richardson, D.J. (2013) Copper control of bacterial nitrous oxide emission and its impact on vitamin B12-dependent metabolism. *Proc Natl Acad Sci U S A* **110**: 19926–19931.

Thauer, R.K., Jungermann, K., and Decker, K. (1977) Energy conservation in chemotrophic anaerobic bacteria. *Bacteriol Rev* **41**: 100–180.

Torres, M.J., Simon, J., Rowley, G., Bedmar, E.J., Richardson, D.J., Gates, A.J., *et al*. (2016) *Nitrous Oxide Metabolism in Nitrate-Reducing Bacteria: Physiology and Regulatory Mechanisms*. 1st ed. New York: Elsevier Ltd.

Van Kessel, M.A.H.J., Speth, D.R., Albertsen, M., Nielsen, P.H., Op den Camp, H.J.M., Kartal, B., *et al*. (2015) Complete nitrification by a single microorganism. *Nature* **528**: 555.

Wang, Y., Qian, P.-Y., and Field, D. (2009) Conservative fragments in bacterial 16S rRNA genes and primer design for 16S ribosomal DNA amplicons in metagenomic studies. *PLoS One* **4**: e7401.

Yamazaki, T., Yoshida, N., Wasa, E., and Matsuo, S. (1897) N2O reduction by Azotobacter vinelandii with emphasis on konetic nitrogen isotope effects. *Plant Cell Physiol* **28**: 263–271.

Yu, K., and Zhang, T. (2012) Metagenomic and metatranscriptomic analysis of microbial community structure and gene expression of activated sludge. *PLoS One* **7**: e38183.

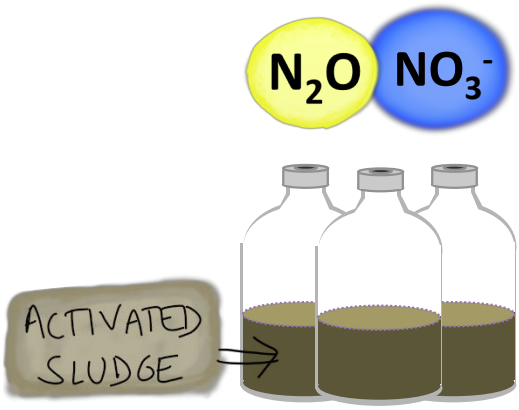
N_2O
NO_3^-
ACTIVATED SLUDGE

6

Denitrification as an N_2O sink

Conthe M, Lycus P, Ramos Da Silva A, Bakken L, Frostegård A, Kuenen JG, Kleerebezem R, van Loosdrecht MCM.

under revision in *Water Research*

+ SUPPLEMENTARY INFORMATION

Denitrification as an N_2O sink

Monica Conthe[1], Pawel Lycus[2], Magnus Arntzen[2], Aline Ramos da Silva[3], Åsa Frostegård[2], Lars Reier Bakken[2], Robbert Kleerebezem[1], Mark C. M. van Loosdrecht[1]

Summary

The strong greenhouse gas nitrous oxide (N_2O) can be emitted from wastewater treatment systems as a byproduct of ammonium oxidation and as the last intermediate in the stepwise reduction of nitrate to N_2 by denitrifying organisms. A potential strategy to reduce N_2O emissions would be to enhance the activity of N_2O reductase (NOS) in the denitrifying microbial community. A survey of existing literature on denitrification in wastewater treatment systems showed that the N_2O reducing capacity ($V_{maxN2O\rightarrow N2}$) exceeded the capacity to produce N_2O ($V_{maxNO3\rightarrow N2O}$) by a factor of 2-10. This suggests that denitrification can be an effective sink for N_2O, potentially scavenging a fraction of the N_2O produced by ammonium oxidation or abiotic reactions. We conducted a series of incubation experiments with freshly sampled activated sludge from a wastewater treatment system in Oslo and found that the ratio $\alpha = V_{maxN2O\rightarrow N2} / V_{maxNO3\rightarrow N2O}$ fluctuated between 2 and 5 in samples taken at intervals over a period of 5 weeks. Adding a cocktail of carbon substrates resulted in increasing rates, but had no significant effect on α. Based on these results – complemented with qPCR and metaproteomic data – we discuss whether the overcapacity to reduce N_2O can be ascribed to gene/protein abundance ratios (nosZ/nir), or whether in-cell competition between the reductases for electrons could be of greater importance.

Introduction

With a global warming potential roughly 300 times greater than CO_2, N_2O can be a major contributor to the greenhouse gas footprint of a wastewater treatment plant (WWTP; Daelman *et al.*, 2013). N_2O accumulates during biological nitrogen removal from wastewater as a byproduct of nitrification by ammonia oxidizing bacteria and/or as a result of incomplete denitrification by heterotrophic denitrifying bacteria in the activated sludge (Kampschreur et al., 2009; Schreiber et al., 2012). The fact that most of the emission of N_2O occurs in aerated nitrification zones in the full-scale could be taken to suggest that nitrification is the primary source of N_2O, but this is far from clear since the N_2O stripped off by aeration could a) originate from non-aerated anoxic zones or b) be produced by denitrification in anoxic microsites within the aerated nitrification zones. Attempts to discriminate N_2O produced via nitrification or denitrification by isotope analyses (Wunderlin et al., 2012) or by correlating a wide range of process variables to emissions in a long term N_2O-monitoring campaign in a full-scale WWTP (Daelman et al., 2015) have not been conclusive. Furthermore, N_2O can be produced via abiotic reactions between intermediates of nitrification and denitrification, e.g. between NO_2^- and hydroxylamine (Soler-Jofra et al., 2016) or reduced iron species (Kampschreur et al., 2011). The relative contribution of all these different processes to N_2O accumulation remains unresolved and makes it a challenge to develop greenhouse gas mitigation strategies in full-scale systems.

Numerous studies have focused on reducing the production of N_2O during nitrogen removal (Lu and Chandran, 2010; Perez-Garcia et al., 2017; Ribera-Guardia et al., 2014; Wunderlin et al., 2012) but far fewer have focused on *increasing* the *consumption* of N_2O as an equally valid - and arguably more simple - strategy to reduce emissions. While AOBs are invariably net sources of N_2O, denitrifying organisms are either net sources or net sinks, both producing and consuming this gas. The propensity of a wastewater treatment system, be it of the activated sludge-type or other, to emit N_2O will be strongly dependent on the intrinsic capacity of its heterotrophic denitrifying community to reduce N_2O. A community with low N_2O reductase (NOS) activity relative to the other reductases (i.e. nitrate reductases, NAR, nitrite

reductases, NIR, and nitric oxide reductases, NOR) will be a strong N_2O-source, while one with high relative NOS activity will emit less N_2O and may even be able to function as a net sink for N_2O produced during nitrification, as observed in nitrification experiments with Leca-particle biofilms in Mao *et al.* (2008).

The degree of NOS activity - and the resulting N_2O sink/source strength - of an ecosystem will ultimately depend on a) the genetic potential of the denitrifying community within and/or b) on the overall physiology of said community (including regulation phenomena, enzyme kinetics, electron affinity of the different reductases, etc). Microorganisms can harbor different combinations of denitrification genes in their genome (Graf et al., 2014; Lycus et al., 2017; Roco et al., 2017; Shapleigh, 2013): e.g. denitrifiers lacking the *nosZ* gene encoding NOS are widespread, as are organisms solely equipped with *nosZ* (coined non-denitrifying N_2O reducers in Sanford *et al.*, 2012; Hallin *et al.*, 2018, and referred to as such from here on). Thus, microbial community structure can play a role in the N_2O sink/source potential of a system. But even in denitrifying organisms harboring all the reductases necessary to complete the denitrification pathway (i.e. NAR/NAP, NIR, NOR, and NOS), transcriptional regulation and post transcriptional phenomena may cause an imbalance in the activity of these enzymes, leading to the release of N_2O and/or other intermediate products (i.e. NO_2^- and NO; Liu *et al.*, 2013; Lycus *et al.*, 2017). Such imbalances have been associated with e.g. the presence of O_2, significant NO_2^- accumulation, storage polymer metabolism and, not the least, rapid fluctuations in these parameters (Foley et al., 2010; Kampschreur et al., 2008; Law et al., 2012; Lu and Chandran, 2010; Otte et al., 1996; Wunderlin et al., 2012).

In order to assess the intrinsic N_2O reduction capacity of activated sludge and its potential use in full-scale N_2O emission mitigation strategies, an inventory was made of literature studies reporting maximum conversion rates for NO_3^-, NO_2^-, and N_2O in a variety of heterotrophic denitrifying systems. Below we compiled the ratios of maximum rates of N_2O production (from NO_3^-) to N_2O-reduction, which in general were not explicitly reported, as a proxy for the N_2O sink capacity of these systems and calculated the steady state concentrations of N_2O ($[N_2O]_{ss}$), an estimation of the N_2O-concentrations at which denitrification changes from being a net source of N_2O ($[N_2O]<[N_2O]_{ss}$) to become a net sink for N_2O ($[N_2O]>[N_2O]_{ss}$). Most studies involved lab-scale sequencing batch reactors (SBRs) run for prolonged periods of time, and the resulting microbial population likely had little similarities to that of the activated sludge used as inoculum. An exception is Wicht (1996), who determined N_2O vs. NO_3^- consumption rates for activated sludge. However, acetate was used as a sole carbon and energy source, neglecting the contribution of microorganisms unable to use acetate in the NO_3^- and N_2O rates reported. In the present study we complement the existing literature by comparing the N_2O and NO_3^- conversion rates of fresh activated sludge from a full-scale WWTP, with and without the addition of a mix of organic electron donors, and at 12°C, a value within the temperature range of the wastewater during most part of the sampling. Furthermore, we address the potential role of (i) the microbial gene and protein abundance in the N_2O sink capacity of the sludge - by quantifying the ratio of *nir* vs. *nosZ* genes and NIR *vs*. NOS proteins - and (ii) of differences in electron affinity amongst denitrifying reductases by means of batch tests with the simultaneous addition of NO_3^- and N_2O. Based on the results obtained, we discuss the reasons why denitrification is potentially a source of N_2O in full-scale systems, and the possibility of exploiting the N_2O sink potential as a mitigation strategy to reduce emissions of this potent greenhouse gas.

Materials and Methods

NO_3^- and N_2O batch tests with activated sludge

Batch tests were performed in 120 ml serum flasks filled with 50 ml of untreated, undiluted, fresh activated sludge from one of the pre-denitrification tanks of the Bekkelaget WWTP, which is a modified Ludzack-Ettinger (MLE)-type plant in Oslo, Norway (see **Figure S1** and for a scheme of the process units, also described inVenkatesh and Elmi, 2013) . Samples were taken over a period of 5 weeks in April and May 2015, and later in October 2015 and May 2017. Immediately after sampling, the activated sludge was transported to the lab on ice, dispensed in serum flasks while stirring for sample heterogeneity, and used for batch tests within 4 hours after sampling. Preliminary tests showed that conversion rates were not affected by which

process unit of the WWTP the activated sludge was obtained from (data not shown).

The flasks, once filled with the 50 ml of activated sludge sample and 3.5 cm long Teflon covered magnets, were sealed with rubber septa and metallic crimps, helium-washed with 6 cycles of vacuum and refilling of the headspace, and placed in the robotized incubation system described in Molstad *et al.* (2007). After a period of 15 min with stirring at 600 rpm for the temperature of the samples to equilibrate with the surrounding water bath at 12°C, the flasks were injected with either 1 ml of pure N_2O gas (using a gas tight syringe, aiming for a final headspace concentration of 1% N_2O) or 1 mM NO_3^- (from a 0.5M stock solution of $NaNO_3$) or both. These batch tests were conducted both with and without the addition of an external electron donor –a mixture of acetate, pyruvate, ethanol and glutamic acid– which was injected into the serum flasks to a final concentration of 0.5 mM for each electron donor, immediately before the injection of N_2O or NO_3^-. The transport coefficient for the transfer of gas between the headspace and the liquid was calculated to be 10^{-3} L s^{-1} at the stirring speed used - 600 rpm -, meaning that roughly 5-6 minutes were necessary for the gas-liquid concentrations to reach an equilibrium, as demonstrated in **Figure S2**. Therefore, to avoid confounding transport and N_2O reduction kinetics a period of 6.3 min was kept between the injection of N_2O and the first sampling of the headspace. Thereafter, the concentration of NO, N_2O, N_2, CO_2, He and O_2 in the headspace was regularly analyzed by the robotized system and the corresponding concentration of NO, N_2O, and N_2 in the liquid calculated as described in Molstad *et al.* (2007). When relevant, 100 μL of broth sample was collected manually for the immediate determination of NO_3^- and NO_2^- concentrations (see below). After verifying that results were reproducible (see **Figure S3**), replicate runs were sacrificed in exchange for a higher time resolution of the conversion rates (the sampling frequency of the robotized incubation system being limited by the length of the GC run and the number of flasks). For our purposes, we only considered the initial consumption rates (i.e. approximately during the first hour of incubation) to avoid the potential effect of changes in enzyme pools or depletion/accumulation of storage polymers (e.g. PHB) on N_2O reduction rates. The buffering capacity of the activated sludge itself was sufficient to maintain the pH in the range of 6.5 to 7.5 during the batch tests (the initial pH being 6.5 ± 0.2; data not shown).

Control experiments with either 15% of acetylene in the headspace or prior autoclaving of the activated sludge (15 min at 121°C; both treatments effectively inhibiting NOS activity) were performed.

Analytical procedures

NO_3^- and NO_2^- concentrations were determined by measuring the amount of nitric oxide (NO) produced by the reaction with vanadium (III) chloride in HCl at 95°C (NO_2^-+NO_3^-) and the reaction with sodium iodide in acetic acid at room temperature (NO_2^- only) using the purger system coupled to the Sievers Nitric oxide analyser NOA280i (Braman and Hendrix, 1989; Cox, 1980). The concentrations of NO, N_2O, N_2, CO_2, He and O_2 in the headspace were determined by gas chromatography as described in Molstad *et al.*, (2007).

qPCR and metaproteomics

Activated sludge samples were fixed in 100% ethanol (1 ethanol : 1 sample) and DNA was extracted using FastDNA® SPIN Kit for Soil (MP Biomedicals). The primers and PCR conditions used are found in **Table S1**. Given the potential PCR biases, and the fact that genes are not always expressed, as evidenced by the lacking correlation between gene numbers and related functions in microbial communities (Rocca *et al.*, 2014; Lycus *et al.*, 2017), we also performed an Orbitrap-based mass spectrometry analysis of the proteins. For this, we used a curated database where all the bacterial genera reported to be abundant in activated sludge, anaerobic digesters and influent wastewater (based on MiDAS survey of 24 Danish wastewater treatment plants Mielczarek *et al.*, 2013) were included. The protein extraction procedure aimed at the periplasmic fraction of proteins adapting the protocol for spheroplasts generation (Kucera, 2003). 50 ml of activated sludge was centrifuged at 10 000 g for 20 min and the pellet was used for protein extraction. The pellet was resuspended in 20 ml of 0.1 M Tris-HCl, pH 8.0, 20% sucrose, 1 mM EDTA, 60 mg lysozyme (Fluka) and incubated for 30 min at 37 °C, followed by addition of 25 ml of ice-cold H_2O and gentle mixing by inverting the tube. The sample was then incubated on ice for

another 10 min and centrifuged at 10000g for 20 min. The supernatant containing water soluble proteins was then concentrated on VivaSpin centrifugal concentrator (Sartorius) with the 30 kDa cutoff. Concentrated preparate was used for proteomic analysis. More details can be found in Supplementary Materials.

Analysis of literature data

We selected studies that reported rates of nitrate reduction at high nitrate concentrations (R_{NO3}), and rates of N_2O-reduction at high N_2O concentrations in the absence of other nitrogen oxyanions (R_{N2O}), which were taken as estimates of the maximum rates of N_2O production ($V_{maxNO3\rightarrow N2O}$) assuming no significant accumulation of intermediates, and the maximum rates of N_2O reduction ($V_{maxN2O\rightarrow N2}$), respectively. We calculated the ratio $\alpha = V_{maxN2O\rightarrow N2}/V_{maxNO3\rightarrow N2O}$ with the data from these studies and we used this data to estimate steady state N_2O concentration during denitrification (at high nitrate concentrations, $>>K_S$, no extra N_2O added). Assuming the gross production of N_2O to be as measured (= $V_{maxNO3\rightarrow N2O}$), and the N_2O reduction rate a simple Michaelis Menten function of the N_2O concentration the following differential equation can be set up:

$$\frac{d[N_2O]}{dt} = v_{\max NO_3^-\rightarrow N_2O} - v_{\max N_2O\rightarrow N_2} * \frac{[N_2O]}{([N_2O]+k_{mN_2OR})}$$

where $[N_2O]$ is the concentration in mol L^{-1} of N_2O in the liquid and k_{mN2OR} is the half saturation constant in mol L^{-1} for N_2O reductase. Solving for $[N_2O]$ when $d[N_2O]/dt=0$ the steady state N_2O concentration ($[N_2O]_{ss}$) can be obtained:

$$[N_2O]_{SS} = \frac{k_{mN_2OR}}{(\alpha-1)} \quad \text{where} \quad \alpha = \frac{v_{\max N_2O\rightarrow N_2}}{v_{\max NO_3^-\rightarrow N_2O}}$$

Results and Discussion

Overcapacity of N_2O reduction in activated sludge and other denitrifying systems

A number of studies in literature report the maximum rates, as measured in batch tests in the absence of substrate limitation, for the different steps of denitrification in activated sludge (Wicht, 1996) and denitrifying SBRs (Itokawa *et al.*, 2001; Pan *et al.*, 2012, 2013; Ribera-Guardia *et al.*, 2014; Wang *et al.*, 2014). We calculated the ratio $\alpha = V_{maxN2O\rightarrow N2} / V_{maxNO3\rightarrow N2O}$, which was not explicitly reported in these studies, as an indication of the N_2O sink (or source) potential of the denitrifiying community in these systems. Interestingly the α values obtained showed that N_2O reduction rates were consistently higher than the corresponding NO_3^- reduction rates, by a factor between 2 and 10 (**Table 1**). We consider α values >1 to represent the overcapacity of the N_2O reduction step relative to the rest of the denitrification pathway (as illustrated in **Figure 1)** and a measure of the potential N_2O sink capacity of the denitrifying community in these systems.

We carried out additional batch experiments to determine the $V_{maxN2O\rightarrow N2}$ and $V_{maxNO3\rightarrow N2O}$ in freshly sampled activated sludge taken during a 5-week sampling campaign at the Bekkelaget WWTP, and on two subsequent occasions (**Figure 2**). The α values obtained from these tests ranged from 2-5, reflecting a persistent N_2O reduction overcapacity of the activated sludge over time (**Figure 3**). The overcapacity was apparent in the batch tests both with and without the addition of a mixture of acetate, pyruvate, glutamic acid, and ethanol carbon substrate (rates increased by a factor of roughly 3 – 5 in the presence of the carbon substrate – **Figure S4**). In the batch tests provided with external N_2O, the measured rate of N_2O depletion sometimes exceeded the measured rates of N_2 production by 5-10% (data not shown) and we considered that this could be due to strong sorption of N_2O to the activated sludge or conversion via an abiotic pathway other than reduction to N_2. However tests with acetylene in the headspace or with autoclaved sludge did not provide any evidence for loss of N_2O and the difference was therefore attributed to error propagation in the calculation of gas-liquid mass transfer of N_2O from the headspace to the sludge which do not affect the N_2 production rates (**Figure S2).**

N_2O overcapacity and NOS/NIR ratio of the microbial community

The *nosZ* and *nir* gene abundance in the activated sludge, determined by qPCR, showed that copy numbers of the genes for NOS (*nosZI* + *nosZII*) were higher but in the same order of magnitude as NIR (*nirK* + *nirS*), with a

Table 1. Ratio of the maximum N_2O consumption and production rates (from NO_3^-) reported in literature and in this study (expressed as α) and steady state concentrations of N_2O ($[N_2O]_{ss}$) during denitrification in these systems, expressed as a fraction of the culture's Ks for N_2O. WW= wastewater

Reference	System	C source	Conditions	α = $\frac{V_{\max N_2O \rightarrow N_2}}{V_{\max NO_3^- \rightarrow N_2O}}$ [a]	$[N_2O]_{ss}$ Fraction of K_s [b]
This study	Activated sludge	Mix[c] + WW		2-5	0.5-1
Ribera-Guardia *et al.*, 2014	Denitrifying SBR[d]	Acetate Ethanol Methanol Mix		3,0 3,6 7,5 3,4	0.5 0.38 0.15 0.41
Pan *et al.*, 2013	Denitrifying SBR[d]	Methanol	pH 7	8,4	0.14
Pan *et al.*, 2012	Denitrifying SBR[d]	Methanol	pH 6 pH 7 pH 8 pH 9	3,3 6,4 8,6 10,5	0.43 0.19 0.13 0.11
Wang et al. 2014	Denitrifying SBR[d]	Acetate	4°C 20°C 34°C	3,3 1,9 1,9	0.43 1.11 1.11
Itokawa *et al.*, 2001	Nitrifying-denitrifying SBR[c]	Acetate	COD/N 3.5 COD/N 5.0	2,2 3,5	0.83 0.4
Wicht, 1996	Activated sludge	Acetate		4,0	0.33
Holtan-Hartwig *et al.*, 2000	Soil			0,5-5	0.33-∞[e]
Hassan *et al.* 2016	*Paracoccus denitrificans*	Succinate	NO_2^-	2[f]	0.14

[a] In the literature studies, $V_{maxNO3 \rightarrow N2O}$ was estimated from RNO_3^- (see text for explanation)
[b] steady state N_2O-concentration expressed as fractions of k_{mN2O} (see text for explanation)
[c] C source mixture included acetate, ethanol, glutamate and pyruvate
[d] SBR inoculated with activated sludge
[e] no steady state concentration is reached if $RN_2ON/RNO_3 < 1$
[f] the value is for cultures grown by denitrification through many generations. Much higher α-values are measured for a period after transition to anoxia because all cells express NOS, while only a fraction express NIR (Hassan *et al.* 2016)

nosZ/(nirS+nirK) abundance ratio of ~2 (**Table S2**). The abundance of NIR and NOS proteins measured by means of a metaproteomic assay, showed that protein numbers were, on the contrary, greater for NIR than for NOS ($3.0*10^9$ NIR *vs*. $1.28*10^9$ NOS), but nevertheless still in the same order of magnitude. Taken together, the gene and protein abundance data suggests that the efficient N_2O reduction in activated sludge is likely not a result (i) of a numerical dominance of NOS over NIR or (ii) of a relatively abundant population of non-denitrifying N_2O reducers in the sludge.

N_2O overcapacity in the context of electron competition in the ETC

Electron competition amongst the different denitrifying reductases could create a bias in the N_2O sink potential reflected in α (note that the total electron flux for an equivalent amount of N_2O-N reduction to N_2 is 5 times greater during

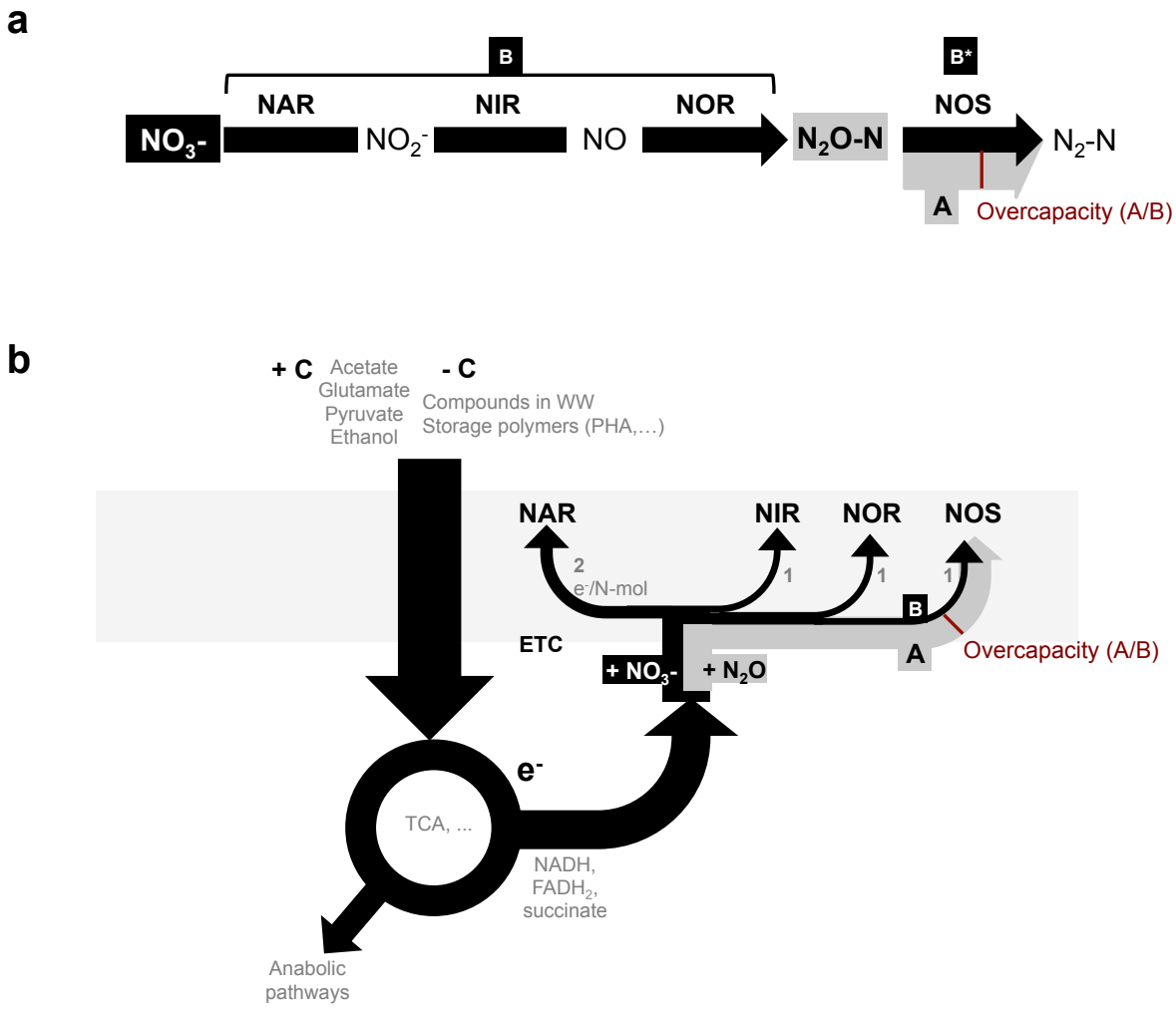

Figure 1 The denitrification pathway visualized in terms of (a) NO_x substrate or (b) electron flow distribution in the ETC. The thickness of black and gray arrows represents the hypothetical proportional flux of N or e^--equivalents during incubation with NO_3^- (assuming no accumulation of intermediates) or N_2O, respectively and the difference in width in N or e^- flux through NOS represents a cell or community's overcapacity for N_2O reduction. In (b) we assume that all 4 denitrifying enzymes share a common electron pool. A more complex mixed culture might be partly (or fully) composed of truncated denitrifiers, meaning that the arrows would be segregated in different cells, and different reductases could have access to electron pools of different sizes depending on the cell's metabolic capacity - or preference - to use some electron donor compounds over others.

the batch tests with NO_3^- than in those provided with only N_2O). Denitrification is a sequential process in terms of substrates, but a branched process in terms of electron flow within the ETC (see **Figure 1**, **a** *vs.* **b**) and there is evidence that, even under conditions of electron acceptor excess, the electron supply rate to the ETC may not match the combined electron accepting capacity of the denitrifying reductases (Pan et al., 2013). To assess whether a lower affinity of NOS for electrons relative to the other reductases, would affect the NOS overcapacity highlighted above (electron competition being absent in our determination of $V_{maxN2O \rightarrow N2}$) we performed additional batch tests providing N_2O and NO_3^- to the sludge simultaneously. In the presence of both N_2O and NO_3^- the total flux going through NOS decreased compared to the N_2O-only experiments (indicating at least some degree of electron competition) but N_2O overcapacity persisted, providing evidence that NOS can effectively compete with the other

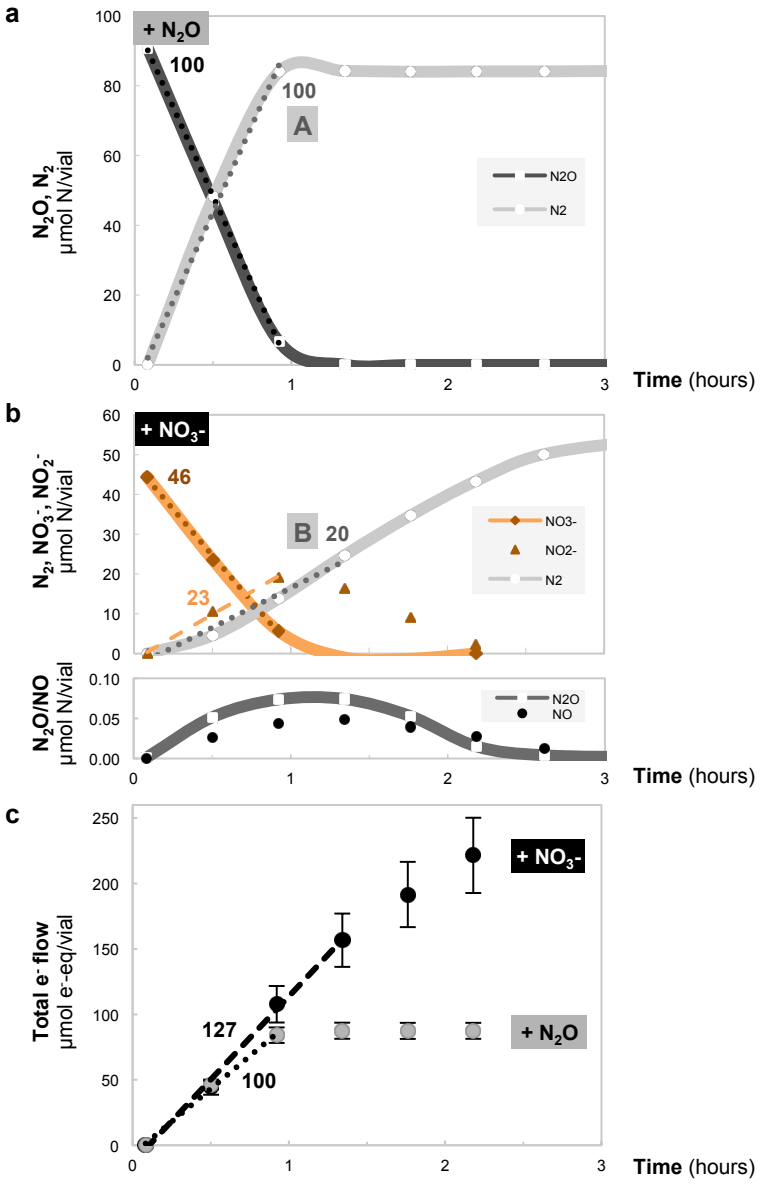

Figure 2 Example of parallel N_2O (a) and NO_3^- (b) batch incubation tests with the activated sludge collected on one of the sampling days. The maximum N_2O reduction and N_2O production rates of the sludge ($V_{maxN2O \rightarrow N2}$; labelled A and $V_{maxNO3 \rightarrow N2O}$; labelled B - in µmol N $vial^{-1}$ h^{-1}) were obtained from the linear regression of the data points during the first hour of the experiments (see Figure 3b). (c) Cumulative electron flux to denitrification in the two treatments.

denitrifying reductases (**Figure 3c**). Similar conclusions can be reached from the results of batch experiments with denitrifying SBR cultures in Ribera-Guardia *et al.* (2014) and Pan *et al.* (2013), though it remains to be seen if the competitiveness of NOS would persist under, for example, more extreme conditions of C limitation, pH, microaerophilic conditions, etc.

Implications for full-scale WWT systems

Given the literature survey and our results, it would seem that (1) a varying degree of N_2O reduction overcapacity is universal in denitrifying (heterotrophic) communities – true for a broad range of pH and temperature values, COD/N ratios, organic electron donors, and irrespective of whether microbial cultures are exposed to fully anoxic or alternatingly oxic-anoxic

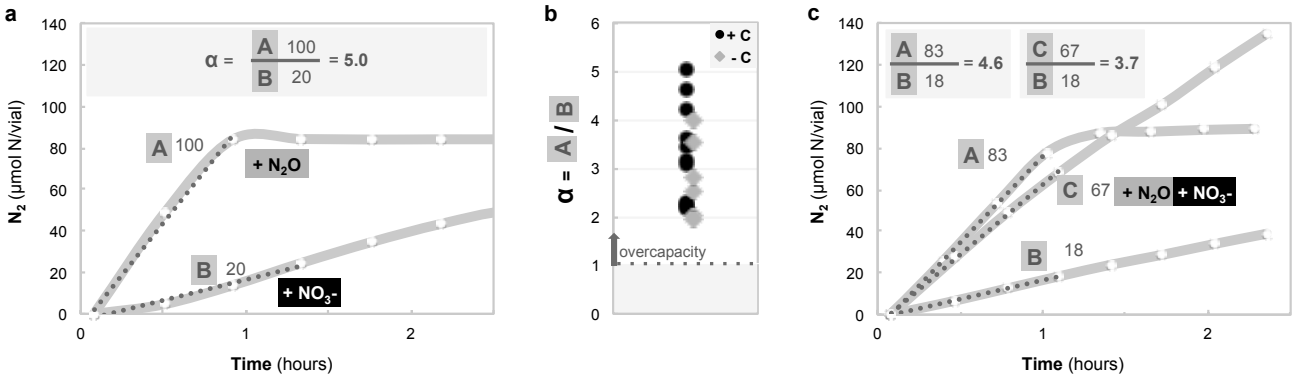

Figure 3 Overcapacity on N_2O reductase activity in the activated sludge samples. (**a**) Example of how the data from the batch experiments in Figure 2 was used to calculate α. For simplicity – we derived $V_{maxNO3 \rightarrow N2O}$ from the production rate of N_2 during the batch tests with NO_3^-, given that N_2O-N accounted for less than 1 % of N_2-N produced during the first hour. The N_2 production rate is a proxy for the N or e^- - equivalent flux through NOS. (**b**) α values determined from the N_2 production rates shown in Figure S4 on different sampling days with (+C) and without (-C) the addition of the cocktail of carbon substrates. (**c**) Example of N_2 production rates during a batch experiment provided with N_2O (A) or NO_3^- (B) or both N_2O and NO_3^- simultaneously (C)

conditions or electron competition phenomena, and (2) that this NOS overcapacity is a physiological characteristic of denitrifying microorganisms rather than a result of the genetic potential of the microbial community. Indeed, NOS overcapacity has also been (non-explicitly) reported for pure cultures of the full-fledged denitrifier *Paracoccus denitrificans:* with conversion rates of N_2O-N 2 to 6 times higher than those of NO_2^- depending on whether the culture had been exposed to oxic conditions shortly before a switch to anoxia or had been growing for a number of generations under anoxic conditions (Bergaust et al., 2012; Hassan et al., 2016).

We are not aware of a conserved regulatory or post-regulatory mechanism hardwiring denitrifying cells to overexpress the N_2O reduction step relative to the other denitrification steps. The existence of such a mechanism would be a surprising explanation given the diversity of denitrifying regulatory phenotypes found even within a same genus (Liu et al., 2013). Furthermore, given that protein numbers of NOS were lower than NIR, NOS overcapacity is more likely to be a result of enzyme activity or electron affinity than of gene overexpression. Whatever the mechanism behind it, a hardwired NOS overcapacity could be a competitive strategy evolved to maximize the effective electron accepting capacity of denitrifying cells, which could be particularly advantageous in systems like WWTP with frequently fluctuating availability of electron donor and electron acceptor limitations (e.g. we estimated that any given denitrifying species in the Bekkelaget activated sludge would be exposed to oxic/anoxic transitions in the range of 14 to 108 times per generation - see **Figure S1**).

Unfortunately, an overcapacity of N_2O reduction (which reflects maximum conversion rates under substrate excess) is not a guarantee that N_2O will not accumulate and be emitted to the atmosphere in a wastewater system. The affinity constant (K_s) of the culture for the N_2O determines the steady state N_2O concentration ($[N_2O]_{ss}$) at which the denitrifying community changes from being a net source of N_2O to become a net sink, and relatively high steady state N_2O concentrations during denitrification imply a greater likelihood of N_2O stripping into the gas phase (the degree of which will depend on the gas-liquid mass transfer of the system). Using the data obtained in literature and in this study, we estimate the steady state N_2O concentrations to be in the range of 0.1-1.1*K_s (**Table 1**), and assuming K_s values for N_2O in the range of 0.6 to 3.4 µM (based on K_m values determined by Hassan et al., 2016 and Pouvreau et al., 2008), this would mean concentrations of 0.07-3.74 µM, equivalent to a partial pressure range 2-100*10^{-6} atm at 10°C (given a solubility of N_2O of 0.039 mol $L^{-1}atm^{-1}$)

or a concentration range of 2-100 ppmv of N_2O in the gas phase (if in equilibrium with the liquid). This relatively low concentration range suggests that denitrification is likely to be a net sink for N_2O in activated sludge systems, able to consume part of the N_2O produced by nitrification or abiotic reactions.

The observation that N_2O reduction overcapacity in denitrifying communities is widespread should be considered in modeling efforts and in the development of N_2O mitigation strategies during nitrogen removal from wastewater. For example, carrousel-type systems, or MLE systems with increased recirculation rates, could be less prone to emissions than e.g. MLE systems with a low recirculation rate since, microbial communities are subjected to more frequent oxic-anoxic shifts. Under such conditions nitrification derived N_2O would be more rapidly transferred to the anoxic zones and readily consumed by N_2O reducing microorganisms, instead of being stripped to the atmosphere.

Conclusions

- The N_2O reducing capacity of denitrifying microbial communities generally exceeds their capacity to produce N_2O by a factor of 2-10, making denitrification a potential N_2O sink in wastewater treatment systems, scavenging N_2O derived not only from denitrification but also from ammonium oxidation and abiotic reactions of NO_2^-.
- Numbers in the same order of magnitude of NIR and NOS, both in terms of genes and proteins, suggest that the overcapacity observed in denitrifying systems is a characteristic of denitrifier physiology, rather than a consequence of the genetic composition of the microbial community.

Acknowledgements

The authors would like to warmly thank Bekkelaget (Morten Rostad Haugen, Tommy Angeltvedt, Jessica Gunnarsson) and VEAS workers (Anne-Kari Marsteng and Ida Skaar)
This work was funded by the European Commission (Marie Curie ITN NORA, FP7-316472).

References

Bergaust, L., van Spanning, R.J.M., Frostegård, A., Bakken, L.R., 2012. Expression of nitrous oxide reductase in *Paracoccus denitrificans* is regulated by oxygen and nitric oxide through FnrP and NNR. Microbiology 158, 826–34.

Braman, R.S., Hendrix, S.A., 1989. Nanogram nitrite and nitrate determination in environmental and biological materials by vanadium(III) reduction with chemiluminescence detection. Anal. Chem. 61, 2715–2718.

Cox, R.D.,1980. Determination of nitrate and nitrite at the parts per billion level by chemiluminescence. Anal. Chem. 52, 332–335.

Daelman, M.R.J., van Voorthuizen, E.M., van Dongen, L.G.J.M., Volcke, E.I.P., van Loosdrecht, M.C.M., 2013. Methane and nitrous oxide emissions from municipal wastewater treatment - results from a long-term study. Water Sci. Technol. 67, 2350–5.

Daelman, M.R.J., van Voorthuizen, E.M., van Dongen, U.G.J.M., Volcke, E.I.P., van Loosdrecht, M.C.M., 2015. Seasonal and diurnal variability of N_2O emissions from a full-scale municipal wastewater treatment plant. Sci. Total Environ. 536, 1–11.

Foley, J., de Haas, D., Yuan, Z., Lant, P., 2010. Nitrous oxide generation in full-scale biological nutrient removal wastewater treatment plants. Water Res. 44, 831–44.

Graf, D.R.H., Jones, C.M., Hallin, S., 2014. Intergenomic comparisons highlight modularity of the denitrification pathway and underpin the importance of community structure for N_2O emissions. PLoS One 9, e114118.

Hallin, S., Philippot, L., Löffler, F.E., Sanford, R.A., Jones, C.M., 2018. Genomics and Ecology of Novel N_2O-Reducing Microorganisms. Trends Microbiol. 26:43-55.

Hassan, J., Qu, Z., Bergaust, L.L., Bakken, L.R., 2016. Transient Accumulation of NO_2^- and N_2O during Denitrification Explained by Assuming Cell Diversification by Stochastic Transcription of Denitrification Genes. PLOS Comput. Biol. PLoS Comput Biol 12.

Itokawa, H., Hanaki, K., Matsuo, T., 2001. Nitrous oxide production in high-loading biological nitrogen removal process under low cod/n ratio condition. Water Res. 35, 657–664.

Kampschreur, M.J., Kleerebezem, R., de Vet, W.W.J.M., van Loosdrecht, M.C.M., 2011. Reduced iron induced nitric oxide and nitrous oxide emission. Water Res. 45, 5945–52.

Kampschreur, M.J., Temmink, H., Kleerebezem, R., Jetten, M.S.M., van Loosdrecht, M.C.M., 2009. Nitrous oxide emission during wastewater treatment. Water Res. 43, 4093–103.

Kampschreur, M.J., van der Star, W.R.L., Wielders, H. a, Mulder, J.W., Jetten, M.S.M., van Loosdrecht, M.C.M., 2008. Dynamics of nitric oxide and nitrous oxide emission during full-scale reject water treatment. Water Res. 42, 812–26.

Kučera, I., 2003. Passive penetration of nitrate through the plasma membrane of Paracoccus denitrificans and its potentiation by the lipophilic tetraphenylphosphonium cation. Biochim. Biophys. Acta - Bioenerg. 1557, 119–124.

Law, Y., Ye, L., Pan, Y., Yuan, Z., 2012. Nitrous oxide emissions from wastewater treatment processes. Philos. Trans. R. Soc. Lond. B. Biol. Sci. 367, 1265–77.

Liu, B., Mao, Y., Bergaust, L., Bakken, L.R., Frostegård, Å., 2013. Strains in the genus *Thauera* exhibit remarkably different denitrification regulatory phenotypes. Environ. Microbiol. 15, 2816–2828.

Lu, H., Chandran, K., 2010. Factors promoting emissions of nitrous oxide and nitric oxide from denitrifying sequencing batch reactors operated with methanol and ethanol as electron donors. Biotechnol. Bioeng. 106, 390–398.

Lycus, P., Lovise Bøthun, K., Bergaust, L., Shapleigh, J.P., Bakken, L.R., Frostegård, Å., 2017. Phenotypic and genotypic richness of denitrifiers revealed by a novel isolation strategy. Nat. Publ. Gr. 11, 2219–2232.

Mao, Y., Bakken, L.R., Zhao, L., Frostegård, Å., 2008. Functional robustness and gene pools of a wastewater nitrification reactor: Comparison of dispersed and intact biofilms when stressed by low oxygen and low pH, in: FEMS Microbiology Ecology. pp. 167–180.

Mielczarek, A.T., Saunders, A.M., Larsen, P., Albertsen, M., Stevenson, M., Nielsen, J.L., Nielsen, P.H., 2013. The Microbial Database for Danish wastewater treatment plants with nutrient removal (MiDas-DK) - A tool for understanding activated sludge population dynamics and community stability. Water Sci. Technol. 67, 2519–2526.

Molstad, L., Dörsch, P., Bakken, L.R., 2007. Robotized incubation system for monitoring gases (O_2, NO, N_2O N_2) in denitrifying cultures. J. Microbiol. Methods 71, 202–211.

Otte, S., Grobben, N.G., Robertson, L.A., Jetten, M.S., Kuenen, J.G., 1996. Nitrous oxide production by *Alcaligenes faecalis* under transient and dynamic aerobic and anaerobic conditions. Appl. Environ. Microbiol. 62, 2421–2426.

Pan, Y., Ni, B.-J., Bond, P.L., Ye, L., Yuan, Z., 2013. Electron competition among nitrogen oxides reduction during methanol-utilizing denitrification in wastewater treatment. Water Res. 47, 3273–3281.

Pan, Y., Ye, L., Ni, B.-J., Yuan, Z., 2012. Effect of pH on N_2O reduction and accumulation during denitrification by methanol utilizing denitrifiers. Water Res. 46, 4832–40.

Perez-Garcia, O., Mankelow, C., Chandran, K., Villas-Boas, S.G., Singhal, N., 2017. Modulation of nitrous oxide (N_2O) accumulation by primary metabolites in denitrifying cultures adapting to changes in environmental C and N. Environ. Sci. Technol. acs.est.7b03345.

Pouvreau, L.A.M., Strampraad, M.J.F., Van Berloo, S., Kattenberg, J.H., de Vries, S., 2008. NO, N_2O, and O_2 reaction kinetics: scope and limitations of the Clark electrode. Methods Enzymol. 436, 97–112.

Ribera-Guardia, A., Kassotaki, E., Gutierrez, O., Pijuan, M., 2014. Effect of carbon source and competition for electrons on nitrous oxide reduction in a mixed denitrifying microbial community. Process Biochem. 49, 2228–2234.

Rocca, J.D., Hall, E.K., Lennon, J.T., Evans, S.E., Waldrop, M.P., Cotner, J.B., Nemergut,

D.R., Graham, E.B., Wallenstein, M.D., 2014. Relationships between protein-encoding gene abundance and corresponding process are commonly assumed yet rarely observed. ISME J. 9, 1693–1699.

Roco, C.A., Bergaust, L.L., Bakken, L.R., Yavitt, J.B., Shapleigh, J.P., 2017. Modularity of nitrogen-oxide reducing soil bacteria: linking phenotype to genotype. Environ. Microbiol. 19, 2507–2519.

Sanford, R.A., Wagner, D.D., Wu, Q., Chee-Sanford, J.C., Thomas, S.H., Cruz-García, C., Rodríguez, G., Massol-Deyá, A., Krishnani, K.K., Ritalahti, K.M., Nissen, S., Konstantinidis, K.T., Löffler, F.E., 2012. Unexpected nondenitrifier nitrous oxide reductase gene diversity and abundance in soils. Proc. Natl. Acad. Sci. U. S. A. 109, 19709–14.

Schreiber, F., Wunderlin, P., Udert, K.M., Wells, G.F., 2012. Nitric oxide and nitrous oxide turnover in natural and engineered microbial communities: biological pathways, chemical reactions, and novel technologies. Front. Microbiol. 3, 372.

Shapleigh, J.P., 2013. Denitrifying Prokaryotes, in: Rosenberg, E., DeLong, E.F., Lory, S., Stackebrandt, E., Thompson, F. (Eds.), The Prokaryotes: Prokaryotic Physiology and Biochemistry. Springer Berlin Heidelberg, Berlin, Heidelberg, pp. 405–425.

Soler-Jofra, A., Stevens, B., Hoekstra, M., Picioreanu, C., Sorokin, D., van Loosdrecht, M.C.M., Pérez, J., 2016. Importance of abiotic hydroxylamine conversion on nitrous oxide emissions during nitritation of reject water. Chem. Eng. J. 287, 720–726.

Venkatesh, G., Elmi, R.A., 2013. Economic-environmental analysis of handling biogas from sewage sludge digesters in WWTPs (wastewater treatment plants) for energy recovery: Case study of Bekkelaget WWTP in Oslo (Norway). Energy 58, 220–235.

Wang, X., Yang, X., Zhang, Z., Ye, X., Kao, C.M., Chen, S., 2014. Long-term effect of temperature on N_2O emission from the denitrifying activated sludge. J. Biosci. Bioeng. 117, 298–304.

Wicht, H., 1996. A model for predicting nitrous oxide production during denitrification in activated sludge. Water Sci. Technol. 34, 99–106.

Wunderlin, P., Mohn, J., Joss, A., Emmenegger, L., Siegrist, H., 2012. Mechanisms of N_2O production in biological wastewater treatment under nitrifying and denitrifying conditions. Water Res. 46, 1027–37.

Zumft, W.G., 1997. Cell biology and molecular basis of Cell Biology and Molecular Basis of Denitrification. Microbiology 61.

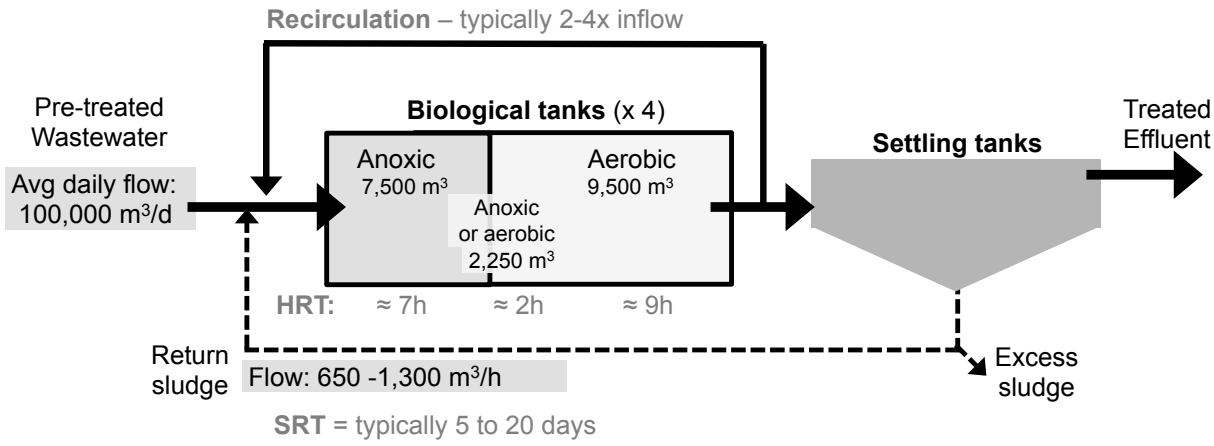

Figure S1: Schematic of the Bekkelaget wastewater treatment plant treating part of the municipal wastewater of Oslo (Norway). The plant is designed and operated as a Modified Ludzack-Ettinger (MLE) plant, with 4 parallel biological tanks consisting of an anoxic "pre-denitrification" zone and an aerated zone, with recirculation for N removal via nitrification-denitrification. Addition of an external source of COD for is typically not required in MLE-type plants (COD from the incoming wastewater is available in the anoxic pre-denitrification zone). However, at the time of our 5-week sampling campaign (April-May 2015), ethanol was being dosed to enhance denitrification. In activated sludge systems the Sludge Retention Time (SRT) depends on recirculation of the biomass from the settling tanks, and is thus independent from the Hydraulic Retention time (HRT). This means that, with an HRT of roughly 18h and an SRT of 5 to 20 days, denitrifiers in the biomass will undergo at least 7 to 27 oxic-anoxic shifts (presumably more taking into account recirculation) All the samples used for the N_2O and NO_3^- incubation experiments presented in this study were taken from the pre-denitrification anoxic zone, after preliminary tests showing that the sampling point did not have an influence on the results of the batch tests.

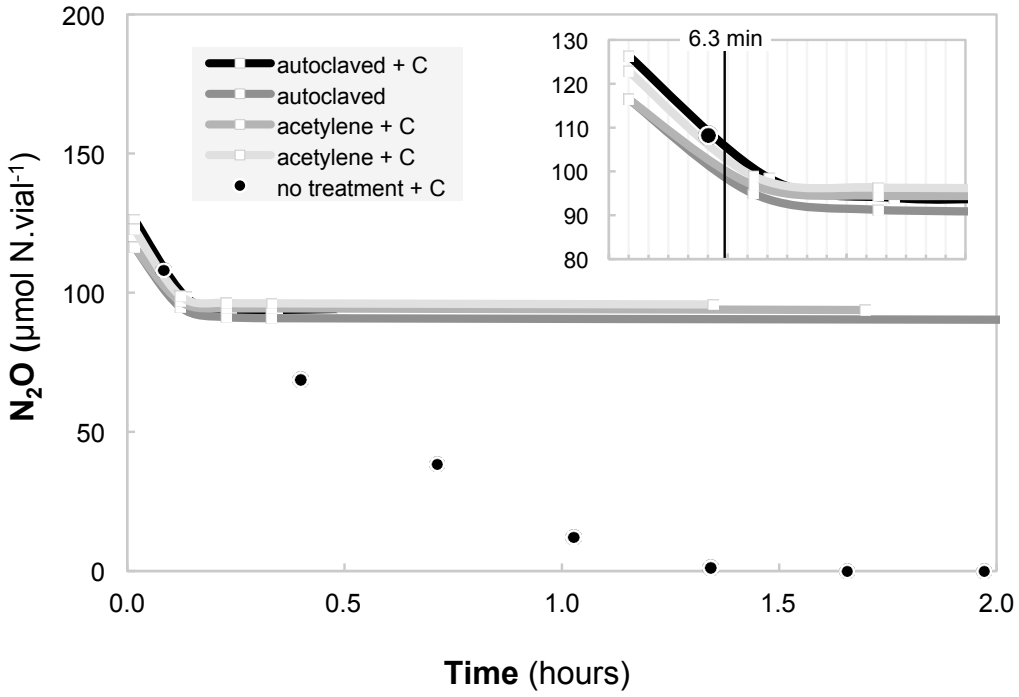

Figure S2 Figure S2 Batch incubation tests with N2O: with either 15 % acetylene in the headspace or with autoclaved samples compared to normal batch incubation test (labelled "no treatment"). The N2O was injected into the flasks at time zero. "+ C" indicates that the mix of carbon sources was added to the sludge.

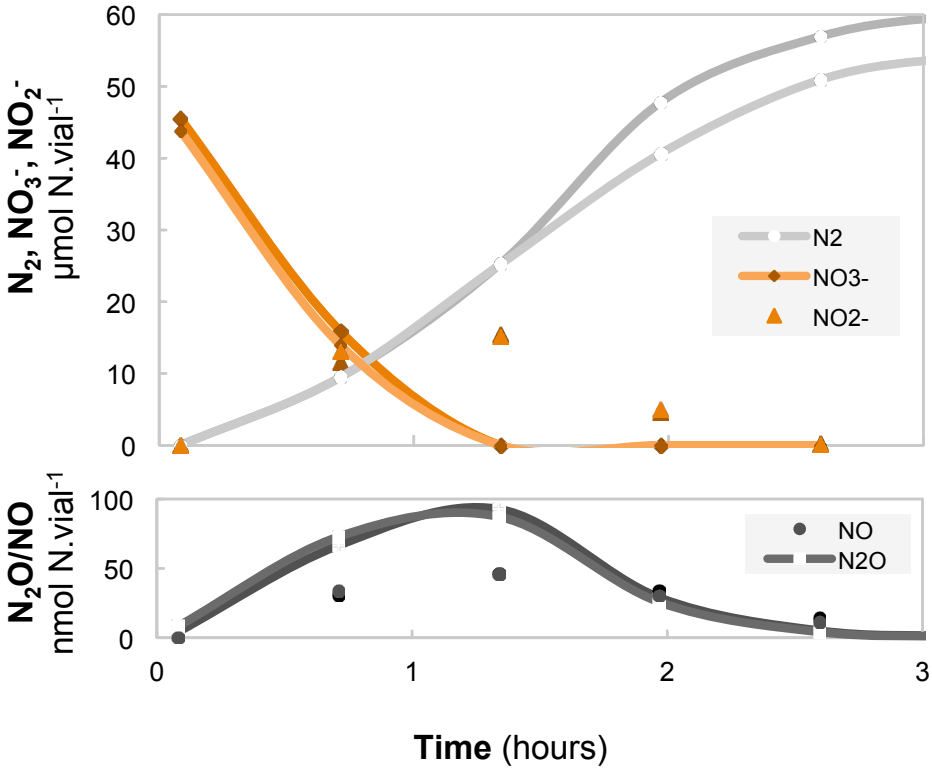

Figure S3 Batch test reproducibility: results from two parallel NO_3^- incubation batch tests (replicate in darker shades).

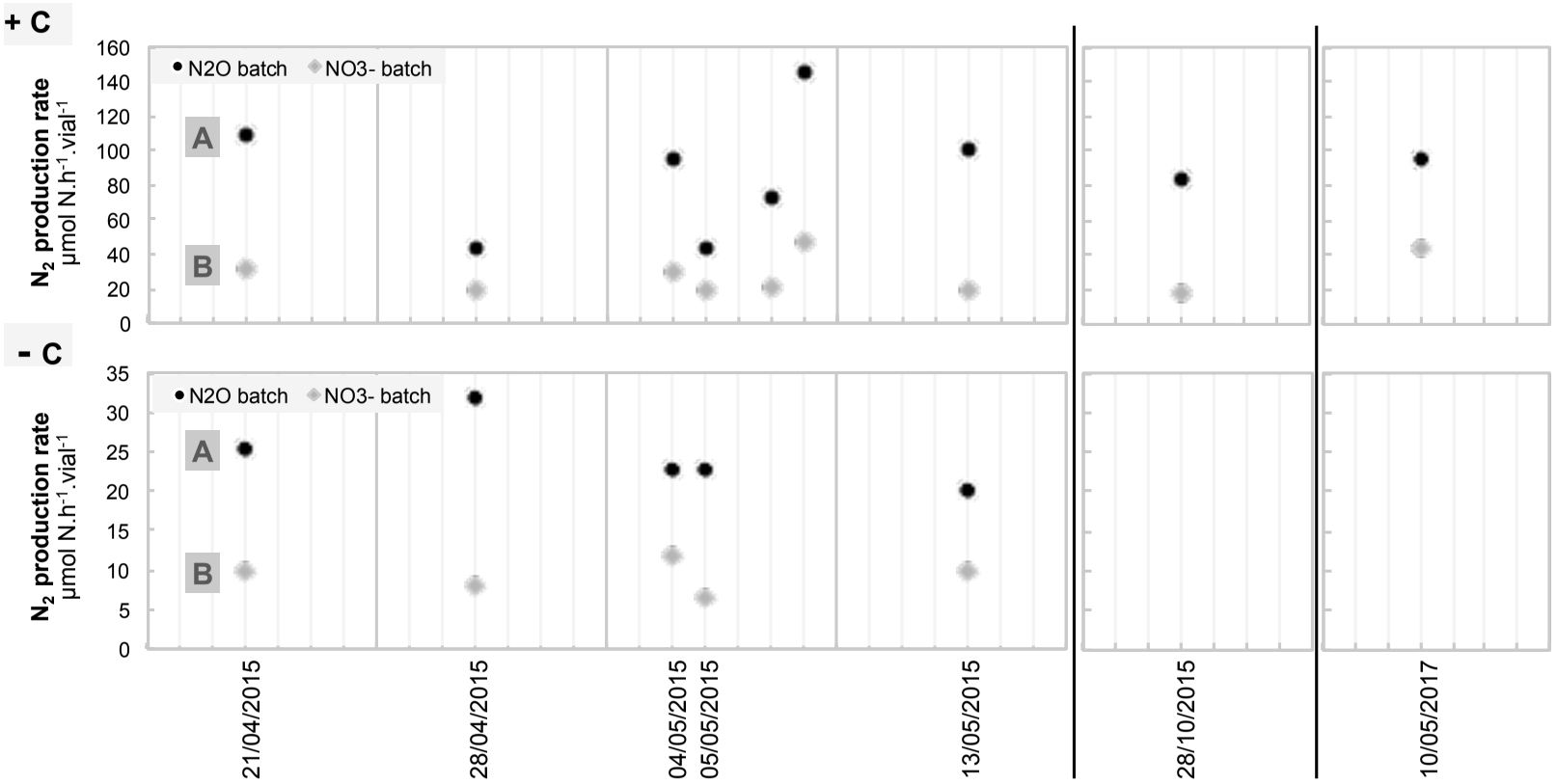

Figure S4 N_2 production rates (a proxy for NOS conversion rates) during either batch test incubations with N_2O (A) or NO_3- (B) used to determine NOS overcapacity (A/B) shown in Figure 2b in the main text. Above, batch tests with a cocktail of carbon substrates (+ C). Below, batch tests without added C source (-C).

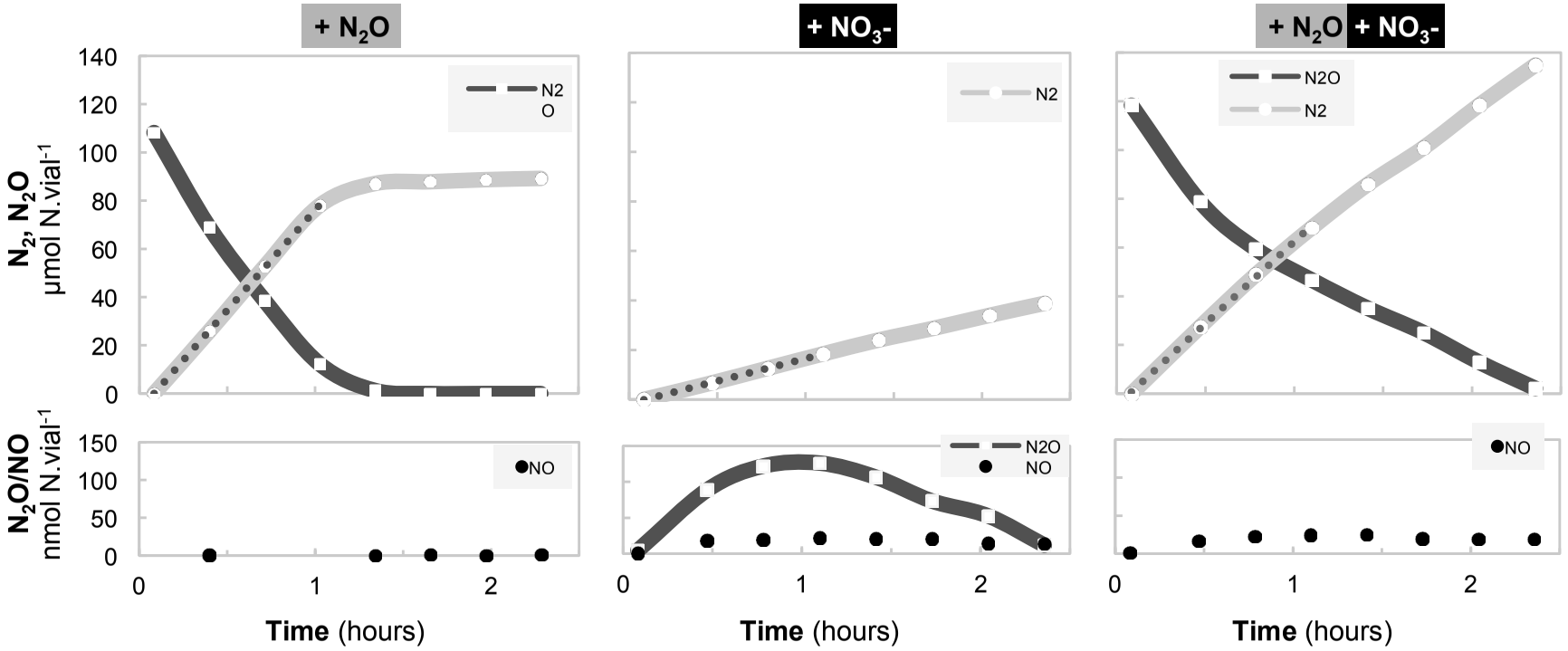

Figure S5 Batch tests with only N_2O, only NO_3- or both N_2O and NO_3- presented in Figure 2c in the main text. The mixture of carbon sources was added to all three experiments. NO_3- and NO_2- concentrations were not measured.

Table S1 - a Primers used for the qPCR

Gene	Primers	Reference
16S rRNA	27F/518R	Lane (1991); Muyzer *et al.* (1993)
*nosZ*I	F/1622R	Henry *et al.* (2006)
*nosZ*II	IIF/IIR	Jones *et al.*(2013)
nirS	Cd3af/R3cd	Michotey *et al.* (2000), Throbäck *et al.* (2004)
nirK	F1aCu/R3Cu	Hallin & Lindgren (1999)
amoA (bacterial)	amoA-1F/amoA-2R	Rotthauwe *et al.* (1997)

Table S1 - b qPCR mixture – according to Takara SYBR® Premix Ex Taq™ II Product manual - 20 μl total volume

Reagent	Volume
SYBR® *Premix Ex Taq*™ II (2x)	10 μl
PCR Forward primer (10 μm)	0.8 μl
PCR Reverse primer (10 μm)	0.8 μl
ROX Ref Dye (50x)	0.4 μl
Template	2 μl (100ng DNA)
dH_2O	6 μl

Table S1 - c qPCR conditions – according to Takara SYBR® Premix Ex Taq™ II Product manual

First Stage	1x	95°C; 30 sec
Second Stage	40x	95°C; 5 sec 60°C; 30 sec
Dissociation stage	1x	95°C; 15 sec 60°C; 60 sec 95°C; 15 sec

Table S2. Gene abundance of 16S rRNA, *nosZ*I, *nosZ*II, *nirS*, *nirK* and bacterial *amoA*

	Activated sludge (copies*ml^{-1} ± SD; n=3)
16S rRNA	$1.93*10^{10} \pm 4.73*10^{9}$
*nosZ*I	$2.30*10^{8} \pm 5.57*10^{7}$
*nosZ*II	$2.47*10^{6} \pm 5.77*10^{4}$
nirS	$1.13*10^{8} \pm 1.15*10^{7}$
nirK	$7.00*10^{6} \pm 1.84*10^{6}$
amoA (bacterial)	$6.03*10^{6} \pm 2.08*10^{6}$

Supplement to the Materials and Methods section

Metaproteomics

Proteins were resuspended in SDS sample buffer and separated by SDS-PAGE using the AnykD Mini-PROTEAN gel (Bio-Rad Laboratories, Hercules, CA, USA) at 240 V for 10 minutes and stained using Coomassie Brilliant Blue R250. The gel lane was cut into four bands and destained two times using 25 mM ammonium bicarbonate in 50% (v/v) acetonitrile. The proteins were reduced, alkylated and trypsinated as previously described (Arntzen et al., 2015). Prior to mass spectrometry, peptides were desalted using C18 ZipTips (Merck Millipore, Darmstadt, Germany) according to manufacturer's recommendations. Peptides were analyzed using a nanoHPLC-MS/MS system consisting of a Dionex Ultimate 3000 UHPLC connected to a Q-Exactive hybrid quadrupole-orbitrap mass spectrometer (both from Thermo Scientific, Bremen, Germany). Samples were loaded onto a trap column (Acclaim PepMap100, C_{18}, 5 µm, 100 Å, 300 µm ID × 5 mm, Thermo Scientific) and back flushed onto a 50 cm analytical column (Acclaim PepMap RSLC C_{18}, 2 µm, 100 Å, 75 µm ID, Thermo Scientific). At the beginning, the columns were in 96% solution A [0.1% (v/v) formic acid], 4% solution B [80% (v/v) acetonitrile, 0.1% (v/v) formic acid]. Peptides were eluted using a 90-min gradient developing from 4% to 13% (v/v) solution B in 2 minutes, 13% to 45% (v/v) B in 70 minutes and finally to 55% B in 5 minutes before the washing phase at 90% B. The flow rate was constant at 300 nL/min. In order to isolate and fragment the 10 most intense peptide precursor ions at any given time throughout the chromatographic elution, the mass spectrometer was operated in data-dependent mode (DDA) to switch automatically between orbitrap-MS and higher-energy collisional dissociation (HCD) orbitrap-MS/MS acquisition. The selected precursor ions were then excluded for repeated fragmentation for 20 seconds. The resolution was set to R=70.000 and R=35.000 for MS and MS/MS, respectively. For optimal acquisition of MS/MS spectra, automatic gain control (AGC) target values were set to 50.000 charges and a maximum injection time of 128 milliseconds.

A database was generated by extracting and concatenating UniProt or NCBI protein entries from all the bacterial genera reported to be abundant in activated sludge, anaerobic digesters and influent wastewater (Cox and Mann, 2008), resulting in a database with 176,175 protein entries. MS raw files were analyzed using MaxQuant version 1.6.0.13 (REF) and the data were searched against the abovementioned community database supplemented with common contaminants such as human keratin and bovine serum albumin. In addition, reversed sequences of all protein entries were concatenated to the database for estimation of false discovery rates. The tolerance levels for matching to the database was 4.5 ppm for MS and 20 ppm for MS/MS. Trypsin was used as digestion enzyme, and two missed cleavages were allowed. Carbamidomethylation of cysteine residues was set as a fixed modification and protein N-terminal acetylation, oxidation of methionines, deamidation of glutamines and asparagines and formation of pyro-glutamic acid at N-terminal glutamines were allowed as variable modifications. All identifications were filtered in order to achieve a protein false discovery rate (FDR) of 1% and further filtering were applied to include at least one unique peptide. For protein quantification, the label-free quantification (LFQ) values reported by MaxQuant were used and summed for NOR and NIS, across species, to calculate the ratio.

Arntzen, M.Ø., Karlskås, I.L., Skaugen, M., Eijsink, V.G.H., Mathiesen, G., 2015. Proteomic Investigation of the Response of Enterococcus faecalis V583 when Cultivated in Urine. PLoS One 10, e0126694. https://doi.org/10.1371/journal.pone.0126694

Cox, J., Mann, M., 2008. MaxQuant enables high peptide identification rates, individualized p.p.b.-range mass accuracies and proteome-wide protein quantification. Nat. Biotechnol. 26. https://doi.org/10.1038/nbt.1511

Hallin, S. and Lindgren, P-E., 1999. PCR detection of genes encoding nitrite reductase in denitrifying… *Appl. Environ. Microbiol*. 65, 1652–1657

Jones, C.M, Graf, D.R.H., Bru, D., Philippot, L.& Hallin, S., 2013 The unaccounted yet abundant nitrous oxide-reducing microbial community: a potential nitrous oxide sink. *ISME J.* 7, 417–26.

Lane, D., 1991 16S/23SrRNA sequencing. Nucleic Acid Techniques in Bacterial Systematics. Stackebrandt E & Goodfellow M, eds, pp. 131–175. JohnWiley & Sons, New York, NY.

Muyzer G., Dewaal E.C., Uitterlinden A.G., 1993. Profiling of complex microbial populations by denaturing gradient gel electrophoresis analysis of polymerase chain reaction-amplified genes coding for 16S rRNA. Appl Environ Microb 59: 695–700.

Michotey V., Mejean V., Bonin P., 2000. Comparison of methods for quantification of cytochrome cd(1)-denitrifying bacteria in environmental marine samples. *Appl Environ Microb* 66: 1564–1571.

Throbäck, I.N., Enwall, K., Jarvis, Å., Hallin, S., 2004 Reassessing PCR primers targeting *nirS*, *nirK* and *nosZ* genes for community surveys of denitrifying bacteria with DGGE. *FEMS Microbiol. Ecol.* 49, 401–417.

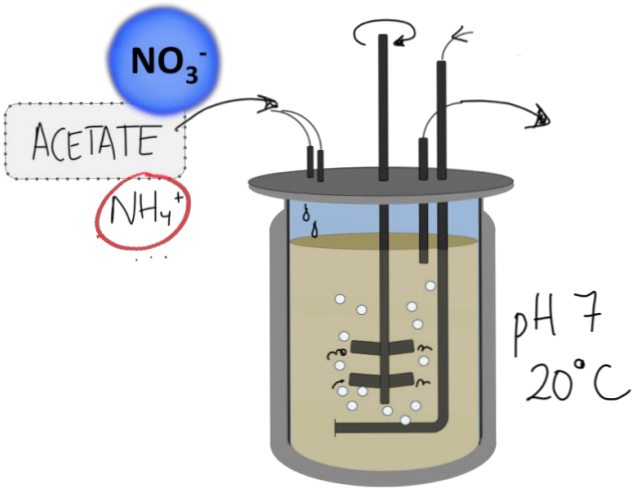
NO3-
ACETATE
NH4+
pH 7
20°C

7

Outlook

A. N_2O accumulation in denitrifying chemostat enrichments (*unpublished data*)

- *Complexity of denitrifying systems on a community and metabolic level*

The research presented in this thesis focuses on to the microbiology of N_2O reduction to N_2, the only microbial conversion known to consume this potent greenhouse gas. However, before shifting our focus to this final step of denitrification, we had been looking into the factors associated to N_2O emission during denitrification in chemostat cultures fed with acetate and NO_3^-. The experimental setup was the same as the one in Chapters 2-5 for the N_2O reducing cultures (i.e. open, continuous flow, anoxic systems initially inoculated with activated sludge) except the cultures were provided with NO_3^- in the mineral medium instead of N_2O in the gas phase (see **Table 7.1**). Two such cultures were run in parallel, one with NO_3^- as a growth limiting substrate and acetate in excess, the other with acetate as a growth limiting substrate and NO_3^- in excess.

Table 7.1: Operational conditions of the different enrichments systems reported in this thesis and in van den Berg *et al.*, (2015). SBR= sequence batch reactor; TE= trace elements. Acetate supplied in the form of sodium acetate and nitrate in the form of sodium nitrate. Yeast extract was used as a source of vitamins but its contribution was negligible as a source of COD

	Denitrifying chemostats	DNRA chemostat	Denitrifying SBR	N_2O chemostats
	Ch 7	van den Berg (2015)	Ch 7	Ch 2, 3, 4, 5
pH (+ HCl)	7	7	7	7
Temperature (°C)	20	20	**30**	20
HRT = SRT (h)	24, 12	**36**	24 (12h cycles)	36, 12
Electron donor	Acetate	Acetate	Acetate	Acetate
Electron acceptor	NO_3^-	NO_3^-	NO_3^-	**N_2O**
Mixing (rpm)	400	400	750	750
Sparging gas	N_2	N_2	N_2	N_2 or Ar + N_2O
Gas inflow (ml/min)	100	50	180	100 – 800 (+ recirculation)
Macro + micro nutrients*	NH_4Cl KH_2PO_4 $MgSO_4$ (Yeast extract) Vishniac TE	-- KH_2PO_4 $MgSO_4$ (Yeast extract) Vishniac TE	NH_4Cl KH_2PO_4 $MgSO_4$ (Yeast extract) Vishniac TE	(NH_4Cl) KH_2PO_4 $MgSO_4$ (Yeast extract) Vishniac TE

* The concentration of macro and micronutrients in each enrichment may have varied. E.g in the experiments of van den Berg (2015) the concentration of trace elements in the medium was higher than in the enrichments in this thesis. Please check individual publications for details, if relevant.

Figure 7.1 shows the evolution of the acetate limited (a) and NO_3^- limited (b) continuous enrichments over time. Aside from the transient NO_2^- accumulation in the acetate-limited system during start-up/operational setbacks, there was no significant accumulation of intermediates of denitrification (NO_2^-, NO, N_2O) during steady state conditions in either enrichment (data not shown). The biomass yields during steady state, presented in **Table 7.2**, served as a reference for the N_2O reducing chemostats. We sporadically interrupted the continuous operation of the chemostats to perform short-term batch tests with the communities enriched (simulating dynamic conditions/disturbances as those encountered in the environment or the anoxic tank of WWTP, e.g. accumulation of nitrite, feast-famine regimes, etc.). Examples of such experiments, one for each of the enrichments, are presented in **Figure 7.3.**

Although interesting trends were observed, deriving strong/general conclusions regarding the factors that may result in N_2O emissions in a denitrifying community proved difficult due to a certain degree of complexity on two different levels: (1) microbial community composition and (2) metabolic adaptations (discussed below). The data presented here remains unpublished but, apart from serving as a useful reference for comparison with the N_2O-reducing chemostats (e.g. regarding biomass yields), we hope it will provide useful insight in the development of new lines of research in the search to mitigate N_2O emissions in wastewater treatment systems and agricultural soils. The tremendously fast advances in "–omic" analysis will likely be the key to fully unravel the complexity of N_2O emissions in N-cycling microbial communities - see for example Perez-Garcia *et al.*, (2017).

Figure 7.1 – next page – Substrate concentrations and microbial community composition - as determined by DGGE - in the (a) acetate limited and (b) NO_3^- limited enrichments over time. NO and N_2O concentrations were negligible and are therefore not shown. Initially, both chemostats were run at a 24h HRT (D= 0.42 h^{-1}). After roughly 40 days, an increase in NH_4^+ concentrations in the NO_3^- limited enrichment, corresponding with the appearance of *Geobacter* sp. in the culture indicated that DNRA was taking place (as in van den Berg *et al.*, 2015). The HRT was decreased to 18 then 12h (D = 0.83 h^{-1}) to select for denitrification rather than DNRA. NH_4^+ concentration in the acetate limited enrichment is not shown, but was always in excess.

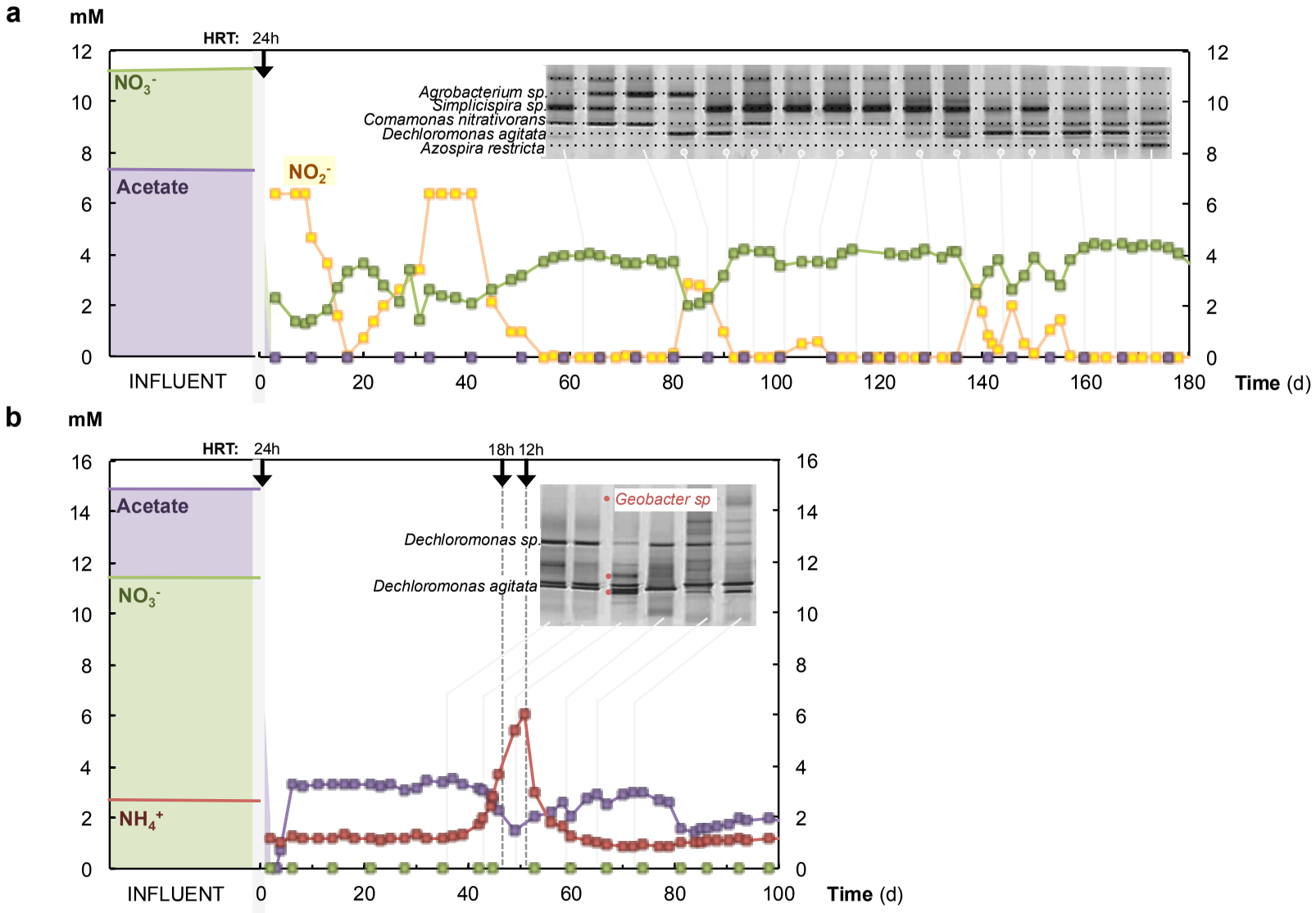
a
mM
HRT: 24h
NO_3^-
Acetate
NO_2^-
Agrobacterium sp.
Simplicispira sp.
Comamonas nitrativorans
Dechloromonas agitata
Azospira restricta
INFLUENT
Time (d)
b
mM
HRT: 24h
18h 12h
Acetate
NO_3^-
NH_4^+
Geobacter sp
Dechloromonas sp.
Dechloromonas agitata
INFLUENT
Time (d)

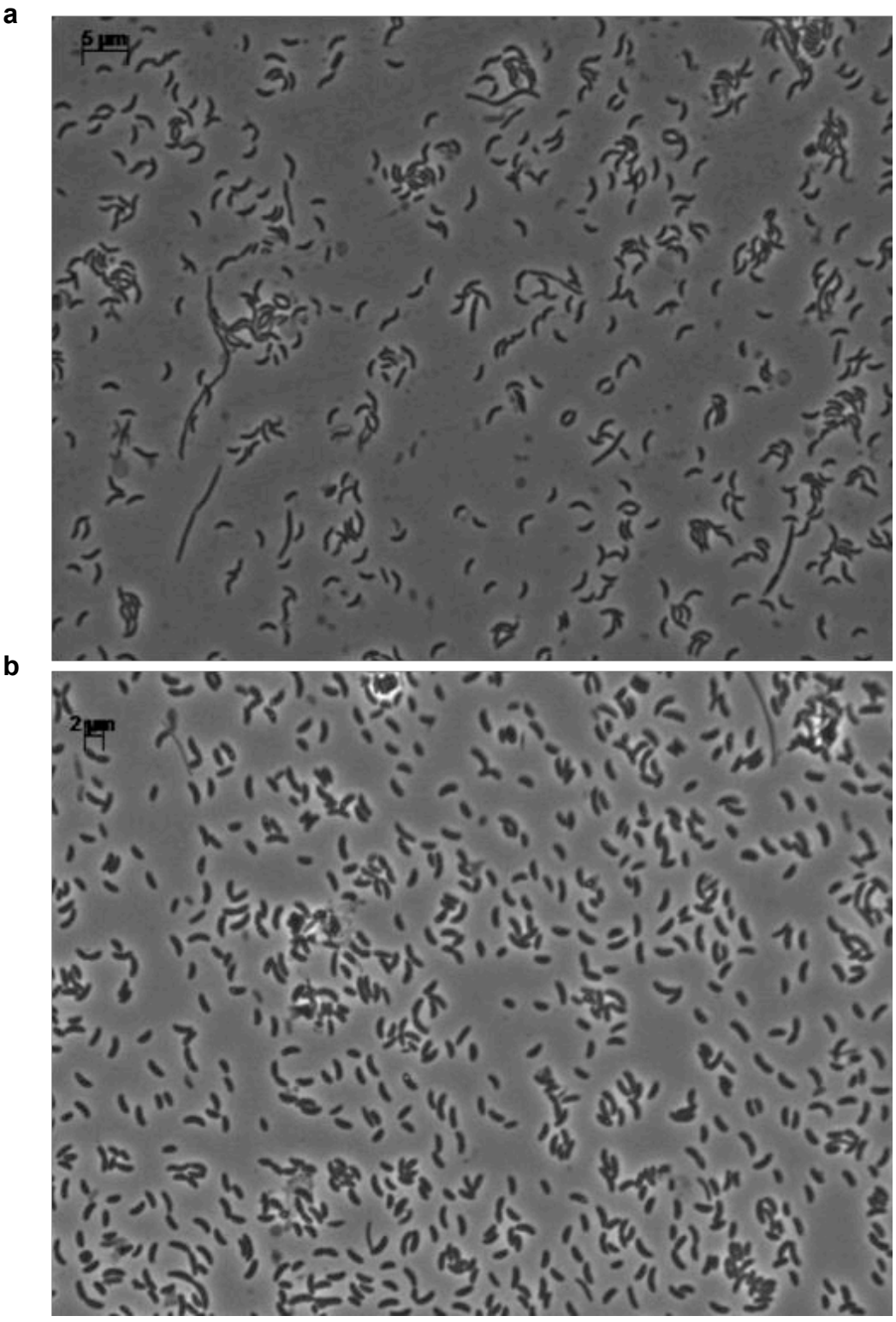

Figure 7.2: Microscope picture of the microbial community in the (a) acetate limited and (b) nitrate limited enrichments on days 329 and 232, respectively. Unfortunately Fluorescent in situ hybridization (FISH) was not much help in determining the diversity of the community, as most of the species selected belonged to Beta-proteobacteria, and we did not have access to more specific probes.

Table 7.2: Biomass yields of enrichments growing on acetate and NO_3^-. SBR = sequence batch reactor, SRT = sludge retention time

Reference	D h^{-1}	Limiting substrate	Y CmolX/CmolS	Y CmolX/molNO_3^-
This study	0.042	Acetate	0.37	0.75
This study	0.083	Acetate	0.39	0.80
This study	0.042	NO_3^-	0.32	0.64
This study	0.083	NO_3^-	0.36	0.78
van den Berg *et al.*, (2015)	0.028	Acetate	0.24	0.48
Kraft *et al.*, (2014)	0.037	NO_3^-, NO_2^-	0.36*	
MSc Thesis Tony Davies		(SBR)	0.25	
Beun *et al.*, (2000)		(SBR)	0.30	

* In Kraft *et al.*, (2014), C source included acetate, glucose and amino acids

- Microbial community composition of the denitrifying enrichments

From the DGGE analysis of the microbial community composition and observation under the microscope it was difficult to judge the degree of diversity in the enrichments but it appeared, in the acetate limited culture in particular, that the cultures were composed of a succession of co-existing species (rather than one stable population of a dominant microorganisms). Strong dynamics in a microbial community composition in a denitrifying chemostat over time, in spite of stable well-defined experimental conditions, had previously been reported in Kraft *et al*. (2014). The main difference was that the culture in Kraft *et al*. was fed with both NO_3^- and NO_2^- and with a mixture of electron donors, including glucose, amino acids and acetate. Hence, part of the microbial community was fermentative and the strong microbial community composition dynamics could be attributed to all sorts of microbial interactions between different microbial populations (e.g. cross-feeding between fermenters and denitrifiers). Our denitrifying chemostats, in contrast, were fed exclusively with acetate as an electron donor (not readily fermentable at the dilution rates used, 0,042 and 0,083 h^{-1}), limiting the diversity of the system to microorganisms carrying out denitrification (or DNRA- see **Figure 7.1-b**). Based on chemostat theory we hypothesized that up to 4 dominant microorganisms could co-exist in the enrichment – provided there was a competitive advantage in specializing in the reduction of NO_3^-, NO_2^-, NO or N_2O. However, one microorganism performing full denitrification would dominate if there was a competitive advantage to harvesting the energy from all the steps of denitrification in the system. We studied both electron donor or electron acceptor limitations in case these conditions would favor one or the other scenario. The common denitrifying genera identified by DGGE (*Simplicispira*, *Dechloromonas*, *Comamonas*, etc.; see **Table 7.3**) suggest that the microorganisms co-existing in the enrichments had the genetic potential for full denitrification. However, with the molecular tools available, we were unable to assess whether these co-

existing microorganism were specializing in specific steps, or simply performing full denitrification in parallel, nor were we able to evaluate the dominance of one microorganism over others (e.g. *Simplicispira sp.* in the acetate limited enrichment from days 100 to 130, or *Dechloromonas sp.* in the NO_{3-} limited enrichment) or understand the reason for the shifts in microbial community composition over time.

Even though the co-existing full denitrifier scenario would contradict chemostat theory strictly speaking (a system with one growth limiting nutrient should yield one dominant microorganism), a certain degree of diversity in cultures starting from a complex inoculum may simply be a result of microbial interactions difficult to detect (e.g cross-feeding; predation, viral blooms). A relatively mixed community and fluctuations in the community composition were also observed in the N_2O reducing chemostats (with the presence of *Gracilibateria*-like bacteria being particularly intriguing in **Ch 2** and **Ch 3**). However, in the long-term open enrichments of van den Berg *et al.*, 2015, with virtually the same experimental set-up as ours, one strongly dominant stable population was consistently obtained in independent enrichments.

The dynamics in microbial community composition might also be explained by the existence of a large diversity of microorganisms capable of denitrification, with very slight differences in affinity (i.e. μmax/Ks) for the limiting nutrient (acetate, NO_3^- or N_2O). In such a case, minor fluctuations in operation could favor one organism, then another, and so on.

- Metabolic “history”

Aside from the variability in microbial community composition, an added difficulty in associating specific factors to N_2O emissions in the full-scale/ecosystems, is the issue of metabolic adaptation, and the possibility that the “history” of a culture in the lab may be very different than that of the same microorganism on the full scale. This is illustrated by two striking observations from the batch experiments depicted in **Figure 7.3:**

(1) the dramatically different response of the two enrichment cultures (in terms of NO and or N_2O accumulation) to a similar disturbance (i.e. a sudden pulse of NO_2^-), despite the fact that the microorganisms composing the enrichments are not very distantly related phylogenetically.

(2) the extent to which metabolic adaptation/cultures history can affect accumulation of intermediates (emissions) as observed in the experiment with two consecutive pulses of NO_2^- in acetate limited enrichment – **Figure 7.3-a**.

A study by Liu *et al.*, 2013 shows that different “denitrification regulatory phenotypes” (coined by the same authors in Bergaust *et al.*, 2011) are observed even amongst species of the same genus (*Thauera*). We wonder if these different “regulatory phenotypes” are a consequence of genetic differences between different species of denitrifiers (or even strains) or if, in fact, these are determined by the “growth history” of the culture (i.e. metabolic adaptations).

Figure 7.3 – next page: Example of two of the batch experiments performed on (a) the acetate-limited enrichment on day 259 of operation and (b) the NO_3^- limited enrichments on day 140. The % of N-moles converted released as NO and/or N_2O is indicated in the figure.

.

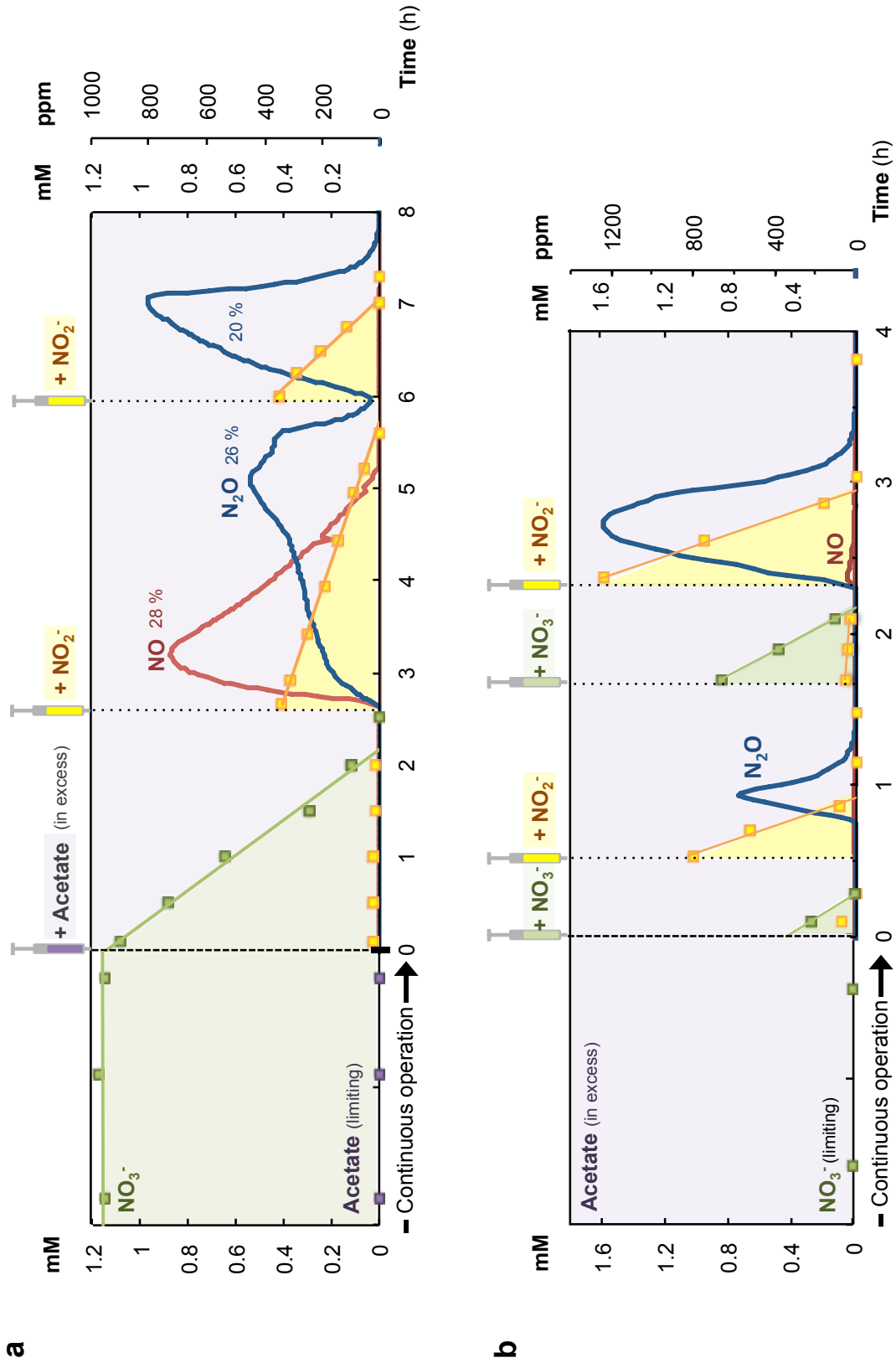
a
mM
ppm
Time (h)
+ Acetate (in excess)
+ NO2-
+ NO2-
NO3-
Acetate (limiting)
NO 28 %
N2O 26 %
20 %
Continuous operation
b
mM
ppm
Time (h)
+ NO3-
+ NO2-
+ NO3-
+ NO2-
Acetate (in excess)
N2O
NO
NO3- (limiting)
Continuous operation

- *Effect of dynamic conditions, NO_2^- and COD/N ratio on N_2O emissions*

In **Figure 1.3** in the Introduction, we summarized some of the factors associated to N_2O emissions in wastewater treatment as described in Kampschreur *et al.*, 2009; Foley *et al.*, 2010, and others. Among the factors linked to increased N_2O emissions during the denitrification step of N removal are: high concentrations of NO_2^-, low COD/N ratios and dynamic conditions. According to our batch experiments:

- Dynamic conditions (*vs*. steady state) can result in the accumulation of N_2O – but do not necessarily do so.

  Pulses of NO_2^- resulted in an important accumulation of N_2O in the enrichments, but pulses of NO_3^- in the NO_3^--limited enrichment or of acetate- in the acetate limited enrichment, did not.

- The sudden presence of NO_2^- resulted in significant N_2O emissions in both enrichments, but for different reasons (not necessarily because NO_2^- inhibits NosZ).

  In the acetate-limited culture, a pulse of NO_2^- resulted in an important peak of NO (nir and nor expression are not always tightly regulated as in *Paracoccus denitrificans*), **Figure 7.3-a**. The NO_2^- conversion rate decreased 5-fold (compared to denitrification with NO_3^-), suggesting there was a strong inhibition of the system, but based on this data we cannot ascertain whether the inhibition was caused by NO_2^- itself (in the form of nitrous acid) or NO.

  In the NO_3^- limited culture, NO_2^- uptake during a pulse was faster than NO_3^- uptake, and only N_2O accumulated significantly, **Figure 7.3-b**. NO accumulation was negligible. Still, the biomass specific conversion rate of N_2O during the NO_2^- spikes was greater than during the NO_3^- spikes. This means that NO2- does not necessarily inhibit NosZ but rather that and NosZ becomes the bottleneck that cannot keep up with NO_2^- and NO reduction rates.

- A low COD/N is ***not*** directly linked to increased N_2O emissions

  The fact that the acetate limited culture produced negligible amounts of N_2O during continuous operation shows that a low COD/N ratio does not necessarily lead to N_2O emissions (and in fact the metabolomics study of Perez-Garcia *et al.*, 2017 suggests the opposite).

This common misconception may have arisen from another interesting observation: a correlation between N_2O emissions and denitrification using storage compounds as electron donor (i.e. PHA), in particular in the presence of NO_2^- (the basis of the CANDO process, see **Box 1.2** in Introduction). Evidence for this phenomenon is show in **Figure 7.4** with data taken from the MSc thesis of Tony Davies (*unpublished data*), although such experiments combined with a metabolomics have yet to explain the metabolic bottlenecks that cause this.

Aside from the correlation between N_2O emissions and PHA metabolism, we could conclude from our experiments that carbon limited cultures may be more prone to emissions in the case of disturbances (e.g. the presence of NO_2^-). However, further research would be required to support this.

Figure 7.4 - next page - (a) Example of one feast-famine cycles in the denitrifying SBR fed with acetate and NO_3^-. NH_4^+ is not shown but was present in excess throughout the cycle. CO_2 in the off-gas was also monitored. **(b)** Effect of a NO_2^- pulse during the famine (above) or feast (below) on N_2O accumulation. Notice than the percentage of NO_3^- naturally accumulating as NO_2^- in this second set of experiments was lower than in the experiment depicted in (a). The length of the feast (i.e. the time in which the acetate is depleted) was also shorter. This could have been due to a difference in microbial community composition and/or metabolic adaptation of the community over time.

a

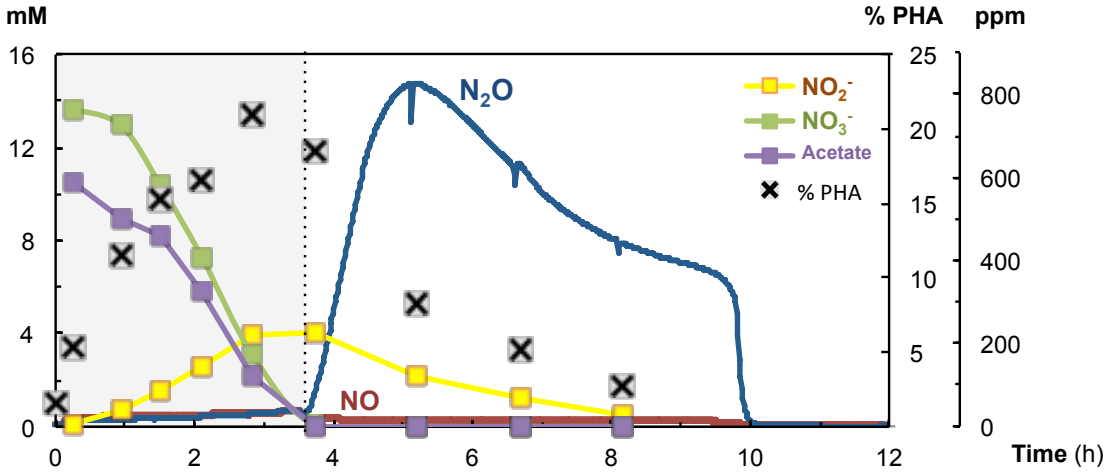
mM
% PHA
ppm
16
12
8
4
0
25
20
15
10
5
800
600
400
200
0
0
2
4
6
8
10
12
Time (h)
N2O
NO
NO2-
NO3-
Acetate
% PHA

b

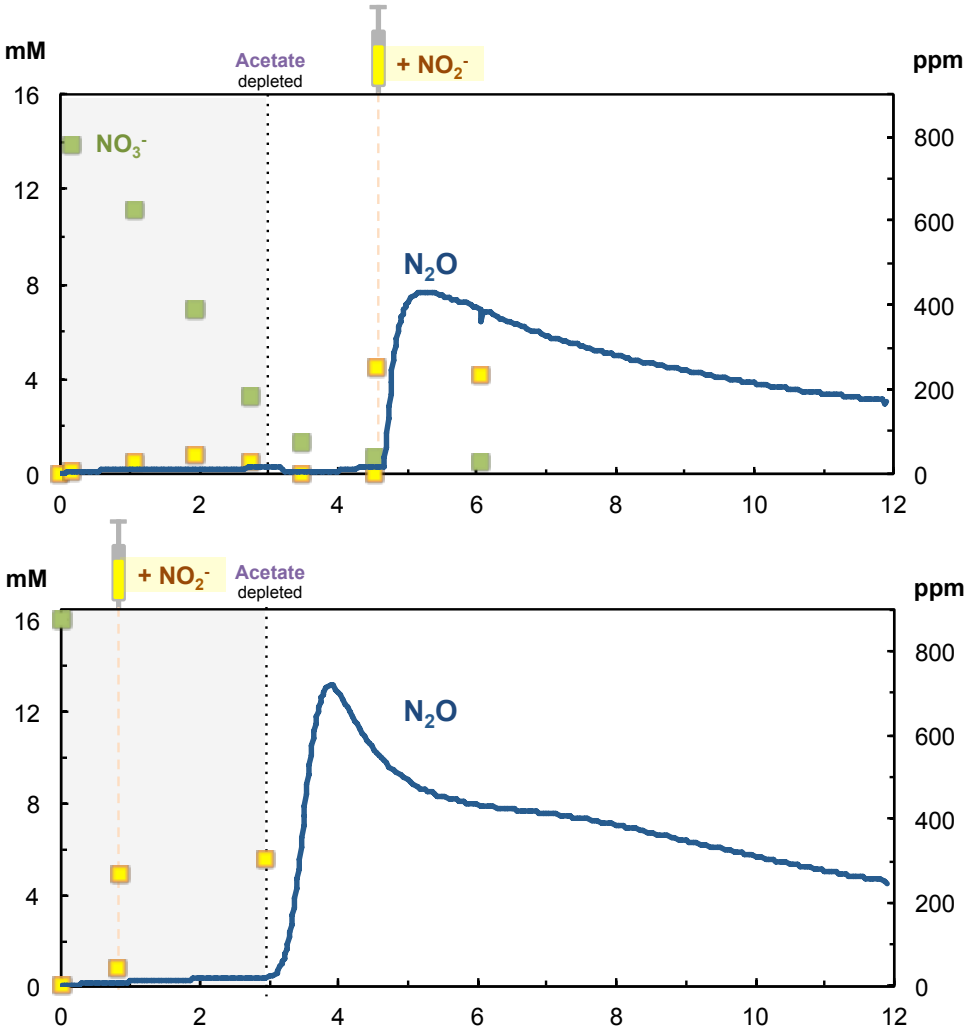
mM
ppm
Acetate
depleted
+ NO2-
NO3-
N2O
16
12
8
4
0
800
600
400
200
0
0
2
4
6
8
10
12
mM
ppm
+ NO2-
Acetate
depleted
N2O

B. Potential and limitations of our experimental approach

- *Acetate as a C source*

The carbon source is an important factor in the selection of a community in any enrichment. We chose acetate as the sole carbon source in the chemostat enrichments for two main reasons:

(1) a single compound, not readily converted in the absence of an external electron acceptor, would limit the growth of organisms other than denitrifying or N_2O reducing microorganisms, reducing the complexity of the communities studied.

(2) acetate is arguably the most relevant single substrate to use in the study of denitrification in WWT systems:

- acetate typically comprises 5–10% of the total COD in municipal wastewater, which is a *much* higher concentration than most other soluble organic compounds (Henze *et al.*, 1994).
- acetate assimilation capacity is common among denitrifiers and the majority of the abundant denitrifying groups in activated sludge consume acetate (Morgan-Sagastume *et al.*, 2008)
- in a study of three different WWTP with N removal, Nielsen and Nielsen, (2002) found that the fraction of bacteria able to consume acetate under anoxic conditions made up between 47% and 93% of the total number of bacteria. Therefore, using acetate would ensure that we would target a significant portion of microorganisms present in activated sludge in our experiments.

However, some important denitrifying groups in activated sludge cannot metabolise acetate: e.g. *Aquaspirillum*-related species (Morgan-Sagastume *et al.*, 2008), *Sulfuritalea* and *Heliangium* (Mcilroy *et al.*, 2016). The potential to grow using acetate - a 2-carbon compound – as a carbon and electron source depends on two enzymes specific to the glyoxylate shunt: isocitrate lyase (encoded by *aceA*) and malate synthase(encoded by *glcB*). In a study of 957 genomes, Ahn *et al*. (2016) found that these genes are not randomly distributed among bacterial species, the major groups harboring both *glcB* and *aceA* belonging to the phyla Proteobacteria (65.2%), Actinobacteria (20.9%), and Firmicutes (9.6%). Interstingly, no bacteria from halophilic, acidophilic, alkaliphilic, or thermophilic habitats were found to possess the shunt and all, but one, of the species harboring the glyoxylate shunt were aerobe or facultatively anaerobe. If there were a reason behind this growth on acetate-aerobic ETC, working with acetate as a C source would exclude the selection of hypothetical N_2O-reducing metabolisms unrelated to the well-known aerobic ETC.

Thus, the deliberate choice to use acetate as a C source in our enrichements arguably had an important role in the selection of the denitrifying/N_2O-reducing microbial populations – and possibly the *nosZ* clade - obtained and studied in this thesis – see **Table 7.3** (note the dominance of Beta-proteobacteria, and the family *Rhodocyclaceae,* in particular*)*

In Chapter 6, we used a mixture of C sources (acetate, glutamate, pyruvate, ethanol) in an attempt to measure the NO_3^- and N_2O reduction rates including as much of the microbial activated sludge community as possible.

Table 7.3 Family/genera of acetate consuming denitrifying/N_2O-reducing microorganisms typically found in Activated Sludge (AS) and in the enrichments in this thesis. The families highlighted in grey belong to the Class Beta-Proteobacteria

Acetate consuming denitrifiers in AS	**Denitrifying chemostats**	**Denitrifying SBR**	**N_2O reducing chemostats**	**N_2O reducing chemostats without NH_4^+**
Literature[abcd]	Ch7 (DGGE)		Ch 2, 3, 4 (DGGE/454/Illumina)	Ch 5 (454)
– *Pseudomonas* [d]			*Pseudomonas*	
Rhodocyclaceae – *Azoarcus* [a,c,d] – *Dechloromonas* [b,e] – *Thauera* [a,b,c,d]	*Rhodocyclaceae* – *Dechloromonas* – *Azospira*	*Rhodocyclaceae* – *Thauera*	*Rhodocyclaceae* – *Dechloromonas* – *Dechlorobacter* – *Azonexus* – *Azoarcus* – uncultured	*Rhodocyclaceae* *Quatrionicoccus* uncultured *Azonexus*
Comamonadaceae – *Acidovoraxb* [a,d] – *Rhodoferax* [e]	*Comamonadaceae* – *Comamonas* – *Simplicispira*	*Comamonadaceae* – *Comamonas*	*Comamonadaceae* – *Comamonas* – uncultured	
Candidatus *Accumulibacter* [c,d]		*Rhodobacteraceae* – *Paracoccus*	*Rhodobacteraceae* – *Paracoccus* – uncultured	
	Rhizobiaceae – *Agrobacterium*		*Rhizobiaceae* – *Rhizobium*	*Rhizobiaceae* *Rhizobium*
	Geobacteraceae – *Geobacter*			
Side-population			*Gracilibacteria*	
		Flavobacteriaceae – Uncultured – *Chryseobacter ium*	*Flavobacteriaceae* – *Flavobacterium* – *Cloacibacterium* – *Moheibacter* – *Chryseobacterium*	
			Chitinophagaceae *Erysypelotrix*	

[a] Thomsen *et al.*, (1994)
[b] Ginige *et al.*, (2005)
[c] Morgan-Sagastume *et al.*, (2008)
[d] Lu *et al.*, (2014)
[e] McIlroy *et al.*, (2016)

- *Molecular methods*

The molecular methods at our reach at the time of this thesis (mostly limited to 16S rRNA phylogeny, whether in the form of DGGE, FISH, or sequencing) fell short in understanding the dynamics of the denitrifying and N_2O-reducing communities enriched in the chemostats. We were often baffled by changes in microbial community composition/metabolic behavior under seemingly constant reactor operation: E.g. unexpected and transient accumulation of PHA in one of the N_2O enrichments (see **Figure 7.5**). No doubt, the ever-accelerating advances in molecular methods will help reap the full benefits of studying enrichment cultures.

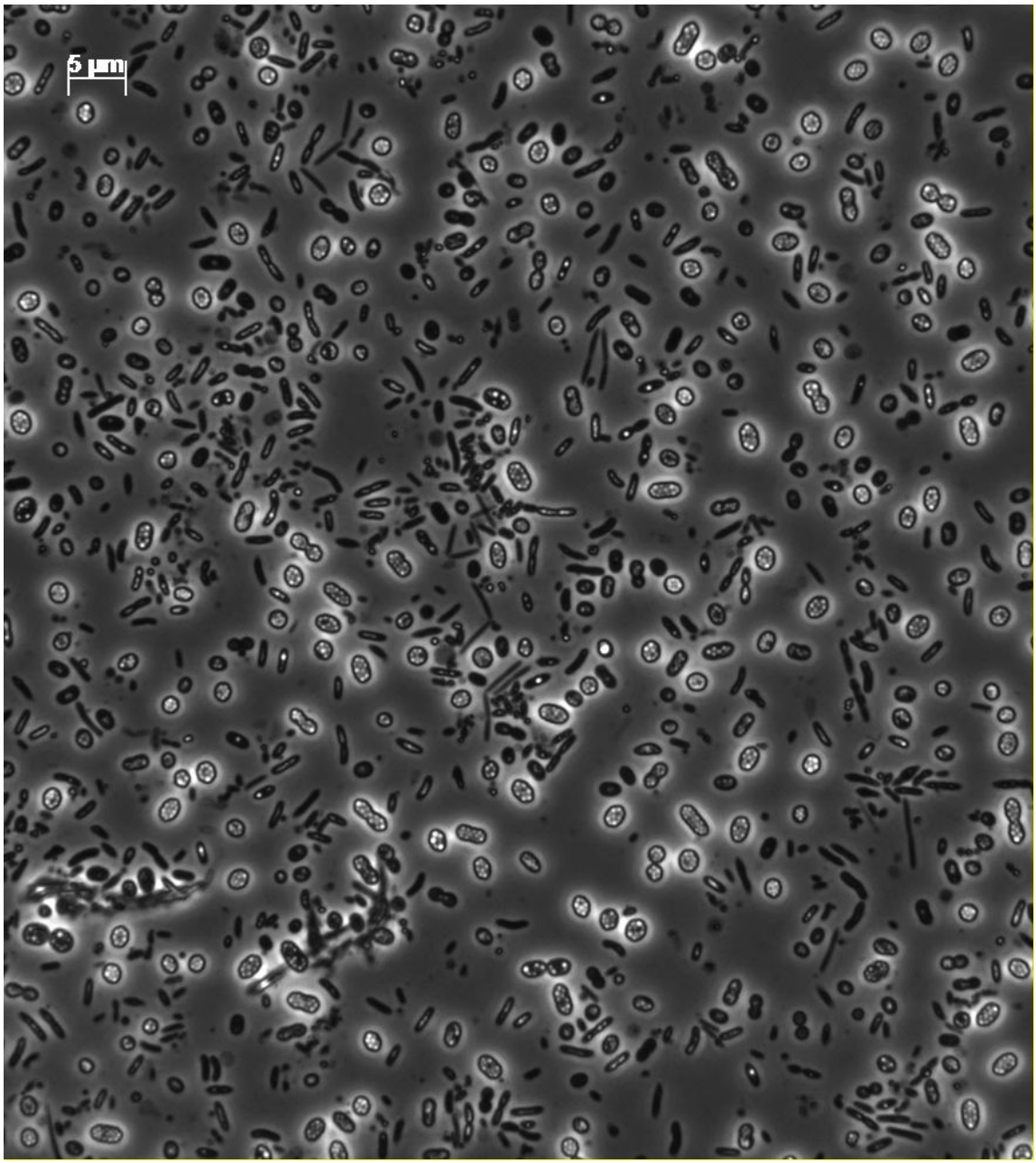

Figure 7.5 Microscope picture of the N_2O reducing microbial community. The white inclusions are a sign of PHA storage within the cells.

- *Online off-gas measurements*

We would like to advocate for a more frequent use of chemostats in microbial physiology studies, but will simply refer to Kuenen 2015 and merely highlight the value of monitoring the off-gas composition of (continuous/batch) cultures online. This can be done either by an infrared offgas analyzer e.g. Rosemount NGA 2000 - data presented in **Figure 7.3** - or automated mass spectrometer – see data Chapter 4, and can be essential to capture important dynamics in (NO and) N_2O production and consumption: see **Figure 7.6** as a particularly interesting example. Such experiments combined with metabolomics would be a powerful tool to understand N_2O emission dynamics in N-cycling ecosystems.

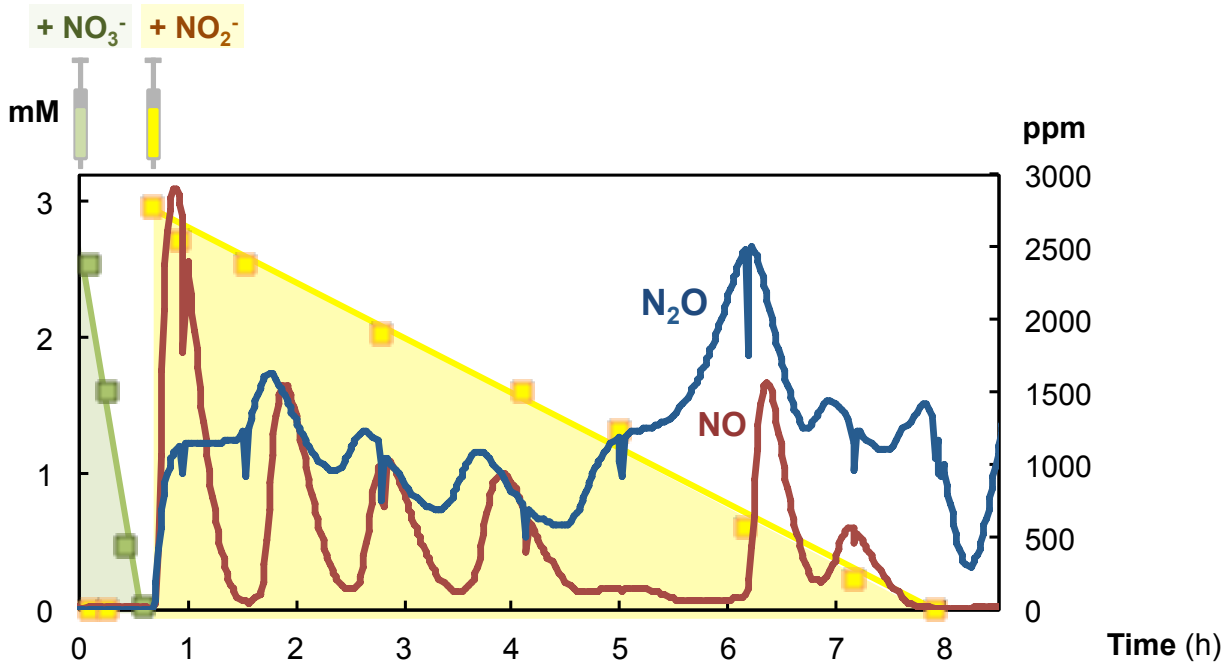

Figure 7.6 Batch experiment with interesting NO and N_2O dynamics performed on day 400 of the NO_3^- limited denitrifying enrichment.

C. Greenhouse gas mitigation strategies in wastewater treatment systems – some clues

It is difficult to extrapolate our findings to general guidelines to mitigate N_2O emissions in full-scale WWTP. However the main take-aways from this thesis would be:

- NO_2^- accumulation should be avoided as it is linked to N_2O accumulation under different circumstances.

- An optimal COD/N ratio (which can be controlled by carefully adjusting the amount – and type - of external C source added, or the recycling rates between aerobic and anoxic zones) could reduce emissions in the denitrification stage of N removal. C limited systems may have higher N_2O-emissions because (i) N_2O accumulation is somehow linked to PHA degradation, generally formed and consumed in C limited processes, and (ii) microorganisms living under these conditions might have a higher tendency to have unbalanced *nir* and *nor* regulation leading to NO and N_2O peaks. On the other hand, C excess is impractical, since the main goals of WWT is the removal of COD (and even for N removal, very high COD/N ratios may lead to DNRA instead of denitrification).

- It may be particularly important to monitor N_2O emissions in systems where denitrification occurs based on storage compounds: i.e. systems relying on biological phosphate removal or with selector systems for bulking sludge control

- Under optimal conditions, denitrifying systems tend to have an overcapacity of N_2O reduction relative to the other dentrification steps. If properly engineered, wastewater treatment systems could use denitrification to scavange the N_2O accumulated as a product of nitrification or abiotic reactions. Systems that might encourage this scavenging on nitrification-derived N_2O could be systems with frequent oxic-anoxic transitions (e.g. carrousel type plants) or with an optimized oxic-anoxic space in the activated sludge flocs or granules.

- N_2O emissions in wastewater treatment plants is a very complex matter. Even focusing on denitrification alone (setting aside nitrification and abiotic reactions), it is difficult to tackle the factors linked to increased N_2O production, since these are dependent not only on the microbial community composition, but also metabolic history The stochastic behavior and irreproducibility of N emissions, and the fact that N emissions are only side-reactions of the main nitrogen conversions, complicates the quantitative identification of factors determining N emissions and the computational modeling (e.g. the ASMN model is inadequate).

Interesting follow-up research would include:

- Metabolomics to unravel the link between NO_2^- reduction driven by PHA consumption and N_2O accumulation.

- Studying the potential cytotoxicity of high N_2O concentrations. Could it affect the denitrifying communities selected in systems with relatively high N_2O emissions?

- Can Cu-limitation in wastewater be associated to emissions (see Felgate *et al.*, 2012)

- How different C sources added to in the denitrification stage may affect microbial communities and thus N_2O emissions (see Hallin *et al.*, 2006, and Ribera-Guardia *et al.*, 2014)

D. N_2O's freakishly high redox potential – a remaining mystery

A lot of the research in this thesis was motivated by the intriguingly high redox potential of N_2O/N_2 pair (see **Figure 1.4** in Introduction). We hoped to select N_2O-reducing specialists, more energetically efficient N_2O reducing ETCs, or previously undescribed N_2O-consuming metabolic pathways.

In summary, we could say that we did not find anything "out of the ordinary":

- No more efficient N_2O reduction systems than those found in model denitrifiers like *Paracoccus denitrificans* (Chapter 2,3)
- No simultaneous consumption of O_2 and N_2O, reflecting the higher redox potential of N_2O compared to O_2 (Chapter 4)
- No new pathways (Chapter 5)

We did however observe other interesting phenomena, perhaps also related to the high redox potential:

- Cytotoxicity of N_2O (Chapters 2, and 5, as in Sullivan *et al.*, 2013)
  (We cannot help but notice a link with the fact that the glyoxylate shunt-required in acetate-consuming cells may play an important role in a cell's tolerance to oxidative stress – see Ahn *et al.* 2016)

- A general intrinsic overcapacity of N_2O reduction in denitrifying cells (Chapter 6)

E. References

Ahn S, Jung J, Jang IA, Madsen EL, Park W. (2016). Role of glyoxylate shunt in oxidative stress response. *J Biol Chem* **291**: 11928–11938.

van den Berg EM, van Dongen U, Abbas B, van Loosdrecht MC. (2015). Enrichment of DNRA bacteria in a continuous culture. *ISME J* **9**: 2153–2161.

Bergaust L, Bakken LR, Frostegård A. (2011). Denitrification regulatory phenotype, a new term for the characterization of denitrifying bacteria. *Biochem Soc Trans* **39**: 207–12.

Beun JJ, Verhoef E V., Van Loosdrecht MCM, Heijnen JJ. (2000). Stoichiometry and kinetics of poly-β-hydroxybutyrate metabolism under denitrifying conditions in activated sludge cultures. *Biotechnol Bioeng* **68**: 496–507.

Davies T, (2015) Enrichment of a Polyhydroxybutyrate Producing Mixed Microbial Culture Under Denitrifying Conditions. MSc Thesis. Environmental Biotechnology Group, TU Delft.

Felgate H, Giannopoulos G, Sullivan MJ, Gates AJ, Clarke TA, Baggs E, *et al.* (2012). The impact of copper, nitrate and carbon status on the emission of nitrous oxide by two species of bacteria with biochemically distinct denitrification pathways. *Environ Microbiol* **14**: 1788–1800.

Foley J, de Haas D, Yuan Z, Lant P. (2010). Nitrous oxide generation in full-scale biological nutrient removal wastewater treatment plants. *Water Res* **44**: 831–44.

Ginige MP, Keller J, Blackall LL. (2005). Investigation of an acetate-fed denitrifying microbial community by stable isotope probing, full-cycle rRNA analysis, and Fluorescent In Situ Hybridization-Microautoradiography. *Appl Environ Microbiol* **71**: 8683–8691.

Hallin S, Throbäck IN, Dicksved J, Pell M. (2006). Metabolic Profiles and Genetic Diversity of Denitrifying Communities in Activated Sludge after Addition of Methanol or Ethanol. *Appl Environ Microbiol* **72**: 5445–5452.

Henze M, Kristensen GH, Strube R. (1994). Rate-capacity characterization of wastewater for nutrient removal processes. In: Vol. 29. *Water Science and Technology*. pp 101–107.

Kampschreur MJ, Temmink H, Kleerebezem R, Jetten MSM, van Loosdrecht MCM. (2009). Nitrous oxide emission during wastewater treatment. *Water Res* **43**: 4093–103.

Kraft B, Tegetmeyer HE, Meier D, Geelhoed JS, Strous M. (2014). Rapid succession of uncultured marine bacterial and archaeal populations in a denitrifying continuous culture. *Environ Microbiol* **16**: 3275–3286.

Kuenen JG (2015). Continuous Cultures (Chemostats). In: Reference Module in Biomedical Sciences. Elsevier, Philadelphia, 2015.

Liu B, Mao Y, Bergaust L, Bakken LR, Frostegård Å. (2013). Strains in the genus *Thauera* exhibit remarkably different denitrification regulatory phenotypes. *Environ Microbiol* **15**: 2816–2828.

Lu H, Chandran K, Stensel D. (2014). Microbial ecology of denitrification in biological wastewater treatment. *Water Res* **64**: 237–254.

Mcilroy SJ, Starnawska A, Starnawski P, Saunders AM, Nierychlo M, Nielsen PH, *et al.* (2016). Identification of active denitrifiers in full-scale nutrient removal wastewater treatment systems. *Environ Microbiol* **18**: 50–64.

Nielsen JL, Nielsen PH. (2002). Enumeration of acetate-consuming bacteria by microautoradiography under oxygen and nitrate respiring conditions in activated sludge. *Water Res* **36**: 421–428.

Perez-Garcia O, Mankelow C, Chandran K, Villas-Boas SG, Singhal N. (2017). Modulation of Nitrous Oxide (N_2O) Accumulation by Primary Metabolites in Denitrifying Cultures Adapting to Changes in Environmental C and N. *Environ Sci Technol* **51**: 13678–13688.

Ribera-Guardia A, Kassotaki E, Gutierrez O, Pijuan M. (2014). Effect of carbon source and competition for electrons on nitrous oxide reduction in a mixed denitrifying microbial community. *Process Biochem* **49**: 2228–2234.

Sullivan MJ, Gates AJ, Appia-Ayme C, Rowley G, Richardson DJ. (2013). Copper control of bacterial nitrous oxide emission and its impact on vitamin B12-dependent metabolism. *Proc Natl Acad Sci U S A* **110**: 19926–31.

Thomsen TR, Kong Y, Nielsen PH. (2007). Ecophysiology of abundant denitrifying bacteria in activated sludge. *FEMS Microbiol Ecol* **60**: 370–382.

Verhagen K, (2015). Obtaining and studying an N_2O-reducing enrichment from activated sludge. BSc Thesis. Environmental Biotechnology Group, TU Delft.

Acknowledgements

The BIGGEST thank you to…

- **Supervisors & coaches**

♥ **Mark**, for giving me the opportunity to do a PhD in such a wonderful group and as part of the NORA ITN. for your kindness, your good example keeping life in perspective and your understanding during rough times.
♥ **Robbert**, former office-mate & invaluable supervisor. You are brilliant, charming, and a force of nature. Thank you for your help and your uplifting energy.
♥ **Gijs**, not all PhDers are so lucky to have private microbiology lessons from the master of chemostats. Not all PhDers are so lucky to have access to such an incredible source of knowledge! Thank you so very much for your great help & dedication.
♥ **Sara**, not officially my supervisor, but deserving a big thank you here for pulling me through my first paper. Without you and Lea I probably would not have made it through - so a million times thank you.
♥ **Åsa**, for all your efforts with the NORA ITN and for welcoming me into NMBU.
♥ **Inge**, for helping me turn from victim to survivor!
♥ **Kristina**, for your support as a mentor.
♥ **José Luis**, por abrirme la puerta al maravilloso mundo de la depuración de aguas.
♥ **Jules VL,** for introducing me to wonderful TU Delft.

- **Lab-mates, Co-authors, fellow ITNers**

♥ **Lea**, the best possible colleague and co-author. for teaching me so many things and for making my stays in Uppsala so nice.
♥ **Pawel**, for running around in the lab with me like “headless chicken”. for your super energy, motivation, and humor.
♥ **Koen**, for being such a wonderful student. for all your help and initiatives setting up the N_2O chemostat. And for providing the nice FISH picture that is in the back cover of this thesis. I have not doubt that a brilliant future awaits you!
♥ **Camiel**, for all your efforts with “Snelle Henkie”! it was lovely to be your MSc supervisor and office-mate.
♥ **Roel**, for all your hard work in the lab.
♥ **Gerben**, for giving us a spot in the Stouten Lab, for all your help, and for your contagious joie de vivre!
♥ **Bart,** for making it so fun to work with R5 ☺
♥ **Tina**, for making NORA summer schools and stays in Uppsala so nice. And your help in the lab!
♥ **Daria**, for being a friend in the Netherlands.
♥ **Linda**, **Manuel**, **Christoph**, **Luiz**, **Phillip:** for a great NORA-time!
♥ **Janne**, for all your hard NORgAnization!

♥ **Laurent**, **Lars**, for your great input &NORA summer school lessons.
♥ **Rob**, for all your thoughtful and helpful input and for welcoming me in VU.
♥ **GWE team,** for making me feel at home!
♥ **EDAR El Torno/ Aqualia team,** for the lessons learned.
♥ **Hayfa**, **Carlotina**, **Ine**, **Ana**, **Patri**, **Mirna,…** por los buenos tiempos en la UAM.

- **EBTers & BTers**

♥ **Udo**, for your help in the lab and measuring greenhouse gas emissions from Olburgen and Amersfoort. EBT is not the same without you!
♥ **Dirk**, for your patience and support setting up the chemostats.
♥ **Ben**, for all your help with the DGGEs, pyrosequencing results, & time.
♥ **Mitchell,** for ALL those DGGEs.
♥ **Song,** for your help and smile!
♥ **Yu mei,** for being such a lovely supportive colleage
♥ **Miranda,** for all the paperwork and insta-ecouragement! ☺
♥ **Janine,** for the cupcakes, songs, and career advice!
♥ **Sjaak**, for all the 10L bottles ordered, your good vibes, and your help with organizing summer schools and events.
♥ **Robert, Nayyar,** for taking such good care of the BT building.
♥ **Astrid**, **Jannie**, **Apilena**, for the innumerable medium bottles autoclaved!
♥ **Max,** for the fun chats and all the GC samples analysed
♥ **Johan,** for the TOC measurements and for making us feel safe!
♥ **Stef,** for your help during practicals…and the fun pubquizes!
♥ **Marc Stampraad,** for letting me use the BOC labs and teaching me about cytochromes and (modified) Clark electrodes
♥ The old EBT crew: **Helena M**, **Helena J**, **Peter**, **Jelmer**, **Andrea**, **Salah**, **Leonie**, **Shiva**, **Mario**, **Tommaso**, **Emmanuelle**, **Marco**, **Matthijs**, for making me want to join EBT.
♥ The new EBT crew: **Jules**, **Victor**, **Simon**, **Laura**, **Michel**, **Leonor**, **Danny**, **David, Hugo, Marta,** … for making it so nice to stay in EBT.
♥ EBT guests from abroad: **Mabel**, **Jose**, **Mariana**, **Borja**, **Lledó**, **Bruno**, **Nuno**,… for bringing some sun to NL.
♥ Fellow CSErs, **Eleni, Robin**, **Florence**, **Yaya**, **Mariana**, **Hugo**, **Sofia**, **Alex,…**
♥ **Eveline** & **Maaike**, for being my N-cycle colleagues, friends and supporters.
♥ **Julio, Cristian,** it was a pleasure to work with you!
♥ **Marissa** for the company singing, for your kindness, & Dutch translations. ☺
♥ **Ingrid & Aina,** for making it so nice to be in the office
♥ **Morez & Donya,** for your support…and for finding me a job! ☺
♥ **Jure,** for offering a tissue when necessary, and for putting things in perspective.
♥ **Michele,** for your encouragement and discussions on N_2O/life

♥ **Pilar**, for being so helpful and nice to be with, inside and out of BT.

- **Adoptive-family**

♥ **Rocio**, for ALWAYS being there. For being our "mommy" in Bastiaansplein and singing along to the guitar. For being such a good friend.

♥ My dear **Maria**, my sister from another mister. For making Delft such a lovely place to live in. For all the fun & silly times. And for your hugs when I most needed them.

♥ **Rober**, the Robertontili to my Monguili. I lava u!

♥ **Bea,** for being Bastiaansplein-family.and an inspiration.

♥ **Sophie**, for the best yoga clases I've ever had. for the nice breakfast and lunches. For forgiveness rituals and being a friend.

♥ **Leni** queridita – platipus leprechaun. Por ser tan maravillosamente maravillosa! Y por las plantitas y calcetines.

♥ Yogi book club girls, **Shoshan**, **Meena**, **Giulianna**, **Olga**, **Shirley**, **Jessica**, **Cora**, **Esther**, for the deep yet light discussions.

♥ Yogi friends. **Boris**, **Didit**, **Neela**, **Yvonne**, **Irina**, **Chantal**, **Isabella**, for the beautiful retreats. **Saskia**, for sharing your adventures.

♥ **Ilias**, for accompanying me so often to the lab out of official hours (when I was scared to go alone). for working next to me so often. For supporting me through my more-often-than-I-would-have-liked crises. For being such a nice, warm, fun osito.

♥ **Kika** love, for being such a soothing presence. For being a role-model (I strive to be more like you ☺). For ALL you help and support.

♥ **Emma**, my sister and biggest support in Delft. For literally feeding me back to life at the worst of times (I will be forever and ever grateful). For your strength and joy for life. It's my lucky day to have you in my life! Thank you for helping me see things a little less dramatically with your humor.

♥ **Tani** dearie, for being a BFF. for flying over to Delft at the blink of an eye and for modelling for me how how to be a wholehearted, strong, independent single woman of the world! And of course for introducing me to HAMILTON! Sissy that walk sistah <3

♥ **Arte, Viki, Cecile, Ana**, for random fun reunions.

♥ **Nerea,** for more random fun reunions,

♥ **Nada**, the Ru to my Michelle Visage & scorpio love-warrior sistah. for being silly with me when I needed it the most <3

♥ **Sandri**, for making my first year in Delft the most fun year of my life - playing reggeaton to our reactors, & running in the snow.

♥ **Miriam**, **Reyesita**, **Pia**, **Ana**, for being my Spanish family in Delft.

♥ **Carmen** & **Iliaria**, por ser tan maravillosas!

♥ **Almudena**, por ser mi familia y apoyo en Cádiz.

- **my Lovely Love-full Family**

♥ my dearest **Maca**, **Eros** & **Lucas**, for the joy you have brought me during these years, just by being you. My auntie love has no limit.

♥ my wonderfully wonderful generous fun soulmate sister **Paula,** for being my rock and unconditional cheerleader. It's my luuuuucky day to have you in my life. I don't know what I (and this thesis) would have done without you.

♥ my wise role-model sister-from-a-previous-life **Ana**. for being a bright bright source of light & love.

♥ **Alvaro** & **Elia**, for making my sisters happy.

♥ **Cloto & Vir**, for being my adoptive sisters. **Vir,** for saving me in Delft, Madagascar, Madrid, or anywhaer.

♥ **Maricarmen**, **Agustin**, for being my adoptive parents.

♥ **Abuela,** por tu apoyo y amor.

♥ **Papi, Mami**, for being the most kind, accepting, and amazingly generous parents I know. For giving me a priviledged international, education & keeping a lovely safe home that I can always come back to.

Any girl should be so lucky.

CV

Monica was born in Madrid, SPAIN, but considers herself a citizen of the world, international environments being her habitat of choice. She studied BIOLOGY (BSc), MICROBIOLOGY (MSc), and is weirdly passionate about wastewater treatment and anaerobic digestion of manure…amongst other wastes. But also about yoga, urban art, musicals, and her little niece/nephews.

Monica thought she would never finish her PhD thesis. She loved her time at TU Delft, but it was also a struggle. Yet she finished, and it wasn't so bad after all. She hopes this will inspire other struggling PhDers not to take things too seriously. And above all, to take care of themselves because, as RuPaul says at the end of every episode, "If you can't love yourself, how in the hell are you going to love somebody else" (and make great discoveries for science)?

This is a picture in the Van Itterson Lab of the old BT building – next to the fumehood which was home to many a happy N_2O-reducing bacteria.